APPLICABILITY OF THE MATHEWS STABILITY METHOD TO OPEN STOPE STABILITY ASSESSMENT AT OLYMPIC DAM MINE

A thesis submitted in partial fulfilment of the requirements for the

Degree of

Master of Science in Engineering Geology

at the

University of Canterbury

by

Jacqueline Emily U'Ren Sharp

2011

Abstract

Olympic Dam underground mine is located in South Australia approximately 520km north-north-west of Adelaide. The copper-gold-uranium deposit is extracted by open stope mining. The empirical Mathews stability method has been applied to open stope stability forecasting at Olympic Dam for the more than 20 years. This method adjusts the rock tunneling quality index (Q') to allow for a rock stress factor, the orientation of any discontinuity and the orientation of the geometric surface formed by the excavation.

The applicability of the Mathews stability method at Olympic Dam was analysed by assessing the volume of over break outside the stope design profile. It was found that 41% of all stope surface predictions were correct, and that 59% (by difference) of all predictions were therefore incorrect. This was found to be primarily due to the method as applied at Olympic Dam, rather than the inherent errors of the Mathews stability method. However there are a number of weaknesses in the Mathews stability method including the inability to identify structural weaknesses in the rock mass, to allow for different stress concentrations around irregular shaped stopes and to account for stope relaxation.

A high resolution non-linear, Hoek Brown, numerical model is capable of providing displacement, velocity and strain rates for points within a rock mass. Velocity is the modelled rate of displacement of the points within the rock mass relative to the stope profile. An existing numerical model of this sort at Olympic Dam was used to investigate the relationship of the velocity of points moving toward a stope, and the probability of them becoming over break. It was found that with increasing rates of velocity the probability of a point becoming over break increased.

The identified limitations of the application of the Mathews stability method are not enough to justify removing the method from the stope design process at Olympic Dam. With the implementation of recommended improvements such as, increasing the frequency of window mapping collection, live stress measurements and detailed post-mining assessment of stopes, an increase in the methods reliability can be expected. These improvements should be incorporated in conjunction with the continued trial of velocity as a stope performance indicator at Olympic Dam.

Table of Contents

List of Figures

List of Tables

Acknowledgements

This thesis would not have been possible without the help of many people. Firstly I would like to thank my supervisor David Bell, for guidance and numerous edits.

Getting started would not have been possible without Josh Bryant providing me with the opportunity to visit and eventually work at Olympic Dam. Big thanks to Glenton Mungur and Don Grant from BHP Billiton who gave up time out of their busy schedules to track my progress and provide any support I needed.

A huge thank you to David Beck, without your extraordinary wealth of knowledge and innovative thinking this thesis would still be in the making. Your passion for your work is inspiring.

To my grammar savvy sister Katherine and her partner Hamish, thanks for spending your weekend proof reading my work.

All my colleagues, friends and family thank you for listening to my worries and whines over the past two years and assuring me that it isn't impossible to write a thesis and that I will eventually get there. In saying that a special mention must go to Josh, he has been through all the highs and lows of studying part-time with me. You have been truly patient and always there to put things into perspective for me, for that I am extremely grateful.

Mum and Dad your consistent encouragement has been one of the main drives for me to finish this thesis, thank you.

Chapter 1. Introduction

1.1 Overview

Olympic Dam mine is an underground operation located in South Australia (Figure 1.1), where a copper-gold-uranium deposit is exploited via open stope mining. Stope stability is of primary importance at Olympic Dam, without it there is no way of achieving reliable and predictable production. By maintaining stable stopes there are fewer threats to the safety of personnel and a greater chance of reaching production targets.

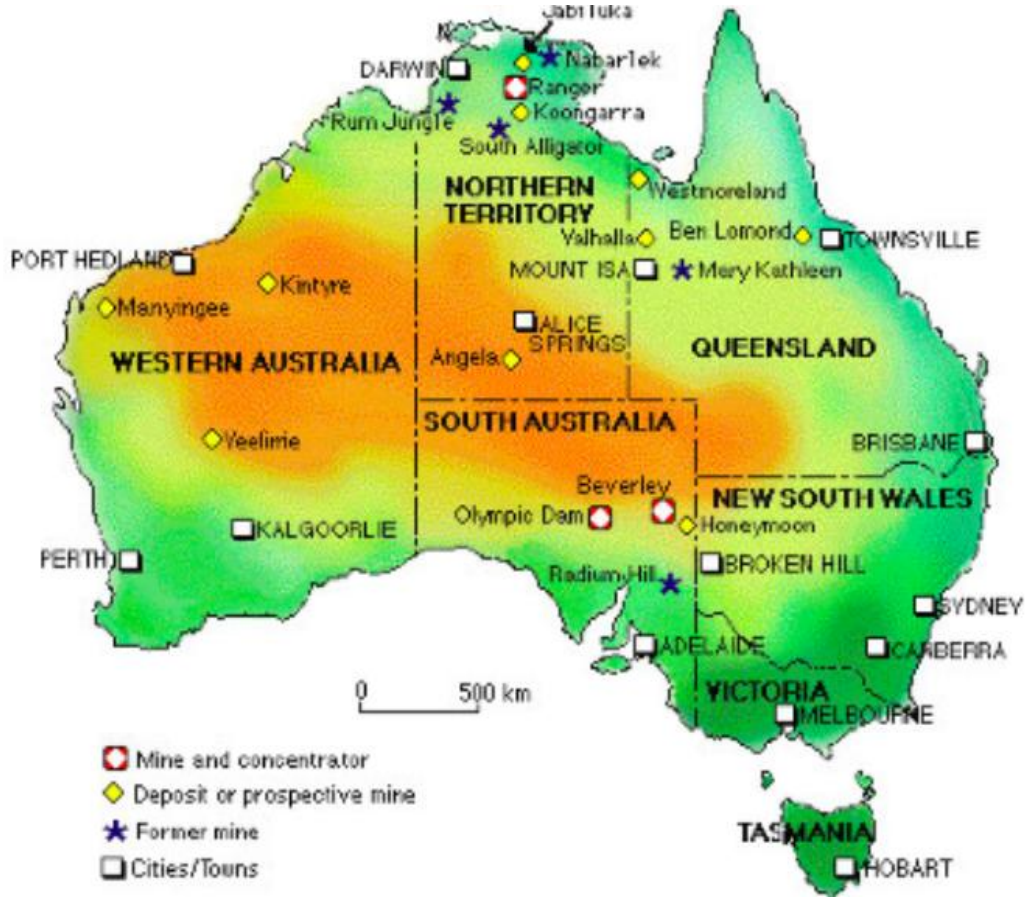

Figure 1.1: Map displaying recent, present and upcoming Uranium mines in Australia (WealthMinerals 2002)

As part of the preliminary open stope design process at Olympic Dam, a version of the Mathews stability method is utilised. The Mathews stability method is an empirical design tool commonly applied during preliminary design of open stopes as a guide to stability.

Built from a database of case studies, the method graphically relates two calculated parameters, the Mathews stability number (N') and the hydraulic radius (HR) (Figure 1.2). The stability number represents the competency of the rock while the hydraulic radius accounts for the geometry of the surface by dividing the area of the stope surface by the perimeter of the stope surface. When plotted together the location of the point on the chart provides the user with an indication of the likely performance.

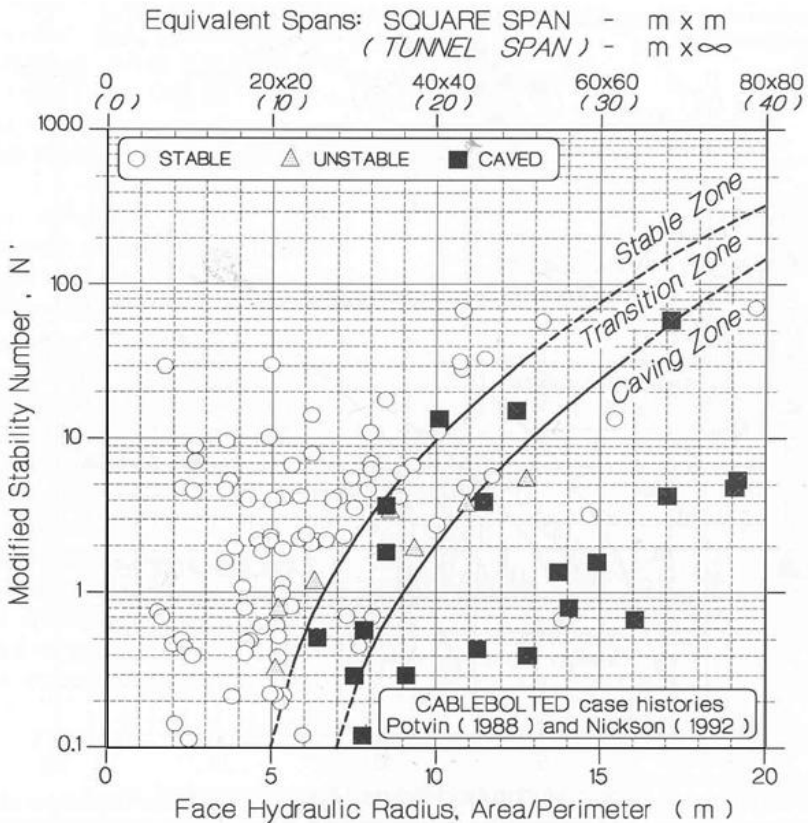

Figure .1.2: Mathews stability chart applied at Olympic Dam for supported surfaces - walls (Hutchinson 1996)

The Mathews method is generally undertaken for five surfaces of each stope. This number will vary if the stope has any mined adjacencies. The five surfaces include the crown, this is the top, or roof of the stope. The remaining surfaces are the four walls (Figure 1.3).

Experience with the Mathews stability method at Olympic Dam has raised concerns with the validity of its application and its usefulness as part of the design process. This is due to the inconsistency between the method's predicted performance and the actual performance of stope surfaces.

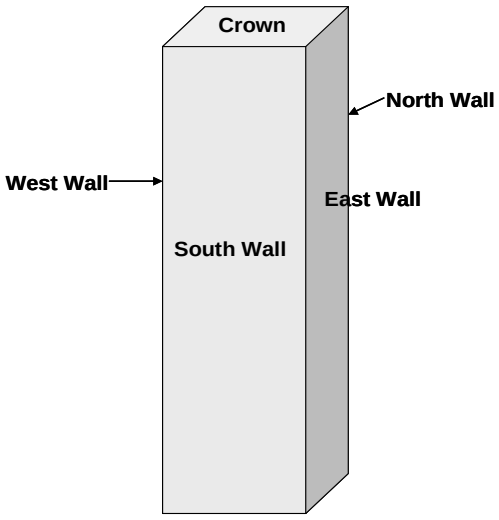

Figure 1.3: Schematic diagram of a basic stope shape and its five surfaces

The stability of each stope surface for this study is measured using the amount of over-break. Over break is any unplanned inclusion of un-blasted material from the walls and crown of the stope which fall into the void. Although stopes at Olympic Dam generally have few stability issues, any unpredicted stope fall off or over break that exists is of concern because it presents potential safety hazards and impacts on future production.

This inconsistency between stope design and performance means there is little trust remaining in the model. This means for example, if a stope surface is plotted in the "caving" zone on the chart the result is disregarded and the stope design will remain unchanged. Instead, designers have begun to rely solely on the experience of the engineer conducting the analysis. The engineer takes into account a range of other stability controls alongside the Mathews plot including, structures and in situ stress patterns in and around the stope. This means the geotechnical analysis of each stope is left to the subjective interpretation of the individual engineer. This is an inefficient and inconsistent approach to mine design and leads to significant variance between engineers.

Although there is a strong belief at Olympic Dam that the Mathews stability method is inaccurate in its predictions there has been no recent study has tested this belief and examined the Mathews stability method against stope performance at Olympic Dam mine. This thesis has undertaken this examination and from the results has identified

some potential improvements to the application of the Mathews stability method at Olympic Dam. An alternative stope surface stability predictive tool for Olympic Dam has also been explored.

1.2 Scope for thesis

There are two primary objectives for this thesis. The first objective is to validate the applicability of the Mathews Stability method to the preliminary stope design at Olympic Dam mine. The second objective is to devise an alternative method to replace the Mathews stability method as the preliminary stope design tool at Olympic Dam.

The subsidiary objectives of this thesis are:

- To define the stability of mined stopes
- To explore what local parameters have an impact or control on failed stope surfaces
- To identify possible improvements to the application of the Mathews stability method at Olympic Dam.
- To gain an understanding of the mechanics of instability including stability indicators.

1.3 Olympic Dam Mine

1.3.1 Location and Reserves

OD underground mine is located in South Australia approximately 520km north-north-west of Adelaide city, close to the township of Roxby Downs. The ~1,600 million year old deposit commonly known as the Olympic Dam Breccia Complex (ODBC) was discovered in 1975 by the Western Mining Company. Hosted by the Roxby Downs granite, the hydrothermal breccia deposit is host to several iron-oxide associated copper-uranium-gold ore bodies. The ore reserves is one of the largest discovered deposits in the world (3,810 Mt at 1.0% Cu, 0.5 g/t Au, 0.04 U_30_8, and 3.6 g/t Ag; (Williams 2005)).

OD mine is located in an arid environment where the average annual rainfall is around 200mm, with temperatures reaching as high as 48ºC in the summer months.

1.3.2 Regional Geology

The Olympic Dam deposit is located on the eastern margin of the Gawler Craton (Figure 1.4). It is unconformably overlain by 300 to 350m of Late Proterozoic to Cambrian age flat-lying sedimentary rocks of the Stuart shelf geological province (Reynolds 2000). The deposit is hosted by the Roxby Downs granite which is part of a Hiltaba Suite batholith. This batholith involved the intrusion of deformed granitoids and metasediments of the Hutchinson Group into the Olympic Dam and Andamooka region. The batholith sub-crops over an expansive area of around 50 by 35 km, with a composition range from syenogranite to quartz monzodiorites (Flint 1993). Campbell et al. (1998) has constrained the intrusion ages of the granites through U-Pb zircon dating. The ages range between 1598 and 1588 million years ago with a plus or minus two error bracket. The Roxby Downs granite is a pink to red coloured, un-deformed, un-metamorphosed, coarse to medium grained, quartz-poor syenogranite (Creaser 1989). The upper parts of the deposit and the Roxby Downs granite were eroded during the Meso to Neoproterozoic (Reeve. 1990). Following this the sedimentary rocks of the Stuart Shelf were deposited. These sediments now have a minimum thickness of 260 meters.

A further literature review, by the author, of South Australian regional geological setting and the Olympic Dam ore body is located in Appendix A.

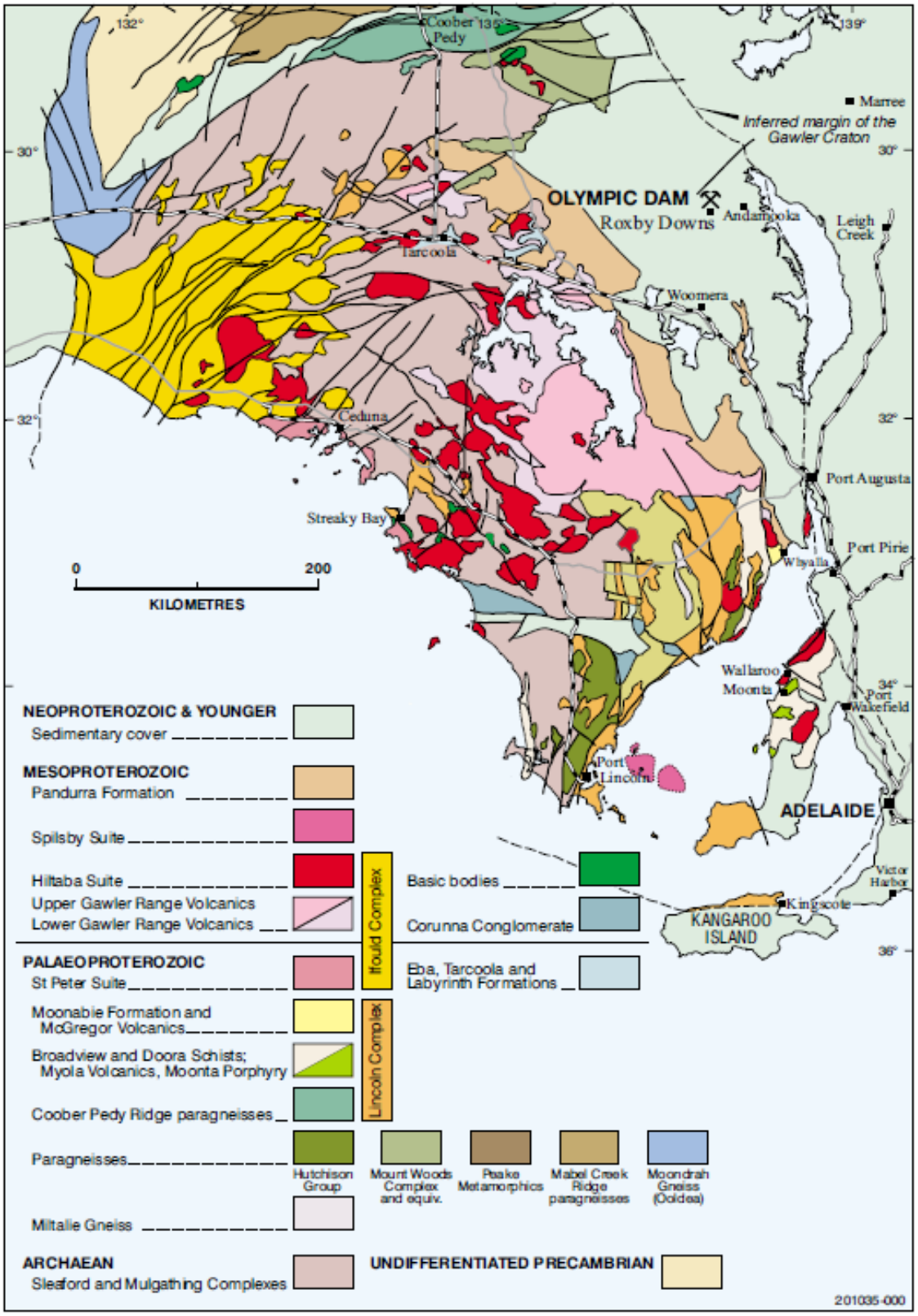

Figure 1.4: Regional geological map showing interpreted subsurface geology of the Gawler Craton, (Daly 1998)and (Reynolds 2000)

1.3.3 Olympic Dam Breccia Complex (ODBC)

The ODBC primarily consists of a funnel-shaped, barren, hematite-quartz breccia core surrounded by an irregular array of variably mineralised and broadly zoned hematite-granite breccia bodies with localised dykes and diatremes (Reynolds 2000). A variety of lithologies are displayed by the breccia body including those which are granite-dominated on the periphery of the complex to those which are intensely hematised equivalents.

Aspects of the deposits origins are still debated, although the most recent models regard the ODBC as stemming from hydrothermal activity. Reeve et al. (1990) and Haynes et al. (1995) concluded that the origin involved the mixing of hot saline water and cooler meteoric water interacting with basaltic and granitic wall rock.

A general increase in hematite content is witnessed in the cross section of the deposit from the margins of the complex to the core (Figure 1.5). A halo of weakly altered and brecciated granite extends out around 5 to 7 km from the core in all directions. In total, hematitic-rich breccias occupy an area of approximately 3 by 3.5 km.

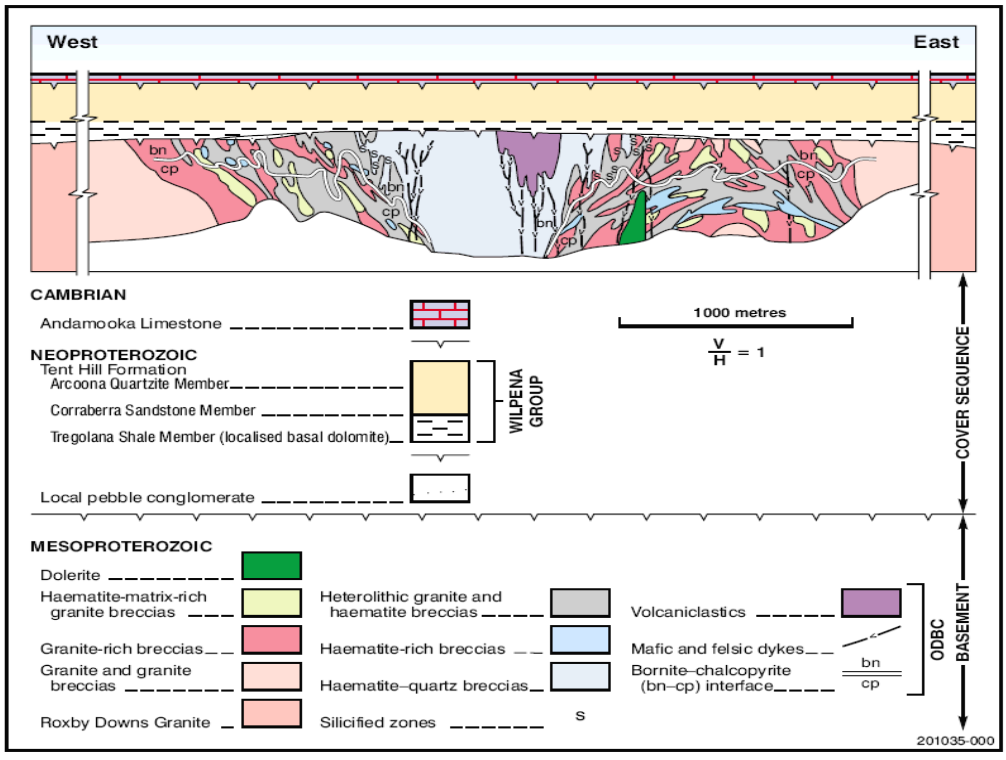

Figure 1.5: Cross section the ODBC showing the variations within the ore body(Reynolds 2000).

Further a 300 to 500 m wide belt extends approximately 3 km to the northwest. The outer and lower boundaries of breccias and alteration have not been accurately located due to a progression into granite host. It has a relatively long and narrow extension to the NW. The limbs extend approximately 1,500 m north-south, 2,000 m east-west, and the limbs are seen to taper with distance from the centre (Figure 1.6). The shape of the deposit is often referred to as a fry pan or a sting ray. The ODBC is poorly explored below 800 m. However exploration drilling has shown that the complex exceeds depths of 1.4 km.

The unconformity which marks the boundary between the ODBC and the overlying sediments is around 260 m below the surface. The unconformity has historically attributed to the unraveling of stope crowns that are within close proximity.

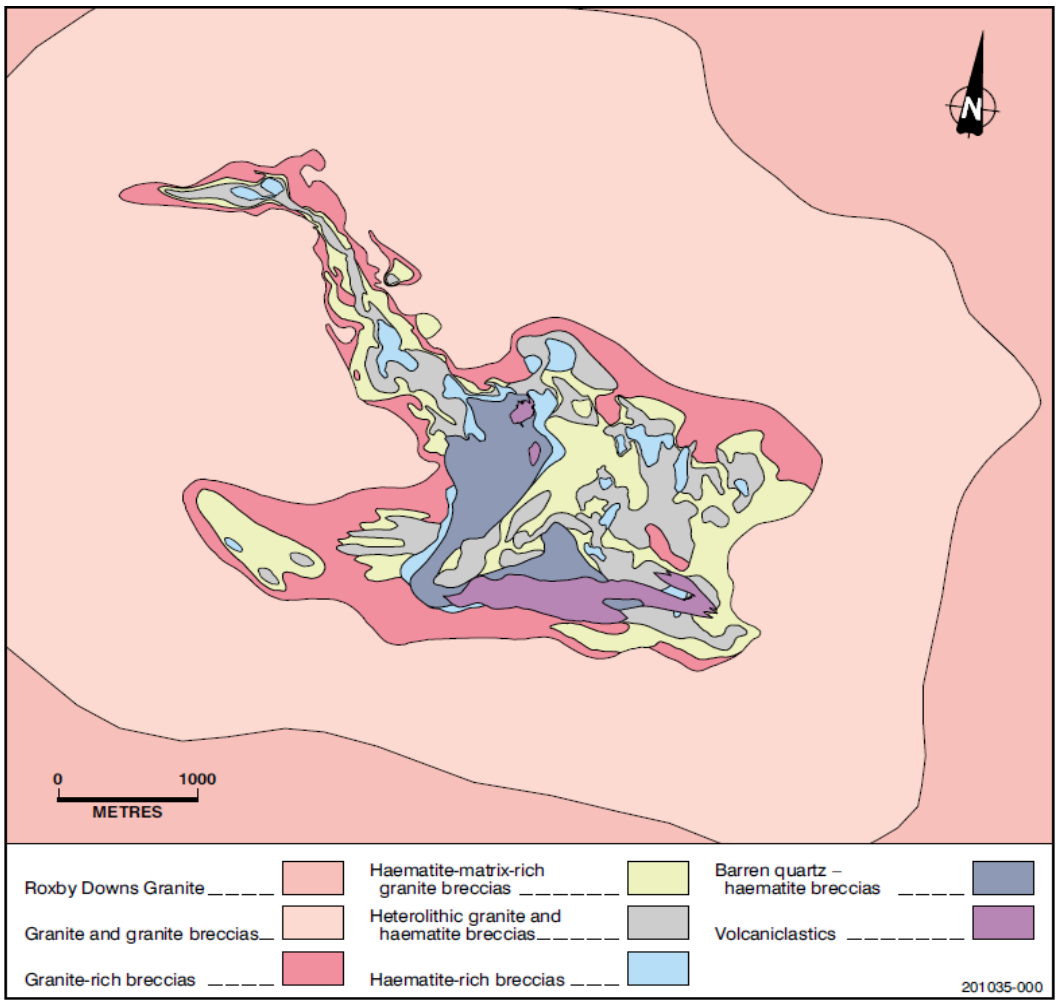

Figure 1.6: Simplified geological plan of the ODBC showing the general distribution of major breccia types. Note the broad zonation from the host granite at the margins of the complex to progressively more hematite-rich lithologies at the center (Reynolds 2000).

As mentioned earlier there are several lithologies found within the Olympic Dam ore body, with the two most prominent types being granite and hematite. Other than the volcanic and sub-volcanic breccias and the dykes the rock types are classified by the dominance of either granite or hematite within them (Table 1.1). There are no sharp boundaries between these rock types. Instead there are gradual transitions throughout the ore body with the principle copper-bearing minerals chalcopyrite, bornite, chalcocite and native copper as well as uranite being present throughout the ore body.

Table 1.1: Olympic Dam ore body rock types and descriptions

	**GRNB:** Brecciated & Unaltered granite as well as fragmental rocks consisting of unaltered granite-derived components. Granite is made up of alkali feldspar (50%, plagioclase (20%), quartz (25%) and mafic minerals (5%).
	**GRNH:** The majority of the unit should be intact, but hematite has either started to crackle brecciate the unit, or the unit is clast supported (predominantly granite). Hematite can replace some of the feldspars, leaving a Ntexturally retentive Órock type.
	**GRNL:** Typically a matrix supported breccia, with the matrix/infill being hematite +/- rock flour components. However, majority of clasts are granitic in composition.
	**HEMH**: Typically a matrix supported breccia (as per GRNL) with the matrix/infill being hematite matrix/replacement, but the clasts are predominantly hematite with a lower proportion of granite.
	**HEM:** Textured or massive; breccias, precipitates, metasomatites . The similarity between hematite clasts and matrix, and the strong hematite replacement/alteration can make individual omponents difficult to recognize.
	**HEMQ** : Classic hematite-quartz breccia. Barren, locally vughy, porous or silicified. No sulphide, sericite or fluorite .
	**HEMV/VHEM:** Breccia containing hematite + um-m volc clasts
	**GRNV/VGRN:** Breccia containing granite + um-m volc clasts
 	**EVD/UMD/FVD:** Generic dyke; volcanic/sub-volcanic textures. Often chlorite or hematite altered. The more mafic dykes have undergone intense texturally destructive sericite and hematite alteration. Felsic dykes commonly have preserved porphyritic textures.

1.4 Mining Method and Equipment

At Olympic Dam the ore-bearing zone lies approximately 340m below the surface, with all mining activities occurring 8-250m below this level. The extensive Olympic Dam deposit is exploited by mechanised underground mining operations. All ore is processed on site, utilizing the onsite facilities including an autogenous mill, concentrator, hydrometallurgical plant, smelter and refinery to produce a marketable product.

Annual production capacity of the mine is around 10 million tonnes (t) of ore, recovering approximately 200,000 t of refined copper, 4,300 t of uranium product (U_3O_8), 80,000 oz gold (Au) and 800,000 oz silver (Ag) (Reynolds 2000).

There is approximately 300 km of tunnelling development extending to depths of around 800m below the surface at Olympic Dam (Figure 1.). Each development heading is completed at a general rate of approximately 20km per annum or 5m per day. The underground is accessed either down the 1.5 km portal in a vehicle or down to the 420 m platform via an electronic personnel cage.

Sub Level Open Stoping (SLOS) is used to extract ore at Olympic Dam, with up to 20 stopes active at any one point in time around different areas of the mine. SLOS mining methods are used to extract large, massive or tabular steeply dipping competent ore bodies. These are surrounded by competent host rocks, which generally have few constraints regarding the shape, size and continuity of mineralisation (Villaescusa 2000).

The development of perimeter drives allows access to the ore zones. The front (footwall) perimeter is primarily used for ore handling systems while the rear (hangingwall) perimeter drive forms the exhaust for the ventilation circuit. This ventilation system is particularly important for controlling the radiation levels in the mine.

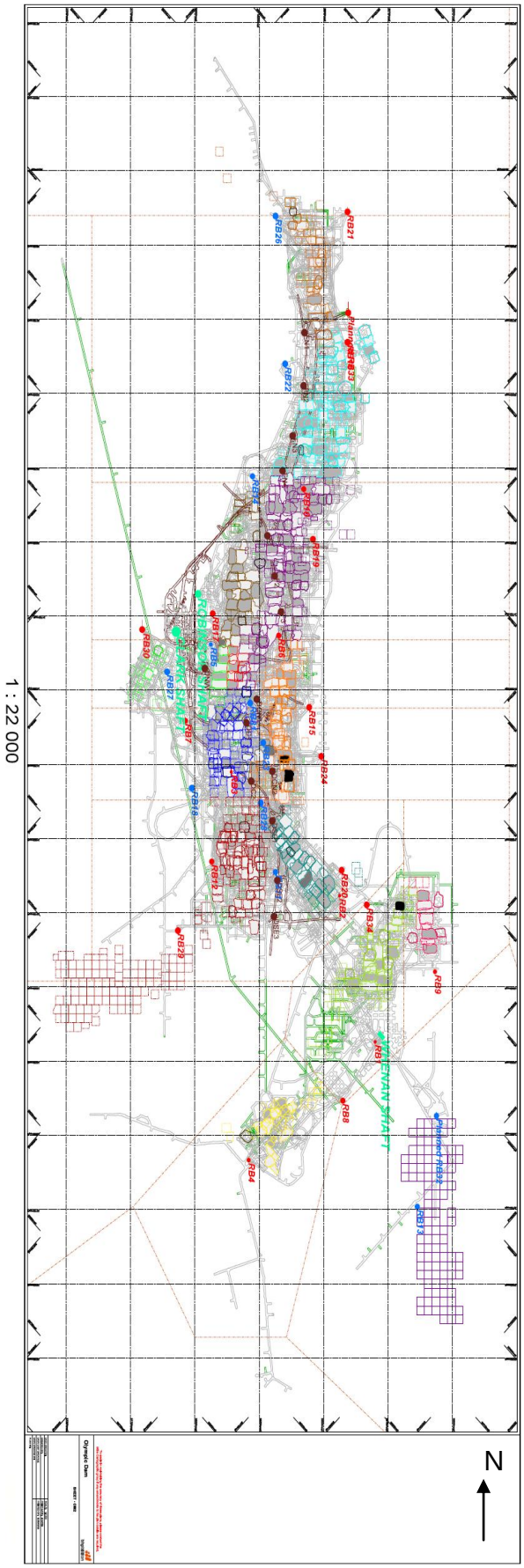

Figure 1.7: Plan of Olympic Dam ore body and the underground workings, with mined and planned stopes highlighted by the colour of which mine area they fall within (Geotechnical 2010) A large copy of this plan is located in the cover of this thesis (Map 1)

Once the access to a stope area has been developed the slot is created. This provides access to the void, and the area that the stope will blast into. The initial void which the slot fills is created by an underground raise (UGR) drilled by a raise drilling rig. These raises are 1.4m in diameter and extend the entire height of the stope. The remainder of the stope is drilled by Simba drill rigs which bore 102mm downholes in the slot, 102mm uphole and 115mm downhole rings on the various drill levels for the stope. The number of drill levels varies from 2 to 6 depending on the size of the stope.

The blast packages are progressively blasted and extracted level by level starting at the bottom. Packages are taken as either full level firings or as undercuts. Using this progressive technique minimizes the exposure of personnel to the open void. Extraction of the fired rock is carried out by front end loaders from the drawpoints. There is a minimum of two drawpoints per stope (Figure 1.8). Once the dirt is within the brow of the drawpoint, tele-remote machinery bogs the stope for the void. Between each stope firing, the stope must be bogged to create enough void to fire into, preventing the stope from becoming blocked and therefore being unable to be bogged.

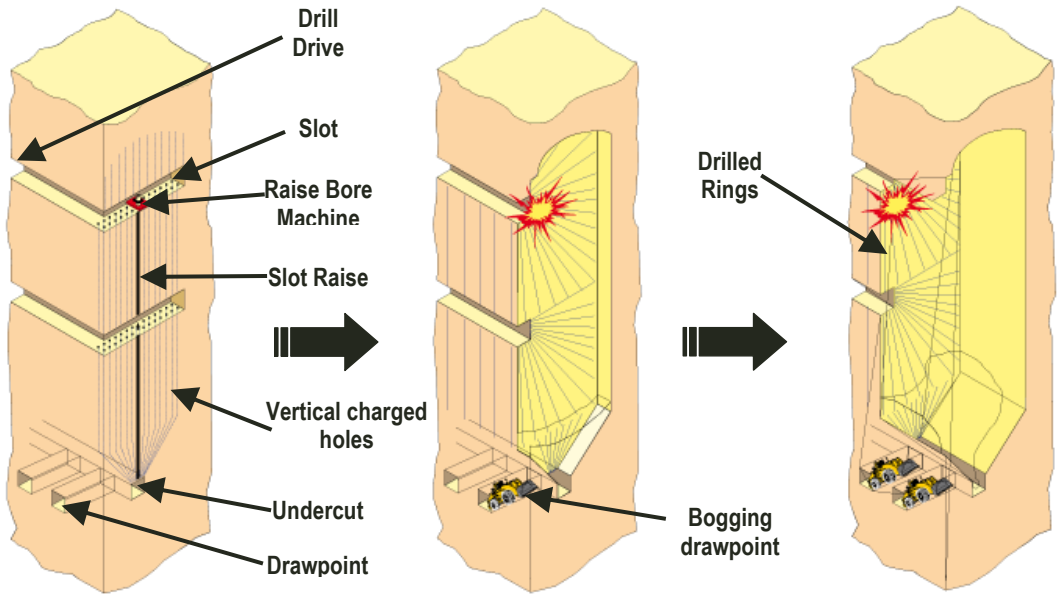

Figure 1.8: Schematic diagram showing the steps of SLOS mining method from drilling to extraction.

The ideal sequence of stope extraction involves always having the adjacent void back filled prior to the commencement of mining (Figure 1.9). A stope which has no backfilled adjacency is a primary stope, with a single adjacency is a secondary stope and with two or more adjacent backfilled stopes is a tertiary stope.

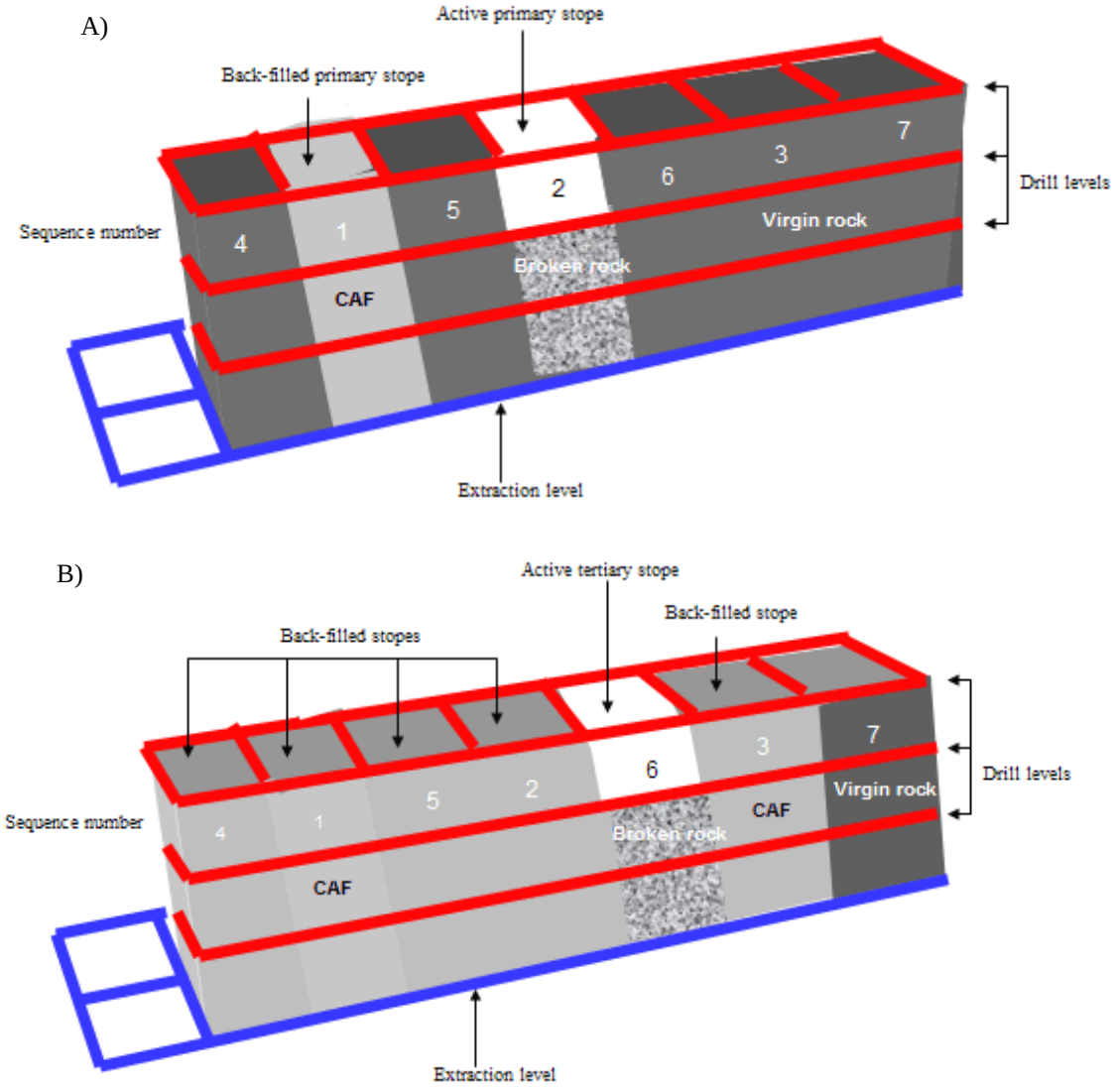

Figure 1.9: Schematic diagram of an ideal stoping sequence, the numbers on each stope indicate the order of extraction while the red lines represent stoping sub-levels (drill levels) and the blue is the production level (extraction level). A) is in early in the sequence. B) Near the end of the sequence.

The benefits of this mining method include, low running costs, the ability to apply highly mechanised equipment, non-entry production, mobile drilling and loading equipment, and high production rates with a minimum level of personnel. Conversely

the downsides of the method include a significant amount of pre-production development requiring a high inherent capital, stopes design requiring regular boundaries for ideal extraction, dilution may occur consisting of waste or mine-fill material, and the risk of insufficient breakage leading to ore production losses (Villaescusa 2004).

Part of the SLOS mining method requires the backfilling of stopes following extraction. At Olympic Dam this is done with cemented aggregate fill (CAF) and waste rock individually, or a combination of both. There are two onsite batch plants which apply specific recipes to define mixes of strengths varying from 0.5MPa to 4.5MPa.

The ingredients involved in batching CAF include:

- Aggregate which is mined from the onsite quarry
- Cement and flyash imported onto site
- De-slimed tailings from the hydromet plant or dune sand (mined locally)
- Water from an onsite dam.

1.5 Thesis methodology

At present there is no process at Olympic Dam, quantifying the performance of a stope in comparison to its designed parameters, unless there was an issue with the stope during production e.g. major over break, under break or freezing. In order to quantify stope performance it needs to be clear what is expected of a stope for it to be considered a success. As this thesis is focused on the Mathews stability method, it is only concerned with the dimension of the final stope surfaces in comparison with the design surfacee. This definition of instability is further discussed in Chapter Three.

To gauge the extent of inconsistency between the Mathews method predictions and stope performance at Olympic Dam, all stopes completed prior to February 2009 that met the data availability requirements had their performance reviewed. The performance was quantified by the application of equivalent linear over break/slough

(ELOS) and classed as stable, unstable or failed. From the stability value a comparison between design stability and actual was undertaken followed by an investigation into some controls of stability specific to Olympic Dam.

There were 124 stopes included in the study; data for these stopes was collected from the mine technical services department at Olympic Dam, using Datamine three dimensional (3D) software, stope dimensions and final cavity survey data, combined with the ELOS quantitative method to measure the performance of each surface of each of stopes. The results of the back analysis lead to the classification of each surface of the 124 stopes as stable, unstable or failed.

Part two of the study was focused on the generation of a possible new preliminary stope design tool for Olympic Dam. The proposed solution applied the understanding of stability indicators with an existing numerical model to forecast stope stability. The method uses well defined criteria for instability and allows a series of points on each stope surface to be considered as opposed to an overall stability classification for the stope surface.

1.6 Thesis format

The outline of the thesis is as follows:

- Chapter Two summarises the geotechnical characteristics of the Olympic Dam ore body and earlier studies, followed by a literature review of the Mathews stability method.
- Chapter Three defines stope surface stability for the purpose of this study, and the details of the methodology and results of investigating the Mathews applicability at Olympic Dam.
- Chapter Four discussed the results of the investigation, other alternative stope surface design methods and possible improvements for the application of the Mathews stability method at Olympic Dam.
- Chapter Five discusses the mechanics of stability in regard to stability indicators and introduces the application of modeled velocity as a stability indicator to forecast stope surface stability at both Olympic Dam and other mines.

- Chapter Six summarises and concludes the thesis, including a section of recommendations and subsequent work necessary to achieve an ideal outcome at Olympic Dam.

Chapter 2. Mathews stability method at Olympic Dam

2.1 Introduction

Historically rock mass classification systems have been used to assist engineers during feasibility and preliminary design stages of a project. As a whole they have been evolving for over 100 years to achieve the most accurate result possible. Several of the systems are based on civil engineering case studies and are continually being adapted to incorporate underground mining case studies. As different systems use differing combinations and have varying motives, it is important that the appropriate system be applied for the project or problem at hand. Some of the common classification systems, including the Mathews stability method, are briefly discussed below.

2.1.1 Mathews Stability Method

The Mathews stability method has been applied for stope stability forecasting at Olympic Dam throughout the mine's operational history. As stated in Chapter One the Mathews stability method is an empirical measurement to forecast an open stopes stability and is found by measuring a surface's material competency (N) and hydraulic radius (HR).

As described by Barton et al (1974), the stability number N' is determined by adjusting the rock tunnelling quality index (Q) value to allow for induced stresses, discontinuity orientation and the orientation of the excavation surface (Equation 2.1):

$$N' = Q' \times A \times B \times C \qquad \text{Equation 2.1}$$

where Q' is the modified Q-Value, A is the stress factor, B is the joint orientation factor and C is the surface orientation factor.

The hydraulic radius (HR) is the consideration of the surface geometry, and is calculated by dividing the area of a stopes surface by the length of its perimeter (Mawdesley 2004). The N' and HR values form the two axes of a chart which has its

area divided into three categories (stable, transition, caving), showing the predicted performance of a stope surface.

2.1.2 Rock Quality Index

The Tunnelling Quality Index (Q) is of particular relevance in this study as it forms the basis of the Mathews stability number. From a growing underground excavations database Barton et al. (1974) generated the Q index for the determination of rock mass characteristics and tunnel support requirements.

The index considers geological, geometric and design/engineering parameters (Hoek. E. 1997). The resulting values range on a logarithmic scale from 0.001 to 1,000, as defined by (Equation 2.2) (Hoek 2006):

$$Q = RQD/Jn \times Jr/Ja \times Jw/SRF \qquad \text{Equation 2.2}$$

Where
RQD is the Rock Quality Designation
Jn is the joint set number
Jr is the joint roughness number
Ja is the joint alteration number
Jw is the joint water reduction factor
SRF is the stress reduction factor

Once the Q value is calculated it can be used to assess the overall condition of the rock mass and assist in choosing a basic support system. The classification of the individual parameters used to define Q is located in Appendix B.

2.1.3 Other classification systems

A descriptive classification system was first developed by Terzaghi (1946). This is based on a rock load concept whereby loads are transferred from crown to sidewalls, and it was initially developed for steel set supports in tunnels. It recognises seven classes of rock (intact, stratified, moderately jointed, blocky and seamy, crushed, squeezing and swelling) and briefly describes the appearance of each.

In 1967, Deere et al (1967) developed the rock quality designation (RQD) to quantitatively estimate rock mass quality from drill cores. This defined RQD as the percentage of intact pieces of core that are longer than 100mm in the total length of the core (Deere 1967). RQD has since been integrated in other classification systems and is applied as part of rock mass classification at Olymic Dam.

One classification utilising RQD in its calculation is the Geomechanics Classification, or more commonly known as the rock mass rating (RMR) system. Initially created in 1973, the system is based on the strength of the material, RQD, spacing condition and orientation of discontinuities, and groundwater conditions. A value is allocated to each of these parameters and the final result is the sum of the values. The original system was not well regarded by the mining industry, resulting in several modifications, as summarised by Bieniawski (1989). The mining version of the Geomechanics classification, mining rock mass rating (MRMR) system is commonly applied to underground caving operations.

Other well-known classification systems include the Rock Structure Rating (RSR) and Lauffer's stand-up time concept (Hoek 2006).

2.2 Geotechnical Data Collection

2.2.1 Rock mass data collection

The Olympic Dam ore body rock mass characteristics have been determined through a combination of underground data collection, laboratory examination and computer analysis. The primary underground data collection method is window mapping.

Window mapping is conducted underground by members of the Geotechnical Department and SRK consultants (SRK) who were employed to generate a database of the rock mass conditions at Olympic Dam. The windows are undertaken on stretches of rock around 20 to 30m long. A window is generally located close to an upcoming stope, providing data for the stope note analysis.

The mapping utilises a template log sheet (Figure 2.1) to observe and record the structures within the rock mass. The data collected as part of this process includes:

- Prominent rock types
- Extent of alteration
- Presence of any weathering
- Groundwater conditions
- Blockiness values
- Estimates of intact material strength
- Any blasting effects
- Potential mode of failure
- Installed ground support
- Rock mass discontinuity data
- Any other relevant or interesting comments

As is often found in data collection, there is an element if subjectivity in the classification of the rock mass. The data which is recorded is dependent on the experience and opinnion of the engineer. However the template log provides a process in order to minimise the degree of subjectivity.

SRK has developed a blockiness index to describe in general terms the rock mass conditions. This index has been developed from approximately 300 completed windows and gives areas of rock a numeric classification between 1a and 8a (Figure 2.2).

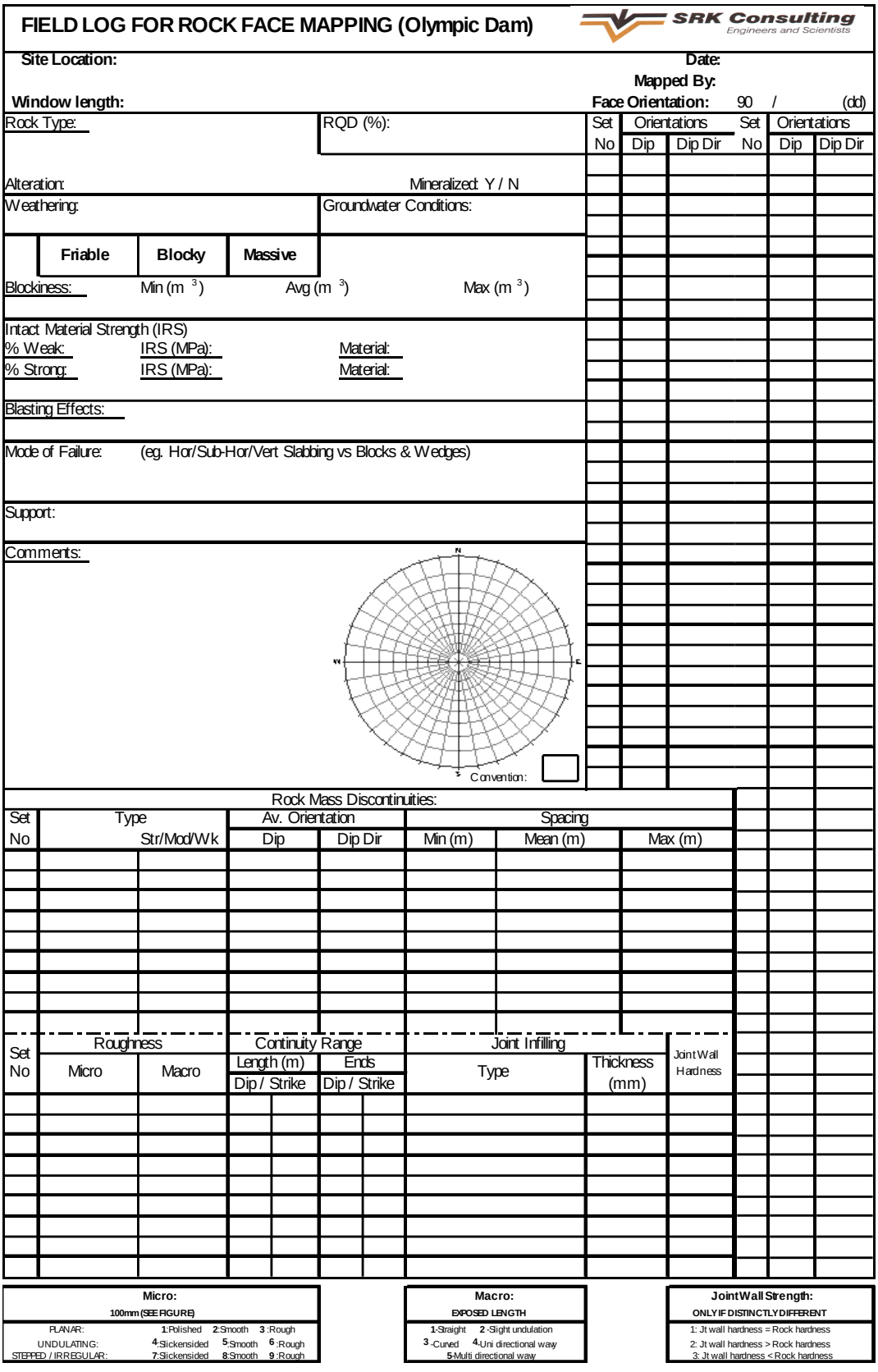

Figure 2.1: Window mapping template used for data rock mass characterisation collection at Olympic Dam

Blockiness Index	Rock Mass Description	Rock Mass Fabric Description: Effective Block Forming Joint Sets	Rock Mass Fabric Description: Joint Continuity	Rock Mass Fabric Description: Joint Spacing	Oversize: Potential for Rock Mass Failure	Oversize: Relative Block Size (average primary fragmentation dimension)	RQD (%)	Figure
1	Massive	Nil, only random	<2m	>5m	Along primary structures and through intact rock	Extremely Large (>20m)	100	
2	Massive	1+random	2-4m	3-5m	Along primary structures, jointing and through intact rock	Very Large (8-15m)	100	
3	Massive to Blocky	2+random	>4m	1-3m	Along joint sets and primary structures and through intact rock	Large (2-8m)	90-100	
4	Blocky to Slabby	Dominated by primaries ..... Rock mass fabric not well defined, or ..... locally in between primaries			Along primary structures and along joint sets	Very Large to Large (2-12m)	80-100	
5	Blocky to Massive	3+random	>4m	1-3m	Along joint sets and along primary structures	Large to Medium (1-5m)	80-100	
6	Blocky	3-5	2-4m	<1m	Along joint sets, may occur in structural corridors	Medium (0.5-1m)	60-90	
7	Blocky	3-6	<2m	<0.5m	Along joint sets	Small (<0.5m)	50-85	
8	Friable	Friable due to low strength, alteration, deterioration, intense fracturing, typically associated with dykes and weak fault planes			Defined by dyke or fault plane	Very Small (<0.10m)	<50	

Figure 2.2: The Geotechnical Blockiness Index (GBI) defined for Olympic Dam (SRK 2000)

2.2.2 Stress measurements

Stress measurements have been conducted at Olympic Dam since the commencement of mining, with the most recent measurements being those undertaken by Australian mining consultants (AMC) in 2007. The database consists of 17 measurements that were collected using a CSIRO Hollow Inclusion (HI) Cell (Figure 2.3). 16 of the measurements were taken in the granite and one in the overlying sediments (Figure 2.4). The HI Cell consists of an array of strain gauges encapsulated in the wall of a hollow pipe with a known elastic modulus. The cell is epoxy grouted into a borehole and monitored for strain response during over-coring.

The AMC report, "In situ stress field for Olympic Dam mine" (Bridges 2007) stated there is no evidence of any sectors within the mine where directions of principal stress are significantly different from the estimated mean orientations by either northing or by depth. This allows the 17 measurements to provide the generic stress measurements for the mine. The present study only discusses the 16 readings from within the granite because there is no current mining undertaken in the sedimentary rock.

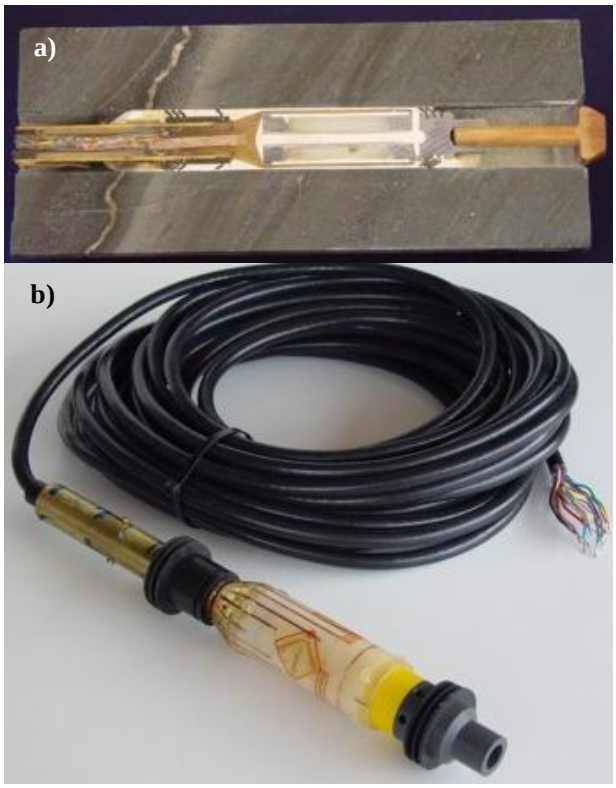

Figure 2.3: Photograph of HI Cell equipment used to obtain in situ stress measurements at Olympic Dam, a) the equipment set in resin inside the drill hole, b)

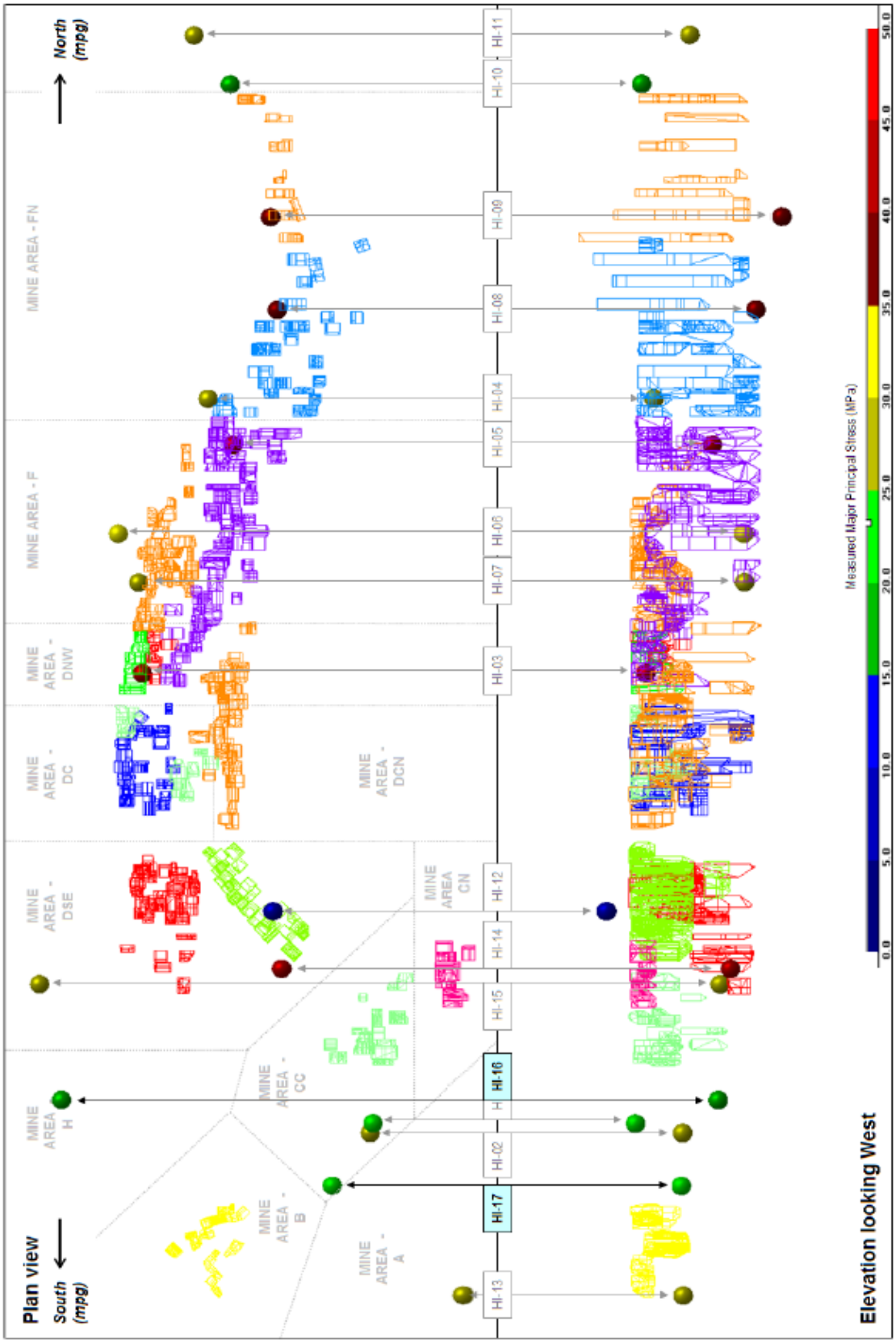

Figure 2.4: Location of in situ stress measurements using CSIRO HI cells at the Olympic Dam Mine, (Bridges 2007).

2.3 In situ stress fields – Granite

2.3.1 Principal in-situ stress field

Directions of intermediate and minor principal stresses spread around a great circle normal towards the mean direction of the cluster of major principal stresses. Using the small clusters and the results from vector summations, allowing for orthogonality, AMC estimated mean directions for principal stresses for granite. For the granite breccia complex the estimated in situ stresses are detailed in Table 2.1.

In table 2.1 the in-situ stress directions are represented as a bearing and plunge, as referenced to the mine-planning grid. The mine grid north is 57.5 degrees west of AMG north. AMG north is 1 degree west of true north. Plunges are positive downwards (right handed system).

Table 2.1: Principal in-situ stresses in the granite at Olympic Dam

Major principal stress	133/02
Intermediate principal stress	224/18
Minor principal stress	037/72

At Olympic Dam, the granite-breccia lies at a minimum depth of 330m below the ground surface. AMC estimated the depth-stress relationship at each of the mean directions of principal stresses, as shown in Table 2.2 (Figure 2.5).

Table 2.2: Estimated depth-stress relationship at each of the mean principal stresses

Major principal stress	6+0.041*D MPa
Intermediate principal stress	2+0.036*D MPa
Minor principal stress	0+0.033*D MPa

Where D is the depth in metres below the ground surface, and respective directions of the major, intermediate and minor principal stresses are the mean directions above (Table 2.1).

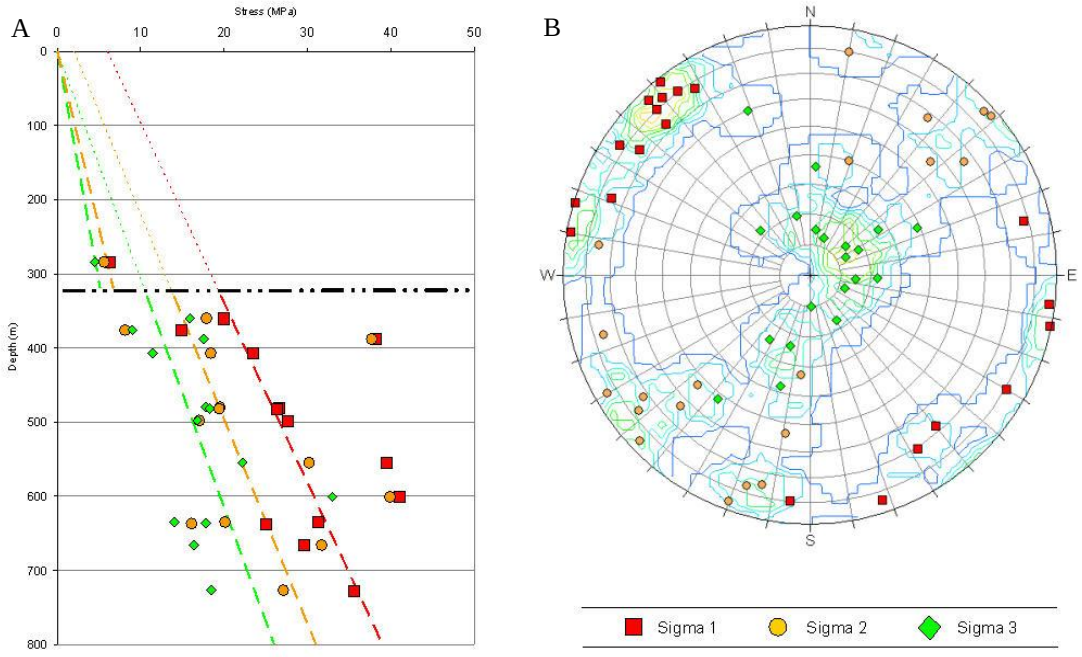

Figure 2.5: A: Magnitude of principal stress versus depth. B: Estimated principal stress orientations (Bridges 2007)

2.3.2 Effect of Mining Induced Stress in Excavation stability

A stope blasting has the potential to increase the stope dimensions and subsequently reduce the rock pillar to a neighbouring stope. Stress concentration through the remaining rock is then vulnerable to elevation. This can potentially result in drill drive deterioration, stope over break and fall-off, longhole squeezing and an increased likelihood of requiring re-drilling.

After the 2007 stress measurements were collected and analysed it was noted on a mine-wide scale that there is a clear inter-relationship between stress and geologic structures in the natural state of the rock prior to disturbance by mining. As mining occurs, the interaction between stress and geologic structures redistributes those stresses sometimes with serious adverse outcomes to stoping activity. The rock mass around these structures will potentially become unstable.

At Olympic Dam, mining induced stress change is modelled with Map3D (Figure 2.6) via stope note and pre-production reporting. However there is no instrumentation in place to physically measure this stress change.Although not directly measured, engineers often look at deformation or damage around voids and interpret them as being caused by mining induced stress changes. They then use the location of the damage to make an “educated guess” as to how the stress field is changing. Although not ideal, this method appears valid on a broad scale.

It is difficult for Olympic Dam to verify the success of educated guesses. This is as there is no investigation of the stress and mining induced changes except for where problems are encountered during the stoping process. Such problems include over break in a stope wall, or damage in a drive near a stope stress analysis. When these occur stress analysis is undertaken as part of the investigation into the stope performance.

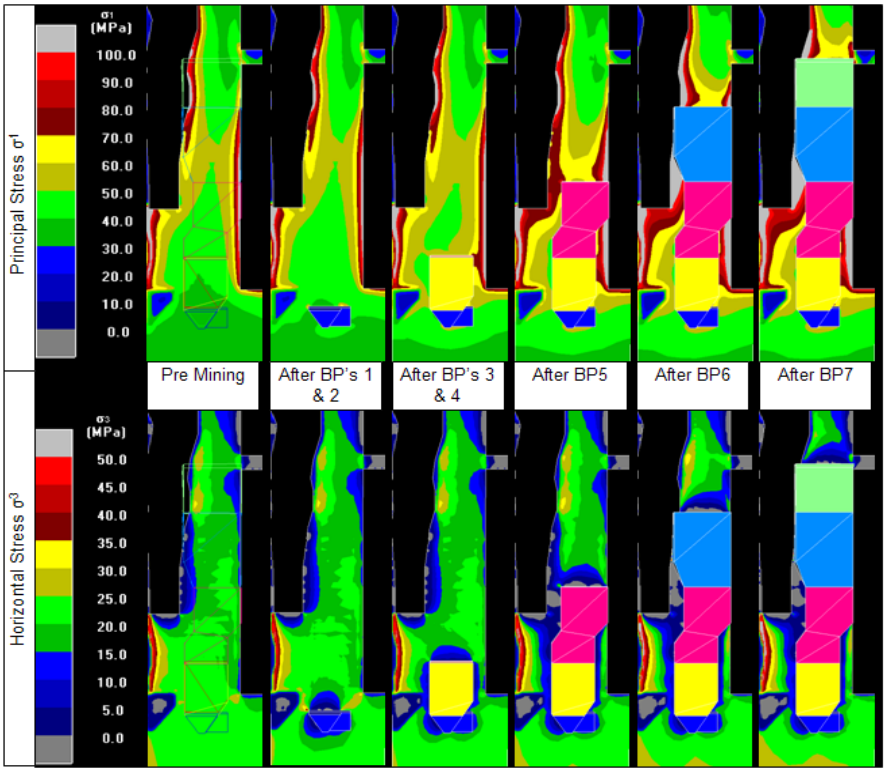

Figure 2.6: Screen shot example of stress modeling undertaken at Olympic Dam prior to the production of stopes displaying expected principal and horizontal stress before and after the firing of each blast packet.

2.4 Intact rock strength at Olympic Dam

During the feasibility stages of the Olympic Dam operations it was determined through a series of laboratory and in situ strength examinations, that the majority of the granite breccia rock types have an average UCS_{50} of around 150MPa with a standard deviation of 75MPa. The large standard deviation suggests a high percentage of the samples tested must have failed by shearing on microstructures or weaknesses that pervade the Olympic Dam intact rock. It can be inferred that similar behaviour will occur around openings throughout the mine, particularly in the small Granite-volcaniclastic (GRNV) deposit portion. Rock strength properties for all Olympic Dam lithologies are located in Appendix D.

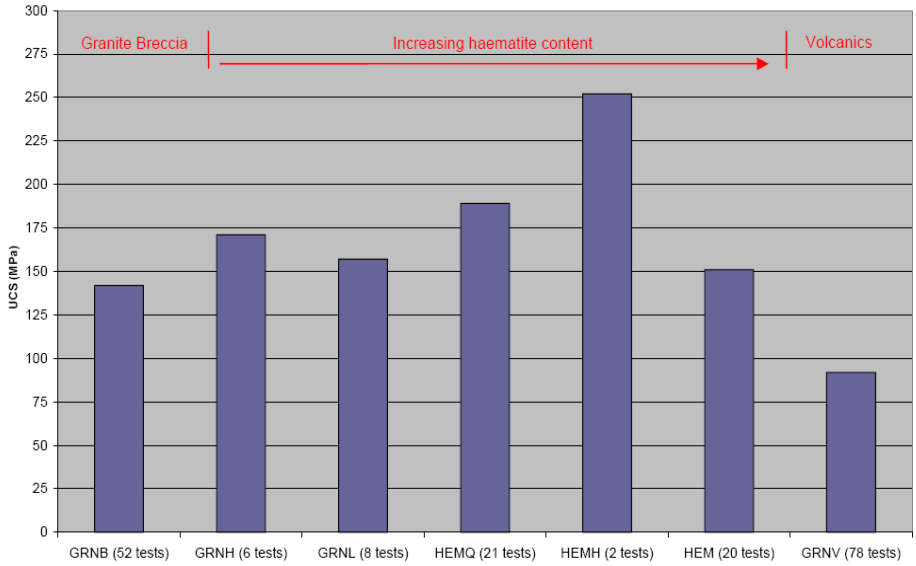

Figure 2.7: Intact rock properties for differing rock types at Olympic Dam. The number of uniaxial compression tests undertaken to achieve the result is noted on the x axis.

2.5 Rock mass Quality Classification

Rock mass quality has been determined using the geotechnical underground window mapping information, assisted by underground observations, with the rock tunnelling quality index (Q index) applied to allocate a value to the rock mass. From the window mapping and blockiness index analysis, Olympic Dam was found to have a range of characteristics.

As described earlier the Q index is based on block size and the joint and stress conditions of the rock. The Q factor values for Olympic Dam are summarized in Table 2.3.

Table 2.3: Rock mass quality Properties for Olympic Dam (BHPBilliton 2010)

	RQD	Jn	Jr	Ja	Jw	SRF	Q'	Q	Description
Best	100	3	3	1	1	2	100	200	Extremely Good
Predominant	100	6	1.5	1	1	2.5	25	10	Good
Expected Worst	75	12	1	2	1	2.5	3.13	1.25	Poor
Worst	55	12	1	4	1	2.5	1.15	0.46	Very Poor

The Q-system parameters are discussed below in regard to Olympic Dam specific values.

2.5.1 Major Structures

Major structures are defined as any discontinuity that has displaced the surrounding rock mass, or that has infill that is significantly weaker than the surrounding rock mass. Major structures are sparse at Olympic Dam. All structures that extend greater than 50m are regarded as regional structures while all others are local. On the local scale structures are mapped as faults, joints and veins.

Data used for joint set depiction and analysis is a combination of geotechnical window mapping data and geological mapping conducted by Olympic Dam mine geologists. Five major joint sets have been recognised and acknowledged as the primary sets at Olympic Dam. The orientations of these five prominent joint sets are summarized in Table 2.4. (Figure 2.8).

Table 2.4: Orientations of the five prominent joint sets

	Geologist Mapping	SRK Mapping
JS1 steep dip - NW/SE strike	90/033 (80-90)/(20-50)	90/045 (80-90)/(30-70)
JS2 steep dip – NNE/SSW strike	88/293 (80-90/270-310)	89/287 (80-90)/(270-310)
JS3 moderate west dip – N/S strike	39/293 (25-50)/(270-310)	38/278 (25-45)/(260-300)
JS4 moderate east dip – N/S strike	32/118 (20-40)/(90/130)	30/082 (20-40)/(60-100)
J5 Flat Dip	-	00/099 (0-20)/(0-360)

Note: Orientations are with respect to Mine Planning Grid North

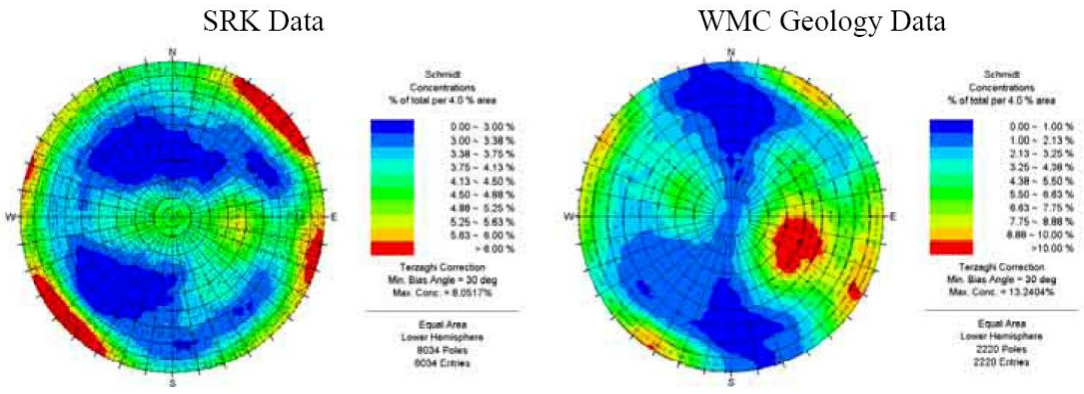

Figure 2.8: Stereographic plots of joint set data (Oddie 2004)

2.5.2 Block size

Block size at Olympic Dam is calculated using the volumetric joint count (Jv) method. This represents the number of joints per unit length for all joint sets and is detailed in Appendix E. A slight variation in RQD values exists across the mine, with the Northern mine end having a wider spread of values than the southern end (Figure 2.9). This variance is not significant enough to suggest that individual RQD values should be used for each section of the mine in analysis.

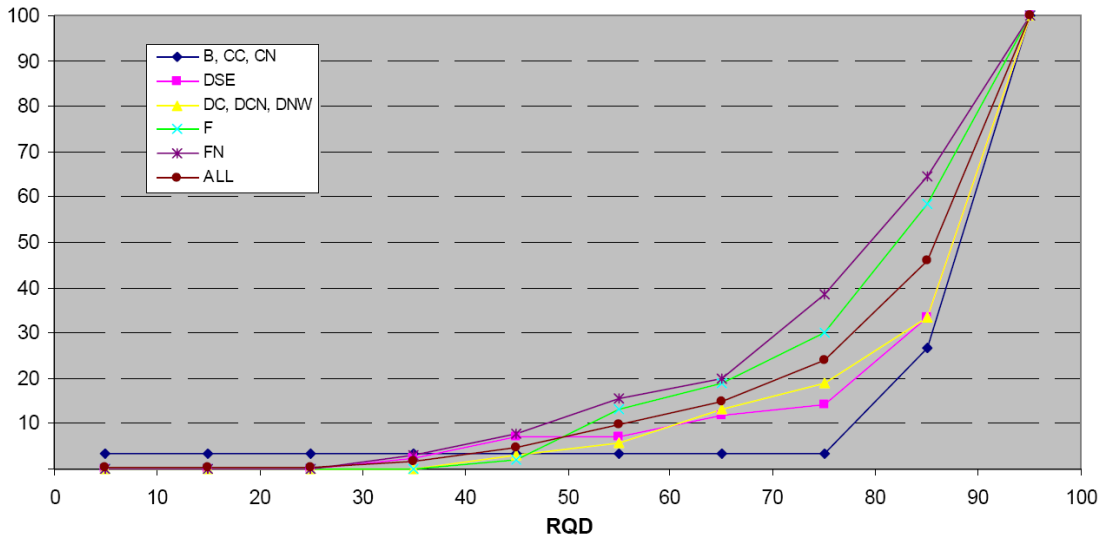

Figure 2.9: Plotted RQD values for mine areas represented in the key by the different letter combinations.

The joint set number (Jn) is a measurement of joint orientation in a rockmass that is judged to influence the stability of an opening. In order to provide a rating system for the rock quality throughout the mine a summary of the different qualities is summarised in Table 2.5.

Table 2.5: Summary block size for Olympic Dam mine (Oddie 2004)

	RQD	Jn	Description
Best	100	3	Excellent RQD, One joint set + random
Predominant	100	6	Excellent RQD, Two joint sets + random
Expected Worst	75	12	Good RQD, Three joint sets + random
Worst	55	12	Fair RQD, Three joint sets + random

2.5.3 Joint surface condition

Joint roughness (Jr) and Joint alteration (Ja) are the two controlling parameters that describe the shape and integrity of the joint surface. They are used to quantify the joint surfaces resistance to shearing.

The joint shapes at Olympic Dam are predominantly “rough planar” but range from “rough undulating” to “smooth planar”. The surfaces are generally unaltered, although with some “surface staining” of sericite, chlorite or salt build up. Occasionally they have a thin coating of less than 5mm of non-softening infill material. A summary of the joint characteristics of each of the five major joint sets is further detailed in Appendix E.

The roughness and level of alteration have been quantified. This showed all joint sets have similar properties with the only difference being in the joint alteration. Joint roughness values average between 1 and 1.5 while the worst joint alterations were around 3 and 4 (Table 2.6).

Table 2.6: Summary joint surface conditions for Olympic Dam rock mass (Oddie 2004)

		Value	Description
Joint Roughness	Best	3	rough or irregular, undulating
	Predominant	1.5	rough or irregular, planar
	Expected Worst	1	smooth, planar
	Worst	1	smooth, planar
Joint Alteration	Best	1	unaltered joint walls
	Predominant	1	unaltered joint walls
	Expected Worst	2	slightly altered joint walls
	Worst	4	softening or low friction clay mineral coating

2.6 Design process

A rigorous design process is critical for safe and successful sub level open stope (SLOS) mining, with input required from Geological, Geotechnical, Survey and Engineering departments. The stope design process at Olympic Dam involves numerous reviews and assessments in order to ensure adequate stability coupled with maximum production.

There are various stages in the design process involving geotechnical input. Initially a front review is conducted. This evaluates the effectiveness of the sequence in order to produce a workable plan for a mine area. This is followed by the preliminary stope design where the conceptual design of the stope is revised. At this stage it is critical to correctly size and shape the stope based on the areas mining sequence.

The next stage involves the most significant amount of quantitative analysis of the rock mass. This analysis is done both in and adjacent to the stope with results driving the stope design. At this stage the Stability Graph Method is used to assess the stability of the stope spans all the data is entered into an Excael spreadsheet which returns a Mathews plot for the crown and one for the walls (Figure 2.10).

The stability graph method works by applying all of the above collected geotechnical properties. Prior to the commencement of production drilling a pre-ring preview and pre-production assessment are undertaken. These review any recent ground control issues and identify any geological structures that have potential to influence interim or final stability. At this stage a stress model is run, analysing the potential influence of structures on each of the blast packets. This influence is investigated by visual analysis.Any changes to stope design identified through the above analysis are processed at this point. The stope assessment is then closed out, allowing production to commence.

All of the above stages and the associated information are compiled into a document called a “stope note”. A stope note details the entire process and includes the preliminary study. Other aspects include the geological background, geotechnical parameters, development design, services design, ventilation plan, drilling and blasting, and backfilling notes.

a)

Mathew's Stability Number $N' = Q' \times A \times B \times C$

Parameter	Crown		East Wall		West Wall	
RQD =	75	GBI, Window mapping and drillholes	75	GBI and Window mapping	75	GBI, Window mapping and drillholes
Jn =	12	Three joint sets + random	9	Three joint sets	9	Three joint sets
Jr =	2	Smooth and undulating joint surface	2	Smooth and undulating joint surface	2	Smooth and undulating joint surface
Ja =	2	Slightly altered joint walls	2	Slightly altered joint walls	2	Slightly altered joint walls
$Q' = \frac{RQD}{J_n} \times \frac{J_r}{J_a}$	6.3		8.3		8.3	
Rock Stress Factor A =	0.3	Conc. Factor 1.55; UCS_{50} 140; σ_{max} 40	1.0	Conc. Factor 0.45; UCS_{50} 135; σ_{max} 12	1.0	Conc. Factor 0.40; UCS_{50} 120; σ_{max} 10
Joint Orientation Factor B =	0.3	Flat dipping structures in crown	0.3	Vertical structures in wall	0.3	Vertical structures in wall
Gravity Adjustment Factor C =	2	Flat crown, Fall	8	Slabbing	8	Slabbing
Mathew's Stability Number N' = Q'xAxBxC =	1.3		16.7		16.7	
	Stable Crown		Stable East Wall		Stable West Wall	
HR for Stability	7		6.5		6.5	
	Design Crown		Design East Wall		Design West Wall	
Design HR	6.1		10.9		10.9	

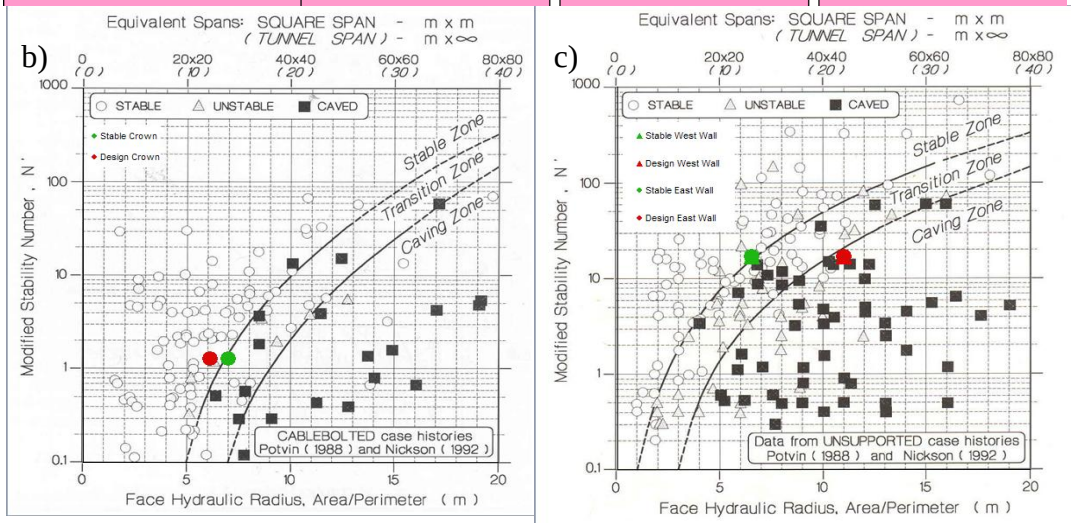

Figure 2.10: Screen shot of a) the input table for the Mathews stability charts in Excel. b) Mathews chart used at Olympic Dam for crowns and c) Mathews chart used for stope walls at Olympic Dam.

2.7 Mathews stability method

2.7.1 Background of the Mathews stability method

Historically empirical civil engineering tools have been applied to open stopes, often resulting in a conservative design. This design is predominantly due to stopes being non-entry areas that allow for a limited amount of fall off . Over time it became clear that no single index is an adequate indicator of the complex behaviour of a rock mass surrounding an underground excavation (Hoek 1990).

Initially designed in 1980, the Mathews method answered the requirement for a more lenient tool for large excavations. It soon became a popular choice, particularly in metaleferous mines, as a preliminary guide to stope dimensioning. The Mathews stability method is an empirical design tool with the original version being based on a restricted data collection from case studies based primarily in North America. It has been revised numerous times since its creation, resulting in the addition of further data now making up the graph. The principal concept of the method is that the size of an excavation surface can be related to the rock mass competence. This gives an indication of stability or instability of a rock mass(Stewart 2001).

The Mathews method provides users with an indication of the likely performance of underground excavations by plotting them on a chart. It is based on a stability graph which relates two calculated factors; the Mathews stability number (N') and the hydraulic radius (HR). The Mathews stability number is a function of rockmass quality, stress, structural orientation and the likely mode of failure, while the hydraulic radius accounts for the size and shape of the surface. For a typical rectangular excavation there will be five surfaces, four sidewalls and the crown/back. The stability graph deals with each of these individually, allowing the five surfaces to fall within different predicted stability zones.

The differing zones on the graph were initially devised by Mathews from 50 case histories compiled from North American mining data (Figure 2.11). The stability of a

planned excavation was then represented by where it was plotted on the graph. The original three zones were stable, potentially unstable and potential caving. Each zone was divided by transitional zones, reflecting the transition and uncertainties of the boundaries.

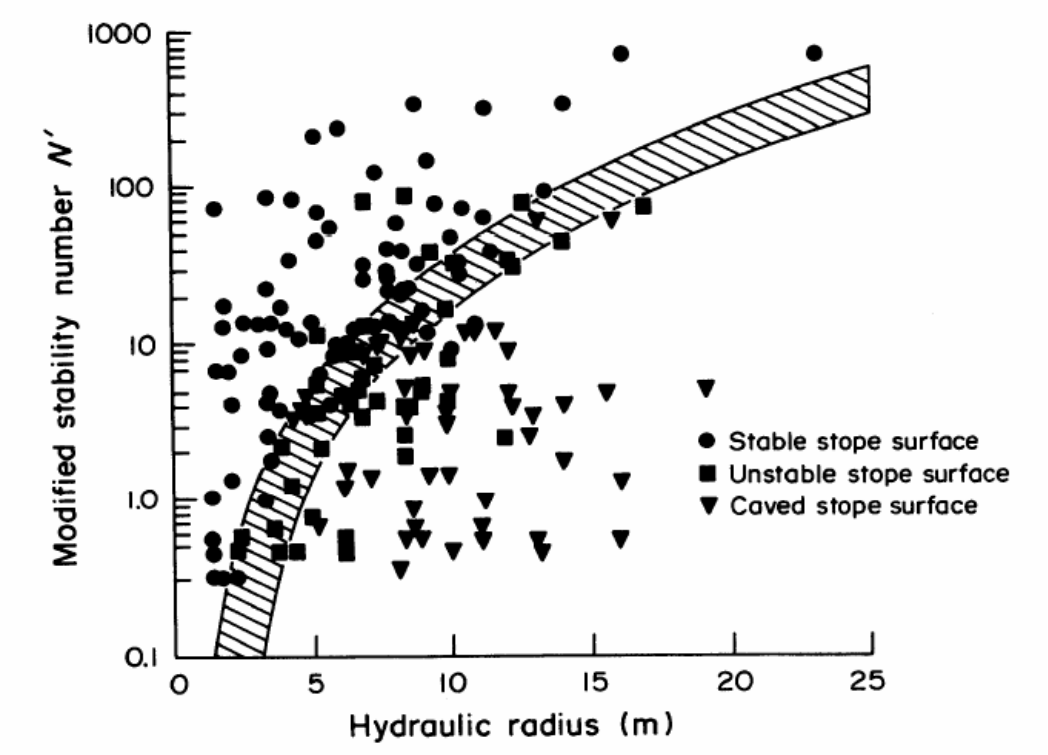

Figure 2.11: The stability graph method plot, the hatched section through the centre of the chart represents the transition zone between the stable zone (above the transition) and the caving zone (below the transition). The points plotted on the chart are mined stopes from the North American case histories, their actual performacne is represented by the shap of the point as depicted in the key (Potvin 1988b).

2.7.2 Modified stability number N'

The stability graph uses the modified stability number, N', as described by Potvin (1988b,1992), Bawden (1993) and Hutchinson (1996) to classify the rock mass.The Modified stability number is a modified version of the rock tunnelling quality index value (Q), as discussed earlier. The Mathews stability number is generated by adjusting the Q' value to allow for induced stresses, discontinuity orientation, and the orientation of the excavation surface.

The stability number (N') is defined by Equation 2.1:

$$N' = Q' \times A \times B \times C \qquad \text{(Equation 2.1)}$$

where;

- *Q'* is the modified Q-value,
- *A* is the rock stress factor,
- *B* is the joint orientation adjustment factor,
- *C* is the gravity adjustment factor.

(Hutchinson 1996)

The rock stress factor, A, is a measure of the ratio of intact rock strength to the surrounding stress. As the maximum compressive stress acting parallel to a free stope face approaches the uniaxial strength of the rock, factor *A* reflects the related instability due to rock yield.

Factor *B* measures the relative orientation of the primary joint set in relation to the excavation surface. Those forming an oblique angle with the free face are most likely to become unstable. Conversely joints that are perpendicular to the free face are taken to have the least influence on stability.

The gravity adjustment factor *C*, represents the potential influence of gravity on the stability of the face. Crowns (backs) or unfavourably oriented structural weaknesses have the maximum influence on potential instability (Hutchinson 1996) (Figure 2.12).

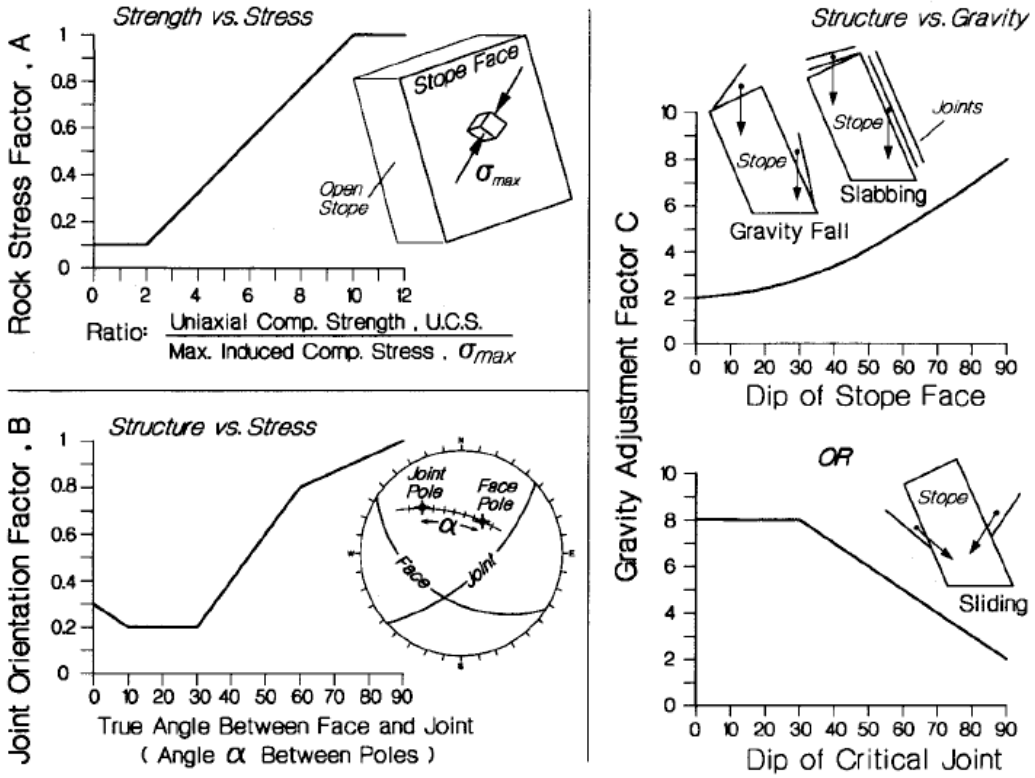

Figure 2.12: Input parameters for the Mathews stability number (Diederichs & Kaiser 1999)

2.7.3 Hydraulic radius

The hydraulic radius (HR) measures the combined influence of the size and shape of the face on excavation stability. The *HR* is calculated by dividing the area of the stope face by the perimeter of that face, shown by Equation 2.3;

$$HR = \frac{\text{Area (m}^2\text{)}}{\text{Perimeter (m)}} = \frac{w \times h}{2(w + h)} \qquad \text{(Equation 2.3)}$$

where

w is the width of the surface

h is the height of the surface (Figure 2.13)

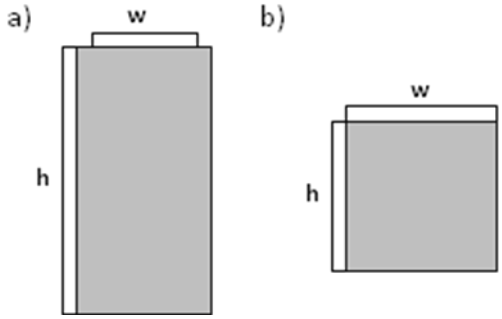

Figure 2.13: Simplified two-dimensional diagram showing the width and height inputs for a) stope walls and b) stope crowns

This calculation differs from those used in other classification systems particularly those of tunnels as it is calibrated for open stopes with finite dimensions and lower priority for safety. It should be remembered that the shape factor of the hydraulic radius is not dimensionless but is expressed in metres (Stewart & Forsyth 1995).

2.8 Evolution of the stability graph

The origins of rock mass classifications lie primarily in civil engineering, and in particular tunnel engineering. It has become evident to many in the industry that a mining specific excavation design tool was needed to replace the tools designed primarily for civil and tunnel engineering. A mining-specific tool was seen as being able to minimise cost and maximise production in underground mines.

In 1980, Mathews, Hoek and Wyllie devised the original stability zones and graph. This empirical solution was published as part of a CANMET report on stope stability in deep Canadian mines. During the initial stages of the method's application in underground excavation projects, it became apparent that there was limited field data supporting the method. This was a result of its design being based on only 50 case histories.

The period since 1980 has allowed the tool to be tested for varying depths and rock mass conditions by numerous authors .This has significantly extended the validity of the tool. Such tests include those by Potvin (1988b), Stewart & Forsyth (1995), Trueman et al.(2000) and Mawdesley (2001). As the method became more widely

applied the database was expanded allowing adjustments to be made to the overall layout of the zones, thereby reducing an element of the method's subjectivity.

The stability graph is defined by zones originally determined by visually fitting boundaries between clusters of data representing stable and unstable stope surfaces, and between the unstable and caved stope surfaces. The mined stope surfaces are defined as stable or unstable after they have been emptied by examining final cavity monitoring survey data with repsect to the designed stope shape. The zone enclosed by the boundaries contains a mixture of stable, unstable and caved stopes. This is labelled the transition zone (Suorineni et al. 2001a).

Subsequent studies have resulted in considerable change to the placement of the original boundaries. These changes are due to the accumulation of additional data, through the re-definition of the stability number, by calibrating boundaries to mine site specific data, the mixing of data from differing versions of the stability number and through human bias.

Potvin (1988b) expanded the original database from 50 to 175 case histories. The enlarged database resulted in the re-calibration of factors *A*, *B* and *C*. Accompanying this was a redefinition of the boundaries between stability states.

Literature subsequent to these changes, such as that by Stewart & Forsyth (1995) and Trueman et al.(2000) noted that the modifications to the calculation of the stability number resulted in no appreciable difference in the methods predictive capability. Consequently the advances were not universally adopted. Note that there is a distinction between those databases based on Potvin's definition of the stability number and those based on the original Mathews factors. This is as the different definitions varying transition boundaries between stability states.

Amongst other changes made by Potvin, the number of zones plotted on the graph was reduced. Potvin's changes left the graph with simply a stable and a caved zone,

with a transition zone separating the two zones. Nickson (1992) later extended this transition zone to incorporate a larger area of the plot.

The choice of the term ‘caved’ has been subjected to much criticism Stewart & Forsyth (1995) noted that the term has a definite meaning in the mining sense that is not consistent with what it represents in Potvin’s modified graph. They also noted that the graph implies too great a level of accuracy as it only uses two zones. Stewart and Forsyth (1995) suggested that new zones be allocated to the graph. These zones were potentially stable, potentially unstable, potential major collapse and potential caving.

The zone of potential caving by Stewart and Forsyth was based on Laubscher’s caving stability graph (Laubscher 1990). They had no data themselves to validate this zone, instead relying on Laubscher’s work (Figure 2.14). Recognising this, Stewart and Forsyth recommended that the user build their own experience and define their own site-specific zones on the graph, rather than arranging data to arrange it to fit the provided zones.

Historically simply visually identifying where the zones should lie was the used to define the location of stability zones on the Mathews graph. These zones were modified with the addition of new data. As the position of these zones on the graph is crucial in the reliability of the method, an alternate method was sought to optimise the locations of the zones.

Mathematical calculations were found to be a satisfactory alternative to visually defining the location of the stability zones. Mathematical calculations were used to identify the zones widths and positions. This is further discussed in Chapter Four. It must be noted that the stability graph method remains a non-rigorous method.

The focus of these developments is in defining the stability graph boundaries and recalibrating existing factors. There is no longer any justification in the use of the original method. As has been shown to be the case with Mathews, empirical design methods can evolve and improve over time with the availability of additional data and increased experience with the method.

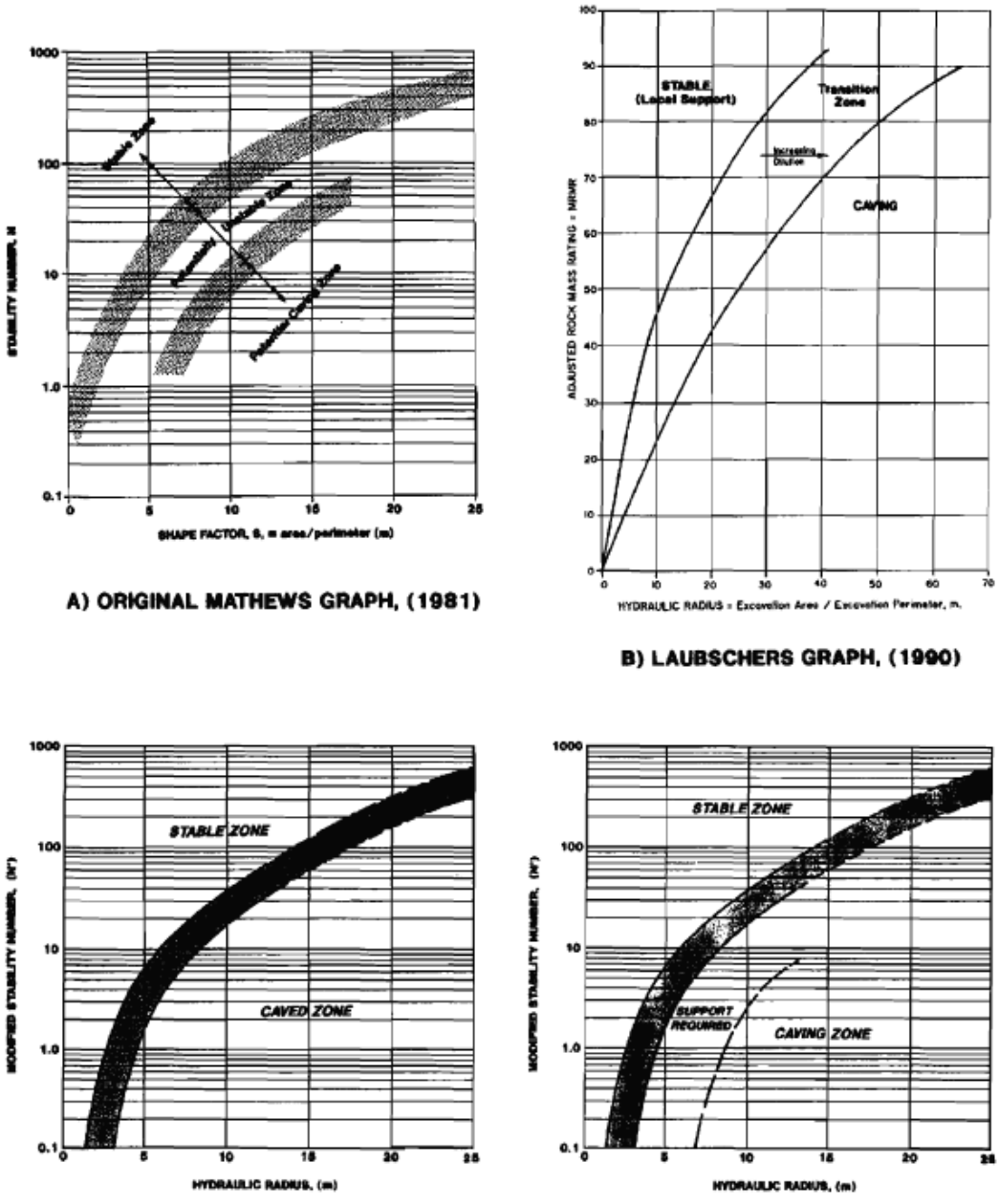

Figure 2.14 Comparison of the different stability graphs (Stewart & Forsyth 1995)

2.9 Application of the Mathews stability method at Olympic Dam

The Mathews stability method has been applied to stope design at Olympic Dam since the mine was first commissioned. The method is used to provide the underlying stability analysis for future stopes and is based on where surfaces plot on the relevant charts. The version applied at Olympic Dam is obtained from "Cablebolting in Underground Mines" (Hutchinson 1996). This particular model differs between un-supported walls, supported crowns and unsupported crowns.

As explained the stope design process at Olympic Dam is compiled into a package called "stope notes". The package includes geological data and interpretation, geotechnical parameters, adjacent development, firing design and sequence along with ventilation and services plans. The modified stability graph is a key part of the geotechnical investigation.

The walls are plotted on the unsupported case histories chart, while the crown is plotted on the supported case histories chart. In the past the crown was plotted on both the unsupported and supported charts to determine whether crown cable bolt support was required. As crown cable support is now mandatory at Olympic Dam the unsupported plot is no longer performed. There is little variation in the parameters applied across the mine area with this technique.

The unsupported chart (Figure 2.15), published in "Cablebolting in Underground Mines", is calibrated from a study of 175 case histories by Potvin (1988a) and another 13 by Nickson (1992). They plotted stopes whose performance was already known as stable, those which exhibited little or no deterioration during their service life, unstable stopes which exhibited limited wall failure and/or block fallout involving less than 30% of the face area, and caved stopes which suffered unacceptable failure. From these plotted case studies they were able to generate the boundaries between the stable, transition and caving zone. The upper boundary of the transition zone is recommended as the "no support" limit for design (Hutchinson 1996).

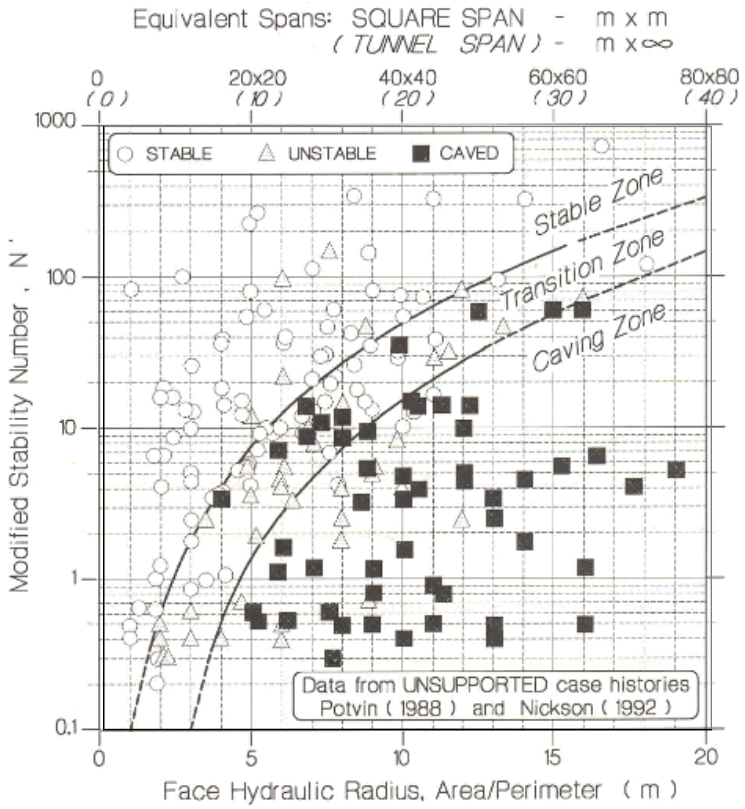

Figure 2.15: Unsupported case histories stability chart used for stope wall stability assessment at Olympic Dam (Hutchinson, 1996).

Potvin (1988a) and Potvin & Milne (1992)also collected 66 case histories of open stopes in which cablebolt support had been used. Nickson (1992) added another 46 case studies to the supported case histories chart (Figure 2.16). Similar to the unsupported wall open stope case history chart, this displays a transition zone with the upper curve represents the limit of reliable cablebolt performance. The lower boundary reflects the reduction in confidence until cables can no longer be assumed to be providing any degree of useful support (Hutchinson 1996).

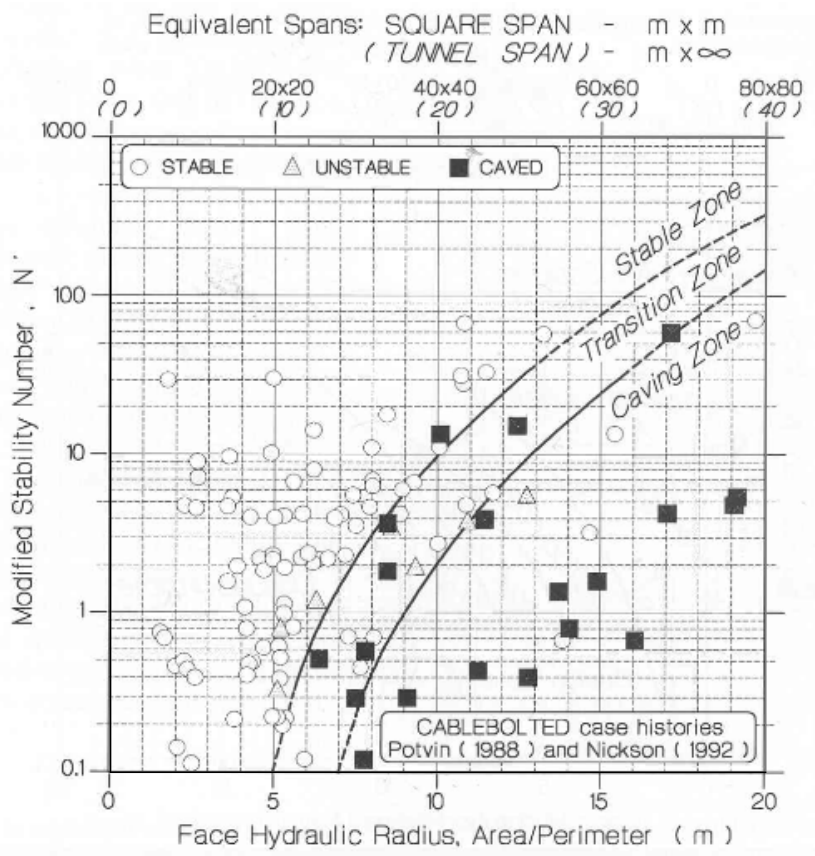

Figure 2.16: Supported case histories stability chart used for stope crown stability assessment at Olympic Dam (Hutchinson, 1996).

Other charts presented in "Cablebolting for Underground Mines" which are used at Olympic Dam assist with the determination of cablebolt reinforcement requirements (Figure 2.17). The chart allows the user to determine, from a calculated value or range of N', the maximum recommended stope size and shape for an unsupported or supported case. With non-entry conditions applying if a stope plots well above the left or uppermost design curve, it is predicted to remain stable without the assistance of support. Conversely a stope which plots far into the right hand section of the graph is likely to undergo serious instability issues. The cablebolt design zone indicates the need and effectiveness of cablebolt application (Hutchinson 1996).

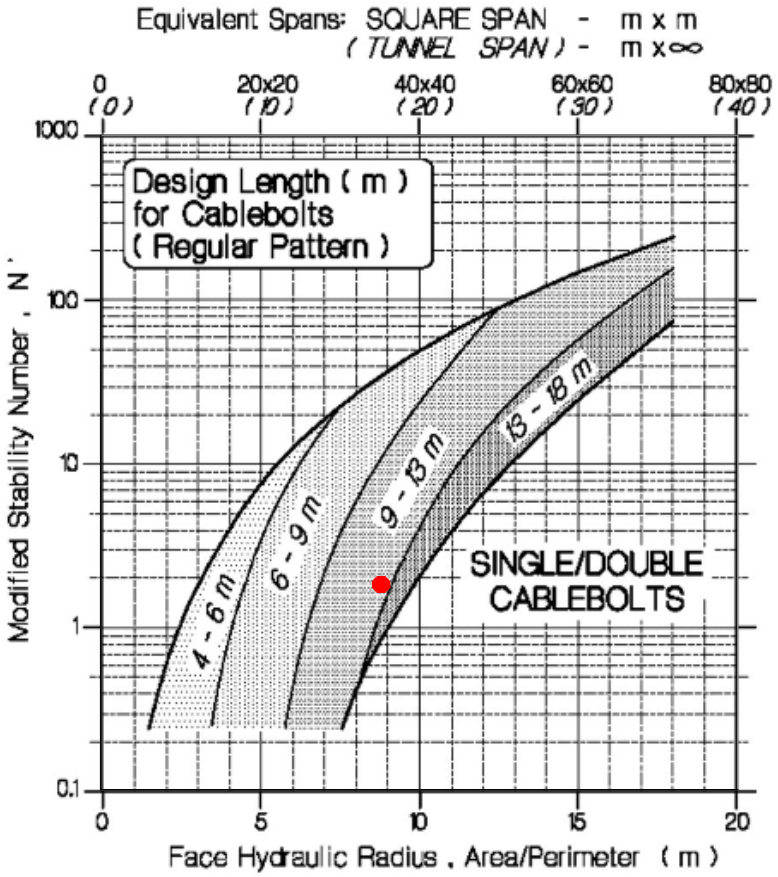

Figure 2.17: Chart used to assist in cablebolt reinforcement requirements at Olympic Dam. The red dot represents an example crown (Hutchinson, 1996).

2.10 Stope stability history at Olympic Dam

Stope history at Olympic Dam has been inconsistent. Over the life of the mine there have been variations in the size of stopes designed, the required stope support and drilling techniques, and also blasting patterns. These changes were in response to reconnaissance studies conducted after problems have been observed with stopes.

A report submitted in 2002 by AMC consultants focused on five stopes within the north (FN) area of the mine. In this area six main controls on stability were identified. These controls were structure, drill and blast design, poor implementation of blast designs, stope shape (size, degree of complexity/undercutting, relationship to structure and stress field), time the excavation is left between firings, bogging and filling. Other contributing controls identified in the report include rock mass quality, Pre-mining stress and stress history and temperature effects (Consultants 2002).

In November 2004 AMC consultants performed a Stability Graph Back Analysis with similarities to the basis of this study. The performance of 92 stopes was used to investigate the confidence that can be placed in the Mathews stability method for the design of open spans at Olympic Dam. Of the 271 stope wall surfaces included in the study 176 (65%) were stable, 78 (29%) unstable and 17 (6%) had failed.

To determine stope effectiveness performance was compared with predicted stability. In relation to the wall surfaces it was concluded that only 10% of the stope walls were in the recommended design zone (unsupported stable zone). 65% of walls were deemed stable, 29% unstable and 6% failed. The performance was based on the examination of the final cavity survey and the design shape of the stope. The design limit of $N' = 0.03xHR^3$ should give an 80% chance of stability, a 20% chance of minor over break and no chance of failure. It was concluded that more stope history in the stable and transition zones were needed to increase confidence in this line. (Consultants 2004).

When looking at crown surfaces, AMC concluded that 95% of the stope crowns were designed in the stable zone and only 50% remained stable. They found 40% of the crowns to be influenced by major structures or the unconformity. Of these only 17% remained stable. Of the 52 acceptable case histories, 28 were supported (cablebolted) and 24 unsupported. The supported crowns were stable in 83% of cases.

The AMC report contained various other general conclusions. They found that calculating the rock stress factor A using methods that consider the influence of low stress did not improve the reliability of the Stability Graph method. They found some existence of time-dependent stope failure at Olympic Dam, but decided further investigations would be required to define this relationship.

In their conclusions AMC stated that Eastern walls have a higher rate of instability, while stopes in the FN have shown poorer performance than other areas of the mine.

There was no strong correlation between rock type or alteration with surface performance. However there appears to be threshold at which low HR values indicate stope surfaces displaying improved stability. For walls this threshold was HR = 10 and for supported crowns HR = 6.

AMC also conducted a further study at Olympic Dam to determine the design practices having a significant influence on the stability of crowns, those determining the length and support capacity requirements for crown cablebolts and recommending design guidelines to help achieve stable stope crowns. These aims were addressed by reviewing the performance of 87 stope crowns at Olympic Dam. This report reiterates that the three main controlling factors on stope crown stability are the distance from the unconformity, cablebolting and crown shape.

The unconformity at Olympic Dam which separates the cover sequence and the breccia lies at 240mRL. If the distance between the unconformity and the crown of the stope is less than the width of the stope, the distance is considered to affect the stability of the crown. The shape of the crown was also determined to be a key influence in the stability of the crown. A crown with an arch shape was found to be the most stable, while those that were stepped in/out being more likely to result in failure.

2.11 Synthesis

The Mathews stability method has been applied during the preliminary design process at Olympic Dam for over twenty years. The version of the method which is currently applied is sourced from Hutchinson's (1996) "Cablebolting for Underground Mines". The database of rock mass characteristics at Olympic Dam that provides the input parameters for the Mathews stability method is continually developing with window mapping data collection an ongoing process.

Previous studies at Olympic Dam have indicated there are inconsistencies between the Mathews stability method predictions and the actual performance of stope surfaces. In order to validate this, the next Chapter compares the predictions and performances of individual stope surfaces.

Chapter 3. Validating the Mathews stability method application at Olympic Dam

3.1 Introduction

Open stope performance is measured by the ability to achieve maximum extraction with minimum dilution (Villaescusa 2004). The following stope performance review focuses only on the shape of the final excavation. The size and quality of ore reporting to the draw points is not in the scope of this thesis.

Since commencing extraction at Olympic Dam, it has been acknowledged there are significant issues with the accuracy of the Mathews stability method. This is generally the case with any empirical method. This has implications for both safety and production. These inconsistencies were not previously quantified and therefore the extent of the problem was unknown. Predicted stope surface performance needs to be calibrated against actual performance to understand the validity of the predictive method.

This study is concerned with the performance of the individual surfaces of each stope. This includes the crown and the side walls. The performance is quantified solely on the amount of over break on each surface. For open stopes, over break can be thought of as any unplanned sloughing or loss of rock from the stope walls or crown. This is not to measure further or potential instability but the performance of the stope at the time of the cavity monitoring survey. Over break is any point inside the actual mined void which is outside the design shape of the stope.

Because it is likely that most surfaces will have over break to some extent, over break has been quantified using the equivalent linear over break/slough (ELOS) method. This method provides a simple number categorising the extent of over break. This is further discussed in the Methodology section of this Chapter.

3.2 Quantifying Mathews stability applicability at Olympic Dam

3.2.1 Methodology

The first objective of this study was to validate the accuracy of the Mathews stability method at Olympic Dam. This is done by completing a back analysis study on mined stopes that were designed and blasted prior to February 2009. These results have then been compared with the Mathews stability analysis component of the stope design. Once this validation was complete any existing relationships between stability and selected parameters, such as the area of the mine the stope is located in, the size of the stope were considered.

The validation involved the following steps:

1) Selection of appropriate stope case histories
2) Data collection and measurement
3) Analysis of the data collected

These steps enabled the effectiveness of the Mathews stability method to be quantified at Olympic Dam. Quantifying the effectiveness is a key step in being able to define the major controls of stope over break and collapse. Quantification also enables the identification of trends in stope performance and helps determine what improvements are required.

All data was collected from the Olympic Dam working database. This included the preliminary stope assessment, production tracking data and the post-production cavity monitoring survey.

A poor correlation between the Mathews stability method's predictions and actual stope performance was expected.

3.2.2 Stope case selection

The stopes analysed were obtained from a database provided by the Production-Tracking Department at Olympic Dam. The names and dates of all stopes developed since January of 1997 were provided. The requirements for a stope to be included in the study were:

1) Stope completed and backfilled prior to February 2009
2) Crown cablebolted
3) All digital wire frames available
4) Stope note data available
5) Final cavity monitoring survey available

For inclusion in the study the stopes must have been completed prior to February 2009. This is the date the present study was commenced. Crowns are also required to be cablebolted prior to this date as this has become a mandatory practice at Olympic Dam. The remainder of the inclusion requirements represent data availability.

The stopes which met the selection included:

- 124 crown surfaces;
- 396 rock wall surfaces; and
- 100 CAF adjacent wall surfaces

3.2.3 Data collection

The stope notes were a primary source of information. These provided Mathews stability method information on the stope as well as other background material. Datamine, a 3D design software package, was applied to look at each stope. This provided a 3D image giving the geometry of each surface.

Each surface of each of the 124 stopes was individually examined. The performance of each surface was then classified as stable, unstable or failed. To ensure consistency across the data range over break was calculated using ELOS, as described by Pakanis (1996).

Adequate stope performance from a stability perspective is difficult to define. ELOS is a simple method for expressing volumetric over break. It works by converting the actual over break, usually varying depths over a well defined portion of the stope face (Figure 3.2), into an average depth spread equally over the entire stope face (Figure 3.1). The following equation (Equation 3.1) displays how the ELOS of a stope surface is calculated.

ELOS = Volume of Over break / Area of stope face Equation 3.1

= (Average depth of over break x Area of over break) / Area of stope face

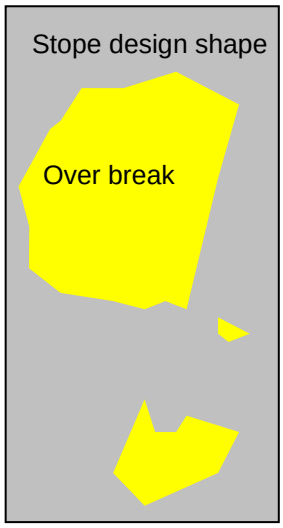

Figure 3.1: Simplified two-dimensional diagram of over break area on a stope surface

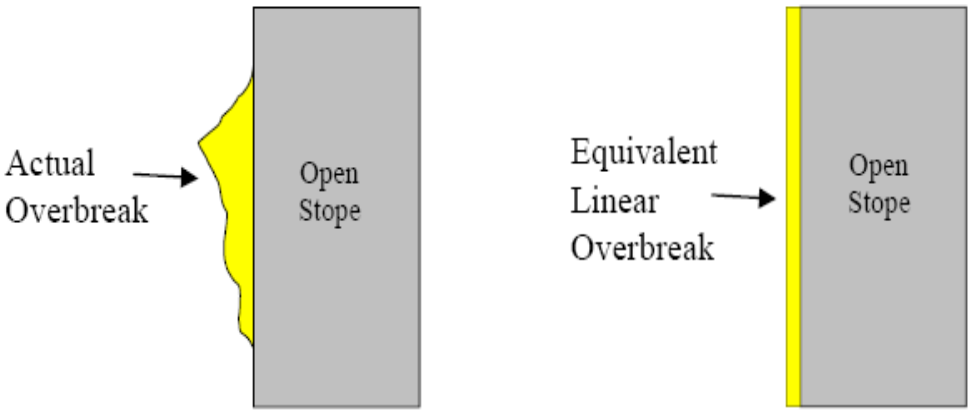

Figure 3.2: Simplified two-dimensional explanation of ELOS.

To quantify the ELOS results, the criteria listed in Table 3.1 were used:

Table 3.1: Quantification of ELOS values

ELOS	Stability Rating	Explanation
0 – 0.75	Stable	Little or no deterioration
0.75 – 2.0	Unstable	Minor failure
> 2.0	Failed	Unacceptable failure

It is important the use of the word “failed” is not miss-interpreted. For the use in this study the meaning is not that the stope or stope surface has entirely collapsed and is un-usable. Instead the word represents the stope surfaces that have over break that has an ELOS value greater than two.

This stability rating discounts the tonnage and grade of the final stope. It simply quantifies the volume of rock over broken.

At Olympic Dam, a cavity monitoring survey is taken of all stopes once they have been bogged for void and prior to the commencement of CAF backfilling. This is an effective diagnostic tool that provides a 3D image of the “actual” shape of the stope. The cavity monitor is a laser device that computes a 3D shape for the void with high precision, allowing a direct comparison of the actual achieved shape with the planned shape.

To calculate the ELOS for each stope surface, the cavity monitoring survey wire frame was overlain the stope design wire frame in Datamine, allowing a comparison between the two. Following this, slices were taken along the face to determine the area of the stope face and the area of the over break. Slices taken perpendicular to the face, along a plane indicating a fair cross section of the over break depths, were used to measure the average over break over an average face cross section gives indicative over break values (Figure 3.3). These values were then manipulated using the ELOS

calculation to provide a final over break value for each surface of the stope. Calculations were also completed for CAF faces, although there is no pre production assessment to compare these results with.

All ELOS values were calculated using the same technique, and judgment, to maintain consistency. The standard design of wire frames in the database has a control on the consistency of the analysis. Some were a combination of blast packets while others were the full design. Stopes that were not simple shapes proved more difficult to measure.

ELOS was used as to quantify over break, due to its straight forward nature and easily comparable results. Its only drawback is that it does not make the distinction between localised versus widespread over break. It is important to remembre ELOS is representing the stope surface over break not its stability.

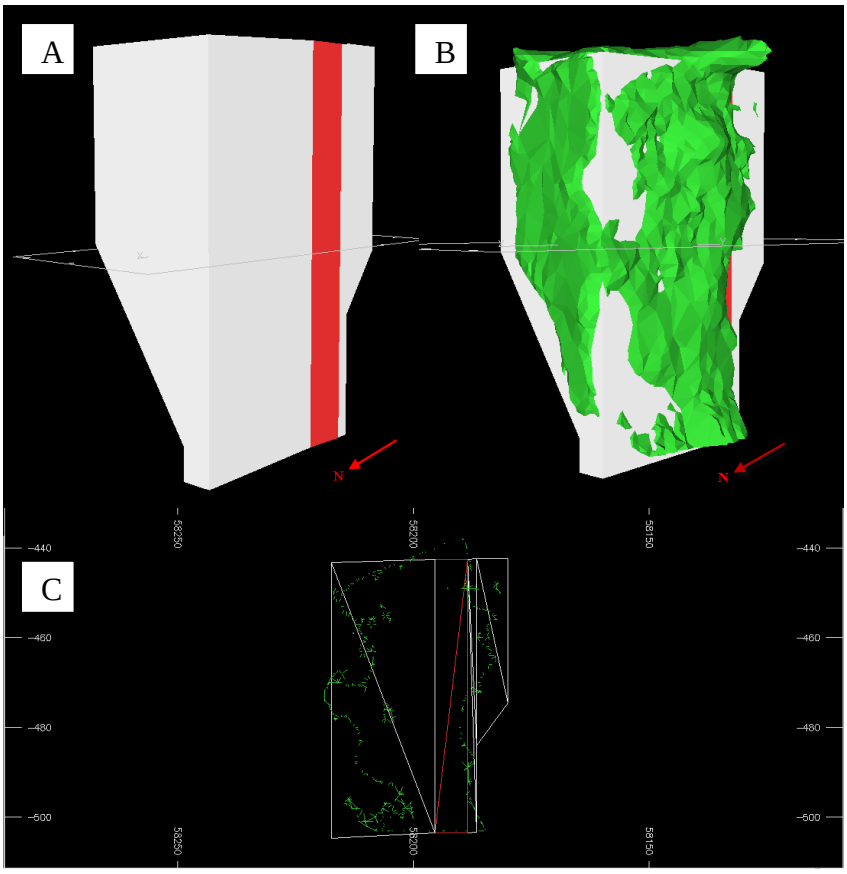

Figure 3.3: A) Stope design wireframe in Datamine. B) cavity monitoring survey wireframe (green) overlain stope design. C) Perpendicular slices through cavity monitoring survey and design wireframe for measuring ELOS inputs.

3.2.4 Analysis

The shape of a mined stope is a function of its design, drilling, blasting, local rock characteristics and over break. Analysis of a stope attempts to understand the over break component. Once all the 124 stopes were analysed, other information on each of surfaces was collected. This information came from stope notes, production tracking and survey. The information was then included in the analysis of all the data. The analysis was performed in Microsoft Excel by plotting relationships in a attempt to identify any correlations in stope performance at Olympic Dam. The Excel spreadsheet containing the raw data for the analysis is saved on disk 1 provided with this thesis.

The 124 crown surfaces were analysed separately from the walls. This is because the crowns at Olympic Dam are supported with cablebolts while the walls are unsupported. The two are therefore not comparable.

The relationships considered during the analysis were:

1) The correlation between the predicted supported and unsupported charts with the completed surfaces stability
2) The Mathews stability number with performance
3) HR with maximum over break
4) HR with performance
5) Mine area with performance
6) Surface orientation with performance
7) Time left open with performance
8) Volume of void with performance

3.3 Results

The data collected generated a database of 124 stopes with 619 surfaces. The raw data is included in Appendix F. Of the 619 surfaces, there were 495 walls. Of these walls 100 were adjacent to CAF backfill and subsequently excluded from the analysis.

The Olympic Dam is divided into 13 areas represented by various letter, such as F, FN, DSE etcetera. These areas are then subdivided into colour groups. For example 'FN' is host to Cyan and Amber. The sample included surfaces from all the primary areas of the mine, although some of the smaller and newer colour groups, such as Green, are not represented in the data (Table 3.1). Further, the data included surfaces with HR measurements ranging between 3 and 20 and N' values from 0.6 to over 160.

Table 3.2: Mine areas and the number of stopes from each included in the study

Mine Area	**Number of stopes**
Amber	10
Blue	12
Brown	2
Cyan	23
Jade	12
Olive	10
Orange	17
Pink	3
Purple	21
Red	1
Scarlet	11
Yellow	2

Of the 124 crowns included in the graph back analysis, 68 were stable, 34 were unstable and 22 failed. 395 of the stope walls in the database remained valid once all CAF adjacent walls had been removed. Of these the performance of 293 was stable, that of 84 was unstable and 22 walls failed (Figure 3.3).

Overall there were 304 inconsistencies between the predicted and actual performance (Figure 3.4). This includes all surfaces which had ELOS values and therefore performances that differed from the Mathews stability method prediction for that stope.

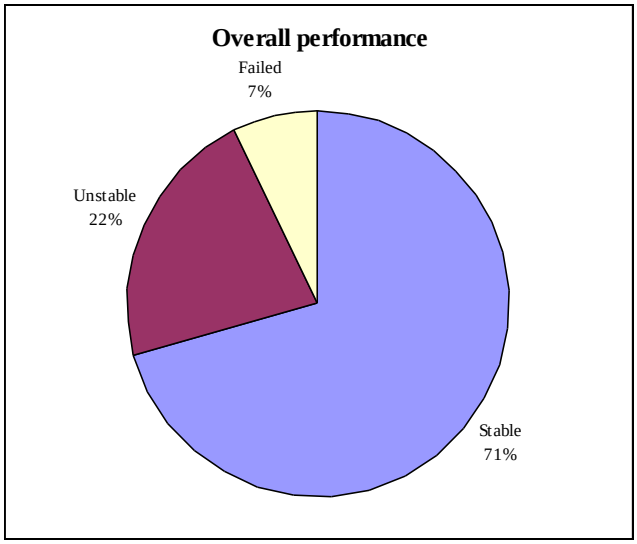

Figure 3.4: The overall performances for all surfaces (crowns and walls)

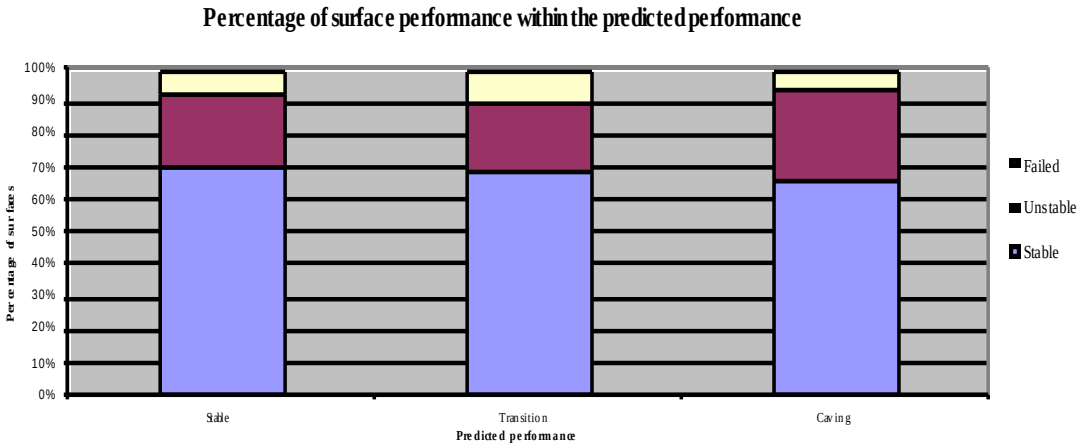

Figure 3.5: The performance of surfaces as a percentage within there forecasted category. Plot shows the majority of forecasted categories performed better than expected with stable (lilac) surfaces dominating each category.

3.4 Discussion of the Mathews stability method evaluation

From the above results, further analysis was completed to identify the underlying relationships and trends within the database. This included considering the results of different areas of the mine and examining surface orientation.

- *Supported graph analysis (Crown):*

There is no correlation when the HR and N' values of crown data is plotted with actual performance on the supported case histories chart (Figure 3.6). A majority of

points fall within the stable zone as expected. This is as the crown is designed generally to be a stable surface with the assistance of cablebolts. However as demonstrated by the number of failed and unstable points, it is obvious the predictions hold little validity. That said, there are a number of points that lie well within the stable zone yet have actually failed or are unstable.

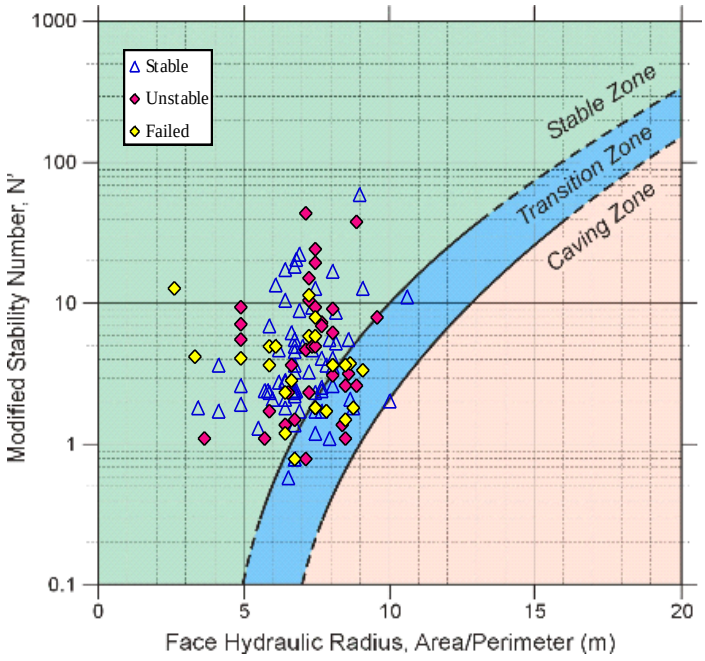

Figure 3.6: Crown surfaces actual performance plotted on the supported case histories chart

- *Un-supported graph analysis (Stope walls):*

There is a loose correlation when the HR and N' values of wall data is plotted with actual performance on the unsupported case histories chart (Figure 3.7). Actual failed surfaces are scattered throughout the three zones. Actual stable walls are also spread throughout the three zones, although they do have a concentration in the transition zone. This concentration means the current design method may be too conservative for the rock type at Olympic Dam. Actual unstable walls have the strongest correlation with actual performance. These are concentrated in and around the boundaries of the transition zone.

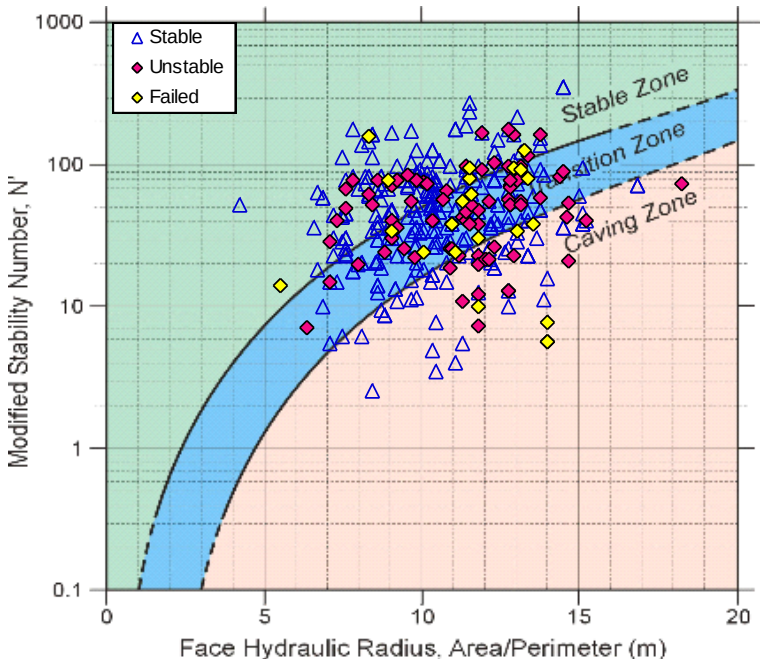

Figure 3.7: Stope walls actual performance plotted on the un-supported case histories chart

- *N'*

There was no relationship between the performance of each surface and their calculated Mathews stability number (N'). This was unexpected as the N' number is one of the two inputs of the stability chart.

- *HR*

HR values were separately plotted against the maximum over break of each wall and crown. This did not expose any relationship. However when HR was plotted against wall surface performance there was a loose correlation between an increase in instability and greater HR values (Figure 3.8). This was not displayed with the crown values.

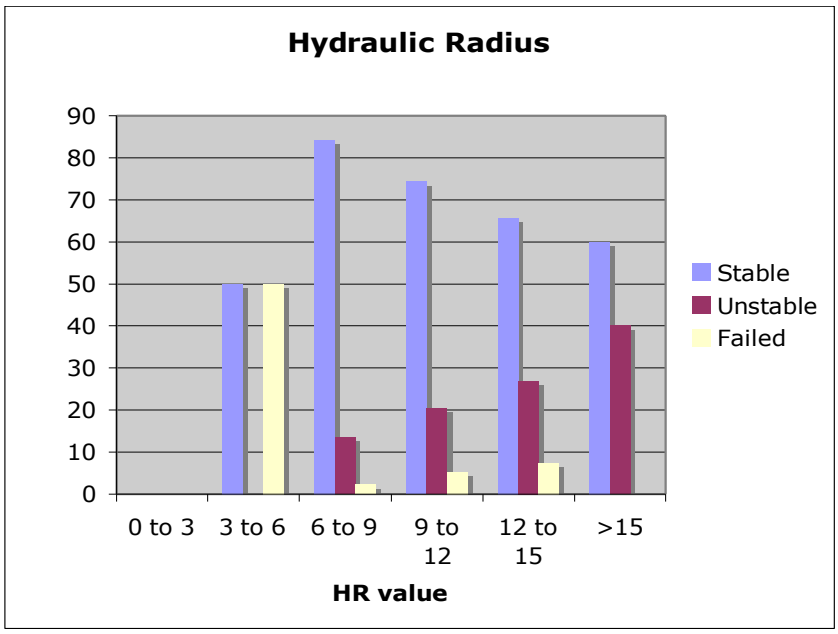

Figure 3.8: Chart showing the relationship between the increase in HR values and increase in instability for stope walls

- *Mine area performance:*

To determine whether the area of the mine hosting the stope has an impact on the stability and accuracy of the prediction, mine area data was plotted against performance. The analysis refers to the mine areas represented by letter combinations, a map of the mine areas can be found in the cover of this thesis.

The FN area of the mine was found to have the highest percentage of surface failures, with just over 10% of the analysed surfaces failing. Several other areas including B, CC, CN and DC, had an unstable performance rate of close to 30% (Figure 3.10). Note that the B and CN areas only make up 2% each of the entire database. This small data size must be taken into consideration when looking at the data (Figure 3.9). The F area had the greatest percentage of stable surfaces. There is no area in the mine with more unstable/failed structures than stable structures.

Based on the above analysis, the mine area comparison is inconclusive. However it does support anecdotal evidence of the FN area being prone to poorly behaving stopes. This is assumed to be due to the area's ground conditions. The rock is notoriously broken up prooving difficult to develop, drill and fire.

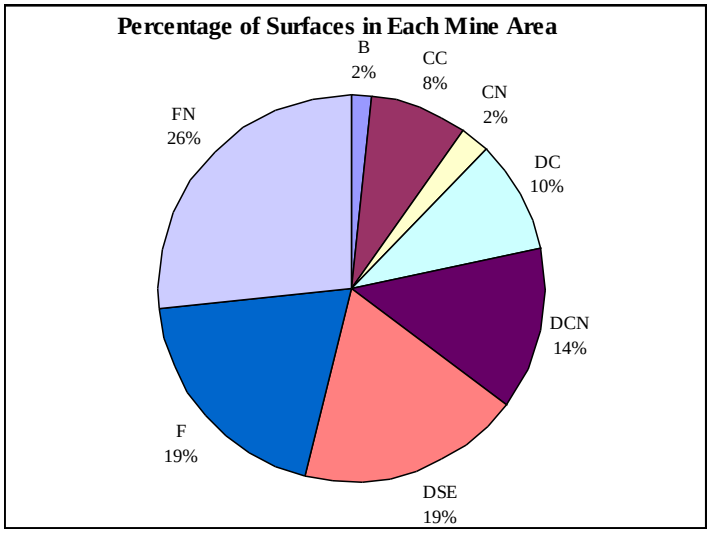

Figure 3.9: Pie chart showing the distribution of stopes included in the study in each area of the mine.

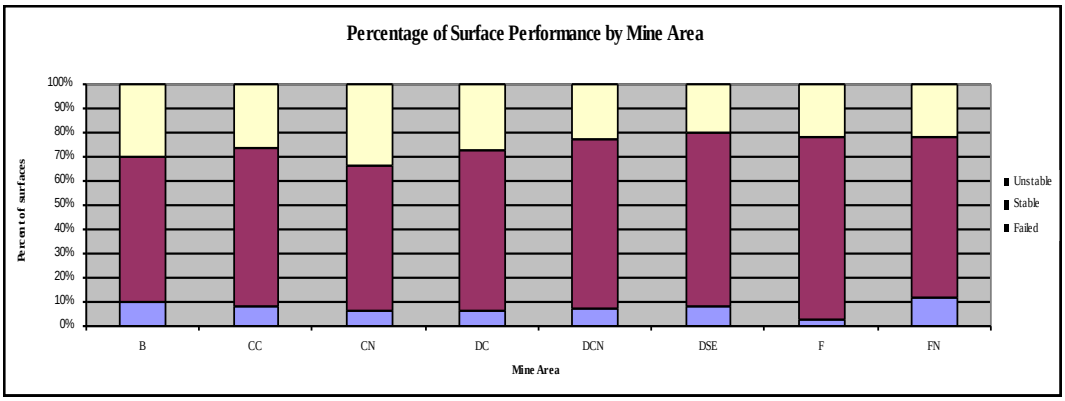

Figure 3.10: Chart displaying the performance of stopes in each mine area

Data from the four largest mine area data sets (FN, F, DSE and DCN) were plotted separately on the supported and un-supported case history charts (Figure 3.11, 3.12, 3.13 and 3.14). As with the combined plot, there was no consistency between the placements of the surfaces on the chart and their final performance.

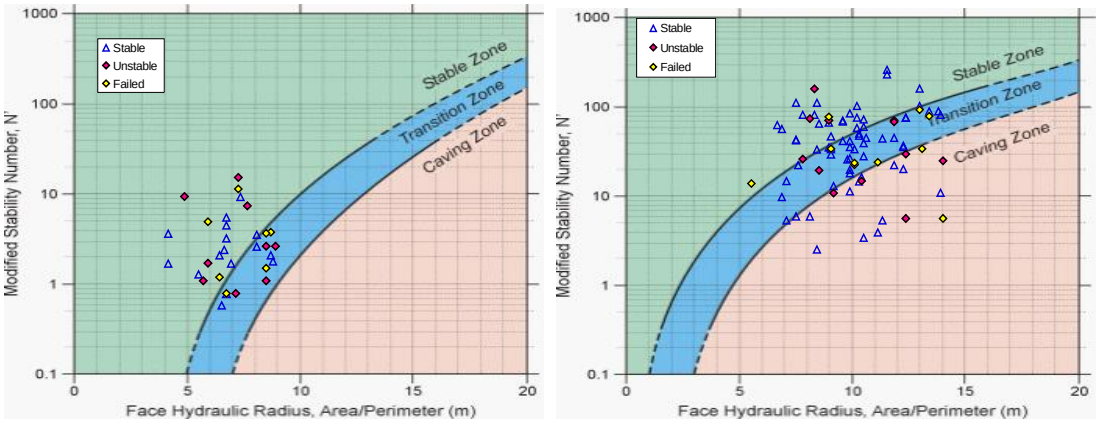

Figure 3.11: Crown (left) and wall (right) plots for the FN mine area.

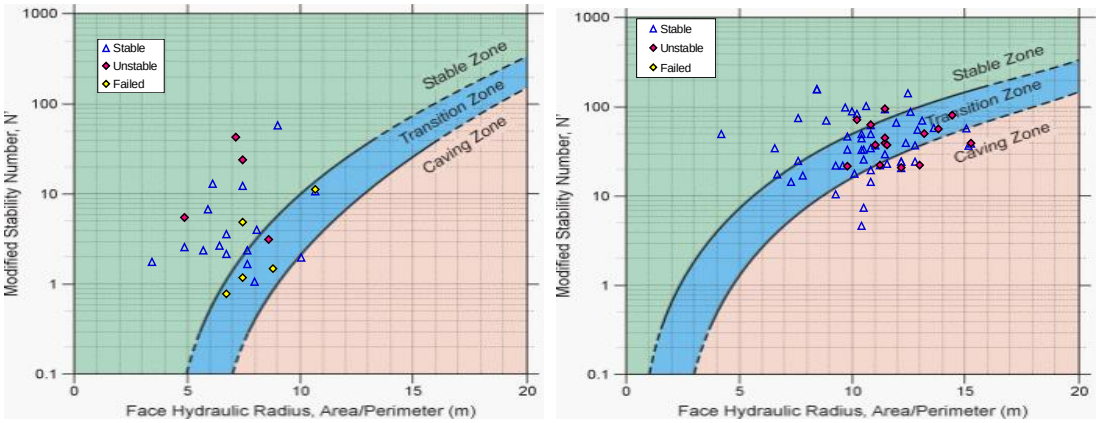

Figure 3.12: Crown (left) and wall (right) plots for the F mine area.

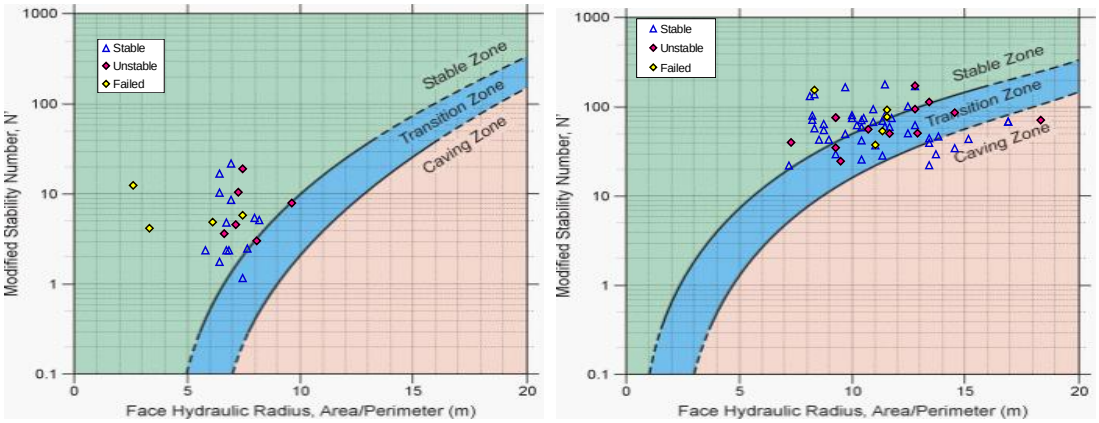

Figure 3.13: Crown (left) and wall (right) plots for the DSE mine area.

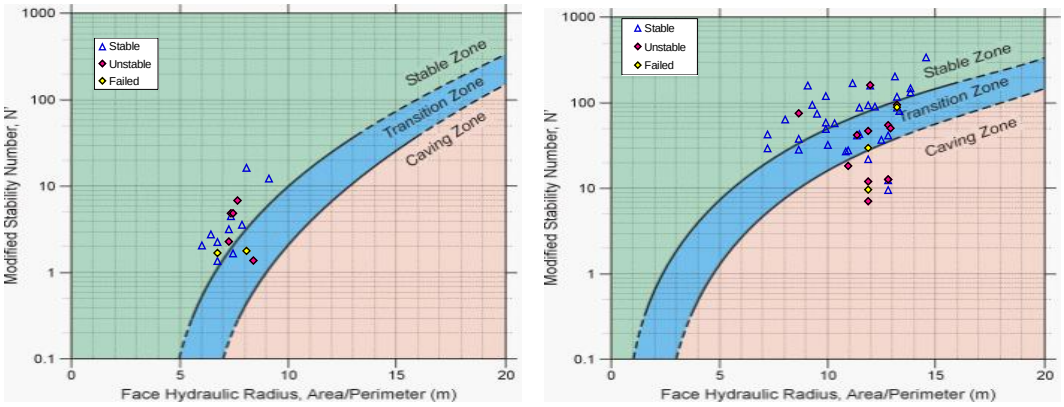

Figure 3.14: Crown (left) and wall (right) plots for the DCN mine area.

- *Surface orientation*:

When looking at the impact of surface orientation on stability there is only sufficient data to look at the five main orientations (being the crown, north, south, east and west) (Figure 3.15). All of the orientations had a majority of the faces that were stable. The crown surfaces show the greatest percentage of failed surfaces with 18% of the crowns failing. The remaining surfaces a fail rate of less than 8%. Southern walls had the greatest percentage of stable surfaces (80%), and no failed surfaces (Figure 3.16).

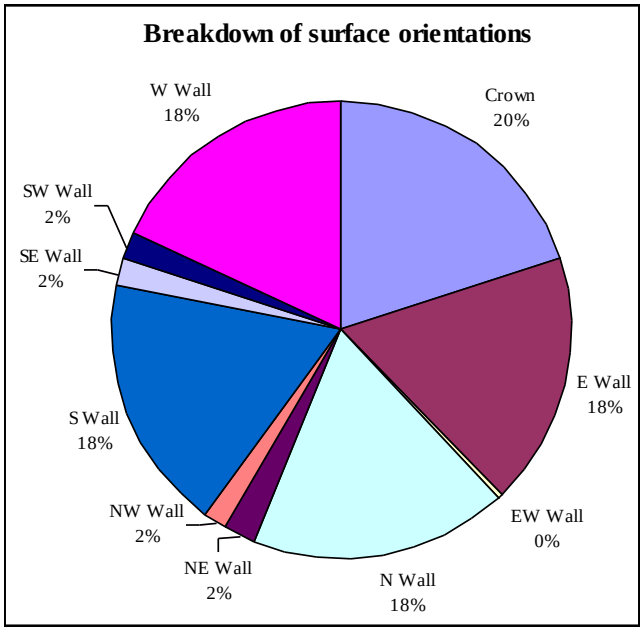

Figure 3.15: Chart showing the breakdown of surfaces included in the study.

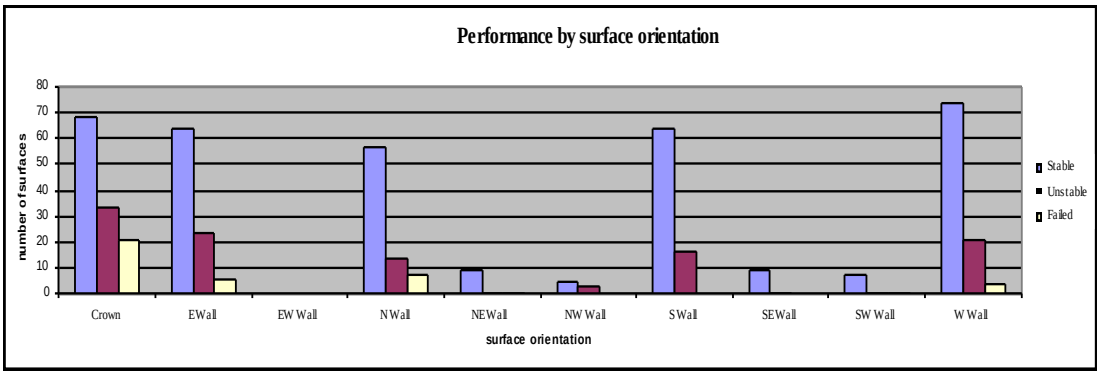

Figure 3.16: Chart displaying performance by stope surface orientation.

- *Time left open*

The impact on stability of the time a void is left open on was also analysed. In performing this analysis, crowns and walls were looked at separately. The time between the completion of a stope's bogging and the commencement of backfilling was calculated.

There is little correlation until a time span of approximately 300 days. At this point the percentage of unstable and failed surfaces and crowns rise. Possible time dependent effects include regional fault movement, stress re-distribution, production blasting, and backfill drainage from adjacent stopes. Blast damage and the effects of water from backfill have potential to move along common structures that truncate a number of stopes.

- *Tonnes bogged*

The volume of tonnes bogged was used to represent the final volume of void. This displayed no trend with stope stability.

Surfaces inconsistent with their prediction

The above analysis does not adequately consider whether performance was consistent with prediction. Of the 519 surfaces included in the analysis, there were 304 (59%) performances inconsistent with their prediction. 216 of these inconsistencies reflected the surface performing better than predicted, while the remaining 88 performed worse than predicted.

The FN mine area had the greatest number of inconsistencies with 92. The area with the least inconsistent predictions was Yellow with 8. However there were only 10 surfaces from this mine area included in the analysis meaning the analysis may not be truly representative of the area (Figure 3.17). Each mine area had greater than 50% probability of their surface's performances predicted incorrectly.

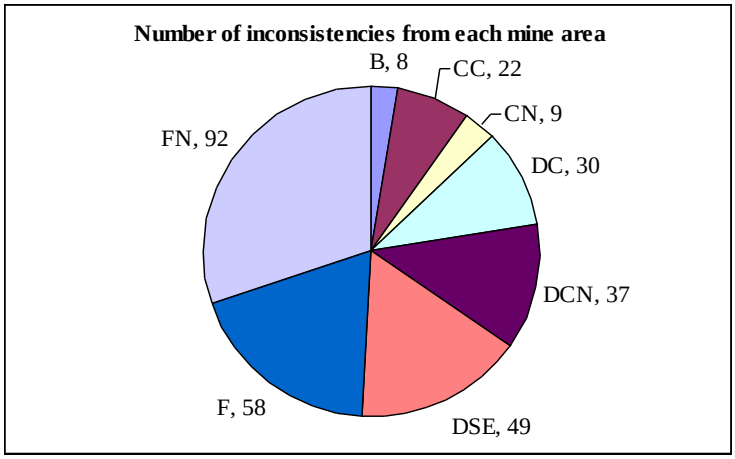

Figure 3.17: Chart displaying the number of inconsistencies from each mine area

With reference to surface orientations, western walls had the smallest number of inconsistencies with 66 (50%) of the walls being inconsistent with predictions. South eastern walls had the greatest percentage of inconsistencies with 90% of all surfaces being incorrectly predicted (Figure 3.18).

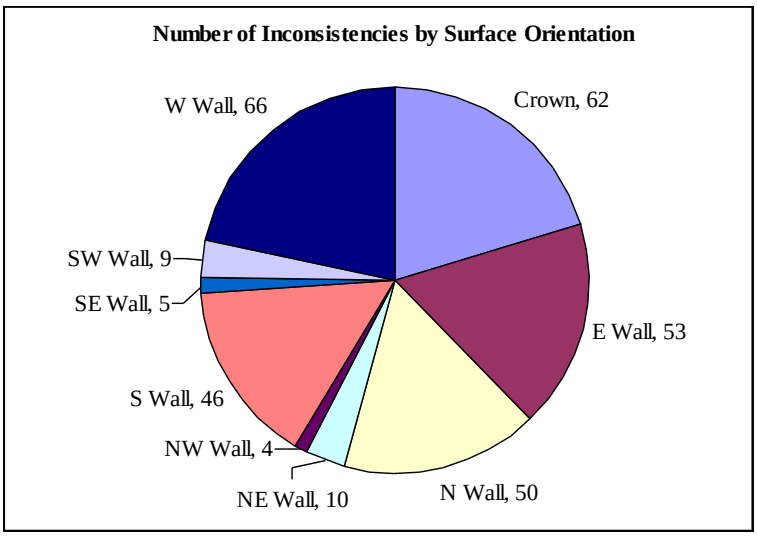

Figure 3.18: Chart displaying the number of inconsistencies from each surface orientation.

Inconsistency was broken into "conservative" inconsistency, where performance was better than predicted, and "underestimation" inconsistency where the performance was worse than the prediction. Of the inconsistencies 71% were conservative, leaving 29% underestimations.

3.5 Statistical Analysis

The apparent error rate (APER), as discussed in (Suorineni et al. 2001a), was used to quantify the reliability of the stability graph for stope performance. Higher values of APER reflected a better correlation between stability graph stope prediction and actual performance.

APER is calculated using the confusion matrix. This is based on the data classification, or alternatively the discriminate rule was used (Suorineni et al. 2001a). This displays the percentage of incorrect predictions by the stability graph. The method differs slightly from that applied by Suorineni (2001) to include all three predicted zones on the chart. The APER is calculated by applying Equation 3.2:

$$\mathbf{APER} = \left(\frac{n_{sm} + n_{um} + n_{fm}}{n_s + n_u + n_f} \right) 100\% \qquad \text{(Equation 3.2)}$$

Where n_{sm} = the number of stable surfaces misclassified as failed, n_{um} = the number of unstable surfaces misclassified as stable, n_{fm} = the number of failed surfaces misclassified as stable, n_s = the number of stable surfaces, n_u= number of unstable surfaces, and n_f= number of failed surfaces.

The present study produces an APER value of 41%. As stated, a high APER value indicates a strong correlation between the predicted data and actual performance. This low APER value in the present study emphasises the need to have the Mathews stability method calibrated to Olympic Dam and adjusted to allow for other controls to effectively assist with stope design at Olympic Dam.

It is important to acknowledge that the 215 correct predictions were not spread across the three stability zones. Of those surfaces that were predicted to be stable 71% were, 22% of all unstable predictions were correct and only 6% of all surfaces expected to fail actually did. This is distribution is displayed by the plot of The plot of predicted performance of the surfaces, as represented by values from 1 to 3 (stable =1, unstable = 2 and fail = 3) with the actual performance of the stope, as represented by ELOS (Figure 3.19).

The majority of the points are clustered in the lower part of the plot, indicating the surfaces were primarily stable despite there Mathews stability predicted performance.

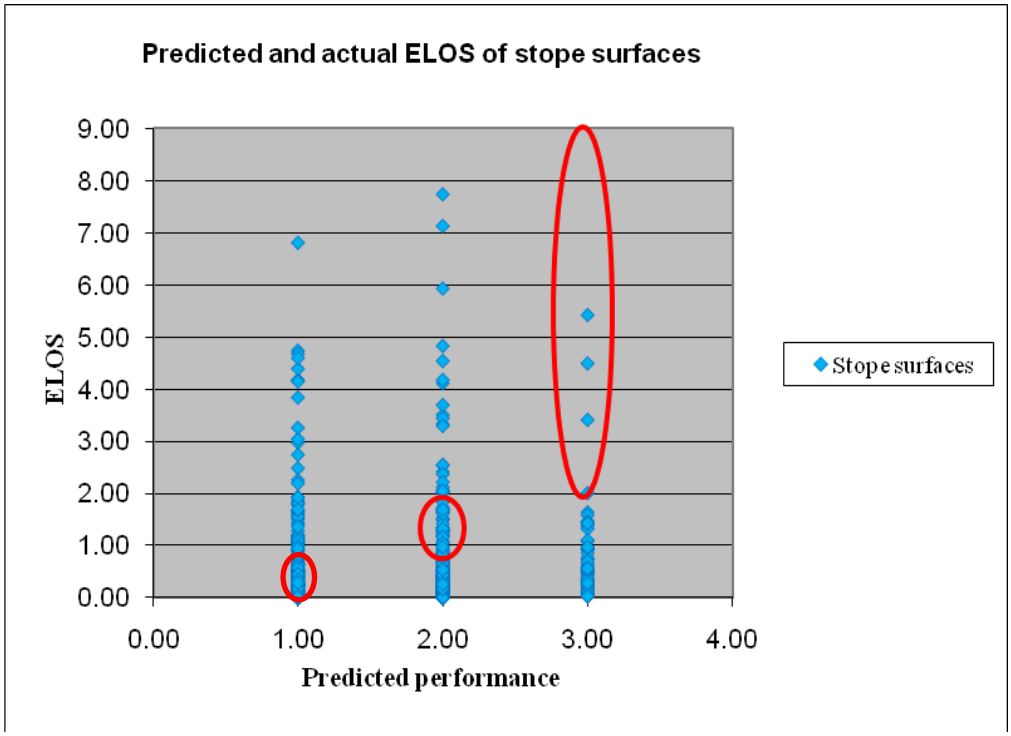

Figure 3.19: Chart displays the predicted performance (1=Stable, 2=unstable, 3=Failed) with the ELOS (actual performance) the red circles around the data represent the estimated areas which all points would fall in if the predictions were 100% correct according to ELOS classification at Olympic Dam

3.6 Failed surfaces

Each of the stopes displaying failure on at least one surface were individually examined in order to discover the failure control mechanism. The individual reports are included in Appendix G.

In summary of the 32 stopes that were examined:

- 17 had some structural influence on the failure
- 9 had high a sericite alteration which may have contributed to the failure
- 10 had adjacent development which has been have attributed to the failure
- 1 crown failure was attributed to the close proximity of the unconformity (Figure 3.20)
- 27 stopes were either secondary or tertiary stopes.

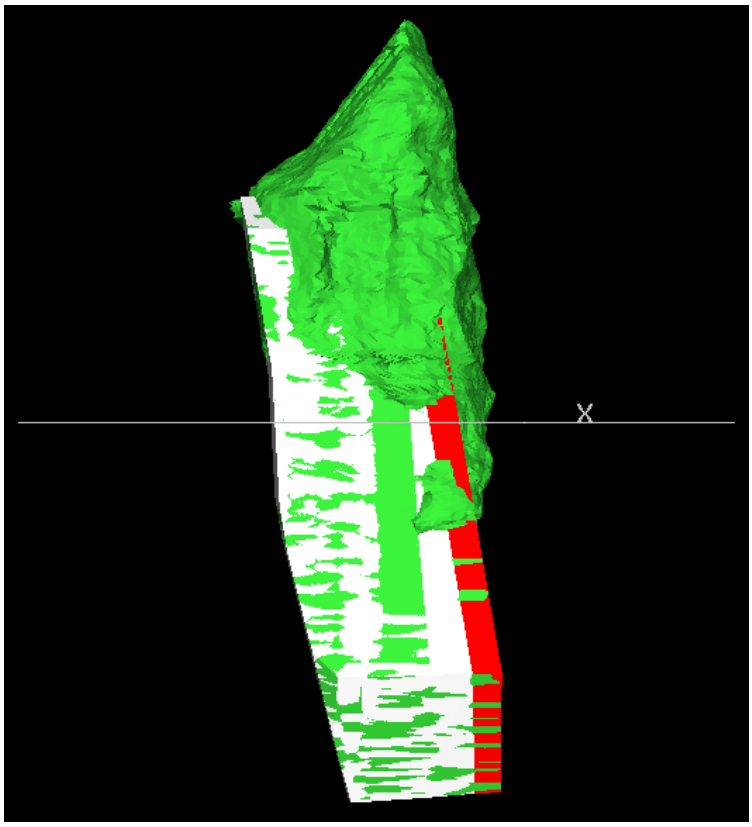

Figure 3.20: View looking North showing crown over break caused by close proximity to the unconformity.

Structure and the presence of adjacent stopes are the two most common parameters present in the 32 failed stopes. Neither of these controls are considered in the Mathews stability graph calculation.

3.7 Limitations and bias of back analysis

The most significant limitation or bias within back analysis is the interpretation of the above data and its associated results. That is, it is important to consider whether a 'correct' stability prediction is in fact correct, or whether the surface's stability is simply the result of a non-event such as failure did not occur (or alternatively non-failure).

Such scenarios have a strong control on results. If stability is due to a non-event, the only predictions that can be classed as truly correct are those that predicted an event that actually occurred. Therefore a correct prediction can only be one where a surface was predicted to fail and the surface did indeed fail.

There are several other limitations within the above analysis that must also be acknowledged. Firstly each stope's parameter data used in the calculation of N' is based on mine wide models. Although the data may be accurate for some areas of, or stopes in, the mine, other areas or stopes may have inaccurate data. Due to the type of deposit at Olympic Dam, it is extremely difficult to produce an accurate model without reducing the scale upon which the model is created.

The results may contain bias as only stopes meeting the required recommendations were included in the analysis, thereby omitting certain stopes from the study. Such stopes are generally from early Olympic Dam production. At that time cablebolting was not mandatory and consequently all required information was not successfully archived.

The ELOS calculation also has numerous limitations. Firstly, as part of the calculation involves human judgment it is unavoidably subject to bias. Further, the method uses the inclusion of drill drives (above the crown surface) as a definition of failure. As the drill drives are not encompassed by the stope design wireframe they become measured as over break. Error in drilling and charging of the stope must also be considered as a factor of over break. Since there is no way of accounting for this, the analysis must assume it is due to poor ground performance. Finally, it must also

be acknowledged that ELOS and the Mathews method were not created in conjunction and therefore the ELOS values determining the stability category may need reviewing.

There are an inconsistent number of stopes included in the study from each area of the mine. This may have contributed to further bias in some of the analysis results.

For completeness, it is also necessary to acknowledge that there are several other factors contributing to stope stability issues that have not been examined. Amongst others, these include stope alteration, pillar adjacencies and previous blast damage.

3.8 Synthesis

The aim of the back analysis was to determine the effectiveness of the Mathews stability method for stope stability forecasting at Olympic Dam. This analysis found that only 41% of the stability predictions were correct. Of the incorrect predictions, 216 were due to the surface displaying less instability than predicted, while 88 showing more instability than expected. Of 124 crown surfaces, 55% were stable, while 18 failed. Of the 395 wall surfaces, 74% were stable and only 6% failed.

Each of the mine areas had greater than 50% of its surfaces incorrectly predicted. The FN mine area had the greatest number of inconsistent predictions as well the greatest number of failed surfaces in the entire study. This indicates that the input values applied in the Mathews stability predictions may not be correct for the surfaces in this mine area.

While 41% of all surfaces conformed to their predicted performance, the analysis discovered the existence of time dependent stability. It also discovered a loose correlation between the increased HR value and increased instability.

The results from the refreshed database in this back analysis showed little variation from the results contained in the 2004 AMC report. The poor correlation and a lack of

improvement confirm that the Mathews stability method is not effectively applied to stope stability forecasting at Olympic Dam.

The limitations of the application of the Mathews stability method at Olympic Dam are discussed in Chapter Four.

Chapter 4. Discussion of the Mathews stability method application at Olympic Dam

4.1 Back analysis results

The results of the previous Chapter support the initial problem statement. That is the application of the stability model at Olympic Dam does not accurately predict stope surface performance. The current rate of correct predictions is around 4 out of 10, the ideal rate of correct predictions would be more like 8 out of 10.

Applying the Matthews stability method at Olympic Dam is problematic as

- Stope performance varies from that forecasted by the stability method
- A large part of the method's application is subjective
- Its successful application relies on engineer experience and expertise
- Design is often conservative reducing the tonnes achieved

When critiquing the Mathews stability method it must be kept in mind that it is an empirical tool. It is not a rigorous method and is only intended to provide a guide to preliminary stope design. However this does not justify the inaccuracy of its application at Olympic Dam, meaning further improvement to the method and its application is necessary.

Calibration of the Mathews stability method to the rock type at Olympic Dam may increase the model's accuracy and efficiency. This can be achieved through altering the relative weighting of the parameters, or through altering the location of the zone boundaries. Alternatively the accuracy of the input data could be improved by reviewing each of the models and increasing the frequency of the mine's window mapping. Further, correlation between actual and predicted stope performance could be increased through the implementation of a new design tool specifically created for application at Olympic Dam.

The following section highlights the limitations of the Mathews stability method and of how it is applied at Olympic Dam and discusses alterations to the method suggested by other authors. Possible improvements for the how the Matthews stability method is applied at Olympic Dam are also identified.

4.2 Limitations of the Mathews stability method use at Olympic Dam

4.2.1 Quality of stability number input parameters

The popularity of the Matthews stability method is attributable largely to its simple application. However as with any method that relies strongly on the subjective interpretation of the user it has several limitations. The limitations are involved in both the method itself and its application at Olympic Dam.

There is a poor correlation between the performance of stope surfaces and their N' value (Figure 4.1). It would be expected that there would be a clear trend between the increase in the N' value and the increase in the stability of stope surfaces. It is difficult to determine whether the poor correlation is due to the accuracy of the input data or the stability number's suitability at Olympic Dam.

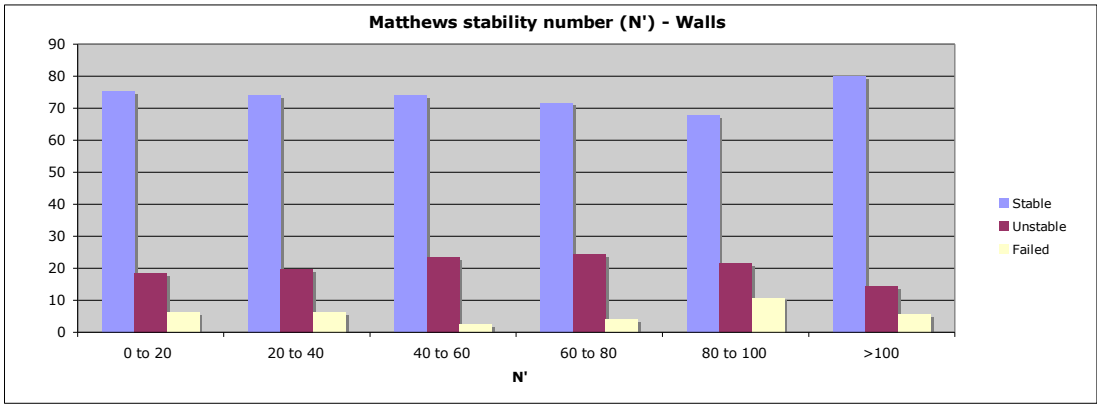

Figure 4.1: The poor correlation between the stability number (N') and the percentage of performance of the wall surfaces.

Data input accuracy is determined by the subjective judgements of the geologist or geotechnical engineer collecting the data during the window mapping process. The collected data is used during the stope note process. Due to the inconsistent coverage of window mapping at Olympic Dam for some stopes this will mean only one

window from a level is entered, which could be as far as 80m away from the actual stope. With an ore body such as the one at Olympic Dam, there can be significant changes in the rock mass characteristics over this distance.

Engineer subjectivity is also involved when applying strength to the rock mass. The average lithology and average extent of sericite alteration are used to define the strength. Each lithology has a designated strength which is reduced to give the final value depending on the extent of alteration. For example, HEMH has a set strength of 235MPa. If the face had a low alteration the HEMH set strength would be reduced by 10% to a final UCS strength of 212MPa. Considering this unavoidable variability in the data inputs, it can be assumed that the poor correlation between the stability number and performance is primarily a result of rock mass data inaccuracy.

4.2.2 Structural influence on stope performance

As mentioned by numerous authors a notable limitation of the Mathews stability method is the absence of any attempt to incorporate the influence of discrete major structures including faults, shears, joints and folds. As the stability graph is designed for a moderately structured rock mass with a distributed or ubiquitous structure, the influence of the structure was not considered as a primary control of instability. Structural influence must therefore be considered separately to prevent unexpected structurally controlled instability.

Ore bodies containing numerous regional and local structures, including faults and joints, are often associated with the SLOS mining method. It is important that while in production the stope remains stable. The intersection of any single structure with the stope can lead to severe unravelling, having detrimental effects on the closing out of the stope (Figure 4.2). The impact of structures on a stope emphasise the importance of considering all structures in stope stability analysis. Other authors have attempted to incorporate such factors into the stability number (as discussed later in this Chapter). No such attempt has been made at Olympic Dam, structural influences are individually considered by visual analysis at the stope note and pre production stage. Because it is unlikely that every single structure has been successfully mapped this is analysis is not always accurate.

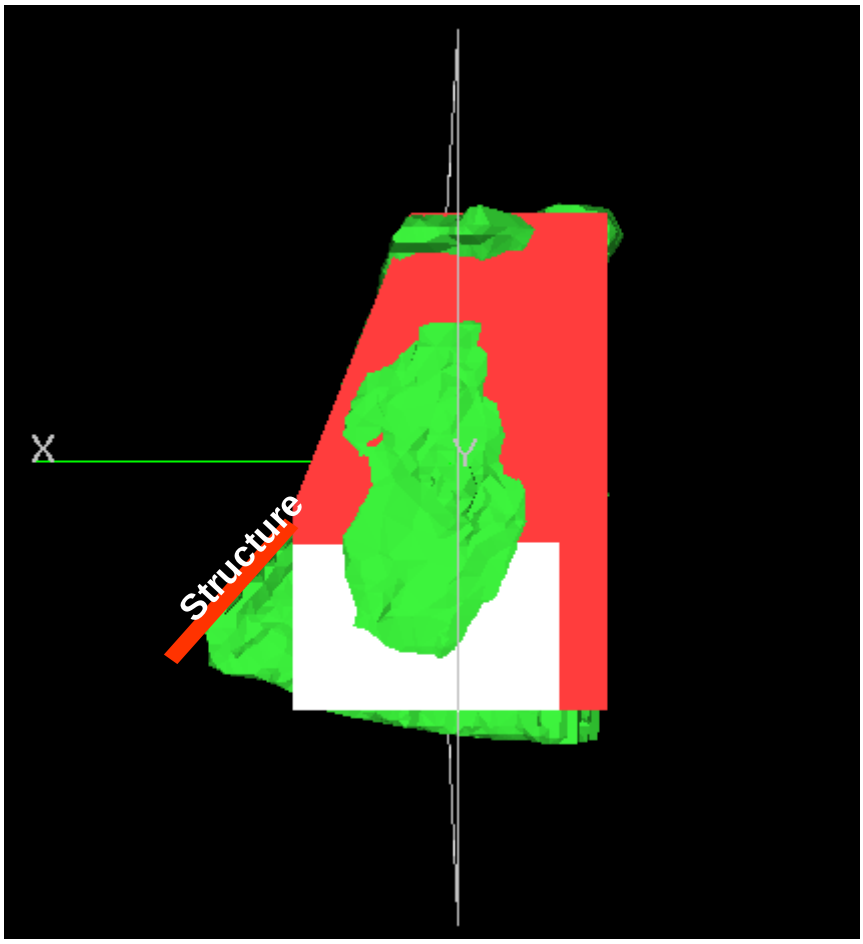

Figure 4.2: Screen shot looking south at a stope design shape (red and white) with the cavity monitoring survey shape (green) showing structurally controlled over break. The ground below the structure has over broken.

Various other factors may lead to stope misclassification. These include rolls or folds located in foliated rocks that may lead to undercutting of structures not anticipated by mapping. This is a risk when the structure was not identified as having the potential to cause failure, whereas if the underlying formation had been identified it would have been. Strength deterioration due to weathering or bias of RQD calculation due to relative orientations of the critical joint sets and drill cores may also lead to misclassification (Stewart & Forsyth 1995). Because Olympic Dam is an underground mine the exposure to weathering is minimal but the possibility of bias in RQD measurements is possible. This bias is difficult to identify and acknowledge.

4.2.3 Adjacent stopes

Another issue relevant to Olympic Dam is the application of the Mathews stability method when designing secondary and tertiary stopes. During the design of secondary or tertiary stope it is assumed the adjacent stopes have been successfully and wholly filled. The surrounding fill must be tight to the walls and the back of the stopes in order for the fill to be considered supporting a element. If this is not the case the assumed span used in the analysis may be much greater than the nominal stope panel. Consequently the stability graph will not appropriately classify the surfaces predicted stability. It is the responsibility of the user to ensure that backfilling of adjacent stopes is completed to tight fill.

At Olympic Dam the Mathews plot is not used for stope surfaces that have direct CAF adjacencies. However it is assumed that a neighbouring mined stope has been tight filled. This assumption may impact the accuracy of the crown surface prediction (Figure 4.3). The only apparent means of eliminating this error is for the user to check back filling reports of adjacent stopes. Any incomplete or incorrect backfilling must be allowed for in the HR calculation of the concerned surface.

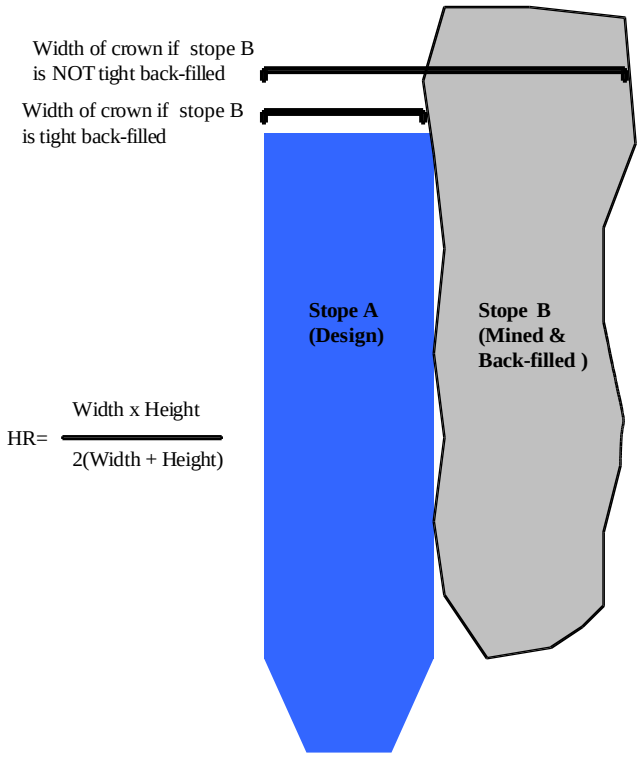

Figure 4.3: Schematic diagram showing how the back fill status of adjacent stopes can affect the crown HR value.

The HR calculation is an improvement on simply accounting for span. However the Mathews curves do not take into account the various stope shapes that could exist with the same HR values (Vongpaisal et al. 2009). This has the potential to be misleading as stress concentrations develop in different formations around different shapes of void.

4.2.4 In situ stresses

As a general practice in SLOS mining, regular shaped stope surfaces are desired for ease of both design and production of the stopes. A rectangular shape stope surface with a "funnel" shaped bottom, or as commonly explained as an "upside down milk carton", cannot always be achieved. This means surfaces take on irregular shapes and therefore have different patterns of stress acting on them (Figure 4.4). The orientation of the stopes relative to this stress field has little influence on the predicted stope performance in the Mathews stability method. At Olympic Dam a stress model is run to identify any of these stress concentrations during the pre-production process. This is as a result of the aspect not being accounted for in the stability number calculation.

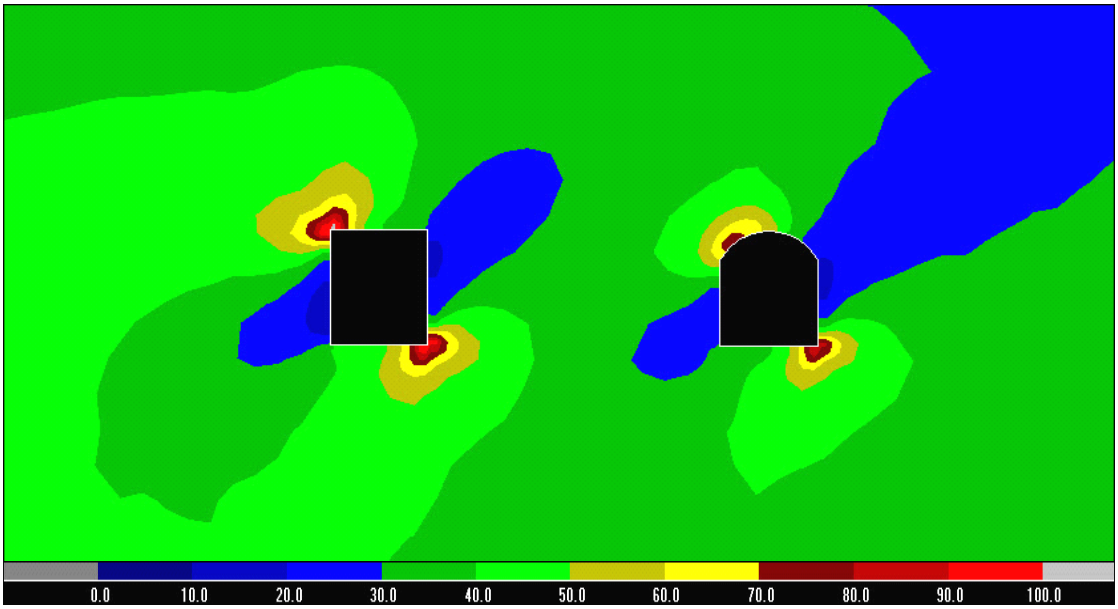

Figure 4.4: Screen shot of stress analysis showing the variation in stress concentrations around different shaped excavations

Another stress-related assumption included in the Mathews stability method is the inability of the stress factor to account for tension. The rock stress factor (A) in the stability number calculation represents the ratio between the intact rock strength to the surrounding compressive strength. Tension is of relevance in areas where there has been a lot of previous excavation with closure pillars, secondary and tertiary stopes particularly as the strength of CAF is not equivalent to that of the rock mass.

4.2.5 Operational impacts on stope performance

There are two production related limitations in the Mathews stability method that can affect the accuracy of predictions. Firstly there is no consideration of blasting effects in the Mathews stability method. Blasting often leads to the degradation of the rock mass by blasting-induced fractures that are likely to cause over break at stope boundaries. Secondly there is an absence of any time factor in the method. It is widely acknowledged that rock mass deterioration increases with exposure time as is seen at Olympic Dam where the number of stable stopes reduced as they remained open longer and the number of failed stopes increased.(Figure 4.5). Accordingly it is preferable to have a stope open for the least time possible.

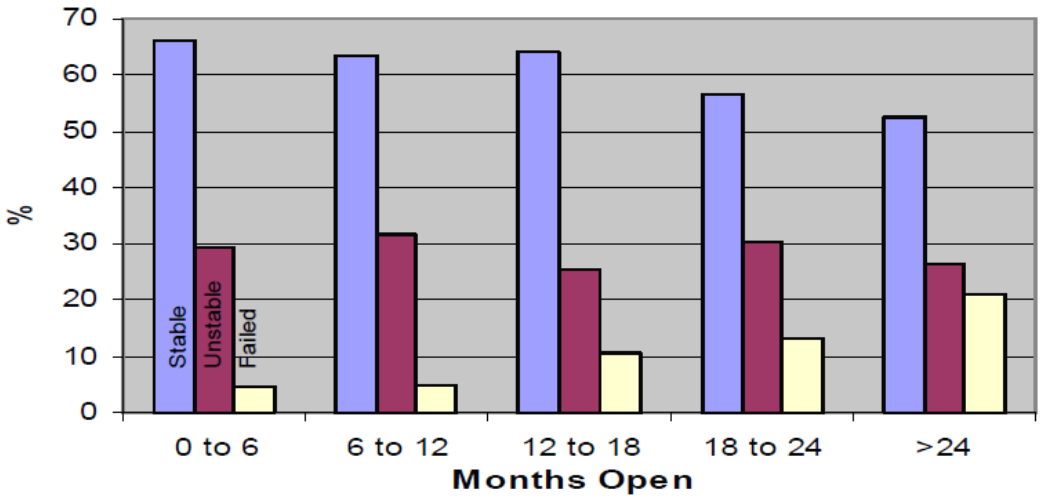

Figure 4.5: Chart by AMC authors showing stope stability deterioration over time at Olympic Dam (Oddie, 2004)

4.2.6 Site specific influences on stope performance

It must be remembered that the Mathews stability method was based on a series of case studies from North American mines. Due to this the stability zones of the graph are unable to allow for differences in site specifics. The requirement for site-specific calibration of the Mathews stability method has long been recognised.

In 2003 Stewart and Trueman looked at the application of the method to narrow-vein stoping. They stated that a reliable stable-failure boundary requires at least 150 case histories. Of these a minimum of 10% should be unstable stope surfaces (Stewart 2003). This requirement is not feasible at new mine sites coming online. Accordingly new sites are forced to rely on clusters of non-continuous data. These define the segments of the graph as the basis for preliminary stope design.

Although the Mathews stability method has some underlying limitations these cannot be assumed the cause of the poor correlation between predicted and actual stope performance at Olympic Dam. For this to be done the method must first be calibrated to Olympic Dam and the database of input parameters for the method must be reviewed.

4.3 Improvements in stope stability forecasting

It is widely acknowledged that despite its wide spread popularity the Mathews stability method has significant shortcomings in the effective application to open stope design including those experienced at Olympic Dam discussed above. As a result, there have been various attempts at making additions or alterations to the method. These have attempted to account for local conditions and other known excavation stability problems.

4.3.1 Incorporation of a fault factor

Suorineni et al. (1999) explored the limitations of the application of Mathew's stability method. They worked toward the incorporation of a fault factor into the stability method. This was intended to account for fault controlled sloughage (Figure 4.6). The fault factor is an adjustment to the stability number that can be applied when

there is a fault which could potentially impact the performance of the stope. It is incorporated in the calculation of the stability number N', as shown in Equation 4.1:

$$N'_f = Q' \times A \times B \times C \times F \qquad \text{Equation 4.1}$$

N'$_f$ is the modified stability number incorporating the fault near the identified stope surface. The F is determined through numerical modelling a variety of given rock mass conditions, in situ stress ratios K, fault friction angles (strength properties) fault geometry and stope geometries (Suorineni et al. 2001b). The equation was created around the most dominant factors that influence the severity of the fault related sloughage.

Suorineni et al. (2001b) showed the effective application of the fault factor at Kidd Mine. It would not be appropriate to apply the fault factor at Olympic Dam due to the inconsistency of the structural mapping and of the areas which have been mapped. This structure mapping includes window mapping, discontinuous models or a discontinuous numerical model.

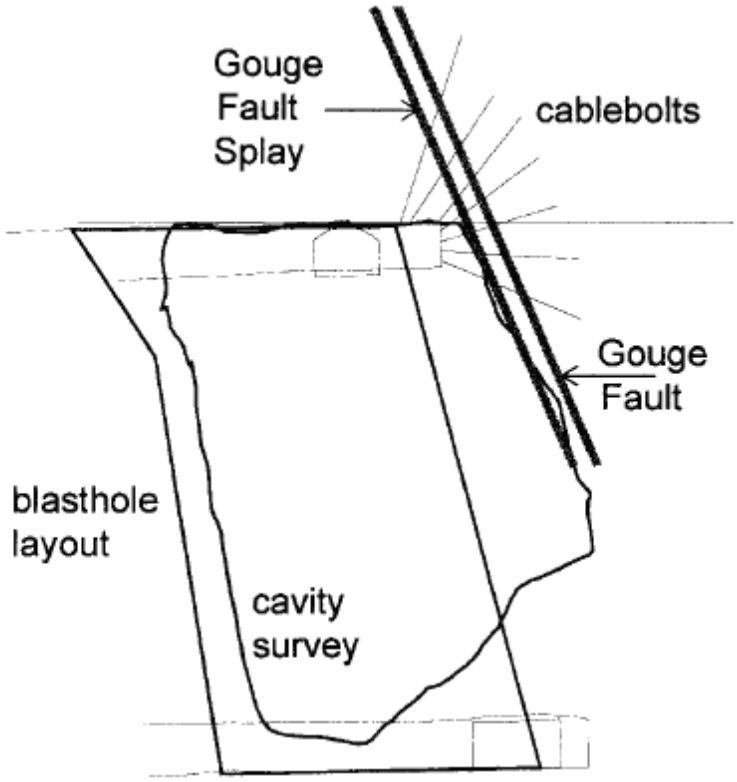

Figure 4.6: Fault-related sloughage of a hangingwall at Kidd Mine, Canada (Suorineni et al. 2001a)

4.3.2 Influence of confining stress

Martin et al (1999) discussed the application of confining stress as an indicator for predicting the amount of dilution to be expected around mine openings. It is well known that the behaviour of a jointed rock mass is predominantly controlled by its confinement. As confining stress approaches zero, the potential for new crack growth increases significantly. This is coupled with the belief that as stress becomes tensile the potential for crack growth grows. From these conclusions a new approach to stope hangingwall stability was presented by Martin et al. (1999). This considered the stress path of stope experiences and the effect of low confinement (Martin et al. 1999).

The hypothesis Martin et al. (1999) study was that confining stress may be an indicator for predicting the amount of dilution around mine openings. To test this, a series of 3D elastic analyses were carried out on stopes of different width and height. The depth at which the confining stress was equal to zero for the hanging wall at mid height was used for the analysis. The results were then expressed as percent of potential dilution. The results were in agreement with both the hypothesis and field observations and found that stope stability is sensitive to the orientation of the stopes relative stress field (Figure 4.7). Although this method was tested with narrow-vein mining the general concept may be applied to open stoping.

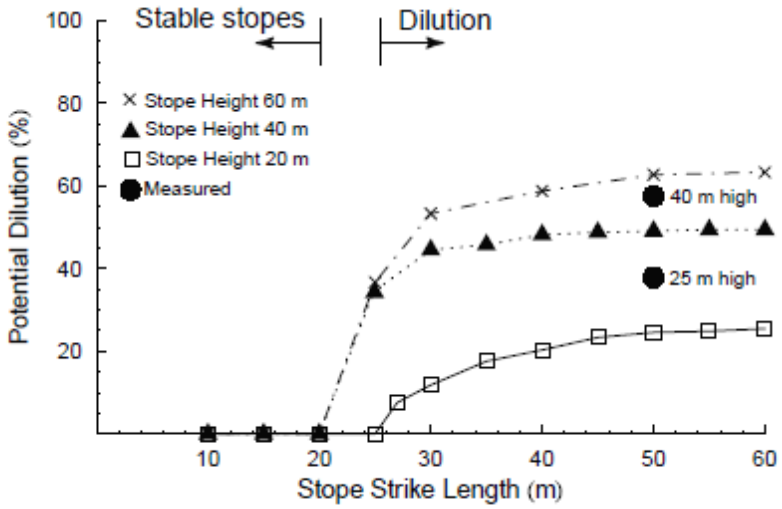

Figure 4.7: The predicted dilution from the numerical analysis compared to measured results (Martin et al. 1999).

4.3.3 Site-specific effects

Despite significant advances in experience and data related to the stability graph, there is substantial evidence that site-specific effects may result in erroneous stability predictions (Stewart & Forsyth 1995). The Mathews stability curves have been based on bias data collected primarily from North America typically representing strong rocks of medium to good quality. The method provides a starting point for design but should be calibrated on site at all mining environments. To do this requires an up to date database of stope dimensions, rock mass parameters and of stope performance. On site calibration allows a more accurate model suited to the local conditions to determine performance and ground support.

A case study completed at Mt Charlotte mine by Stewart and Trueman (2001) used logistic regression to generate site-specific zone plots on the graph. These displayed higher accuracy as a prediction tool than the generic stability graph (Figure 4.8). The performance of stope surfaces at Mt Charlotte mine were represented by the stable, failure and major failure. These are the equivalent of the stable, unstable and failed used at Olympic Dam.

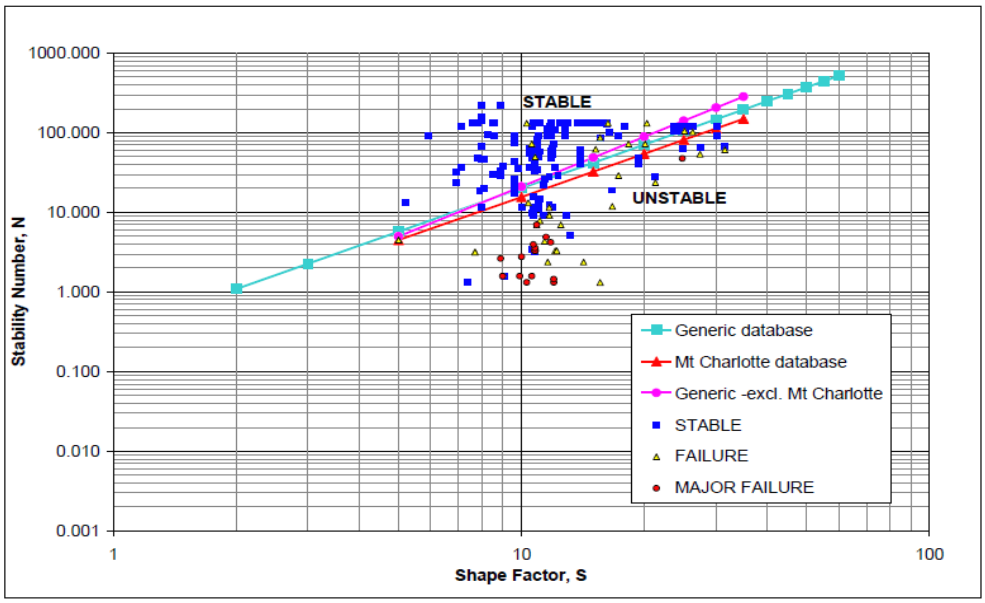

Figure 4.8: Mt Charlotte site-specific stable-failure boundary compared to the generic boundary after logistic regression (Stewart 2001).

Caution must be used when undertaking a site-specific model with a database that is adequate to make changes to the boundaries. Such changes must avoid the reflecting a

short-term operational condition rather than a relevant site-specific controlling factor. Stewart and Trueman (2001) recommend a site-specific database of at least 150 case histories of which at least 10 percent must be unstable. This number of case histories must be obtained to minimize variance in a stable-failure boundary. The authors note that these requirements apply only within the range of the current database.

The primary aim of underground excavation design should be to utilize the in situ rock for its structural properties without relying on the installation of rock and surface support to assist stability. The Mathews stability method has been validated as an appropriate empirical design tool for the preliminary design of stopes. This means it has been recognised as a helpful guide to stope stability during the early stages of design. Over time experience with the model, the increased size of the database across a broad range of surface geometries and rock mass conditions, and the use of statistical analysis has resulted in minimal associated variability when it is correctly applied to a mine site. This has optimised the method as a prediction tool. The method is recommended as a useful open stope design tool, but it must be recognized that it is not a rigorous design method.

4.3.4 Statistical improvements

With the use of logistic regression the risks associated with using the Matthews technique has been quantified and applied. This is as has been recommended by several authors (Trueman & Mawdesley 2003). Optimising the placement of the stability zones on the stability graph is a critical to improving the reliability and minimising the inherent subjectivity of the Mathews stability method (Mawdesley 2004).

Stability graphs are a simple, non-rigorous design approach based on case histories and logistic regression. They can be applied to reduce the subjectivity through statistical delineation, placement optimisation, and through calculating the accuracies and probabilities of stability boundaries (Mawdesley 2004). The process also allows isoprobability contours to be calculated and drawn on the stability graph. This is a valuable design tool in quantifying the uncertainties of the Mathews design tool.

Although the zones can be determined by visual placement based on the scatter of site-specific case studies, human bias and unknown errors are introduced when there is no statistical guidance.

Mawdesley (2004) states logistic regression is used due to the failure of traditional regression techniques to appropriately deal with binary or categorical outcomes. A key benefit of this technique is its capability to allow the user to quantify the accuracy of a given model. Applying regression techniques to a sufficiently large database is currently the best option for minimising the influence of subjective data (Mawdesley 2004).

It is important to remember that the proceeding statistical analysis does not justify the use of the stability graph as a rigorous design tool. Logistic regression enables the engineer to allow for site specific calibration. However logistic regression is nothing more than a short-term solution to the shortcomings of the Matthews method and the application at Olympic Dam. To improve stope stability forecasting in the long-term, the methods discussed in the previous section are preferable.

4.3.5 Applying numerical modelling

Rose & Hungr (2007) apply varying rates of velocity with the inverse-velocity method to forecast potential slope failure in open pit mines. The inverse-velocity method, developed by Fukuzono (1985) uses surface displacement measurement data to determine the onset of failure. Based on laboratory tests during the development of his method, Fukuzono simulated a rain-induced landslide. This landside indicated that the logarithm of surface displacement acceleration increased in proportion to the logarithm of surface velocity. When the inverse-velocity was plotted the values approached zero. This allowed a prediction of time of failure to be determined (Figure 4.9).

The method was applied successfully to the three slope case studies in 2001 by Rose and Hungr (2007). This was the first time it had been tested in an open pit mining environment. They concluded that the inverse-velocity plot often approaches linearity, especially during the final stages before failure, which enhances the utility of the

method as a instability indicator (Rose & Hungr 2007). They stated that the method could be extended to the forecasting of any unstable phenomena.

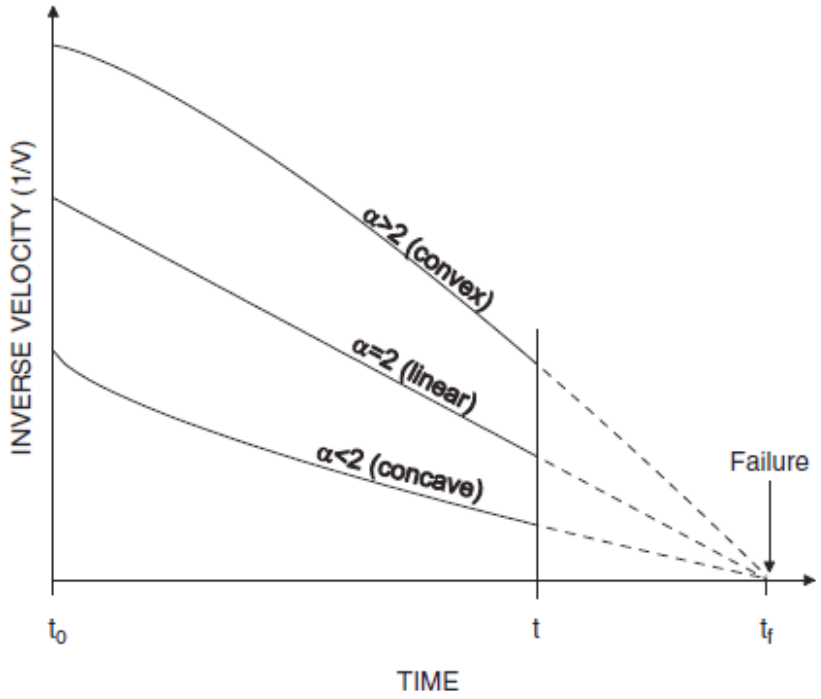

Figure 4.9: Inverse - velocity versus time relationships preceding slope failure (Fukuzono, 1985)

The application of velocity and plastic strain as stability indicators was investigated by Cepuritis et al (2010) at the Kanowna Belle gold mine. They used back analysis of over-break to investigate non-linear elasto-plastic relationships and stability. Their modelling was done in Abaqus Explicit, a 3D analysis product, and selected velocity and plastic strain as their stability indicators. Velocity and plastic strain were plotted against points which had been classified as either stable or unstable (Figure 4.10). The point's classification was determined by their location relative to the void boundary. The results showed a clear relationship between an increase in velocity and the increased likelihood of instability.

The Kanowna Belle mine study has similarities to one undertaken at Panda mine in Canada's NW territories. There velocity, displacement and plastic strain were applied as stability indicators to define the boundaries of instability. This was used as accurately as possible to differentiate between stable and unstable material (Reusch 2008).

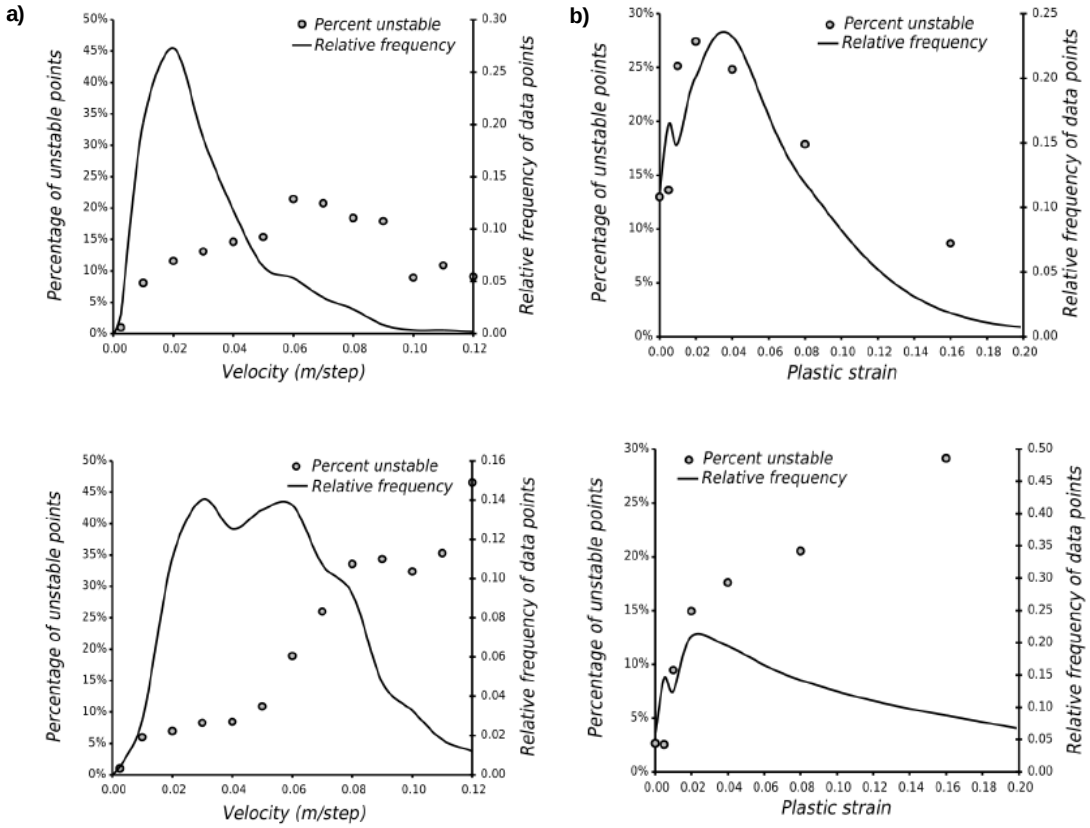

Figure 4.10: Percentage of unstable points (left hand y-axis) versus a)velocity and b) plastic strain for two different stoping areas from the Kanowna Belle gold mine case study (Cepuritis 2010)

Every point on a surface has its own complex history of stress and strain (Reusch 2008). The methods of stability forecasting introduced by both the Kanowna Belle Mine and Panda mine case studies acknowledge this by assessing the potential instability for each point on the surface rather than on the surface as a whole. The Panda mine study confirms that this method can be used and tested at a site that does not have a small-scale structure model available. The application of instability as a criteria to define stability indicators is discussed later in this thesis.

The preceding section is merely a summary of the works completed in this field. There are numerous other authors and topics which have not been mentioned due to the vast collection of work available.

4.4 New stope stability analysis tool for Olympic Dam

The relationship between the actual performance of stope surfaces at Olympic Dam does not correlate with the predictions of the Mathews method (Figure 4.11) Historically it has been recommended that the zones on the chart be altered to suit the Olympic Dam ore body. This recommendation alone is not enough to entirely correct the Mathews model.

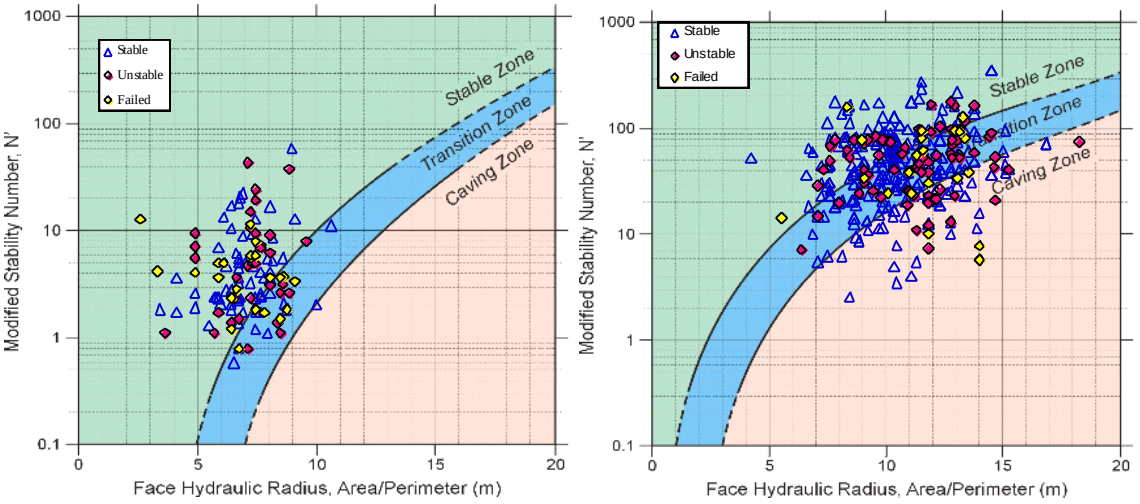

Figure 4.11: The actual performance of a) crowns and b) walls defined by their HR and N' values, showing a poor correlation between stope performance prediction and performance at Olympic Dam**.**

The results from Chapter Three indicate that the Mathews stability method is not effectively applied at Olympic Dam. For the successful application of the method it is required that it is calibrated to the Olympic Dam ore body. If the Mathews method is continued to be used at Olympic Dam there are some recommendations which should be adhered to in order to improve the methods application:

1) Implement a detailed quality assurance quality control (QAQC) system to track the performance of mined stopes with reference to the design.
2) When applying ELOS during the QAQC process add another category to the classification of surface performance. Currently any stope surface which has over break with an ELOS value of two or over is classified as failed. Another

catrgory should be added to separate the surfaces with catastrophic failures from those which have extensive over break.

3) Undertake more window mapping close to upcoming stopes to strengthen the accuracy of the database.
4) Install a series of live stress measuring stations around the mine. With particular focus on stress relaxation around mined stopes.
5) Attempt to incorporate structures into the Mathews stability number.
6) Perform statistical analysis such as logistic regression to ensure the zones on the Mathews chart are the best fit possible to Olympic Dam.

4.5 Summary

After working through both the results of the analysis in Chapter Three and the discussion in this Chapter it is clear the issues with the Mathews stability method as a design tool at Olympic Dam appear to primarily result from how the method is applied. One limitation that exists within the method itself which is worth noting is the lack of acknowledgement of structurally controlled failure.

There are several ways the application method at Olympic Dam could be improved to achieve more accurate stability predictions. The main limitations with the application at Olympic Dam and possible solutions are shown in Table 4.1

In the following chapter, a new method is devised that appears to provide accurate forecasts of stope surface stability at Olympic Dam. Before the development of this new method it is important to understand the mechanics and criteria of instability, as well as the indicators most suited to forecasting this.

Table 4.1: Major limitations of the application of the Mathews stability method at Olympic Dam and possible solutions and improvements

Limitations of application at Olympic Dam	Possible solutions
The quality and coverage of the database of stability number input parameters.	Increased frequency of window mapping, particularly in and near upcoming stopes.
Lack of incorporation of structural influence on stability in the stability number	Attempt to incorporate structures into the Mathews stability number specific to the Olympic Dam rock mass.
Insufficient in situ stress data	Install a series of live stress measuring stations around the mine or increase the regularity of measurements. Also increase the number of measuring stations. Particular focus should be placed on stress relaxation around mined stopes.
Unknown status of adjacent stopes	A detailed QAQC process should be undertaken for all stopes not only those which do not perform as expected to develop a detailed database of stope performance history.
No site-specific calibration	Perform Logistic Regression on the current stope histories to determine the relocation of the stability zones on the stability chart to best fit the Olympic Dam conditions.

Chapter 5. Numerical model for stope design at Olympic Dam

5.1 Introduction

At Olympic Dam, a high resolution non-linear numerical model of stoping already exists. This model is able to replicate the extent and magnitude of damage well and utilises a 3D discontinuum, Hoek Brown, strain softening and explicit finite element modeling. This encapsulates a majority of completed stopes at Olympic Dam. The data represented in these models includes displacement, velocity and plastic strain.

This chapter develops a new stability prediction tool to improve the non-linear numerical model currently in use at Olympic Dam. This new model is based on velocity, or incremental displacement, as a stability criterion. Note that stress and strain-based approaches were not investigated as the estimate of velocity, or incremental displacement, is predetermined by stress and strain.

The suggested new tool uses the existing numerical model to examine trends in the movement of individual points, otherwise known as material instability. Completed stopes were investigated to determine their material instability. From this a model for future application at Olympic Dam has been produced. Cepuritis et al (2010) has previously utilised similar numerical modelling and analysis at Kanowna Belle Gold Mine .There the ore body is simultaneously mined in underground and open pit operations.

The application of velocity as a stability indicator is incomparable to the Mathews stability method. It is based on a numerical model and is not geologically based. The use of the terms stable and unstable in this section should not be confused with the use of the terms in regard to the Mathews stability method.

5.2 Mechanics of instability

Over break arises from rock mass instability at the excavation surface due to a number of mechanisms. These include:

Wedges and blocks formed by existing discontinuities
Rock mass comminution (crushing and disassembly of rock mass)

Unstable volumes bound by a combination of existing discontinuities and induced damage surfaces.

Estimating the potential for kinematic instability, that is the dislodging of block or wedges formed solely by discontinuities, requires an understanding of the distribution of discontinuities. This understanding is not usually complete but rather is a function of geometry. The mechanics of this geometry are simple and well understood. Sloughing by this mechanism is not the focus of this thesis.

Over break due to rock mass damage, or alternatively combined damage and structure, is more relevant to this thesis. This requires consideration of both material and kinematic instability. Material instability refers to the stability of a point within a material (a comparison of stress and strength to estimate the accumulated yield), while kinematic instability refers to the freedom of a volume within a mass to displace and fail.

5.2.1 Empirical stability indicators

In the past the application of mechanistic analysis tools to rock mass was thought of as a difficult task. To simplify this complexity rock empirical rock mass classification systems were introduced. Most empirical classifications originally applied in mining were based on civil engineering case studies. These case studies included rock quality designation (RQD), rock mass classification (RMR), Q and the modified rock mass classification (MRMR). These were in addition to the Mathews stability method.

The application of the empirical indicators has altered over time as more case histories have been applied, testing and calibrating the indicators. It is usually recommended that the methods be calibrated to each site, because they rely on local rockmass patterns to be effective, but this is rarely done, and few of them account well for the 3D geometry of the mine or the excavation, the stress history, structure or interactions between multiple voids. The most commonly employed empirical stability method is the Mathews Method, or the Modified Stability Graph.

5.2.2 Physics based stability indicators

The purpose of stability indicators is to identify the timing, magnitude and extent of instability. The criteria for instability are generally defined by a certain critical limit

of a chosen parameter. The criteria will be applied to analyse results over a certain timeframe. For open stoping this timeframe is typically between the completion of the stope's production firing and back filling (Cepuritis 2010). As discussed in Chapter Three the Olympic Dam criteria, volume of over broken rock, is measured at the time of the cavity monitoring survey (after bogging, before back-filling).

For an engineering assessment of the potential for 'combination' mechanisms of instability several criteria are frequently used. These are classified as the lower or upper bounds, depending on whether they infer potential for instability, or whether they constitute explicit instability. Stress is lower bound, because highly stressed rock may or may not be unstable, while high velocities are upper bounds as something which is accelerating is by definition not at equilibrium.

The stress criterion is generally applied for the assessment of excavation performance. This is typically expressed as a ratio between peak strength and an elastic model's estimate for stress. This ration is the strength Factor of Safety Factor (FOS). The criterion states that there is a level of stress above which instability will occur. The approach is qualitatively simple but limited in excavation stability assessments. This is because stress is poorly correlated with kinematic permissibility for failure. Further, rock mass damage is not simply correlated with any single component of stress, because stope failures generally occur in de-stressed parts of an excavation rather than in the highly stressed parts.

There are also practical considerations for the estimate of stress. As materials yield the capacity to bear load reduces and stresses are redistributed. Analysis that does not capture this softening, the subsequent redistribution of stress or the ultimate equilibrium accounting for damaged parts of the rock mass will not properly estimate the stress field. That is the stress estimate for FOS calculations may be invalid if the mechanism of yield and instability are not sufficiently captured. Around stopes a single safety factor for strength or stress does not meet the needs of an operator (Martin et al. 1999).

Critical strain criteria are frequently applied in the assessment of instability. This assessment uses the magnitude of damage or deformation to estimate the likelihood of

instability. Critical strain criteria are most often used when the kinematic constraints are easily accounted for. Such circumstances occur where there are known unfavourable geometric intersections with structure, for pillars, or where the level of strain in the pillar core directly indicates the residual strength. The level of residual strength is the level of strain where pillar strength reduces significantly and the pillar will continue to deform even at constant or reducing load.

The main limitations of the critical strain criteria are the sufficiency requirements for reliable non-linear analysis to compute strain values. It is also a lower bound on instability in most cases as a rock mass may be damaged but still stable. This is as it may not be kinematically capable of sloughing, or may retain sufficient strength to be able to reach a stable equilibrium. This is in terms of the particular stress configuration, strain, strength and structure. For example on the floor where the damage can be deep but there is no issue with the rock remaining at rest.

Despite the limitations if the extent and magnitude of the damage and deformation is sufficiently forecast, critical strain criteria are more satisfactory than stress criteria. This is as the accounting for stress, strain and strength in the structure is implicit, when in stress criterion additional assumptions are needed.

Any point within the rock body that is moving at a high velocity is unstable. The velocity and acceleration of a point within a mass can therefore be considered an upper bound criterion for instability. The velocity value represents the rate of movement within the rock mass, generally measured relative to some point. In the case of stope stability it is toward the void or designed void, for example points above the crown that are moving in a downward vertical movement toward the crown have positive modelled velocity values.

The load factor derived from a kinematically admissible velocity field is an upper bound on the true collapse load factor (Yu 2006). Thus, the velocity criteria is applicable for estimating the stability of all mechanisms including unstable blocks bound by structures that have low levels of internal comminution, and high levels of comminution (Cepuritis 2010).

In terms of velocity, instability in a rock mass can be divided into three phases:
An unstable phase: during this phase velocity increases at a constant or near constant rate
Active failure: during this phase there is an onset of more rapid accelerations leading to failure.
Failure: this phase is signified by collapse.

Beck (2009), when discussing slope failure forecasting in open-pit mines, said the displacement rate (velocity) is commonly considered the best indicator of the failure process. There is no doubt that it is the simplest criterion to understand. In open pits for example radar are used to monitor slope movements and alarms are triggered using velocity criteria, not stress or strain.

Numerical models estimate the movements in the rock mass. From one point in time to another, from these values the distance they movies divided by the time passed. The outcome is the velocity of the point the modelled velocity is the modelled distance that any point moves in real time.

When applied to the result of numerical analysis, the main limitations of velocity based stability criteria are the very high level of model similitude required before the velocity estimates can be considered reliable. Essentially the displacements, and therefore the extent and magnitude of damage modelled, must be a sufficient representation of the real problem for the modelled velocities to correlate well with actual measurements. It is only recently that the most sophisticated physics based models have been considered to have high enough resolution and precision for this task.

5.3 Method for applying velocity as a stability indicator

The method uses commercial modelling packages and should be easily applied at most mine sites. The basic requirements to apply the stability indicators at different sites are:

A strain softening dilatant finite element numerical model, preferably a discontinuum model. The model needs a high resolution, implying fine meshing, higher order elements and small extraction steps.

- A database of mined stope.
- The model will be more accurate if a large number of case histories are available.
- Cavity monitoring survey data must be available for each of the stope case histories.

The first step is to use the cavity monitoring survey shapes of mined stopes to determine a stability classification for each point of available data in and around the stope (Figure 5.1). Unstable points are those which were over break when they should still be standing, they became over break because they are unstable. To define this each point lying between the planned stope outline and the cavity monitoring survey outline is classed as unstable, while those outside the cavity monitoring survey outline are classed as stable (Figure 5.2). This must be completed for a volume large enough to bound all unstable points above (crown analysis) and beside (wall analysis) the void.

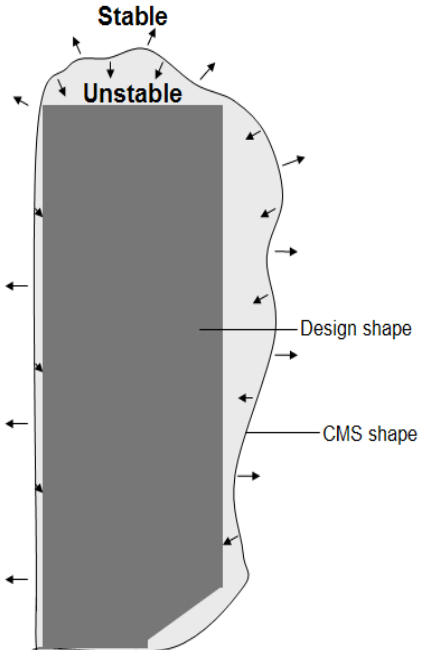

Figure 5.1: Schematic showing any points within the numerical model which fall within the shape of the mined stope (cavity monitoring survey outline) are classed as unstable and any points which remain in place (outside cavity monitoring survey outline) are stable**.**

Once each point has been classified the relationship between unstable points and modeled velocity can be examined (Figure 5.3). This is done by computing the proportion of unstable points in each velocity range to those that are stable to estimate a probability function.

Ideally, this relationship should display an increase in instability with an increase in velocity. It is expected that all rock masses, irrespective of local properties, should display this general relationship. This is one of the reasons why velocity is an upper bound stability indicator. By completing the analysis using site-specific case studies, a direct reflection of the behaviour of the local rock mass is achieved.

The output graph can be applied as a stope stability forecasting tool using the relationship between the probability of instability and the velocity values for the points in and around the designed stope.

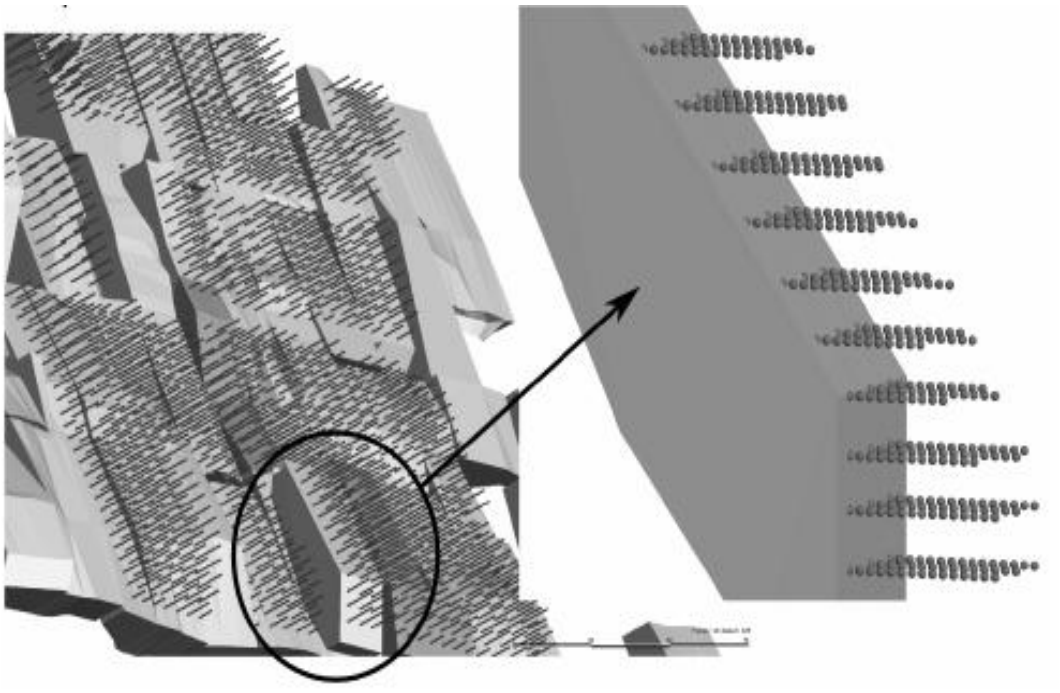

Figure 5.2: An example of how the arrangement and distribution of points may look in the numerical model, this one is from KBGM using Abaqus software. Each of these points has a value for plastic strain, velocity and displacement (Cepuritis 2010)

The Kanowna Belle mine case study (Cepuritis 2010) provides examples of the analysis possibilities. This includes plotting the rate of velocity with the probability of instability (Figure 5.3). The probability of a stopes surface's instability can be visualised (Figure 5.4) in a cross section allows the potential shape of any over break to be estimated (Figure5.4).

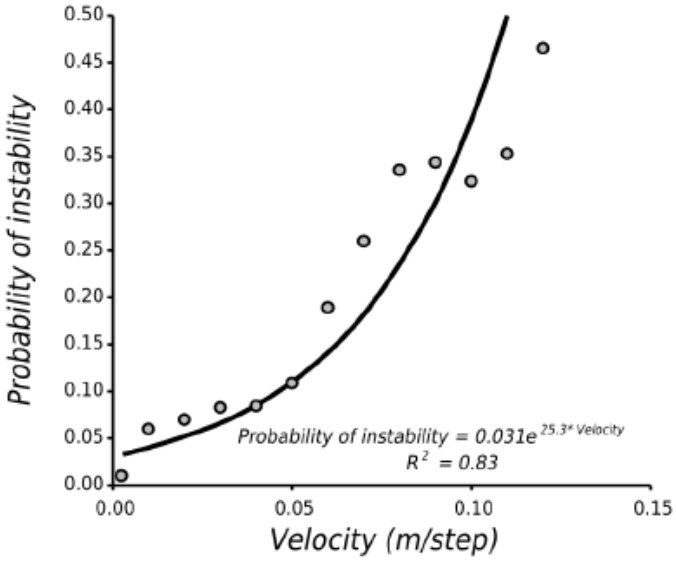

Figure 5.3: Instability criteria based on velocity only for Kanowna Belle mine. The measurements were taken in one month steps (Cepuritis 2010)**.**

As further mined stope case histories become available they will be added to the database. This helps calculate the probability of instability and the velocity relationship. The mine is then able to improve accuracy and ensure the model remains up to date with the mines conditions.

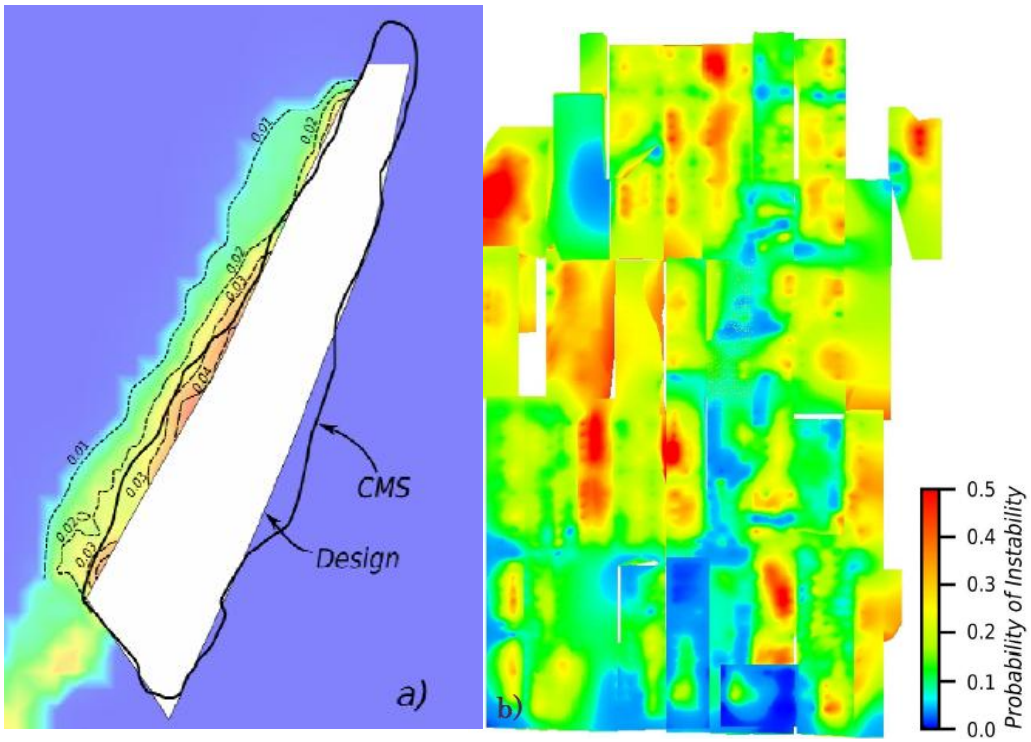

Figure 5.4: a) Cross section showing design and cavity monitoring survey geometries together with modelled velocity (m/step) and b) long section of a section of stopes showing the probability of hangingwall instability, estimated from the velocity instability criteria at Kanowna Belle mine (Cepuritis 2010).

5.4 Application at Olympic Dam

The relationship between velocity and unstable points has been investigated at Olympic Dam to generate a guide for forecasting stope surface stability. Although there are still areas for improvement the initial trial as discussed below, has produced excellent results. This method is completely separate from the Mathews stability method.

5.4.1 Numerical modelling

The existing numerical model of stoping at Olympic Dam was created by Beck Engineering. It was generated using Abaqus Explicit, a general purpose, 3D, non-linear, continuum or discontinuum finite element analysis software.

The Levkovitch Reusch (LR2) model was used by Beck Engineering. In the model softening, weakening and changes in other material properties are all described as a function of strain. This enables softening to occur gradually and simulates, as closely as possible, what is observed in 'real' rock (Beck 2009). As all of the parameters in

the model can vary at different rates, with respect to the strain changes, approximation of complex stress-strain behaviour can occur.

Initially a global model was created. This incorporated all mined and planned stope geometries, access development and mapped mine-scale structures. There were no new measurements taken for the rock mass model, instead relying on existing information. The stress field that was used is based on the measurements from AMC's report "In situ stress field for Olympic Dam mine" (as discussed in Chapter Two) (Figure 5.5).

The Olympic Dam Geotechnical Department provided the material properties. A copy of the table provided is given in Appendix I. The softening parameters were estimated using conventional ratios for moderate strength rocks.

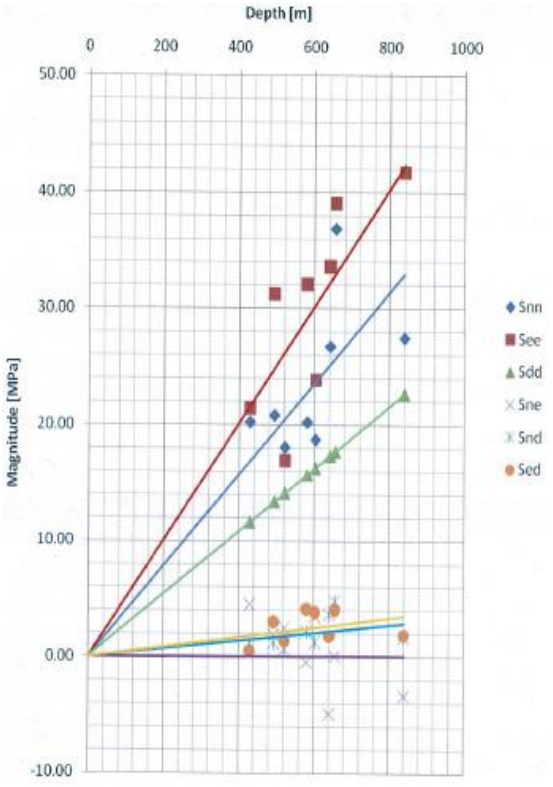

Figure 5.5: Simple logistic regression to estimate far-field stress inputs for the model (Beck 2009).

From the global model, three smaller more detailed sub-models were created. These incorporate the main areas of mining activity in the Olympic Dam ore body (Table 5.1) (Figure 5.6). Strain outputs and tractions of the global model defined the boundary conditions of the sub-models for each extraction step. The evaluation points in the sub-model used for stability function calculations are spaced between one and two metres apart. The steps in model are one month apart (plus or minus one week).

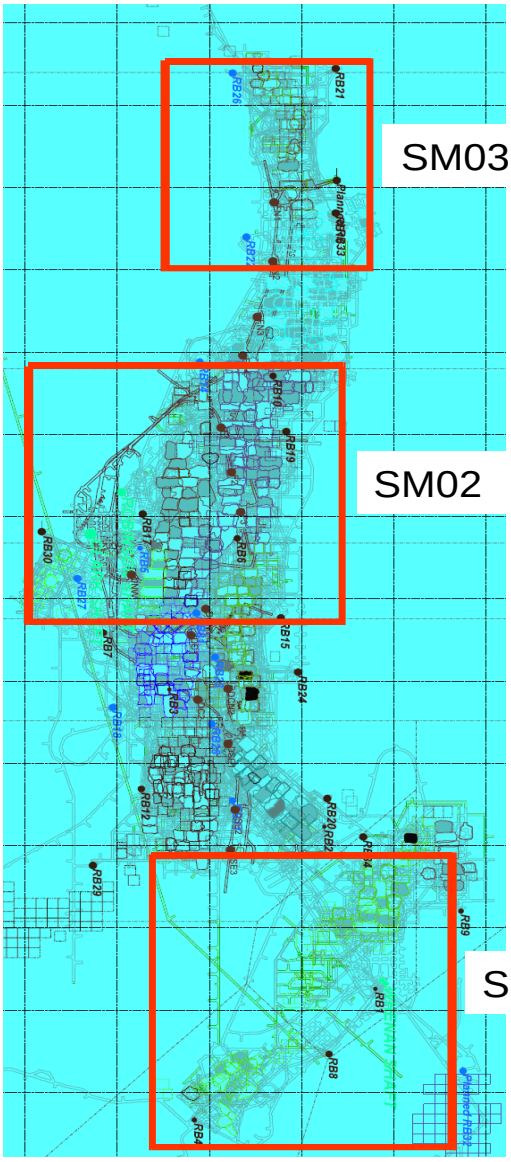

Figure 5.6: Approximate location of the three sub-models on the mine plan.

Table 5.1: Sub-model naming convention and coordinates (mine plan grid)

Sub-Model	Approximate coordinates
SM01	33000mN to 33800mN
SM02	34500mN to 35000mN
SM03	35500mN to 36150mN

5.4.2 Velocity analysis at Olympic Dam

The workflow, as outlined in the previous section, was undertaken at Olympic Dam with the assistance of David Beck of BE. The 3D visualisation was undertaken using Voxler 2. All further analysis was completed using Microsoft Excel.

The stopes included in the numerical modeling at Olympic Dam had to meet two criteria. Firstly they needed to be included in the back analysis undertaken in Chapter Three and secondly to fall within one of the three stope sub-models. This provided a database of 42 completed stopes; 11 stopes from sub-model 1(SM01), 15 from sub-model 2 (SM02) and 16 from sub-model 3 (SM03).

To categorise the stability of points in and above the crown of each of the stopes, the cavity monitoring survey data for each stope was opened with each of the points surrounding the mined stope being classed as either stable or unstable. This classification was dependent on whether they fell within or without the confinement of the cavity monitoring survey void. Unstable points were allocated a number 1 and stable points a number 2. The volume of the points above the crown varied for each stope. This ensured all unstable points were included (Figure 5.7).

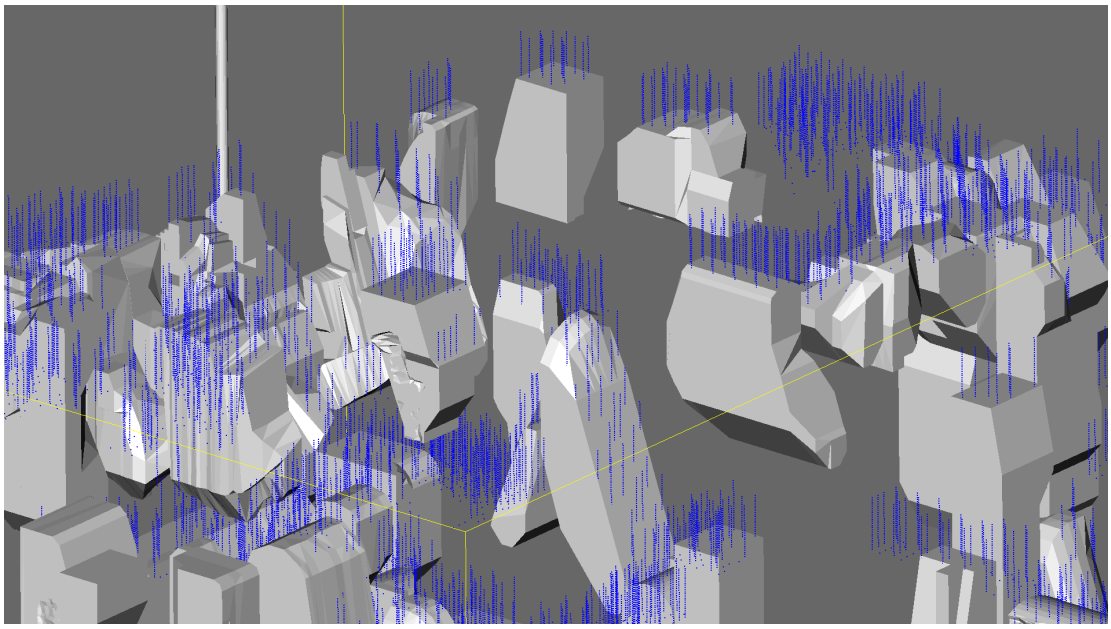

Figure 5.7: Screen shot of point arrangement above stope (design shapes) crowns in Voxler 2.

The reason why the points became unstable is because the balance of stress/strain/strength/structure wasn't sufficient for them to stay connected to the rest of the rock. The numerical model applied in to the rock mass simulates this exact same balance.

Once the points had their stability classification (stable or unstable) they were then plotted with their modeled velocity values. The velocity is the rate of downwards movements in a stope crown (Figure 5.8). The velocity value for each point was derived from the sub-model data, allowing a probability relationship to be derived based on the value of velocity and the likelihood of the points instability. This is simply comparing modelled velocity for points that fell off, to points that didn't fall off.

In the initial plot, 42,822 points from within and above the 42 stope crowns provided a strong correlation with a R^2 value of 0.8299 (Figure 5.8). A clear relationship can be seen with the increase of velocity and the increase of the likelihood of instability. That is if a single point moves 100mm in a single step (1 month) it is expected that the point will become unstable greater than 40% of the time. In other words the rock mass which that point represents has a probability of around 40% of becoming over break.

The strong relationship between velocity and the likelihood of instability was in some respects unexpected due to the absence of a small scale structure component in the numerical model. This may suggest that rock mass damage combined with structure is the dominant mechanism of over break. That is to say a continuum representation captures much of the over break. It is only instability which is solely structurally controlled which cannot be captured by a continuum model.

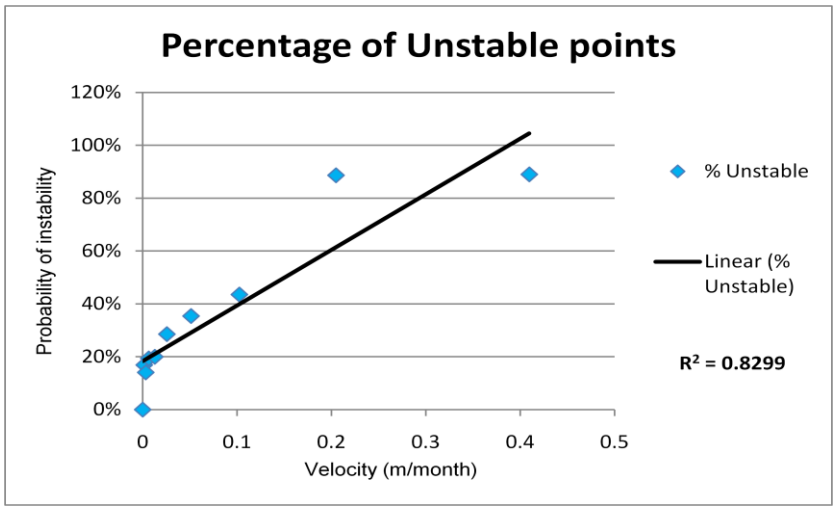

Figure 5.8: Initial plot comparing the modelled velocity and probability of rock mass instability at these velocities.

In order to ensure the relationship accurately reflects the behaviour of the rock mass at Olympic Dam on a stope by stope basis, the velocity rates were compared with the actual over break of a range of stopes from across the three sub-models. A majority of the mined stopes with cavity monitoring survey shapes conformed to the probability of instability relationship while others showed a weaker relationship.

Above the crown of a stope located near the centre of SM02 (Figure 5.9), the only points remaining located outside of the cavity monitoring survey shape have velocity values that reflect a low (0 – 25%) probability of instability. If the model was incorrect, it would display a series of points remaining stable (outside the cavity monitoring survey shape) with high percentages of probability of sloughing. This scenario was witnessed in another stope from SM02 (Figure 5.10). Although the probability values do not exceed 30% they are still significant. If this stope had been designed using the new method a more conservative design may have been adopted in recognition of the probability percentage.

There are numerous explanations for why or how these points remained stable. One such explanation is that an error may have occurred with the sequencing in the model, resulting in incorrect values being displayed. Another explanation is that crown cablebolts effectively held the ground in place, particularly as the final crown shape is uniform across the crown with very little over-break across the entire surface. Further, under-break around the corner of the stope would not have been picked up in the model. This is of particular relevance with this stope due to its previously mined, backfilled adjacency. Other possibilities include good design and rigid implementation of drilling and blasting procedures. Advantageous ground conditions may also have contributed.

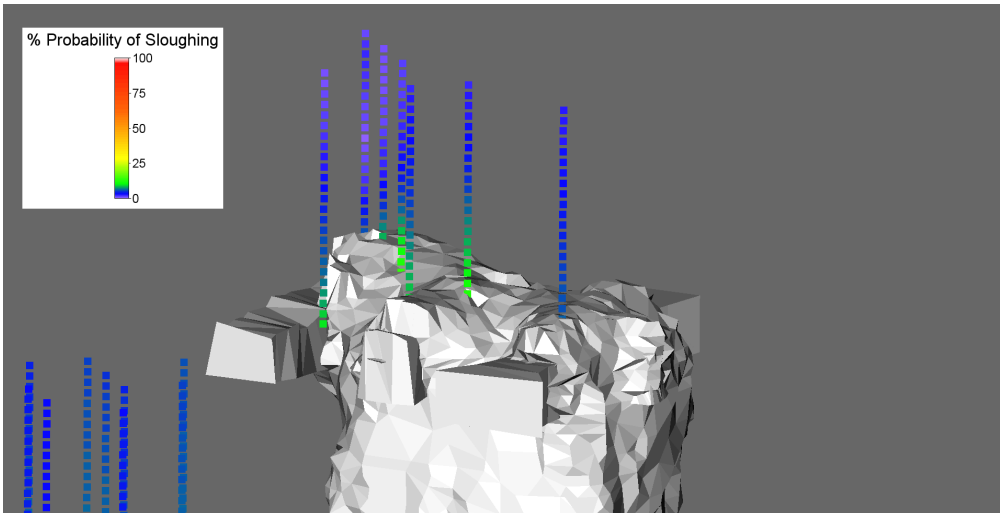

Figure 5.9: Screen shot from Voxler showing the cavity monitoring shape of a mined stope from SM02, the coloured points represent the % probability of sloughing as quantified by the scale shown. The probability scale was defined from the initial plot of unstable points and there modelled velocity from the mined stopes at Olympic Dam.

The majority of the stopes loaded with cavity monitoring survey having a percentage probability of sloughing reflected the expected relationship. This indicates that the method will be adequate as a stability indicator for stope crowns. Around 60% of the sample stopes clearly reflected the relationship (Figure 5.11). Less than 15% of the stopes were a poor match. The remainders were a strong qualitative match, falling inside the general category of over break (for instance high or low).

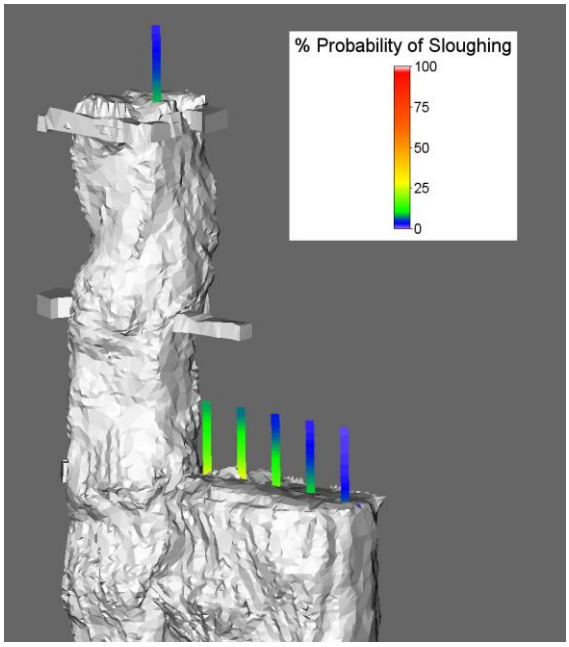

Figure 5.10: Screen shot from Voxler where the crown of the lower stope remained stable despite the percentage probability of sloughing being around 30%

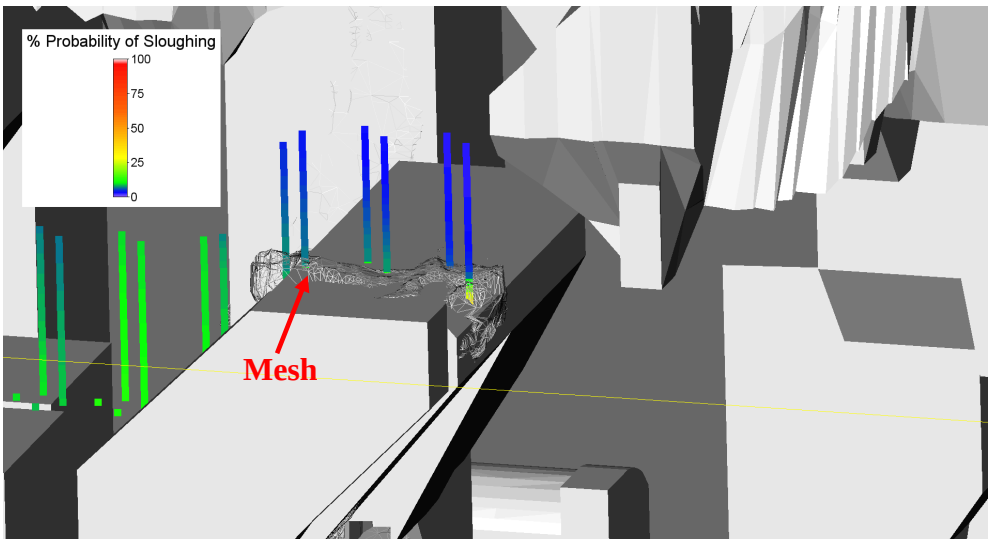

Figure 5.11: Screen shot from Voxler where stope crown behaviour reflects the expected performance based on velocity values. The block shapes represented stope design and the mesh represents the cavity monitoring survey shape.

5.4.3 Applying velocity as a stability forecasting tool

The initial modelled velocity and instability probability plot infers that the larger the modeled velocity value for a point within the material surrounding a stope, the more likely that point is to become over break. This strong correlation can be utilised as a tool to predict stope stability. It can be concluded that a stope crown's probability of instability can be estimated using the rate of modeled velocity (as computed by a model).

The most effective way of applying this relationship is visually. By opening the stope design shape in Voxler, or other similar software and applying the percentage of probability scale. The final crown shape can be estimated or the overall stability of the crown can be determined (Figure 5.12). The engineer can then consider factors not accounted for by the model, such as better or worse than normal blasting practice and the influence of structures.

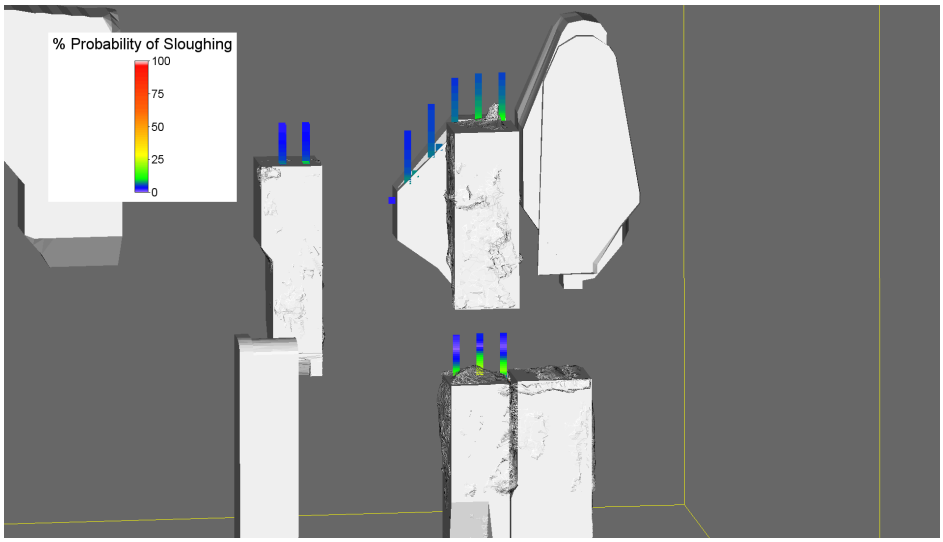

Figure 5.12: Screen shot from Voxler, the designed stope shapes are the solid blocks while the actual performance (cavity monitoring data) is displayed by the mesh.

5.5 Conditions and limitations of results

The above results are a promising start in the development of a stope stability forecasting tool for Olympic Dam. However there are some limitations that must be considered before the method is implemented.

As the method assumes that surface failure will be preceded by increasing rates in displacement (velocity), failures that are bound by persistent structure will only be accurately forecast if the structure is modelled explicitly. This limitation could be avoided with the addition of more structural data collected at Olympic Dam, and with the generation of a mine-scale structural model being incorporated into the numerical model. Current computational capacity allows for this, but would limit the choice of software to a few select codes.

If a point is moving at a high velocity, such as 400mm a month at Olympic Dam, it is unstable. Therefore instability and high velocity are essentially one and the same. This makes velocity an ideal stability indicator. One limitation of the application is that it is difficult to accurately model velocity. This limit is unavoidable and is therefore acknowledged but accepted because the same model is used for all stopes within the ore body. This limits high-end and high-accuracy analysis as outlined at

Olympic Dam. This is becoming more commonplace, but is not currently standard in Australian mines.

Only current sub-model stopes were included in the calibration of this model. Future stopes, particularly new stoping areas, will require the extension of the sub-models in order to use this method.

Although the general idea of the model may be applied at other mines, the model developed in this thesis will only be suitable for application at Olympic Dam. This is of particular importance as the mine has significantly harder rock and an unusual lack of prominent structures. This is unlike most other SLOS method mines. To be accurately applied at other sites the workflow depicted earlier will need to be emulated in local conditions.

As mentioned in the discussion of the results the crown cablebolts contribute to conservative analysis. In some cases as they support material that otherwise may be unstable. Allowing for this support during the design stage of the stope will assist avoiding conservative design.

5.6 Possible Improvements and Recommendations

After experimentation with modelled velocity as a stability indicator at Olympic Dam, it can be concluded that the model can be effectively utilised during crown stability forecasting. Due to the rate of design and the turnover of stopes at Olympic Dam, a period of at least five years is required to truly assess and calibrate the proposed new model. It is recommended a five year trial be implemented. This trial period would allow the model to be applied in the design of new stopes and for the final results to be compared with the predicted stability. This testing would be performed through a back analysis the same as or similar to the one completed in Chapter Three.

A major improvement, as identified earlier would be the incorporation of a mine-scale structural model into the model. Although the current model is adequate for long term planning, the addition would allow potential structurally controlled failure to be

identified and mitigated prior to production. Neither the Mathews method nor the new method are currently capable of this. More structure would also allow detailed local scale analysis. This would allow the assessment of sequencing options for an individual stope.

In addition, the numerical model applied in the Olympic Dam case study was not generated with over break analysis in mind. Improvements may be seen if the model was re-run, incorporating the entire mine and with a better reconciliation with current schedule and design data. Once the model is up and running, the periodical addition of new data would ensure that the conditions at Olympic Dam are reflected as accurately as possible.

The instability relationship identified by velocity or the probability of instability has the potential to indicate the amount of over break that can be expected from a designed stope surface. Using an agglomerate of points with known velocity values, the likelihood of instability of a geometric failure can be defined. By combining the likelihood of a point being unstable with the known tones of a designed stope, the final surface may be estimated. Therefore the volume of over break can be estimated.

Crown cables are designed to mark the top of the stope. They ensure material cannot continue to unravel into the void and become over break. They are intended to aid potentially unstable material to remain stable. Incorporating this as a factor in the model would assist in avoiding overly conservative crown design.

The velocity analysis should be undertaken not only for the crown of the stope but also the walls. There is a possibility the results would be similar. Therefore one scale percentage of sloughing probability could be used for all five stope surfaces. However the workflow completed in this study in relation to the crowns needs to be repeated for walls. This would develop the most accurate relationship possible.

It is worthwhile determining whether one relationship could be used for the design of all walls despite their orientation and location. Alternatively a series of guidelines could be developed for each of the stope walls. Such guidelines would define the relationship for each wall individually and then compare the variance in results.

5.7 Success of velocity as a stability indicator at Olympic Dam

As a stability indicator, velocity allows the user to consider what the material will do, rather than what the excavation's behaviour will be. While the Mathews method gives an aggressive and broad yes or no type answer for each surface, the velocity based model determines whether each individual point within the material is stable or unstable. From this, a percentage of the surface can be deemed as stable or unstable. There is no apparent reason why the velocity method could not also be successfully applied to the wall surfaces. With some fine tuning the method has the potential to be effectively applied at Olympic Dam.

5.8 Synthesis

As noted in the introduction to this Chapter the application of modelled velocity as an indicator of stability and the Mathews stability method are very different and completely separate approaches to stope stability forecasting.

The Mathews stability method is based on a series of parameters based on rock mass characteristics. The final method was calibrated based on a series of case history mined stopes. The application of modeled velocity is based on material stability and the recommended relationship is derived from the behaviour of previously mined stopes at Olympic Dam.

While both methods have their own strengths and short comings one similarity the two methods have is the inability to predict structurally controlled failure. The remainder of the limitations in the application of the Mathews stability method at Olympic Dam that were acknowledged in this thesis are primarily related to how it is applied, rather than within the method itself.

It is difficult to identify all of the limitations of applying modeled velocity as a stability indicator until it is applied during the design of stopes and is validated. Ideal validation would be similar to the analysis undertaken on the Mathews stability method in Chapter Two, Recommendations for the effective implementation of the modeled velocity method at Olympic Dam are made in Chapter Six.

Chapter 6. Summary and Conclusions

6.1 Thesis objectives

This thesis was focused on the application of the Mathews stability method at Olympic Dam mine. The empirical method is based on a modified version of Barton et al. (1974) tunnelling quality index. The modified tunneling quality index is incorporated with a hydraulic radius value which accounts for the geometry of the stope surfaces.

There were two primary objectives for this thesis.

1) To validate the applicability of the Mathews stability method at Olympic Dam.
2) To investigate an alternative stope stability forecasting tool at Olympic Dam.

This thesis was undertaken at the request of the Geotechnical Department at Olympic Dam due to ongoing concern with the inconsistency between Mathews stability method predictions and stope performance.

The applicability of the Mathews stability method at Olympic Dam was investigated by classifying the performance of mined stope surfaces, specifically the crown and sidewalls. The performance was classified by comparing the shape of the mined void with the stope design shape. Any rock within the mined void which was outside the design shape was classed as over break. This over break was quantified by equivalent linear over break./slough (ELOS) which calculates a numerical value by dividing the volume of over break by the area of the stope face. The performance of each surface was classified dependent on the amount of over break as shown in Table 6.1:

Table 6.1: Classification of stope performance based on ELOS values

ELOS	Performance
<0.75	Stable
0.75 - 2	Unstable
>2	Failed

From the results and subsequent analysis it was discovered the inaccuracy of the Mathews stability method predictions at Olympic Dam is primarily a result of the quality of input data and the application, not the method itself.

6.2 Mathews stability method

The Olympic Dam Breccia Complex is host to a copper-gold-uranium ore body, this ore is extracted by sub level open stoping (SLOS). The validity of the application of the Mathews stability method at Olympic Dam was quantified by performing a back analysis study of open stope performance. The performance was quantified solely on the amount of over break on each surface.

This analysis of stope performance at Olympic Dam confirmed there are inconsistencies between the Mathews stability method classification of stope surfaces and their performance. The results showed 41% of all the Mathews predictions were correct and the remaining 59% were incorrect. Of all the predictions 42% were conservative. Only 6% of failed predictions were correct, 22% of unstable predictions were correct and 71% of stable predictions were correct.

The hypothesis assumed that the Mathews stability method was not suited to the Olympic Dam rock mass, however the majority of the identified limitations were a result of how the method is applied not the method itself. Some possible solutions to these limitations were identified:

1) Implement a detailed quality assurance quality control (QAQC) system to track the performance of mined stopes with reference to the design.
2) When applying ELOS during the QAQC process add another category to the classification of surface performance. Another catrgory would separate the surfaces with catastrophic failures from those which have extensive over break.
3) Undertake more window mapping close to upcoming stopes.
4) Install a series of live stress measuring stations around the mine.
5) Attempt to incorporate structures into the Mathews stability number.

6) Perform statistical analysis such as logistic regression to ensure the zones on the Mathews chart are the best fit possible to Olympic Dam.

6.3 Velocity as a stability indicator

Alternative methods to the Mathews stability method which could potentially be implemented at Olympic Dam for stope stability forecasting were researched. Velocity was selected and successfully trialled as a stability indicator at Olympic Dam. The method is based on a high resolution non-linear numerical model where modelled values of displacement, strain and velocity are allocated to evenly spaced points within the rock mass. The modelled velocity value represents the rate of movement of the points within the rock mass, relative to the designed stope.

The method of applying velocity as a stability indicator was trialled at Olympic Dam using an existing high resolution non-linear numerical model. The points from the model, were allocated a stability classification. They were classed as unstable if they fell within the mined void but outside the design shape of the stope. These unstable points were then used to depict the relationship between modeled velocity and the probability of instability. A strong correlation between the increase in modelled velocity and the increased probability of instability was achieved, for example a point which is being displaced at a velocity of 0.2m/month has a 60% probability of becoming unstable.

Velocity is an upper bound stability indicator, therefore there are advantages of applying it to stope surface stability forecasting. The velocity method does not rely on the broad model but specific points. Because the Olympic Dam ore body is heterogeneous relying on one generic model to cover the entire mine in regards to rock properties and behaviours is unrealistic.

Some limitations of the velocity have been identified, such as the inability of the method to predict structurally controlled instability. The relationship that was defined in this study only depicts the behaviour of the Olympic Dam rock mass. It should not be generically applied to other rock masses.

. For effective application at other mine sites these recommendations are made:

1) Must have a non-linear elasto-plastic finite element numerical model available, inclusion of a small-scale structure model is preferred particularly at a mine where structurally controlled failure is dominant.
2) Perform a back analysis study to ensure the model is accurately predicting stope surface performance.
3) Allow for a trial period so the stopes which are analysed with the new method during their design period to be examined after mining to validate the methods applicability.

6.4 Recommendations for future work

These improvements will allow modeled velocity to be confidently applied as a stope stability indicator at Olympic Dam mine:

1) This study has successfully applied velocity as stability indicator. However it is recommended that a five year trial is instilled giving the mine technical services department the opportunity to apply the model in design of stopes and see the results once stopes completed.
2) The creation of a discontinuum model for Olympic Dam. Discontinuum models are approximately 15% more expensive than a continuum model but much more effective in prediction than continuum by providing a small-scale structural model. Structure needs to be explicitly represented to accurately forecast overbreak.
3) In order to best learn through experience, it is important to have a thorough and consistent stope performance-monitoring schedule. This should be done by implementing a thorough quality assurance quality control (QAQC) program. The details of the stope design and it's underlying assumptions and the history of the stopes performance from initial firing through to backfilling should be included as part of a stope record. The stope record should include notes from throughout the design and production as well as a back analysis.
4) Drill hole deviation should be recorded and controlled.
5) Live or more regular stress measurements should be undertaken.

6) The LR2 model should be updated regularly to ensure data is parallel with the mines current conditions.

6.5 Conclusions

The Mathews stability method correctly predicted the performance of 41% of the surfaces from 124 stopes included in this study at Olympic Dam. To be classed as a reliable predictive tool this percentage should be the order of 80%. There were several improvements that could be made to the application of the method at Olympic dam to achieve this. All of the recommended improvements are achievable. Therefore it is not recommended that the Mathews stability method be completely removed from the stope design process at Olympic Dam.

It is recommended that the application of modeled velocity as a stope stability indicator is trialled over a five year period to gain a comprehensive understanding of its applicability. This should be undertaken in conjunction with the improvements to the Mathews stability method. This may be a permanent arrangement or only carried out until one method can be justified as more applicable to stope design at Olympic Dam than the other.

References

Barton N., LR, Lunde J. 1974, 'Engineering classificationof rock masses for the design of tunnel support', *Rock Mechanics*, vol. 6, pp. 188-236.

Bawden, WF 1993, 'The use of rock mechanics principles in Canadian underground hard rock mine design', in Hudson (ed.), *Comprehensive Rock Engineering: Principles, Practice and Projects*, vol. 5, Pergamon Press, Oxford, pp. 247-90.

Beck, D 2009, *Olympic Dam, Global Open Pit and Underground Interaction*.

BHPBilliton 2010, Olympic Dam Underground Control Management Plan, BHP Billiton, Olympic Dam 4814.

Bieniawski, ZT 1989, 'Engineering rock mass classifications: a complete manual for engineers and geologists in mining, civil, and petroleum engineering', *Engineering rock mass classifications: a complete manual for engineers and geologists in mining, civil, and petroleum engineering*.

Bridges, MC 2007, *In situ stress field for Olympic Dam*, Australian Mining Consultants.

Campbell, IH, Compston, DM, Richards, JP, Johnson, JP & Kent, AJR 1998, 'Review of the application of isotopic studies to the genesis of Cu-Au mineralisation at Olympic Dam and Au mineralisation at Porgera, the Tennant Greek district and Yilgarn Craton', *Australian Journal of Earth Sciences*, vol. 45, no. 2, pp. 201-18.

Cepuritis, PM, Villaescusa,E., Beck, D., Varden., R. 2010, 'Back analysis of Over-break in Longhole Open Stope Operation using Non-Linear Elasto-Plastic Numerical Modelling', in *44th US Rock Mechanics Symposium and 5th US.-Canada Rock Mechanics Symposium*, Salt Lake City, UT, June 27-30 2010.

Consultants, A 2002, *Review of Stope Performance Issues*, 202014.

Consultants, A 2004, *Olympic Dam Operations, Stability Graph Back Analysis*, 104078.

Creaser, R. A. 1989 *The geology and petrology of Middle Proterozoic felsic magmatism of the Stuart Shelf, South Australia.Ph.D. Thesis*, Melbourne, La Trobe University.Unpublished

Daly, SJ, Fanning, C.M., Fairclough, M.C. 1998, 'Tectonic evolution and exploration potential of the Gawler Craton, South Australia', *AGSO J. Australian Geol. Geophys.*, vol. 17, no. 3, pp. 145 - 68.

Deere, DU, Hendron, A.J., Patton, F.D., Cording, E.J. 1967, 'Design of surface and near surface construction in rock', *Failure and breakage of rock, proceedings 8th U.S symp, rock mech.*, ed. C.Fairhurst, Society of Min.Engrs, Am. Inst Min.Metall. Petrolm Engrs, New York, pp. 237 - 302.

Diederichs, MS & Kaiser, PK 1999, 'Tensile strength and abutment relaxation as failure control mechanisms in underground excavations', *International Journal of Rock Mechanics and Mining Sciences*, vol. 36, no. 1, pp. 69-96.

Fukuzono, TA 1985, 'A new method for predicting the failure time of a slope.', *Fourth international conference and field workshop on landslides.*, Japan Landslide Society, Tokoyo, Japan, pp. 145-50.

Haynes, DW, Cross, KC, Bills, RT & Reed, MH 1995, 'Olympic dam ore genesis: a fluid-mixing model', *Economic Geology*, vol. 90, no. 2, pp. 281-307.

Hoek, E, Brown, E.T. 1990, *Underground excavations in rock*, Taylor & Francis, Abingdon, Oxon.

Hoek. E., KPK, Bawden. W.F. 1997, *Support of Underground Excavations in Hard Rock*, 1st edn, A.A.Balkema Publishers, Rotterdam.

Hoek, E 2006, 'Practical Rock Engineering'. Evert Hoek Consulting Engineering Inc, North Vancouver, Notes.

Hutchinson, DJ, Diederich, M.S 1996, *Cablebolting in Underground Mines*, BiTech Publisher Ltd, British Columbia.

Laubscher, DH 1990, 'A geomechanics classification system for the rating of rock mass in mine design', *Journal of South African Institue of Mining and Mettalurgy*, vol. 90, no. 10, p. 16.

Martin, CD, Kaiser, PK, Tannant, DD & Yazici, S 1999, 'Stress path and instability around mine openings', *20th Century Lessons, 21st Century Challenges.*, pp. 311-5.

Mawdesley, C, Trueman, R & Whiten, WJ 2001, 'Extending the Mathews stability graph for open-stope design', *Mining Technology: Transactions of the Institute of Mining & Metallurgy, Section A*, vol. 110, no. 1, p. 27.

Mawdesley, CA 2004, 'Using logistic regression to investigate and improve an empirical design method', *International Journal of Rock Mechanics and Mining Sciences*, vol. 41, no. SUPPL. 1, pp. 3A 07 1-6.

Nickson, SD 1992, *Cable support guidelines for underground hard rock mine operations*, University of British Columbia.

Oddie, ME 2004, *Minimum Ground Support Requirements for Development Headings at Olympic Dam*, Australian Mining Consultants, Melbourne.

Pakanis. R., NS, Lunder. P., Clark. l., Milne. D., Mah. P. 1996, 'Emperical Methods for the design of Mine Structures', in *Colleque en controle de terrain de l'Association Miniere* Quebec, 12 March 2006..

Potvin, Y 1988a, *Emperical Stope design in Canada*, University of British Columbia, Canada.

Potvin, Y, Hudyma, M., Miller, H.D.M.S. 1988b, 'The stability graph for open stope design', in *90th CIM AGM*, Edmonton.

Potvin, Y, Milne, D. 1992, *Emperical cable bolt support design*, Rotterdam

Reeve., ea 1990, 'Olympic Dam copper-uranium-gold-silver deposit', in Hughes (ed.), *Geology of the mineral deposits of Australian and Papua New Guinea. Australasian Institute of Mining and Metallurgy*, pp. 1009 - 10035.

Reusch, F, Beck, D., Tyler, D. 2008, *Quantitative forecasting of sidewall stability and dilution in Sub-level Caves*.

Reynolds, LJ 2000, 'Geology of Olympic Dam Cu-U-Au-Ag-REE Deposit', in Porter (ed.), *Hydrothermal Iron Oxide Copper-Gold & Related Deposits: A Global perspective*, vol. 1, PGC publishing, Adelaide, pp. 93-104.

Rose, ND & Hungr, O 2007, 'Forecasting potential rock slope failure in open pit mines using the inverse-velocity method', *International Journal of Rock Mechanics and Mining Sciences*, vol. 44, no. 2, pp. 308-20.

Stewart, PC, Trueman, R. 2001, 'The extended Mathews stability graph: Quantifying case history requirements and site-specific effects', in *International Symposium of Mining Techniques*. CIM, Quebec, p. 9, 2001, Conference paper.

Stewart, PC, Trueman, R. 2003, 'Applying the Extended Mathews stability graph to stress relaxation, site-specific effects and narrow-vein stoping', in *Ground Control in Mining*, ed. BK Hebblewhite. UNSW School of Mining Engineering, Scientia, UNSW, p. 7, 2003, Conference paper.

Stewart, SBV & Forsyth, WW 1995, 'The Mathew's method for open stope design', *CIM Bulletin*, vol. 88, no. 992, pp. 45-53.

Suorineni, FT, Tannant, DD & Kaiser, PK 1999, 'Determination of fault-related sloughage in open stopes', *International Journal of Rock Mechanics and Mining Sciences*, vol. 36, no. 7, pp. 891-906.

Suorineni, FT, Kaiser, PK & Tannant, DD 2001a, 'Likelihood statistic for interpretation of the stability graph for open stope design', *International Journal of Rock Mechanics and Mining Sciences*, vol. 38, no. 5, pp. 735-44.

Suorineni, FT, Tannant, DD & Kaiser, PK 2001b, 'Incorporation of a fault factor into the stability graph method: Kidd mine case studies', *Mineral Resources Engineering*, vol. 10, no. 1, pp. 3-37.

Terzaghi, K 1946, 'Rock defects and loads on tunnel supports', in RV Proctor, White, T.L. (ed.), Rock tunneling with steel supports, vol. 1, Commercial Shearing and Stamping company, Youngstown, OH, pp. 17-99.

Trueman, R & Mawdesley, C 2003, 'Predicting cave initiation and propagation', *CIM Bulletin*, vol. 96, no. 1071, pp. 54-9.

Trueman, R, Mikula, P, Mawdesley, C & Harries, N 2000, 'Experience in Australia with the application of the Mathews' method for open stope design', *CIM Bulletin*, vol. 93, no. 1036, pp. 162-7.

Villaescusa, E 2000, 'A review of sublevel stoping', *Australasian Institute of Mining and Metallurgy Publication Series*, 7 edn, pp. 577-90.

Villaescusa 2004, 'Quantifying open stope performance', in *MassMin*, Santiago Chile, August 2004.

Vongpaisal, S, Li, G, Pakalnis, R & Brady, T 2009, 'New 3D engineering curves for predicting stope stability and mining dilution in longitudinal blasthole mining operations', *International Journal of Mining, Reclamation and Environment*, vol. 23, no. 2, pp. 92-102.

WealthMinerals 2002, *Wealth mining*, Wealth minerals Ltd, Vancouver. Retrieved 10/01/2011, from www.wealthminerals.com/s/UraniumMining.asp

Williams, PJ, Barton, M.D., Fontbote, L., de Haller, A., Mark, G., Oliver, N.H.S., Marschik, R. 2005, 'Iron oxide-copper gold deposits: Geology, space-time distribution, and possible modes of origin', *Economic Geology*, vol. 100, pp. 371 - 405.

Yu, HS 2006, *Plasticity and Geotechnics*, Springer Science+Business Media, LLC, New York.

Appendices

Appendix A: Olympic Dam Geological and Geotechnical literature review.

Introduction to Olympic Dam Geological and Geotechnical Background

1. Introduction

The Olympic Dam Cu-U-Au-Ag-REE deposit is located in the Stuart Shelf geological province of South Australia, on the eastern most margin of the Gawler Craton. The deposits lie wholly within the Olympic Dam Breccia Complex (ODBC) populating only a small portion of the breccias volume with mineralised ore. In the following summary the geological framework of South Australia was explored and reviewed by accumulating information from a variety of sources. Rockmass quality explored includes the identification and investigation of the five major joint sets at Olympic Dam. The block size analysis aspect showed RQD values ranging from 55 (worst) to 100 (best). Further investigation of joint surface conditions showed a variety in roughness between rough undulating and planar smooth exists with little in the way of surface alteration, very rarely low friction clay minerals were identified (worst).

The Olympic Dam deposit is a giant iron-oxide associated copper-uranium-gold-silver-REE deposit in barren South Australia, near the township of Roxby Downs around 520 km north-north-west of Adelaide (Hitzman, 2005). Discovered in 1975 by exploration studies conducted by Western Mining Company (WMC) the deposit contains ore reserves in excess of 600 Mt averaging 1.8% Cu, 0.5 kg/t U_3O_8, 0.5 g/t Au and 3.6 g/t Ag (Reynolds, 2000). The ore is exploited by underground open stope

extraction methods at a rate of around 9 million tones of ore per annum, with all the ore being processed to a marketable product on site.

2. South Australian Geological Framework

Modern South Australia is a tectonically stable region of the crust, punctuated only by relatively minor epirogenic movements highlighting the unique setting of the island continent Australia. There are no modern mountain ranges related to crustal or intercrustal collisional zones and no volcanic or seismic activity.

A little over a million years ago the island continent of Australia was attached to Antarctica along its present southern margin. It was a component of the much larger Gondwana 'super-continent'. South Australia was adjacent to Wilkes Land and George V Land; as a result the state shares many of the same geological units with these land masses. Comparable units such as late Archaen to earliest Proterozoic hypersthene Gneiss, amphibolite and granitoid gneisses can be seen in both South Australia and Commonwealth Bay (Parker, 1983).

Prior to separation from Antarctica the southern margin of Australia was dramatically thinned by extension of the crust offshore from mainland South Australia. The zone of extension was related with the eruption of Jurassic Basalts (e.g. Kangaroo Island) and the commencement of thick sediment accumulation, including the Otway, Duntroon and Bight Basins. The basement and younger rocks of Australia represent over 80 percent of the entire geological history of the earth, with sediments, lavas and igneous and metamorphic complexes as old as Archaen (more than 2,300 million years old). This divergence of Australia and Antarctica occurred about 95 million years ago

Deep crustal structure

The composition of the mantle underlying South Australia is not well defined but is assumed to be like the mantle under most stable crustal plates. Deep crustal structures below Australia are limited as there are no actively subducting plates, no major zones of upwelling mantle and no intracontinental rift zones; this is reflected in the absence of any ridge related volcanism on the surface. A deep root crustal

structure lies beneath the main uplands of Mount Lofty and the Flinders Ranges and irregularities can be seen in the Moho topography below the prominent Adelaide geosyncline structure generated by extensional faulting. All depressions or geosynclines appear to have displayed continual activity throughout geological time.

The Precambrian crystalline basement

Knowledge of the Precambrian rocks is still inadequate, but geological mapping, isotopic dating and geophysical surveys have increased this knowledge significantly in decades passed. The Australian Precambrian shield rock mass, forms a basement beneath a relatively unaltered younger cover rock sequence. High grade metamorphism in the eastern area of the state due to folding and granite intrusions interferes with the interpretation of basement rock.

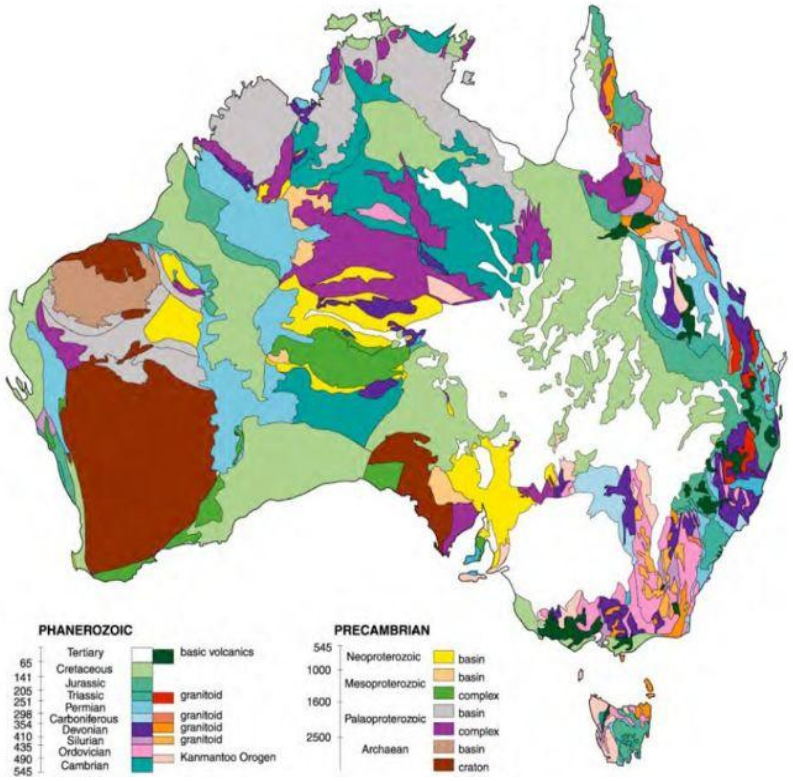

Fig 2.1: Geological units of Australia (Ludbrook, 1980)

There are differing views on the subdivision of the Precambrian, the scheme discussed here is based around the stratigraphic positioning and layering of volcanic units and there isotopic derived ages. Three major sedimentary basins appear to have preserved complete Proterozoic records with the Adelaide Geosyncline being the only one located in South Australia.

Tectonic framework

The crustal rock movements of the South Australian region can be divided into three parts; the Gawler Platform, Adelaide Geosyncline orogen and the great

Musgrave Block. An array of major faults, shears and hinge lines reflects the shields fragmentation, wide extremes of pressure and temperature and variations of fold patterns show the shield has undergone more than one cycle of folding and metamorphism. As much as 80,000 feet of sediment was accumulated in this area in the time interval 1,400 and 600 million years ago. An overall northeasterly trend is abundant in many of the fold belts in South Australia. Some basement areas are discussed in more detail below, particular emphasis is based on the Grawler Craton.

Grawler Craton

Through geological mapping, geophysical surveys and exploratory drilling it has been determined that a vast partly buried basement of Precambrian metamorphic, intrusive or extrusive crystalline rocks extend over the majority of South Australia. This shield extends northward and westward most probably to the Continental shelf. Individual basement areas have been identified, the Grawler craton is the prominent of these discrete areas in the state.

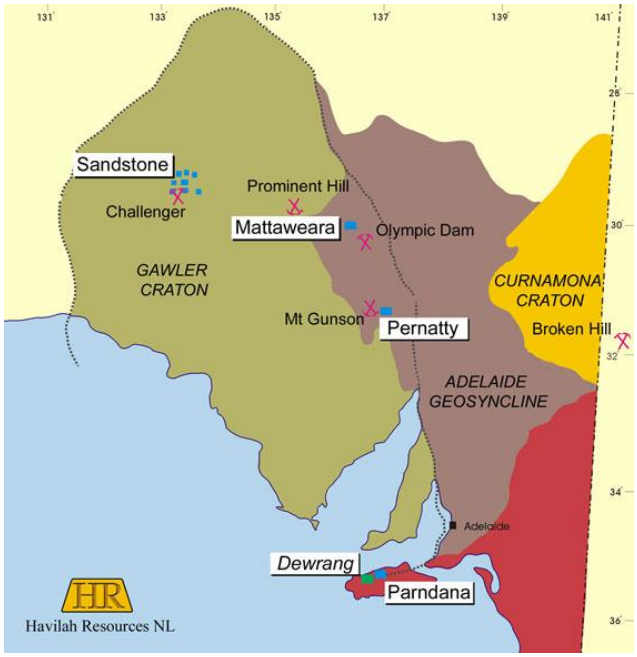

Fig 2.2: Gawler craton and neighbouring sedimentary basins (Havilah Resources, 1992)

Comprised of Archaean to Mesoproterozoic rocks mantled in part by thin platformal sediments and regoliths of Neoproterozoic to Cainozoic age (Parker, 1983). The craton is a stable crystalline basement with little evidence of deformation and remobilization, it is essentially the extension of the great shield of Western Australia interrupted by the depressed area of Eucla Basin. The eastern and southern boundaries are clearly defined while the north, northwest and west are difficult to pin point due to thick Neoproterozoic and Phanerozoic cover, however it has been confirmed the craton basement extends far into Western Australia under the Nullarbor Plain.

The craton is subdivided in to several tectonic sub-domains, these differentiations are based on metamorphic, structural and stratigraphic properties. Because boundaries are often difficult to depict they are located along prominent linear structures for convenience. The Grawler ranges are an important sub-domain of the craton which display little to no deformational history and an irregular distribution. The volcanics and sediments which compile the sub-domain are relatively flat-lying.

The Musgrave Block

Compiled of crystalline basement terrain which extends into the Northern Territory and Western Australia is a deep crustal rock which is now exposed after a complex series of tectonic events. Rotation in the trend of foliation and layering of granulites, granites and gneisses can be witnessed as the Northern Territory is approached related to global shear systems. The shear system in the Musgrave Block appears to be responsible for a chain of basic and ultrabasic intrusives which compile the Giles Intrusive Complex (Sprigg and Wilson, 1958).

A belt of well layered metamorphic rocks form the *Musgrave-Mann Metamorphics* which compile the region. Granulite facies are the dominant members, the rocks are generally completely free of hydrous minerals due to distressing. Locally intruded coarse grained feldspathic gneisses suggest certain layers were converted magma, overall the layers appear to be in there original order.

Adelaide Geosyncline

Extending from beyond Kangaroo Island in the south to the Barrier Ranges at the northern most past of the Flinders Ranges, The Adelaide Geosyncline is a Neoproterozoic to Middle Cambrian complex of rift and sag basins flanking the eastern margin of the Gawler Craton (Parker, 1990). The trough is host to more than 50,000 feet in thickness of sediment deposits from Proterozoic times. The sediments were stripped from the shield to the west as the geosyncline was sinking during a period of lithospheric stretching (Parkin, 1969). Investigations have shown that the vast thicknesses of sediment were deposited in a shallow water environment, Glacial debris is amongst the accumulated sediments.

The deeply subsident sedimentary basin underwent at least four main phases of rifting in
the Adelaidean (Neoproterozoic) and one in the Early Cambrian; 12 major transgressive–regressive cycles (sequence sets) in the Adelaidean and three in the Early to Middle Cambrian. Break up of the geosynclinal trough commenced in the early Paleozoic, when plate movements changed and the area experienced the Delamerian Orogeny (~500Ma). The orogeny is one of the four major tectonic periods disrupting sedimentation in the trough, it was related to major folding, mountain building and the intrusion of granites. Newly formed structures proceeded to undergo a long period of stripping but there is o evidence of these sediments in the area preceding the Permian only the debris from the Permian glaciation period.

The ancient geosynclinal trough is represented by the Great Artesian Basin, the Murray Basin and the Eucla Basin in the modern day. Permian marine sediments line the bases of these areas. These basins continued to sink throughout the Mesozoic and Tertiary, evidence of their mobility is identified up to reasonably recent times. However not the entire geosyncline has been disturbed deposits can still be seen on the Stuart Shelf today.

The Adelaide Geosyncline records the formation of the eastern margin of the Australian continent, to which juvenile crustal elements were subsequently accreted to during the Palaeozoic in the Tasman orogenic system. The North Flinders Zone and Nackara Arc may have faced an opening ocean at least during the later stages of evolution, but continental crust is likely to have extended at least as far ast as the South Australia and Victoria border.

Precambrian Basement Cover

At its thickest in the Adelaide geosyncline this great belt of relatively unaltered Precambrian sediments is the cover sequence of the crystalline basement. The term *Adelaidean* has been allocated to sediments of this time interval in respect to the colossal exposures seen in the Flinders ranges section of the shield. The rock sections preserved in the Adelaide geosyncline represent a time span from about 560

million years back to approximately 1,400 millions years, these dates are based on sparse isotopic dating but persistent markers throughout the shield support these ages.

The rocks of the geosyncline have been subdivided into four major units. The oldest of these units is the Callanna, associated with basic volcanic rocks including basalts and andesites as well as altered limestones. Cast structures in within the unit infer a evaporative deposition environment. Some of the recognised formations recognised in the Callanna unit include the Paralana Quartzite, the Wyawyana formation, Wooltan and Roopean volcanics.

The Burra group overlies the Callanna unit, it marks the commencement of a major sedimentary cycle of dominantly carbonate siltstones. The depostional environment of these successions was mainly lagoonal to shallow marine. This particular unit reaches thicknesses of up to 20,000 feet in the depression of the geosyncline. The age of the oldest member of this unit is around 1 million years, the Rhynie sandstone. Other members include the Skillogalee Dolomite, Woolshed Flat formation, Undalya Quartzite and the Auburn Dolomite.

The Umberatana group is associated with cycles of sedimentation related to tillites. The unit clearly indicates that two major late Precambrian ice ages occurred in South Australia. These events were also registered not only in adjacent states but in other continents around the globe including Central Africa, minimum ages of these glacial periods have been placed at around 750 million years. Thicknesses of the unit fluctuate between 12,000 and 20, thousand feet across the extent of the unit. Members of the unit include the Yudnamutana Sub-Group, the Farina Sub-Group, the Tarcowie Siltstone, the Angepena formation, the Elatina formation and the WIllohra sub-group.

The uppermost of the Precambrian units is the Wilpena group, deposited as a result of sea-level rise these shallow water and continental sediment deposits have generated an extensive blanket across the geosyncline. A transition from carbonate-sandstone-siltstone to siltstone occurs with time. In some regions the top sequence of the unit is missing meaning the deposits become 10,000 feet thick while in other areas they are 20.000 feet thick. In the Woomera area the unit is around 13,000 feet thick and appears to be thickening northward. Brachina formation, ABC Range Quartzite,

Bunyeroo formation, Wonoka formation and the Pound Quartzite are several of the Wilpena unit members.

Paleozoic Era

The onset of the Paleozoic era is characterized by the appearance of animals with external skeletons which could be preserved as fossils in sedimentary rocks. The period extends from about 580 million years to 225 million years before the present including Cambrian, Ordovician, Silurian, Devonian, Carboniferous and Permian periods. Only those sediments from the Cambrian and Permian periods are extensively preserved in South Australia.

The Cambrian Period

The Adelaide geosyncline is host to the most prominent deposition of Cambrian sediments in South Australia. The sediments are highly exposed in surface outcrops extending from Kangaroo Island to the northern Flinders Ranges. Cambrian sediments are also found in the Cooper Basin, but here they underlie Permian sediments at great depths and are not exposed as surface outcrops.

Much of the Flinders ranges are capped with Cambrian deposits, directly overlying the earlier mentioned Permian Pound Quartzite. In the trough these sediments mark the last deposition prior to the final deformation event.

Basal Cambrian units are characterized by a thick succession of dark coloured carbonates and shales. The remainders of the Cambrian sediments were deposited in evaporite "red-bed" and carbonate environments. The mobile behaviour of the Adelaide Geosyncline means Cambrian deposits are characterized by regular fluctuations in thicknesses and facies resulting in interbedded units, these sediments are collectively referred to as the Hawker Group (Parkin, 1969). Rock groups included in this collaboration include the Parachilna Formation, Kulpara Limestone, Bunkers Sandstone and the Oraparinna Shale.

The beginning of the middle Cambrian is marked by a brief interval of basin-wide shallow water deposition occurred. This is now seen as an excellent marker horizon in the Flinders Ranges. The marker is the last of carbonate deposits and is followed by red and green clastics which extend into the upper Cambrian.

The Ordovician period

Outcrops of Ordovician period rocks are limited in South Australia but can be seen in the northwest in the Mount John and Indulkana Ranges. In some regions Ordovician sediments rest on a sharp angular unconformity on steeply dipping Precambrian tillites whereas in other localitites they are underlain conformably by Cambrian greywacke siltstones and conglomerates.

At the surface outcrops the Ordovician deposits are compiled of lower and upper sandstone units separated by about 150 feet of marls and calcareous siltstones. The lower sandstone unit is medium grained quartz sandstone, with occasional lenses of conglomerate. The overlying marl beds are poorly exposed but tend to be finely micaceous. The upper sandstone is fine to medium grained with low angle current bedding. Bedding in this unit is thinner than in the lower sandstone with frequent changes in the apparent current direction.

The Silurian and Devonian Periods

Devonian period rocks have only recently been identified in the deep basins of South Australia while those of a Silurian age are yet to be reliably identified. Sandstones, conglomerates and some red beds of the Devonian period are known to underlie the west-central Simpson Desert.

Overall it has been discovered by several authors that there is very little sediments of Silurian and Devonian age in South Australia.

The Permian period

Early in this period much of South Australia was covered by ice, striated and grooved rock was discovered in 1859 by a geologist by the name of Selwyn. The discovery of marine foraminifera in Permian rocks has significantly enhanced the understanding of the nature and duration of Permian sedimentation. The Gulf St. Vincent Region, Murray Basin, Great Artesian basin and Eucla Basin are all host to Permian deposits.

Mesozoic Era

The Mesozoic era covers around 160 million years, commencing around 225 million years ago. The era comprises the Triassic, Jurassic and Cretaceous periods, in South Australia these periods represent large-scale down warping of the earths crust. At the beginning or the era South Australia's was tectonically stable, the negative movements related to the crustal down warping reached their maximum in the Cretaceous period reflected in the development of most of the states major sedimentary basins.

The Triassic period

Rocks of this period exist in only the Cooper and Great Artesia Basins and do not outcrop, but are often intersected in oil exploration drilling. The rocks are generally dolomitic sandstones and siltstones with a complete absence of marine fossils, the specific age of these sediments has not been pin pointed.

Other South Australian Triassic deposits are small and rare fresh water sediments, the most well known being the Leigh Creek Coal Measures. All Triassic sediments have been affected by post-depositional tectonic movements, resulting in the faulting, tilting and folding of the strata. This tectonic activity may explain the sparse remaining deposits of Triassic sediments in South Australia.

The Jurassic period

These sediments represent a terrestrial fresh water depositional cycle which may have exceeded the Jurassic period, the resulting sediments can be found reasonably consistently through the entire South Australian segment of the Great Artesian Basin.

These sediments provide the aquifers for the pressure water of the Great Artesian basement making them of great economic importance.

The Cretaceous period

Cretaceous rocks cover the entire South Australian portion of the Great Artesian Basin making the most extensive deposits of the Mesozoic era. Sediments were deposited following a major marine transgression at a time of stable basin

conditions. A clear transition can be seen from the terrestrial-freshwater deposits of the Jurassic to the marine environment in the lower Cretaceous.

Sediments deposited in the Cretaceous period are also present in the Murray Basin, Eucla Basin and the Otway Basin.

The Tertiary period

The beginning of the tertiary period in South Australia saw the development of much of the southern part of the state and several of the major sedimentary basins including the Murray, St. Vincent and Eucla basins. These depressions were formed by subsidence counteracting the tectonic uplift in the region.

The best Tertiary exposures can be seen in St. Vincent Basin, Kangaroo Island, Murray Basin and Eucla Basin. Rocks ascend from carbonaceous sands and silts with lignite beds to marine limestones and marls, rich in fossils predominantly molluscs.

The Quaternary period

Extending back around only two years the Quaternary period is comprised of the Pleistocene and Holocene epochs, representing a small pocket of time on the geological scale. Due to there adolescence Quaternary deposits are well preserved providing a vast insight to the past two million years and displays these development of most modern day geomorphological features.

The tectonic processes which resulted in the break up of the South Australian Tertiary basins carried to through to the Quaternary, there is no doubt that in areas such as the Flinders Ranges this tectonic uplift is continuing. Volcanic activity which occurred south of Kangaroo Island and in the south east of the state appeared to occur in two separate phases. The younger phase is aged at about 1,700 years ago while the older of the events is around 4,700 years old.

There is no evidence of Quaternary glaciation in South Australia on the resultant climatic effects represented in shell fragments and dune preservation.

3. The Olympic Dam Cu-U-Au-Ag-REE Deposit

The ~150 million year old deposit more commonly known as the Olympic Dam Breccia Complex has been the focus of several studies since its discovery in 1975 by the Western Mining Company. The majority of existing literature on the deposit has been published as a component of exploration studies. The geological interpretation and genesis of the Olympic Dam deposit has been the subject of considerable discussion and debate predominantly due to its potential economic value. In the case of Olympic Dam, a number of factors, in particular the unique nature of the deposit and its deep burial beneath unrelated rocks, have resulted in considerable changes in geological thinking over few decades since its discovery.

Geology

Regional setting

The Olympic Dam deposit is located on the eastern margin of the Gawler Craton, and is unconformably overlain by 300 to 350 meters of Late Proterozoic to Cambrian age flat-lying sedimentary rocks of the Stuart shelf geological province (Reynolds, 2000). The deposit is hosted by the Roxby Downs granite which is part of a Hiltaba Suite batholith which involved the intrusion of deformed granitoids and metasediments of the Hutchinson Group into the Olympic Dam and Andamooka region. The batholith sub-crops over an expansive area of around 50 by 35 km, with a composition range from syenogranite to quartz monzodiorites (Cross, Daly, Flint, 1993). Cooper et al has constrained the intrusion ages of the granites through U-Pb zircon dating, ages ranging between 1598 and 1588 million years ago, with plus or minus two error bracket. The Roxby Downs granite is a pink to red coloured, undeformed, unmetamorphosed, coarse to medium grained, quartz-poor syenogranite (Creaser 1989).

The upper parts of the deposit and the Roxby Downs Granite were eroded during the Meso- to Neoproterozoic (Reeve et al 1990). Afterwards the sedimentary

rocks of the Stuart Shelf were deposited. These sediments now have a minimum thickness of 260 meters.

Olympic Dam is one of the several coincident magnetic-gravity anomalies on the Stuart Shelf, most probably caused by hydrothermal iron-oxide alteration in the basement. The breccia complex and surrounding granite form a local basement high on a broader regional uplift.

Fig 3.1: Map of Australia showing the location of the Olympic Dam (Campbell et al. 1998)

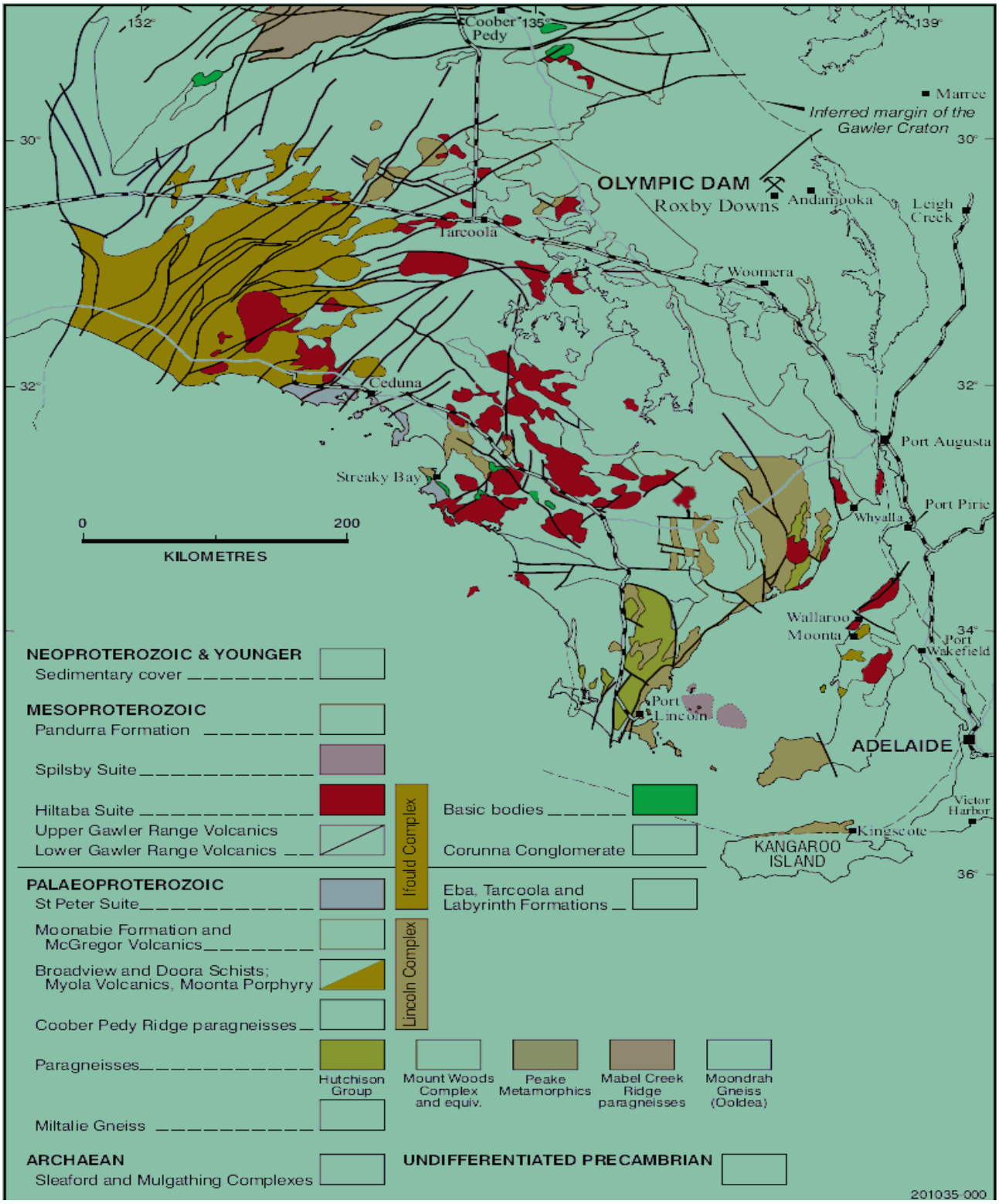

Fig 3.2: Geological units of the Gawler Craton, South Australia.

Deposit Host Rocks

Olympic Dam Breccia Complex (ODBC)

The complex primarily consists of a funnel-shaped, barren, hematite-quartz breccia core surrounded by an irregular array of variably mineralised and broadly zoned hematite-granite breccia bodies with localised dykes and diatremes. A variety of lithologies are displayed by the breccia bodies including those which are granite-dominated on the periphery of the complex to those which are intensely hematised equivalents. (Reynolds, 2000)

A general progressive increase in hematite content is witnessed from the margins of the complex to the core. A halo of weakly altered and brecciated granite extends out around 5 to 7 km from the core in all directions. In total, hematitic-rich breccias occupy an area of around 3 by 3.5 km, and a 300 to 500 meter wide belt extends around 3 km to the northwest (Cross, Daly, Flint, 1993). The outer and lower boundaries of breccias and alteration have not been accurately located due to progression into granite host. it has relatively long and narrow extension to the NW. The limbs extend around 1,500 meters north-south and 2,000 meters east-west, limbs are seen to taper with (Cross, Daly, Flint, 1993). The ODBC is poorly explored below

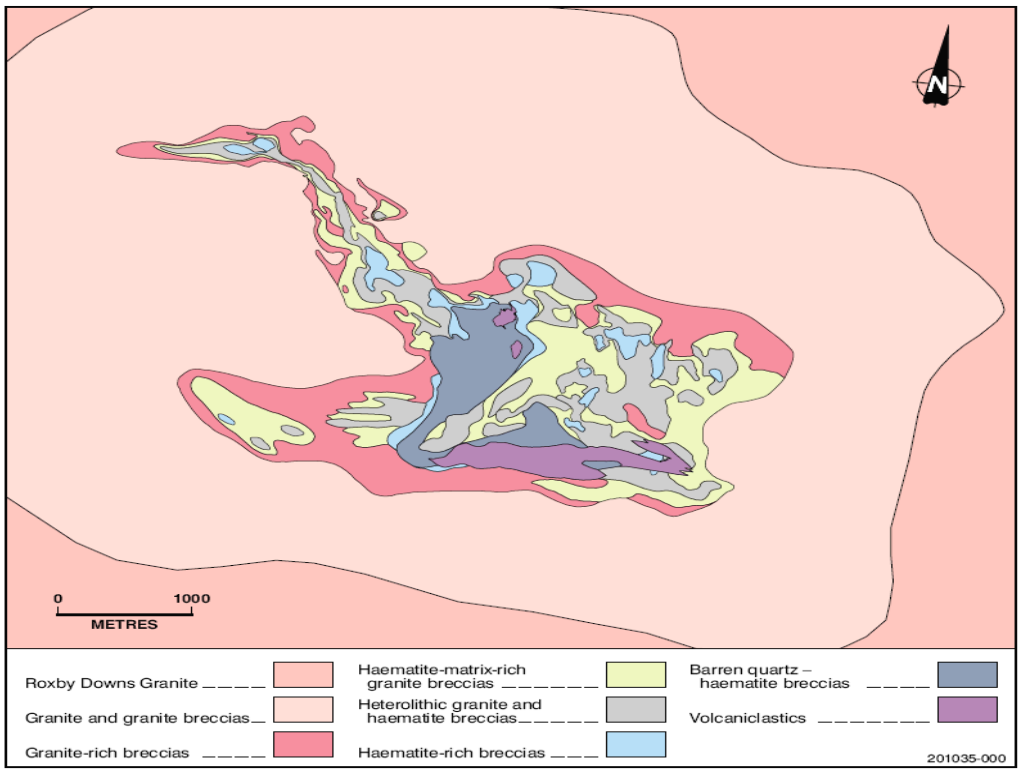

Fig 3.3: Simplified geological plan of the ODBC showing the general distribution of major breccia types. Note the broad zonation from the host granite at the margins of the complex to progressively more hematite-rich lithologies at the center (Reynolds 2001)

800 meters, but exploration drilling has shown that the complex exceeds depths of 1.4 km.

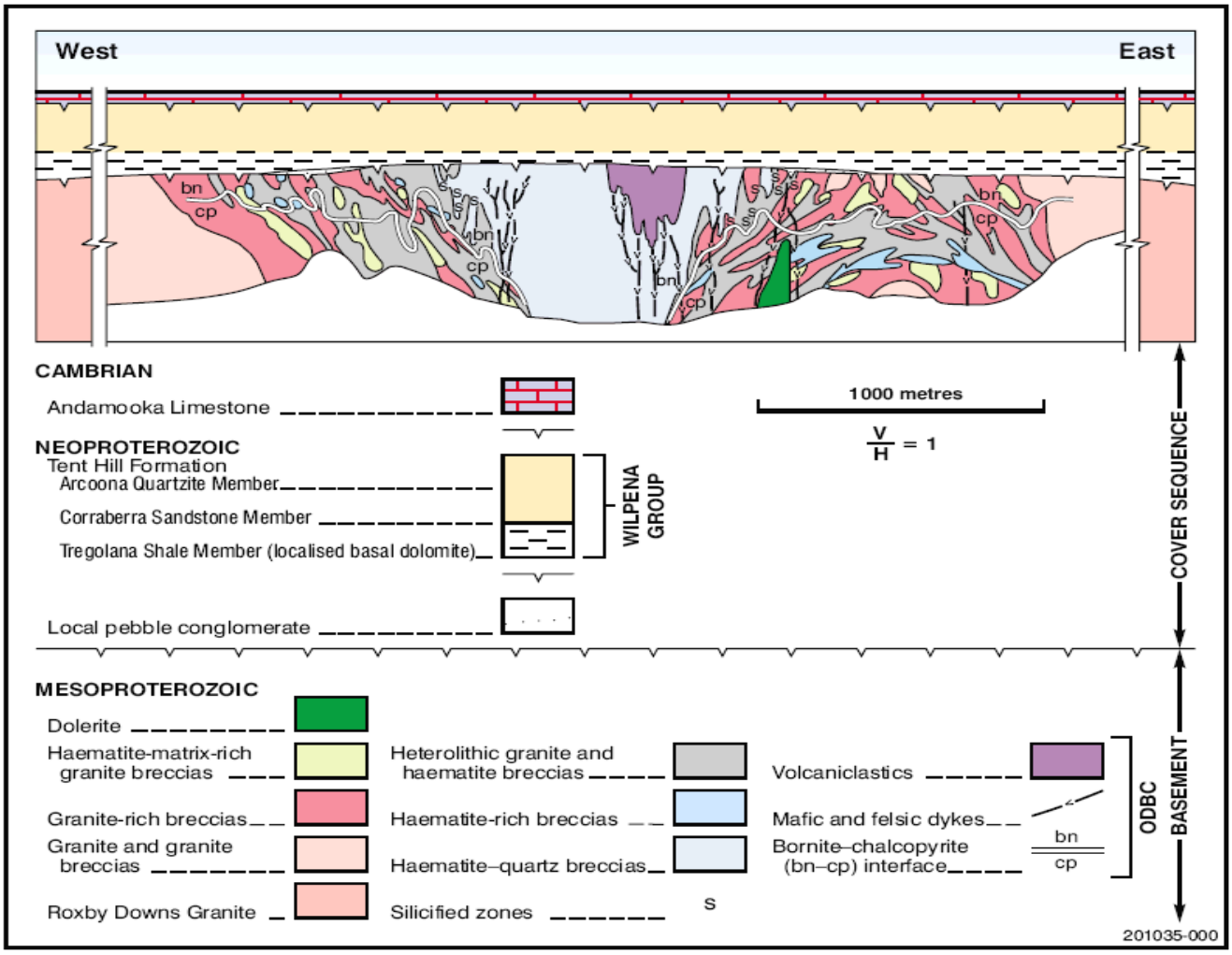

Fig 3.4: Schematic east–west cross-section through the ODBC (after Reeve et al., 1990).

Other Lithologies

The hematite breccia bodies within the ODBC show very little pattern in terms of shape and size, they are however generally elongate and steeply dipping. Variability in mineralization can be seen within single breccia as well as between adjacent breccias. Reeve *et al* interpreted the formation of the breccias to be related to five processes; tectonic faulting, hydraulic fracturing, chemical corrosion, phreatomagmatism and gravity collapse.

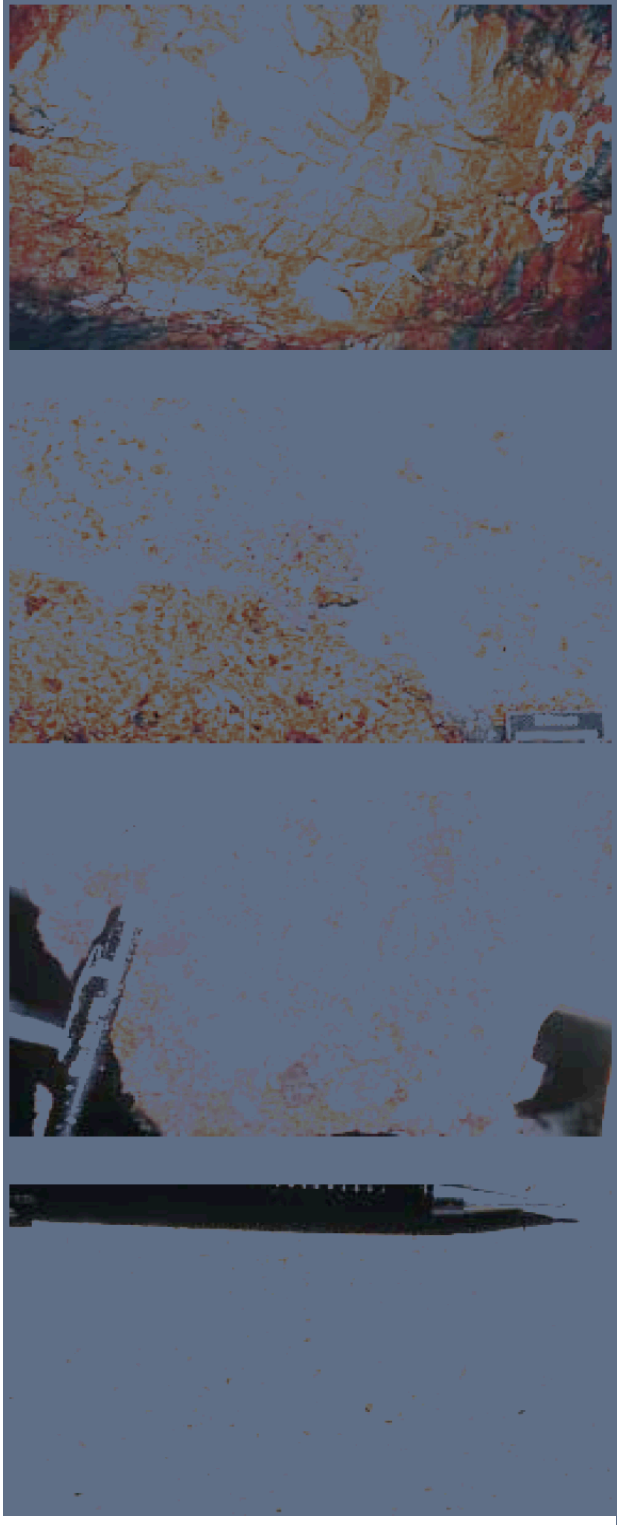

Fig 3.5: Photos from top to bottom:
Weakly brecciated Roxby Downs Granite. The breccia matrix primarily consists of sericite and hematite, and occupies steep dilated joints and cross-cutting fractures. Typical granite-rich breccia with abundant hematite-rich matrix. Note the partial disaggregation of the larger granite clasts. Heterolithic hematite breccia containing a variety of hematite-rich,granitic and transitional clast types. Hematite-quartz breccia containing hematite as clasts and matrix.Minor white disseminations are barite. (Reynolds 2000).

When inspected in detail the breccia zones often display the same grading outward trend; hematite rich cores grading out to fractured granite that can be seen on the larger scale complex (Reynolds, 2000).

The porphyritic felsic volcanic clasts within the ODBC may be derived from coherent extrusive lava flows correlated with the Gawler Range Volcanics' (Reynolds 2001). Reeve et al. (1990) interpreted that these rocks lay above the Roxby Downs Granite and intruded during the development of the hydrothermal system into the breccia complex or, rather, that they were epiclastic in origin. The Dykes within the ODBC intrude mineralized and barren breccias. In the northwest section brecciated aplitic and microgranitic types prevail but in the other parts ultramafic, mafic, and felsic types are dominant. The laster specified units indicate that shattering and alteration occurred in wet, poorly lithified sediments and breccias. (Haynes et al. 1995)

There are a lot of veins within the ODBC and in the surrounding granite. These narrow mono- or polymineralic veins are made up of haematite, sericite,

chlorite, siderite, barite, fluorite, quartz, sulphides or pitchblende in a variety of combinations. These minerals are the prevailing alteration and mineralisation phases throughout the breccia complex. (Reynolds 2001) The degree of alteration intensity can immediately linked to the abundance of brecciation (Reynolds 2001). Fig. 3.6 shows the systematic patterns of alteration and mineralisation within the ODBC. 'The characteristic hydrothermal alteration mineralogy at Olympic Dam is sericite-haematite, with less abundant chlorite, silica, carbonate (siderite) and magnetite' (Reynolds 2001).

Alteration

In general the degree of alteration intensity is associated with the amount of brecciation, leaving the weakly brecciated granite halo only very slightly altered. All publications confirm the characteristic hydrothermal alteration at Olympic Dam is sericite-hematite, with less abundant chlorite, silica, carbonate (siderite) and magnetite.

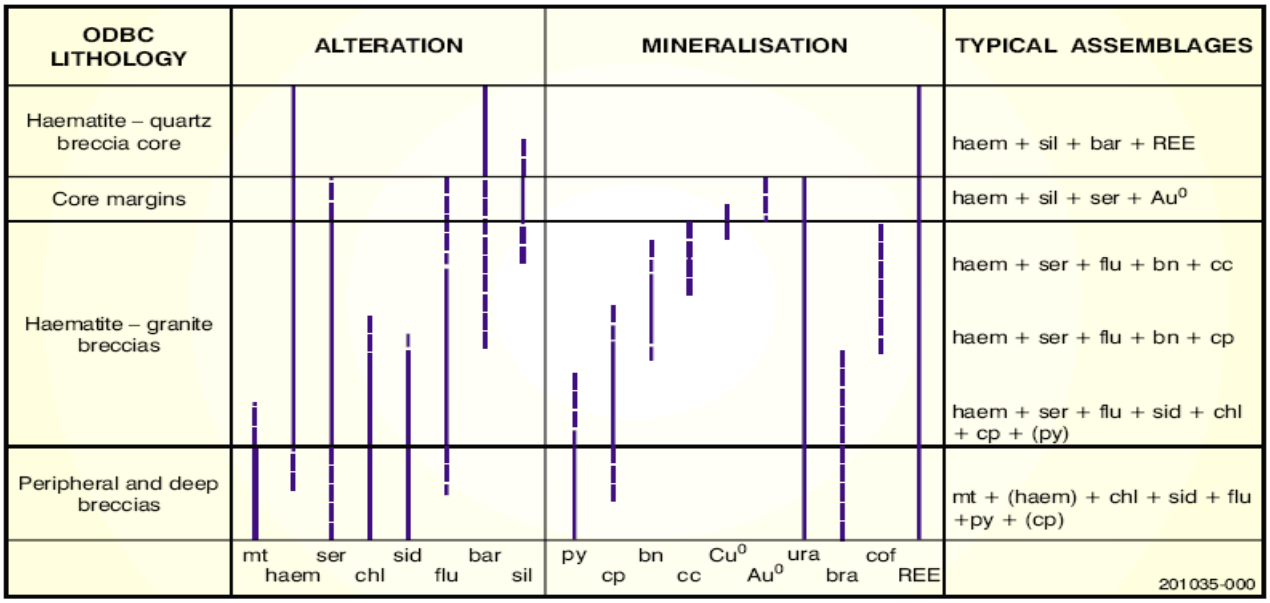

Fig 3.6: Generalised alteration and mineralisation patterns within the ODBC with some typical mineral assemblages. More common components of the ODBC shown in solid lines; neither absolute nor relative abundances are implied. mt=magnetite, haem=haematite, ser=sericite, chl=chlorite, sid=siderite, flu=fluorite, bar=barite, sil=silicification, py=pyrite, cp=chalcopyrite, bn=bornite, cc=chalcocite, Cuo=native copper, Auo=free gold, ura=uraninite, bra=brannerite, cof=coffinite, REE=lanthanum and cerium. (Reynolds 2000).

In the breccia complex two iron oxide alteration product minerals exist, magnetite and hematite. Magnetite is in good condition at depth and within the breccia on the frontier of the ODBC, which are obviously not well developed. (Reynolds 2001). Reynolds (2001) suggests that magnetite could be 'the earliest phase of iron oxide alteration within the breccia complex' and that it has been signed over by hematite alteration. Hematite occurs mainly in the center of the deposit and regional represents >95% of the rock whereas magnetite make up 20% of the rock in strongly altered breccia zones. Reeve et al. (1990) documented that hematite generally displays 'pre-existing minerals, including primary granitic components, dykes and secondary hydrothermal or vein minerals'. But it can also 'precipitated from solution in veins and vugs' (Reynolds 2001). Hematite is closely connected with copper mineralisation at all scales. (Reynolds 2001) Apart from the magnetite and hematite alteration there is silicate alteration. Table 3.1 provides more information about the original minerals, their alteration products and their appearances within the ODBC.

Table 3.1: Silicate Alteration (after Reynolds 2001)

Alteration product	Original mineral	Appearance within the ODBC
Sericite	Feldspar	-widespread within all breccias, except the haematite-quartz core
Pseudomorphic chlorite	Feldspar	-patchy, but widespread within the breccia complex -generally of low to moderate intensity
Siderite	Carbonate	-generally weak within mineralized breccias
Quartz		-minor present throughout the breccia complex

It should also be noted that 'chlorite and siderite alteration is more abundant at depth and on the periphery of the breccia zones' (Reynolds 2001). It is also connected with 'more magnetite-dominated alteration and chalcopyrite mineralisation' (Reynolds 2001). The boundary of the central core of hematite-quartz breccias possesses a high silicification and these zones are expected to have a higher gold mineralisation.

Mineralisation

Olympic Dam ore body is a complex mixture of more than 40 minerals (Pickers, 2005). The principle copper-bearing minerals are chalcopyrite, bornite and chalcocite accompanied by a small amount of native copper (Reynolds, 2000). The primary uranium bearing mineral is uranite, while gold and silver are related to the copper sulfides. Oreskes & Einaudi (1990) have determined bastnaesite to be the main REE-bearing mineral and this conclusion has remained throughout exploration. Haynes et al. (1995) publicized 'three distinctive mineral associations in the orebody'. Association I, which is paragenetically the first of these three, is magnetite ± hematite, chlorite, sericite, siderite, pyrite, chalcopyrite, and pitchblende. The appearance of association II contains partially or almost totally the oxidized minerals of association I and is 'more characteristic of the middle to late stages of mineralisation episodes' (Haynes et al. 1995). Association II is hematite, sericite, chalcopyrite, bornite, pitchblende, barite, fluorite, and chlorite. The greatest amount of chlorite and sericite exist in association I an II, and the hydrothermal quartz in association II is regionally defined and unusually in combination with sulphides. The third association is composed of 'porous, vuggy, or massive hematite, granular quartz, and vein barite, with localized zones of silification ± quartz veining' (Haynes et al. 1995). The quartz veining is in general brecciated. Association III mainly belongs to the later stage of mineralisation and seldom contains fluorite and silicates except for quartz. These three associations coincide more or less in temporal and spatial regard. It exists 'a gross vertical zonation from III at higher levels, to I at depth' (Haynes et al. 1995). Reeve et al. (1990) observed that the cone- or wedge-shaped sectors of association III acuminate to lower levels into II and in this area subsist 'a lateral zonation outward from III to II' (Haynes et al. 1995). But sporadic spikes of II protrude upward into association III. (Haynes et al. 1995)

Beyond the classification after Haynes (1995) it is important to know that massive

Ore is seldom in the ODBC that means the mineralisation basically appears within the matrix of the breccias. Copper ore minerals are found as 'disseminated grains, veinlets and fragments within the breccia zones' (Reynolds 2001). Gold, silver and uranium always occur with sulphides, for example the uranium mineral pitchblende (uraninite) mainly appears as 'fine-grained disseminations within hematitic breccias,

intergrown with sulphides and hematite' (Reynolds 2001). Silver mostly is present 'in solid solution with the sulphide minerals' (Reynolds 2001) and gold appears as strongly bound particles within and in connection with
copper sulphide grains. The rare earth elements mainly La and Ce are found all over the breccia zones and especially in the central hematite quartz core its concentration is commonly higher (Reynolds 2001). In addition a sulphide zonation has developed. At depth pyrite is the prevailing sulphide mineral, 'grading upward into chalcopyrite-dominant zones' (Campbell et al. 1998) and finally passing into bornite, chalcocite and bornite + chalcocite zones (Oreskes & Einaudi 1990, Reeve et al. 1990). In defined and complex zones within and around the silicified borders of the hematite quartz core exist gold zones that are of a higher grade (Reynolds 2001).

.

Cross, Flint and Reynolds all exclaim only minor portions of the entire ODBC volume are populated by ore zones. Within these ore zones there is a general correlation between higher grade copper-uranium mineralisation and more hematitic

Fig 3.7: Diamond drill core samples from Olympic Dam displaying from left to right Chalcocite mineralisation, Bornite mineralisation and Chalcopyrite mineralisation.

altered rocks (Reynolds, 2000). However it has recently been noted by several publications that the central hematite-quartz breccia zone is essentially barren of copper-uranium mineralisation.

Variations exist within the publicized copper grades; this is due to the process of averaging the values across the ore zones. Cross *et al* determined that the grades of delineated copper ore commonly vary between 1 and 5%, while gold varies from between 0.3 and 1.0 g/t in 1993, these values have varied only very slightly in Reynolds more recent summary. Reynolds suggests copper grades between 1 and 6% and average gold grades of 0.6 g/t. The areas of ore within the ODBC are displayed in the map below.

Common rock types found at Olympic Dam

GRNB: Brecciated & Unaltered granite as well as fragmental rocks consisting of unaltered granite-derived components. Granites is made up of alkali feldspar (50%) , plagioclase (20%), quartz (25%) and mafic minerals (5%).

GRNH: The majority of the unit should be intact, but hematite has either started to crackle brecciate the unit, or the unit is clast supported (predominantly granite). Hematite can replace some of the feldspars, leaving a "texturally tentative" rock type.

GRNL: Typically a matrix supported breccia, with the matrix/infill being hematite +/- rock flour components. However, majority of clasts are Granitic in composition.

HEMH: Typically a matrix supported breccia (as per GRNL) with the matrix/infill being hematite matrix/replacement, but the clasts are predominantly hematite with lower proportion of granite.

HEM: Textured or massive; breccias, precipitates, metasomatites. The similarity between hematite clasts and matrix, and the strong hematite replacement/alteration can make individual components difficult to recognize.

HEMQ: Classic hematite-quartz breccia. Barren, locally vughy, porous or silicified. No sulphide, Sericite or fluorite.

HEMV/VHEM: Breccia containing hematite and volcanic clasts.

GRNV/VGRN: Breccia containing granite and volcanic clasts.

EVD/UMD/FVD: Generic dyke; volcanic/sub-volcanic textures. Often chlorite or hematite altered. The more mafic dykes have undergone intense texturally destructive Sericite and hematite alteration. Felsic dykes commonly have preserved porphyritic textures.

A basal conglomerate directly overlies the unconformity, it is a clast support pebble conglomerate containing rounded clasts of hematite and granite in a granular hematite and quartz matrix. Overlying the conglomerate there is a transition in sediments from shale, sandstone, quartzite and limestone.

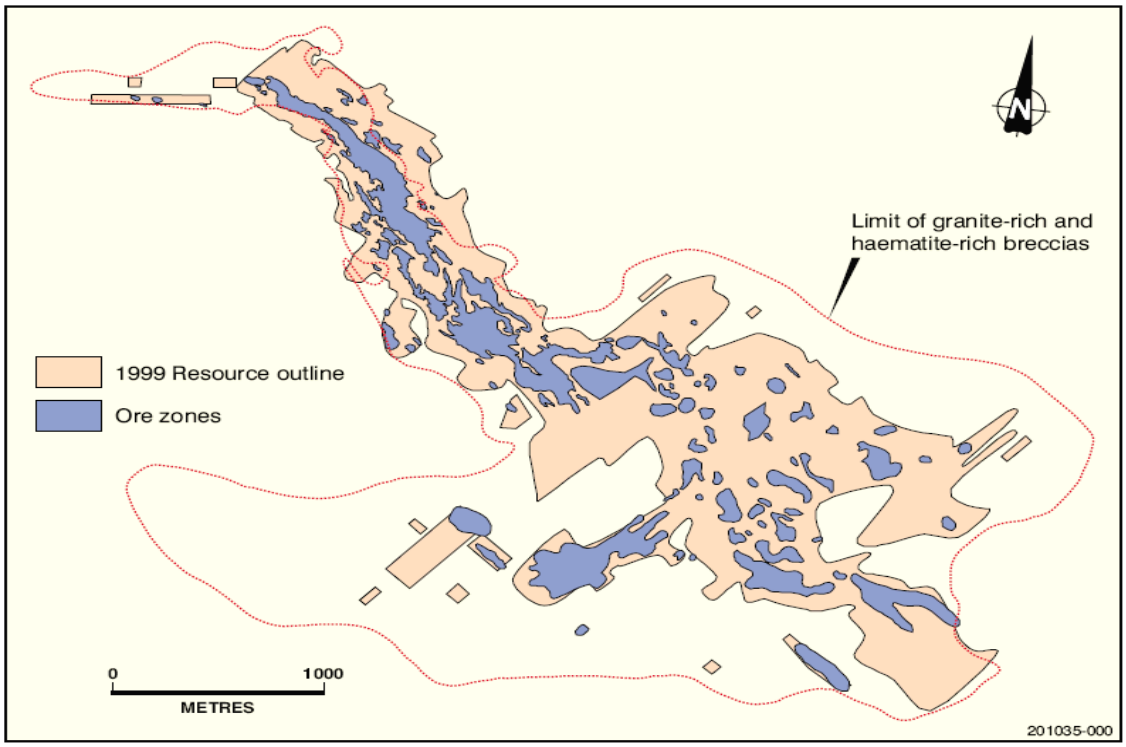

Fig 3.8: Olympic Dam resource outline at the 41 Level + 100 m, showing distribution of ore zones.

Structure

The majority of publications refer to summaries of the deposits structures by Sugden & Cross (1991). They observe the general north-west to north-north-west trend which the ore bodies generally display. Early structures and controls on structure have probably been obliterated during the on-going processes of brecciation and alteration (Reeve *et al*, 1990; Sugden & Cross, 1991).

O'Driscoll (1985) suggested the pattern of breccia bodies within the deposit may represent an en-echelon fault zone, however further literature has questioned that those faults presumed to be the bounding faults and whether they are just surficial. On the mine scale the deposit is criss-crossed by a complex array of brittle faults and

veins of variable orientations and magnitudes. Sugden & Cross (1991) indicated it is evident that most of these structures post date breccia-forming events, there study also subdivided them into syn-hydrothermal structures, early strike-slip faults, reverse faults, and late-stage conjugate arrays. Late stage conjugate arrays have been interpreted to have formed during the Delamarian Orogeny (Sugden & Cross, 1991; Reynolds, 2000)

Individual faults are generally minor structures with small displacements, generally less than ten meters, these minor features are often hard to trace due to short strikes. There are a few structures however which display displacements of up to 100m and display cataclastic zones (Reynolds, 2001).

4. Olympic Dam ground surface characteristics

Before commencing this section of the review it is important to note that the following rock strength and stabilisation data is relevant for the current environment at Olympic Dam, these characteristics should be reviewed regularly to allow for change. The main source for the proceeding information is a document produced by AMC consultants, spreadsheet rock strength data from the Olympic Dam database and Rock Technology Pty Ltd regarding rock strength. Little other studies of the kind have been conducted.

General

The underground mining operations at Olympic Dam are highly mechanized including automated rail transportation and underground crushing. The primary method of ore extraction is long-hole open stoping, this process involves the firing of a slot followed by the progressive blasting of the stope through ring drill and blasting, stopes vary greatly in volume generally averaging around 150m tall. The ore is then bogged from an extraction point and the open stope is refilled with a cement aggregate fill known as CAF, which is produced at the onsite CAF plant. The open stoping method allows for large equipment to achieve high productivity and maximum ore recovery.

On the base level (rail level) of the mine an automated rail transports the ore to the crushers, where the ore is crushed and then hoisted to the surface via the main Clark shaft or the Wheenan shaft.

Once at the surface the ore is fed into two grinding circuits by a conveyor system. After grinding, the resultant slurry passes to a flotation circuit where a series of flotation stages and further grinding activity produces a copper concentrate. This concentrate is then passed through a leaching circuit which is principally designed to extract uranium from the copper minerals. Uranium is extracted in a solvent extraction plant, producing yellow-cake, which is subsequently calcined to produce uranium oxide concentrate, this is the product which is package and exported. The remaining copper concentrate is then fed through a flash furnace smelter to produce a slag. The remainder of the process involves the copper being transferred into anodes which are transported to the refinery to produce cathodes. Residual slimes are then further processed to extract gold and silver.

Underground development

There is approximately 300 km of tunneling development extending to depths of around 800m below the surface at Olympic Dam. Development of these tunnels is done at a general rate of around 20kn per annum or 5m per day. Underground is accessed either down the 1.5 km portal in a vehicle or down to the 420 metre platform via an electronic cage. Around 20 stopes are being operated at one point in different areas of the mine. The mine has been divided into the sub-areas displayed on the following map of mine development.

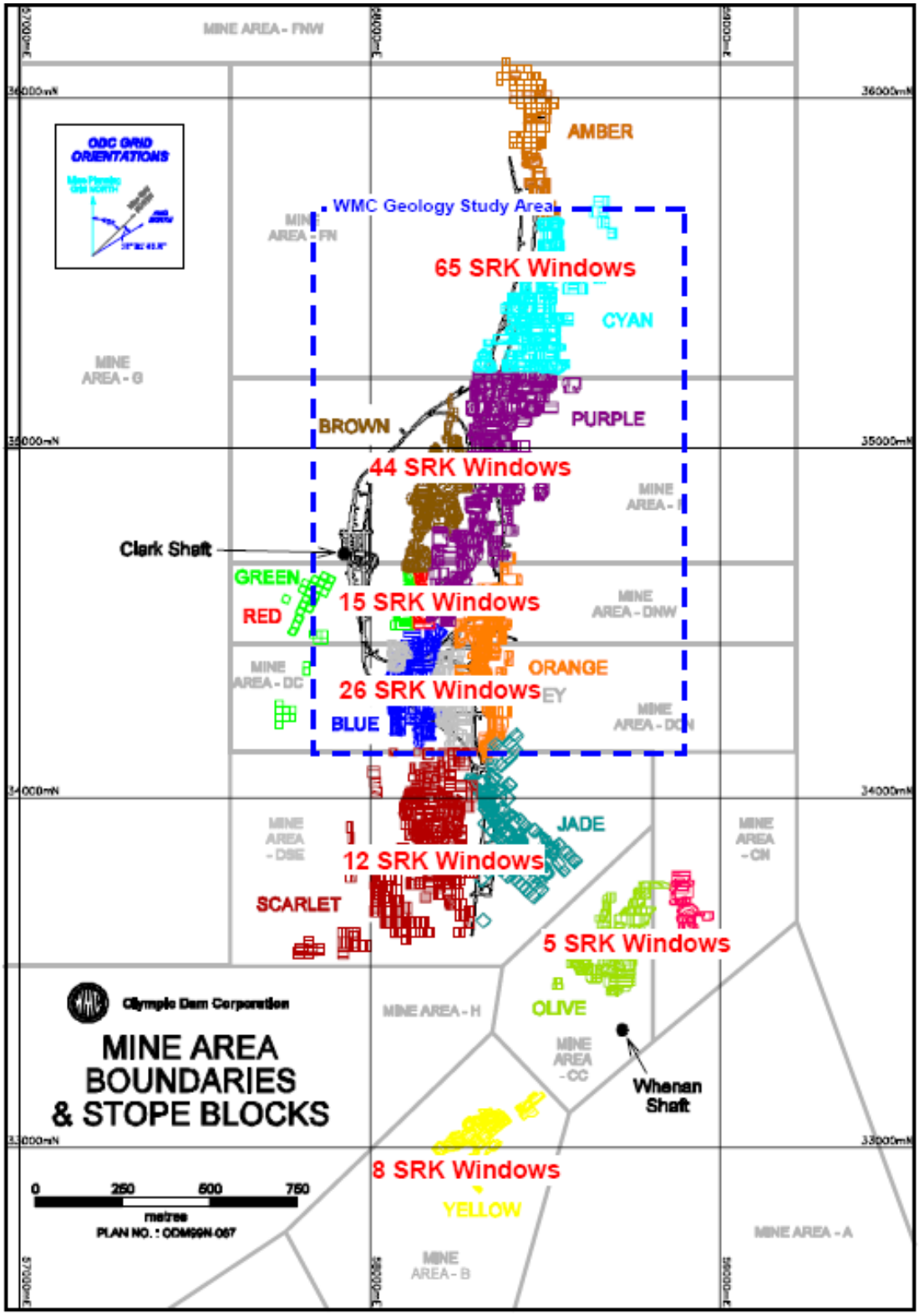

Fig 4.1: Mine area map and stope blocks

References

AMC Consultants, 2007a In Situ stress field for Olympic Dam Mine. Unpublished AMC Consultants report 106113 to BHPBilliton August.

AMC Consultants, 2007b OD seismic Pillars – Phase 1. Unpublished AMC Consultants report 107090 to BHPBilliton December.

BHP Billiton 2006 Olympic Dam Underground Control Management Plan. BHP Billiton, Unpublished Internal Report, April.

Baldwin, G. & Grice, A. Engineering the new Olympic Dam Backfill System. MassMin 200. Brisbane, QLD, Australia. Oct 2000. Pp 721-734.

Campbell I H, Compston D M, Richards J P, Johnson J P, Kent A J R (1998) Review of the

application of isotopic studies to the genesis of Cu-Au mineralisation at Olympic Dam

an Au mineralisation at Porgera, the Tennant Creek district and Yilgarn Craton. AustralianJournal of Earth Sciences 45: 210-218

Creaser, R.A., 1989. The geology and petrology of Middle Proterozoic felsic magmatism of the Stuart Shelf, South Australia. Umpublished Ph.D, thesis, La Trobe University, Melbourne, Australia.

Enghardt, J. 2004. The Olympic Dam Cu-U-Au-Ag-REE deposit, South Australia. Institute of Geology, University of Mining and Technology Freiberg, Germany

Flint, R.B, (Comp), 1993. Mesoproterozoic. *In*: Drexel, J.F., Preiss, W.V. &Parker, A.J. (eds), The geology of South Australia, v 1, The Precambrian, Geological Survey of South Australia, Bulletin 54.

Grice, A et al. Reports to Olympic Dam on Backfilling. Consultancy reports from AMC.

Haynes, D.W., Cross,K.C.,Bills, R.T., & Reed, M.H., 1995. Olympic Dam ore genesis: A fluid mixing model. Economic Geology v. 90, pp 63-74

Hitzman, M.W., Oreskes, N., & Einauddi, M.T., 1992. Geological characteristics and tectonic setting of Proterozoic iron oxide (Cu-U-Au-REE) deposits. *Precambrian Research* v 58, pp 241-287

Hitzman, M.W & Valenta R.K., 2005. Uranium in iron oxide-copper-gold (IOCG) systems. *Economic Geology* v. 100, pp 1657-1661.

Johns, R.K. 1968. "Geology and Mineral Resources of the Andamooka-Torrens Area", Bulletin No 41, Geological Survey of South Australia, Adelaide, pp 7 – 46.

Ludbrook, N.H. 1980. *A guide to the geology and mineral resources of South Australia*, D.J Woolman government printer, South Australia.

O'Driscoll, E.S.T., 1985. The application of lineament tectonics in the discovery of the Olympic Dam Cu-U-Au deposit at Roxby Downs, South Australia. *Global Tectonics and Metallogeny* 3 (1), pp 43-57

Olympic Dam: Some developments in geological understanding over nearly two decades, 1993,

Conference Series - Australasian Institute of Mining & Metallurgy, Australasian Inst of Mining & Metallurgy, Parkville, pp 113-118

Oreskes, N. & Einaudi, M.T., 1990. Origin of rare earth element-enriched hematite breccias at the Olympic Dam Cu-U-Au-Ag deposit, Roxby Downs, South Australia. *Economic Geology* 85, pp 1-28.

Oreskes, N. & Einaudi, M.T., 1992. Origin of hydrothermal fluids at Olympic Dam: Preliminary results from fluid inclusions and stable isotopes. *Economic Geology* v. 87, 64-90.

Parkin, L.W. (ed) 1969, Handbook of South Australian Geology, Geological Survey of South Australia, Adelaide, Australia.

Pickers, N. & Maturana, F. Mineral Resource Report and Estimation Procedure, August 2005.

Reeve et al. (1990) Olympic Dam copper-uranium-gold-silver deposit. *In*: Hughes (Ed.), Geology of the mineral deposits of Australian and Papua New Guinea. Australasian Institute of Mining and Metallurgy. Monograph Series 14: 1009-10035

Reynolds, L.J. 2000. Geology of Olympic Dam Cu-U-Au-Ag-REE Deposit; in Porter (Ed.), Hydrothermal Iron Oxide Copper-Gold & Related Deposits: A Global perspective, v. 1; PGC publishing Adeaidelaide, pp 93-104.

Sugden, T.J. & Cross, K.C., 1991. Significance of overprinting fault systems in the Olympic Dam Breccia Complex. Structural Geology in Mining and Exploration, extended abstracts, University of Western Australia, Publication No. 25, 93-98.

WMC Resources, Olympic Dam Numerical Modelling of Stoping Schedule, September 2005. AMC document number 105018.

WMC Resources, Olympic Dam Operations – Geotechnical Review – September 2003. AMC document number 103099.
WMC Resources, Olympic Dam Operations – Geotechnical Review – May 2004. AMC document number 104035.
WMC Resources, Olympic Dam Operations Stability of Stope Crowns, February 2005. AMC document number 104028.
WMC Resources, Olympic Dam Operations Stability Graph Back Analysis, November 2004. AMC document number 104078.

Appendix B: Classification of Q value input parameters

Rock mass classification

Table 6: Classification of individual parameters used in the Tunnelling Quality Index Q

DESCRIPTION	VALUE	NOTES
1. ROCK QUALITY DESIGNATION	***RQD***	
A. Very poor	0 - 25	1. Where *RQD* is reported or measured as ≤ 10 (including 0),
B. Poor	25 - 50	a nominal value of 10 is used to evaluate *Q*.
C. Fair	50 - 75	
D. Good	75 - 90	2. *RQD* intervals of 5, i.e. 100, 95, 90 etc. are sufficiently
E. Excellent	90 - 100	accurate.
2. JOINT SET NUMBER	J_n	
A. Massive, no or few joints	0.5 - 1.0	
B. One joint set	2	
C. One joint set plus random	3	
D. Two joint sets	4	
E. Two joint sets plus random	6	
F. Three joint sets	9	1. For intersections use ($3.0 \times J_n$)
G. Three joint sets plus random	12	
H. Four or more joint sets, random,	15	2. For portals use ($2.0 \times J_n$)
heavily jointed, 'sugar cube', etc.		
J. Crushed rock, earthlike	20	
3. JOINT ROUGHNESS NUMBER	J_r	
a. Rock wall contact		
b. Rock wall contact before 10 cm shear		
A. Discontinuous joints	4	
B. Rough and irregular, undulating	3	
C. Smooth undulating	2	
D. Slickensided undulating	1.5	1. Add 1.0 if the mean spacing of the relevant joint set is
E. Rough or irregular, planar	1.5	greater than 3 m.
F. Smooth, planar	1.0	
G. Slickensided, planar	0.5	2. J_r = 0.5 can be used for planar, slickensided joints having
c. No rock wall contact when sheared		lineations, provided that the lineations are oriented for
H. Zones containing clay minerals thick	1.0	minimum strength.
enough to prevent rock wall contact	(nominal)	
J. Sandy, gravely or crushed zone thick	1.0	
enough to prevent rock wall contact	(nominal)	
4. JOINT ALTERATION NUMBER	J_a	ϕr degrees (approx.)
a. Rock wall contact		
A. Tightly healed, hard, non-softening,	0.75	1. Values of ϕr, the residual friction angle,
impermeable filling		are intended as an approximate guide
B. Unaltered joint walls, surface staining only	1.0	25 - 35 to the mineralogical properties of the
C. Slightly altered joint walls, non-softening	2.0	25 - 30 alteration products, if present.
mineral coatings, sandy particles, clay-free		
disintegrated rock, etc.		
D. Silty-, or sandy-clay coatings, small clay-	3.0	20 - 25
fraction (non-softening)		
E. Softening or low-friction clay mineral coatings,	4.0	8 - 16
i.e. kaolinite, mica. Also chlorite, talc, gypsum		
and graphite etc., and small quantities of swelling		
clays. (Discontinuous coatings, 1 - 2 mm or less)		

Table 6: (cont'd.) Classification of individual parameters used in the Tunnelling Quality Index *Q* (After Barton et al 1974).

4, JOINT ALTERATION NUMBER	J_a	ϕr degrees (approx.)	
b. Rock wall contact before 10 cm shear			
F. Sandy particles, clay-free, disintegrating rock etc.	4.0	25 - 30	
G. Strongly over-consolidated, non-softening clay mineral fillings (continuous < 5 mm thick)	6.0	16 - 24	
H. Medium or low over-consolidation, softening clay mineral fillings (continuous < 5 mm thick)	8.0	12 - 16	
J. Swelling clay fillings, i.e. montmorillonite, (continuous < 5 mm thick). Values of J_a depend on percent of swelling clay-size particles, and access to water.	8.0 - 12.0	6 - 12	
c. No rock wall contact when sheared			
K. Zones or bands of disintegrated or crushed	6.0		
L. rock and clay (see G, H and J for clay	8.0		
M. conditions)	8.0 - 12.0	6 - 24	
N. Zones or bands of silty- or sandy-clay, small clay fraction, non-softening	5.0		
O. Thick continuous zones or bands of clay	10.0 - 13.0		
P. & R. (see G.H and J for clay conditions)	6.0 - 24.0		
5. JOINT WATER REDUCTION	J_w	approx. water pressure (kgf/cm^2)	
A. Dry excavation or minor inflow i.e. < 5 l/m locally	1.0	< 1.0	
B. Medium inflow or pressure, occasional outwash of joint fillings	0.66	1.0 - 2.5	
C. Large inflow or high pressure in competent rock with unfilled joints	0.5	2.5 - 10.0	1. Factors C to F are crude estimates; increase J_w if drainage installed.
D. Large inflow or high pressure	0.33	2.5 - 10.0	
E. Exceptionally high inflow or pressure at blasting, decaying with time	0.2 - 0.1	> 10	2. Special problems caused by ice formation are not considered.
F. Exceptionally high inflow or pressure	0.1 - 0.05	> 10	
6. STRESS REDUCTION FACTOR ***a. Weakness zones intersecting excavation, which may cause loosening of rock mass when tunnel is excavated***		***SRF***	
A. Multiple occurrences of weakness zones containing clay or chemically disintegrated rock, very loose surrounding rock any depth)		10.0	1. Reduce these values of *SRF* by 25 - 50% but only if the relevant shear zones influence do not intersect the excavation
B. Single weakness zones containing clay, or chemically disintegrated rock (excavation depth < 50 m)		5.0	
C. Single weakness zones containing clay, or chemically disintegrated rock (excavation depth > 50 m)		2.5	
D. Multiple shear zones in competent rock (clay free), loose surrounding rock (any depth)		7.5	
E. Single shear zone in competent rock (clay free). (depth of excavation < 50 m)		5.0	
F. Single shear zone in competent rock (clay free). (depth of excavation > 50 m)		2.5	
G. Loose open joints, heavily jointed or 'sugar cube', (any depth)		5.0	

Table 6: (cont'd.) Classification of individual parameters in the Tunnelling Quality Index *Q* (After Barton et al 1974).

DESCRIPTION		VALUE		NOTES
6. STRESS REDUCTION FACTOR			***SRF***	
b. Competent rock, rock stress problems				
	σ_c/σ_1	$\sigma_t\sigma_1$		2. For strongly anisotropic virgin stress field
H. Low stress, near surface	> 200	> 13	2.5	(if measured): when $5 \leq \sigma_1/\sigma_3 \leq 10$, reduce σ_c
J. Medium stress	200 - 10	13 - 0.66	1.0	to $0.8\sigma_c$ and σ_t to $0.8\sigma_t$. When $\sigma_1/\sigma_3 > 10$,
K. High stress, very tight structure	10 - 5	0.66 - 0.33	0.5 - 2	reduce σ_c and σ_t to $0.6\sigma_c$ and $0.6\sigma_t$, where
(usually favourable to stability, may				σ_c = unconfined compressive strength, and
be unfavourable to wall stability)				σ_t = tensile strength (point load) and σ_1 and
L. Mild rockburst (massive rock)	5 - 2.5	0.33 - 0.16	5 - 10	σ_3 are the major and minor principal stresses.
M. Heavy rockburst (massive rock)	< 2.5	< 0.16	10 - 20	3. Few case records available where depth of
c. Squeezing rock, plastic flow of incompetent rock				crown below surface is less than span width.
under influence of high rock pressure				Suggest *SRF* increase from 2.5 to 5 for such
N. Mild squeezing rock pressure			5 - 10	cases (see H).
O. Heavy squeezing rock pressure			10 - 20	
d. Swelling rock, chemical swelling activity depending on presence of water				
P. Mild swelling rock pressure			5 - 10	
R. Heavy swelling rock pressure			10 - 15	

ADDITIONAL NOTES ON THE USE OF THESE TABLES

When making estimates of the rock mass Quality (*Q*), the following guidelines should be followed in addition to the notes listed in the tables:

1. When borehole core is unavailable, *RQD* can be estimated from the number of joints per unit volume, in which the number of joints per metre for each joint set are added. A simple relationship can be used to convert this number to *RQD* for the case of clay free rock masses: $RQD = 115 - 3.3\ J_v$ (approx.), where J_v = total number of joints per m^3 ($0 < RQD < 100$ for $35 > J_v > 4.5$).
2. The parameter J_n representing the number of joint sets will often be affected by foliation, schistosity, slaty cleavage or bedding etc. If strongly developed, these parallel 'joints' should obviously be counted as a complete joint set. However, if there are few 'joints' visible, or if only occasional breaks in the core are due to these features, then it will be more appropriate to count them as 'random' joints when evaluating J_n.
3. The parameters J_r and J_a (representing shear strength) should be relevant to the weakest significant joint set or clay filled discontinuity in the given zone. However, if the joint set or discontinuity with the minimum value of J_r/J_a is favourably oriented for stability, then a second, less favourably oriented joint set or discontinuity may sometimes be more significant, and its higher value of J_r/J_a should be used when evaluating *Q*. The value of J_r/J_a should in fact relate to the surface most likely to allow failure to initiate.
4. When a rock mass contains clay, the factor *SRF* appropriate to loosening loads should be evaluated. In such cases the strength of the intact rock is of little interest. However, when jointing is minimal and clay is completely absent, the strength of the intact rock may become the weakest link, and the stability will then depend on the ratio rock-stress/rock-strength. A strongly anisotropic stress field is unfavourable for stability and is roughly accounted for as in note 2 in the table for stress reduction factor evaluation.
5. The compressive and tensile strengths (σ_c and σ_t) of the intact rock should be evaluated in the saturated condition if this is appropriate to the present and future in situ conditions. A very conservative estimate of the strength should be made for those rocks that deteriorate when exposed to moist or saturated conditions.

Appendix C: OD intact rock properties

D.1 Summary of rock property data for OD

Summary rock property data for Olympic Dam rocks*

Rock Code			Specific Gravity Tm^{-3}	UCS MPa	UCS_{50} MPa	UTS MPa	E GPa	v	P wave ms^{-1}	S wave ms^{-1}
Granite Breccia		Number	63	62	52		57	35	27	16
	GRNB	Average	3.00	142	139		58	0.30	5117	3257
		Std Dev	0.39	71	72		16	0.18	993	694
Increasing haematite content		Number	7	7	6		6	2	3	2
	GRNH	Average	3.55	171	175		64	0.20	5235	3313
		Std Dev	0.22	91	95		21	0.04	950	140
		Number	9	9	8	1	17	13	5	4
	GRNL	Average	3.66	157	148	8	63	0.30	5537	3116
		Std Dev	0.71	110	113		22	0.18	1787	550
		Number	22	22	21		21	1	2	1
	HEMQ	Average	3.51	189	186		75	0.35	5217	3217
		Std Dev	0.58	104	105		29		872	
		Number	2	2	2		2	2	2	2
	HEMH	Average	3.92	252	250		80	0.36	6896	3745
		Std Dev	0.49	10	10		1	0.09	359	11
		Number	20	22	20	3	22	7	5	5
	HEM	Average	4.01	151	157	8	69	0.33	6840	3348
		Std Dev	0.43	70	72	1	21	0.05	1231	355
Volcanics		Number	78	78	78		62			
	GRNV	Average	2.74	92	97		48			
		Std Dev	0.07	53	51		15			
Cover Sediments		Number	9	9			2		9	
	ZWA	Average	2.53	124			56		3567	
		Std Dev	0.08	56			18		763	
		Number	3	3			1		3	
	ZWC	Average	2.23	85			30		3733	
		Std Dev	0.06	11					321	
		Number	12	12			9		3	
	ZWT	Average	2.79	88			33		3267	
		Std Dev	0.11	77			20		1415	

* Rock properties for OD have been collected over the mine's history. The database contains over 200 test results. Most of the tests were conducted prior to 1997 and the advent of the new rock code nomenclature. This has meant that there is some confusion in correctly allocating alteration and rock codes. The adjacent samples are being reviewed to accurately determine their description and alteration.

C.2 UCS and UCS Vs sample diameter plots for different rock types at OD

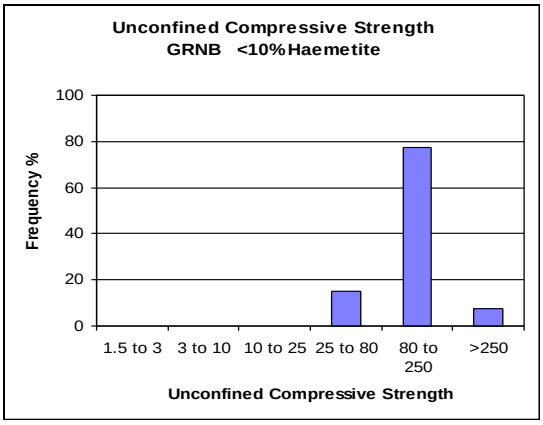

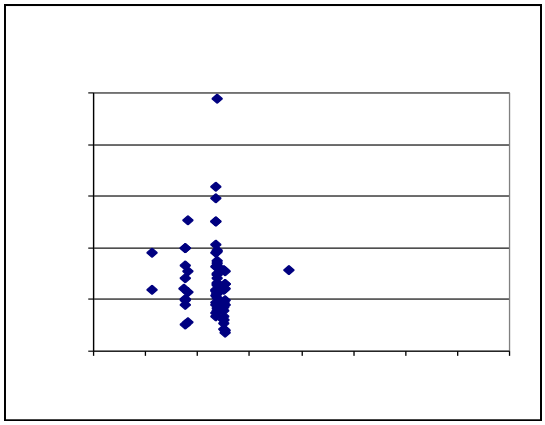

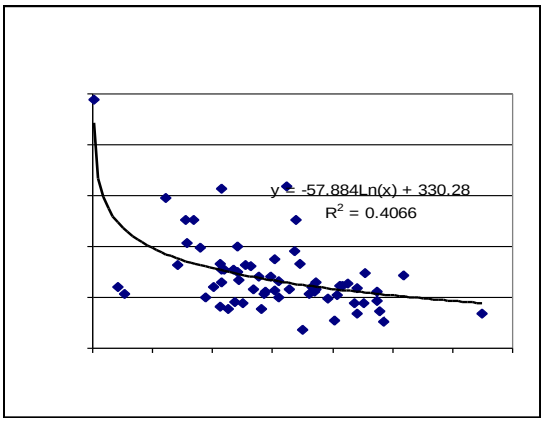

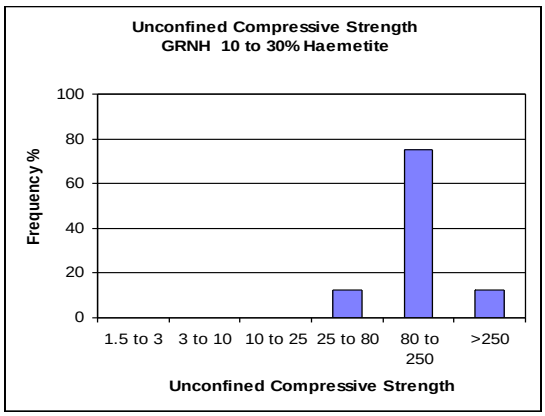

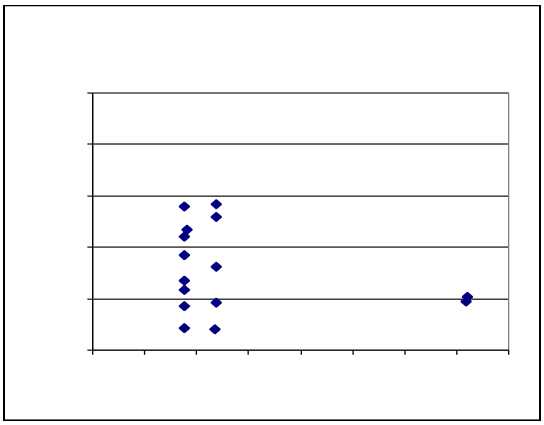

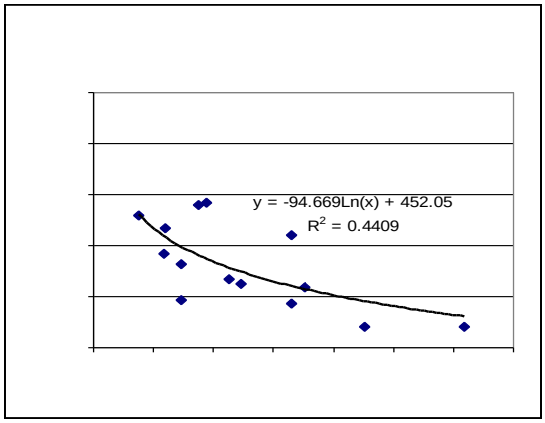

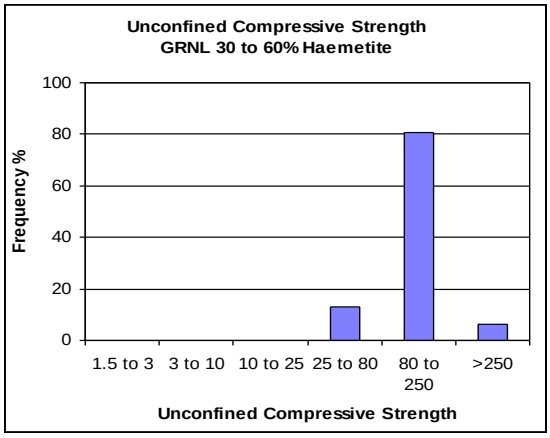
Unconfined Compressive Strength
GRNL 30 to 60% Haemetite
Frequency %
100
80
60
40
20
0
1.5 to 3
3 to 10
10 to 25
25 to 80
80 to 250
>250
Unconfined Compressive Strength

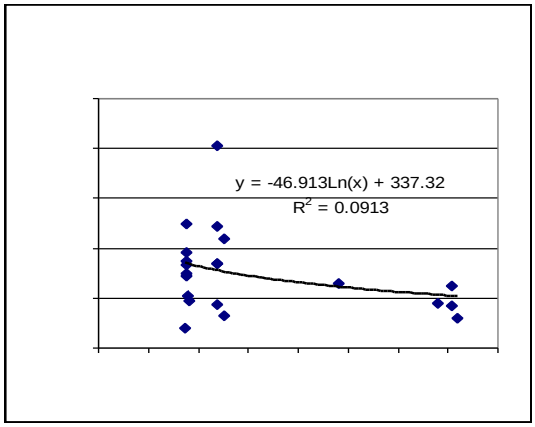
y = -46.913Ln(x) + 337.32
R2 = 0.0913

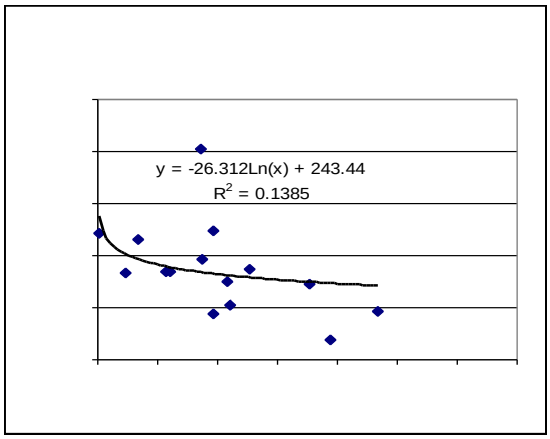
y = -26.312Ln(x) + 243.44
R2 = 0.1385

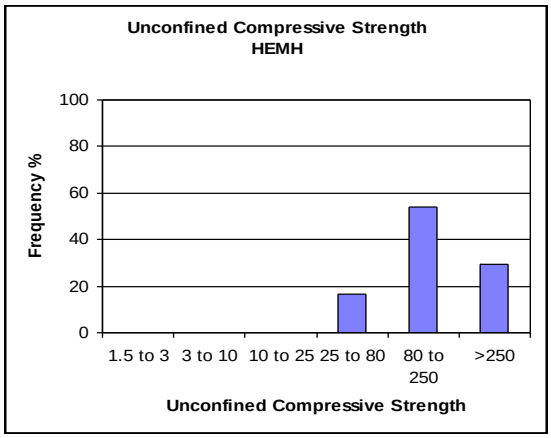
Unconfined Compressive Strength
HEMH
Frequency %
100
80
60
40
20
0
1.5 to 3
3 to 10
10 to 25
25 to 80
80 to 250
>250
Unconfined Compressive Strength

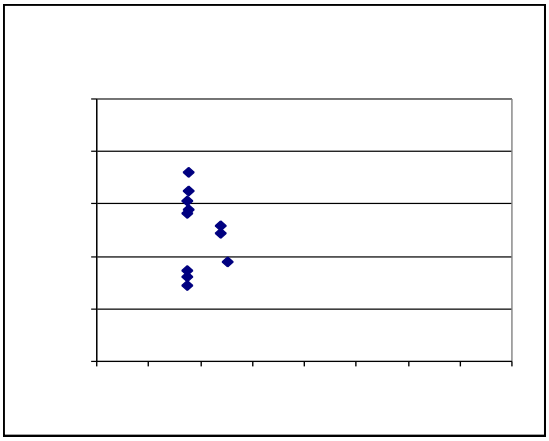

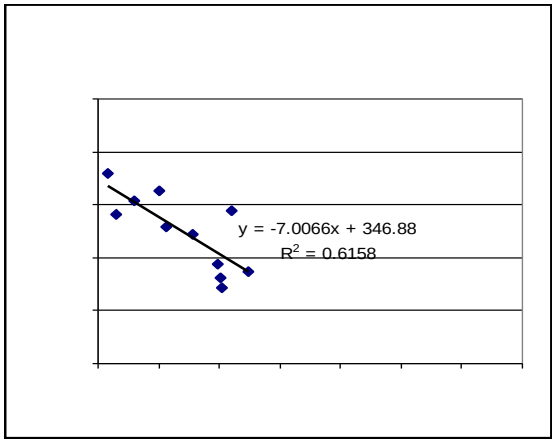
y = -7.0066x + 346.88
R2 = 0.6158

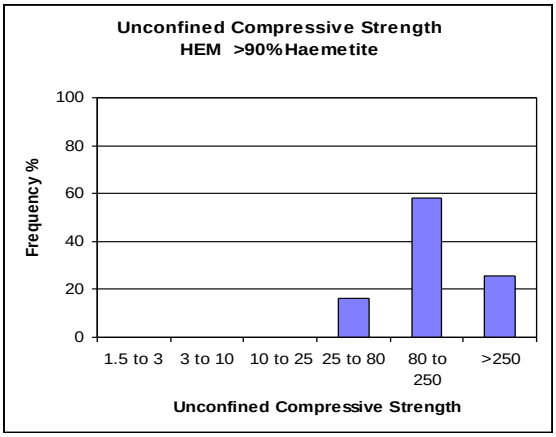
Unconfined Compressive Strength
HEM >90% Haemetite
Frequency %
100
80
60
40
20
0
1.5 to 3
3 to 10
10 to 25
25 to 80
80 to 250
>250
Unconfined Compressive Strength

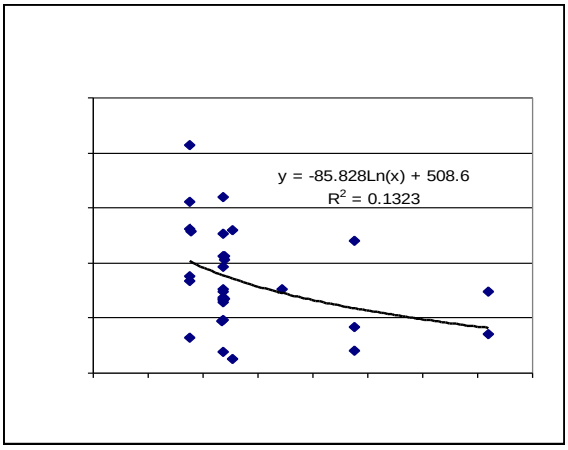
y = -85.828Ln(x) + 508.6
R2 = 0.1323

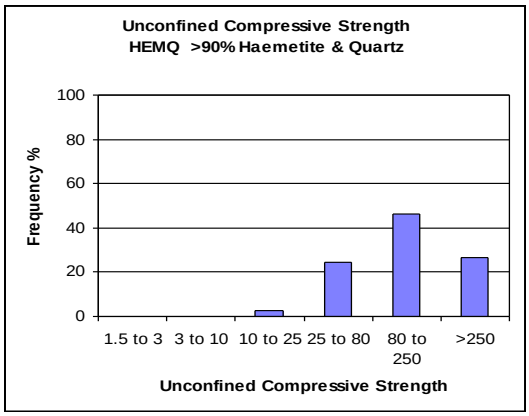
Unconfined Compressive Strength
HEMQ >90% Haemetite & Quartz
Frequency %
100
80
60
40
20
0
1.5 to 3
3 to 10
10 to 25
25 to 80
80 to 250
>250
Unconfined Compressive Strength

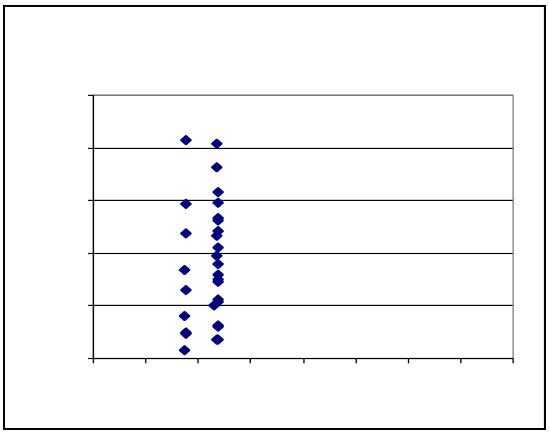

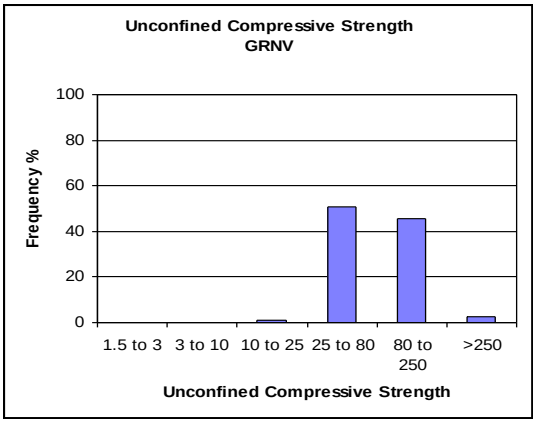
Unconfined Compressive Strength
GRNV
Frequency %
100
80
60
40
20
0
1.5 to 3
3 to 10
10 to 25
25 to 80
80 to 250
>250
Unconfined Compressive Strength

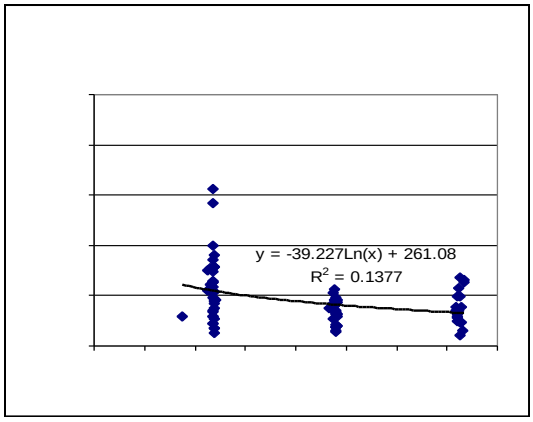
y = -39.227Ln(x) + 261.08
R2 = 0.1377

Appendix D: OD joint properties

E.1 Joint roughness and orientation

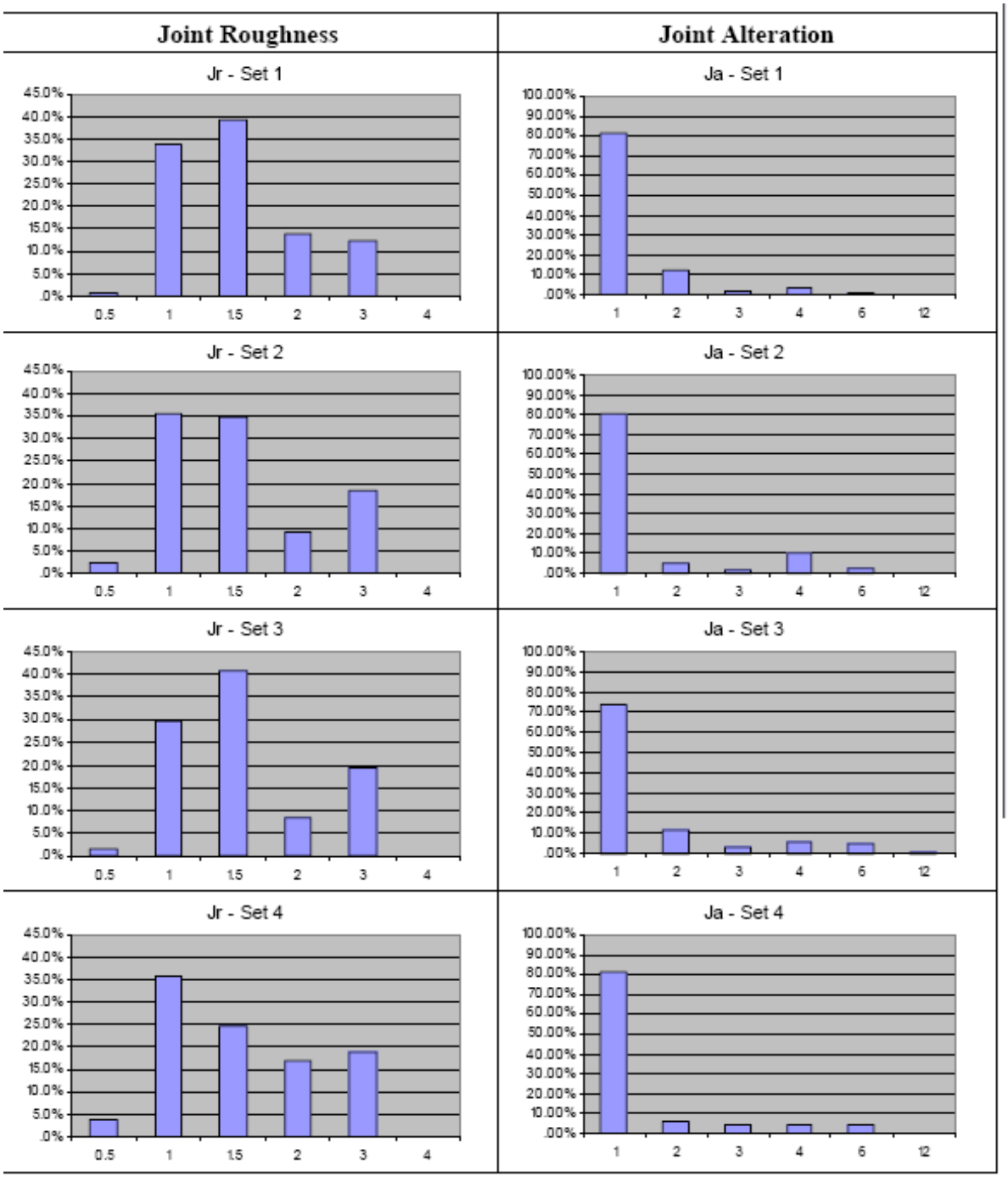

Joint Roughness	Joint Alteration
	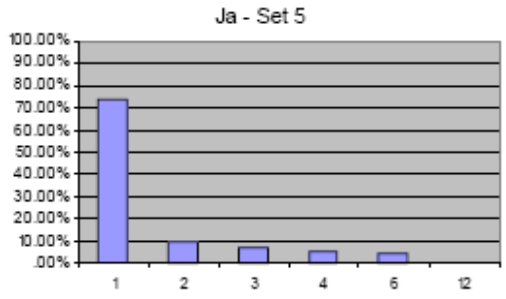
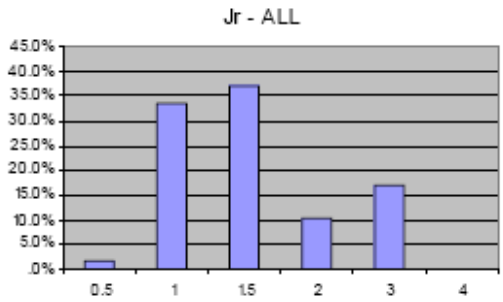	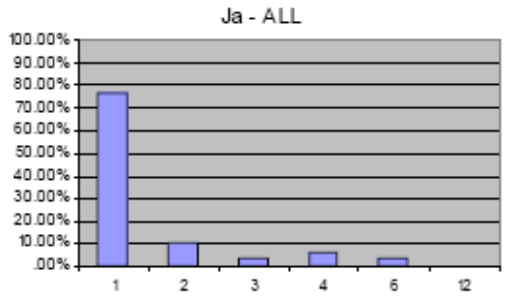
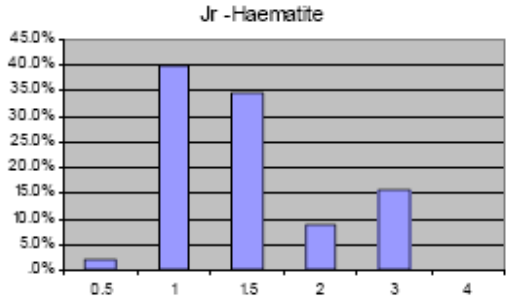	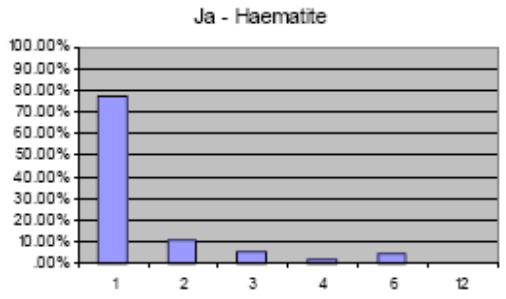
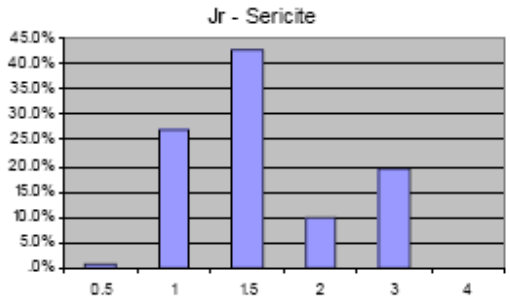	

D.2 Mine area joint orientations

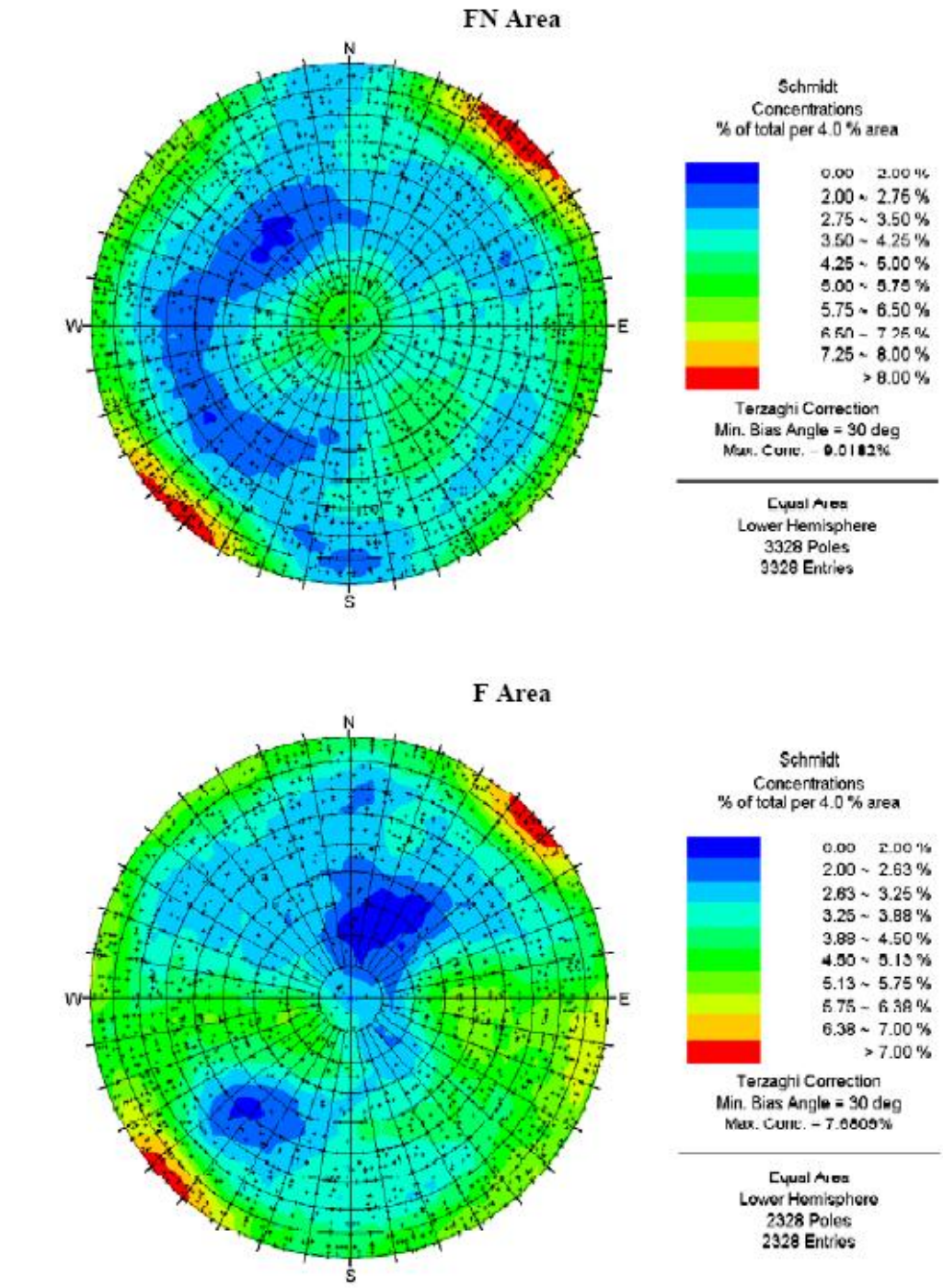

DSE Area

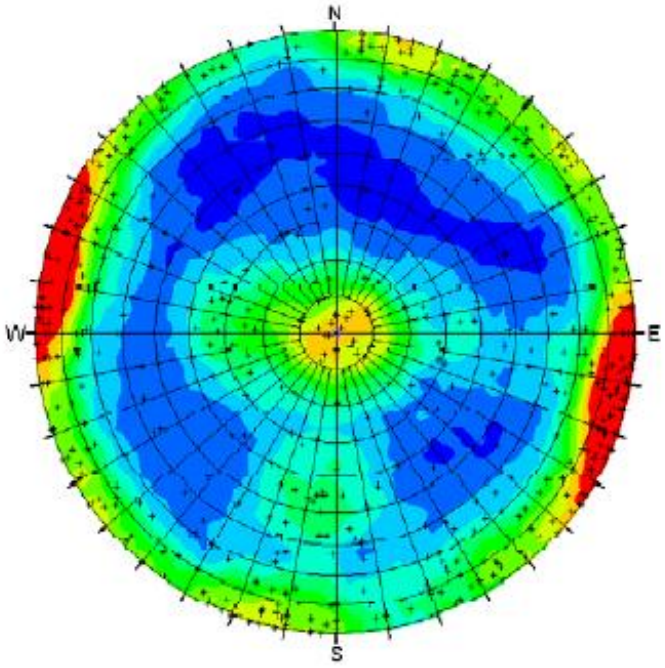

Schmidt
Concentrations
% of total per 4.0 % area

0.00 - 1.00 %
1.00 - 2.13 %
2.13 - 3.25 %
3.25 - 4.38 %
4.38 - 5.50 %
5.50 - 6.63 %
6.63 - 7.75 %
7.75 - 8.88 %
8.88 - 10.00 %
>10.00 %

Terzaghi Correction
Min. Bias Angle = 90 deg
Max. Conc. = 14.7940%

Equal Area
Lower Hemisphere
594 Poles
594 Entries

B, CC and CN Areas

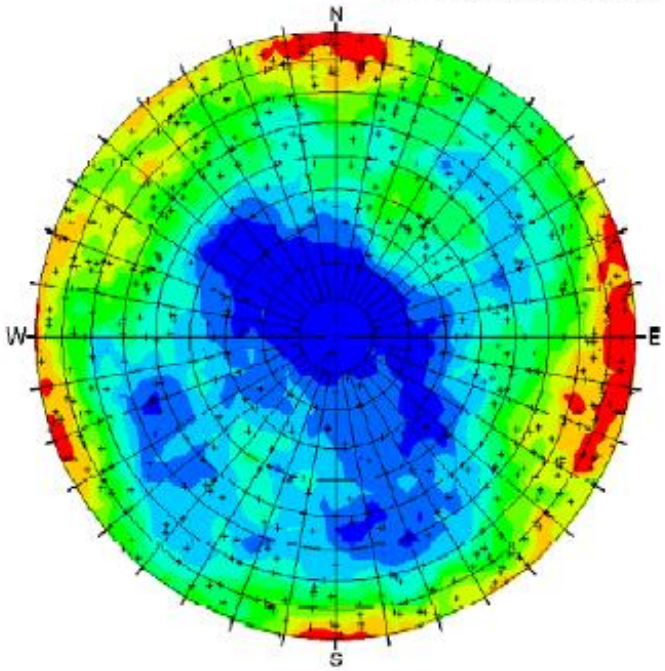

Schmidt
Concentrations
% of total per 4.0 % area

0.00 - 2.00 %
2.00 - 2.63 %
2.63 - 3.25 %
3.25 - 3.88 %
3.88 - 4.50 %
4.50 - 5.13 %
5.13 - 5.75 %
5.75 - 6.38 %
6.38 - 7.00 %
> 7.00 %

Terzaghi Correction
Min. Bias Angle = 90 deg
Max. Conc. = 8.2365%

Equal Area
Lower Hemisphere
656 Poles
656 Entries

Appendix E: Explanation of failed surfaces

STOPE NAME: **Amber 137**
Commenced: September 2004 Completed: November 2004 Backfilled:
Lithology: The stope was predominantly composed of GRNH and HEM lithologies Alteration: Moderate to high
Stope adjacency's: Primary stope Stress condition: Moderate
Overbreak: Both the North & East walls failed.
Comments: The crown was plotted as stable but performed with an ELOS of 1.87 (unstable), around 50% of the surface had some overbreak with the greatest being 11.4 metres but the indicative only 2.9. The failure was centered around the slot raise indicating this was the cause of the localized failure.

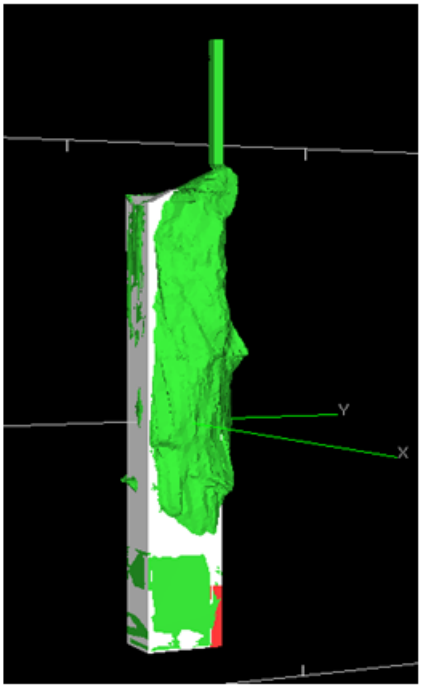

View looking NW

Comments:

The North wall produced an ELOS of 3.34 while it was predicted to be a transition face, the close proximity of Amber 012 may be to answer for this failure. Over 85% of the face experienced some overbreak with the indicative measurement at 3.9 metres.

The Southern wall performed better than was expected with an ELOS of only 0.05. The question raised here is why was the design conservative for this face.

Like the North wall the East wall significantly under performed, 72% of the face had some over break with parts ovrebreaking by 9.8 metres. The indicative failure was reasonably consistent at 5.8 metres contributing to an ELOS of 4.12. Conjugate sub-vertical faults in the area may have played a role in this failure.

The West wall also failed, this face is adjacent with the CAF filled AMBER 012 so there was no preliminary study completed for this face. It can assumed the stresses generated by the pillars between these two stopes are accountable for this failure.

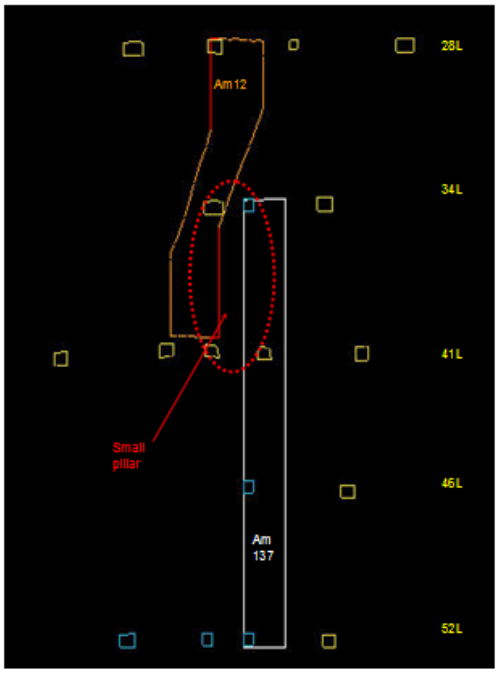

W-E cross section through Amber 012 & Amber 137 showing the small pillar between.

STOPE NAME: **Amber 193**	
Commenced: June 2006 Completed: September 2006 Backfilled:	
Lithology: Predominantly GRNL & GRNH Alteration: Moderate to high sericite alteration	
Stope adjacency's: Secondary stope, Amber 024 abuts the entire eastern wall of Amber 193. Stress condition:	
Overbreak: The crown suffered failure with an ELOS of 2.55	
Comments: The CMS showed all the surfaces were stable other than the crown which failed. The failure appears to be initiated by the raise and intersecting structures. The crown plotted in the Transition Zone on the Stability Chart of supported case histories chart.	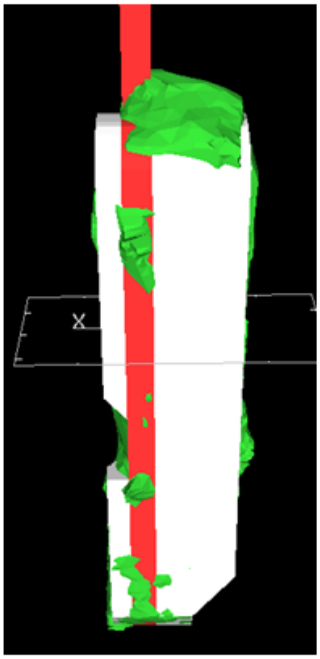 View looking south

Comments:
The crown design profile was arched which is a naturally more stable shape than a flat backed stope. To support the crown, long downhole cables were installed from the 27 level.

The north and south stope walls both plotted within the Transition Zone on the Stability Chart for the unsupported stope case histories. Some falloff and overbreak can be expected from these walls as a result. The west wall plotted well within the Caving Zone on the Stability Chart of unsupported stope case histories. The stability of this wall differed from the north and south wall due mostly to unfavourable orientation of structures (and high frequency).

A number of moderate to steeply SW dipping structures were identified which intersect the crown of Amber 193. The structural influence study identified structures throughout the 41 and 46 levels with potential to cause wedges in the walls. The west wall is particularly exposed to unfavourable orientations of structures

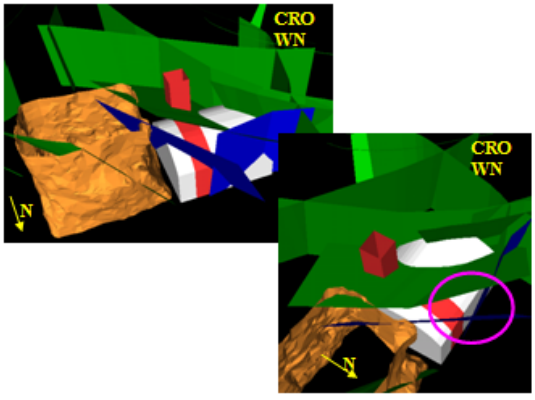

STOPE NAME: **Amber 302**	
Commenced: May 2007 Completed: October 2007 Backfilled:	
Lithology: Within Granitic rocks GRNH-GRNL Alteration: High	
Stope adjacency's: Three mined adjacency's, with Amber 106 which abuts the Southern wall being the only directly adjacent one. Stress condition: Moderate	
Overbreak: Both the Crown & North wall displayed failures.	
Comments: The crown was plotted as stable due to favourable development crown cablebolt coverage. The crown displayed an extraordinary case of failure where 99% of the face over broke in some way. 4.	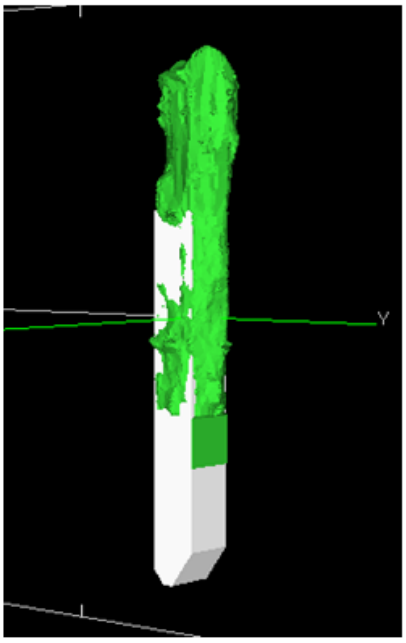 View looking SW

Comments:
The maximum overbreak was a staggering 75.05 metres high and the indicative overbreak used for ELOS calculation was 67 metres, generating an ELOS of 66.04.

The rock in the crown was ranked at 120MPa with moderate to high Sericite alteration with a GBI of 5 indicating a large blocky makeup and a stress figure of 34MPa. None of the above indicated such drastic failure, from this it can be assumed the structure that intersected the Northern side of the crown was the primary unraveling behind the crowns stability. It appears the structure acted as an instigator of the unraveling which reached the unconformity. The structure was acknowledged in preliminary studies but the extensive cablebolting was assumed to prevent failure.

The Northern face was plotted in the transition zone although there was significant concern for the stability based on the expected stress elevation created by the elevation in pillar stress between the Northern side of Amber 302 and Amber 137, coupled with the close proximity of development on the 41 and 46 levels. A stress measurement of 44MPa was measured for this face.

The ELOS calculated for the Northern wall was 4.19 leading it to be classed as a failed wall. 62% of the face over broke in some way with the maximum overbreak being 11.25 metres the indicative overbreak was 6.8 metres. Upon inspection of the overbreak it appears a shallow dipping regional structure in the 46 level has contributed to the failure coupled with the elevated stress environment.

Both the East and West wall were expected to be unstable but recorded stable ELOS figures. The east wall was expected to perform in a similar manner to the Northern wall due to stress changes and interaction with several structures on the 41 and 46 levels. The West wall with a stress measurement of 6MPa was distressed due to Amber 108, stress relaxation of confinement was expected to result in the unraveling of structures on this wall. Very minimal overbreak was experienced on each of the faces, only 29% of the East wall over broke with a maximum of 4.2 metres, while less than 1% of the West wall over broke, a indicative overbreak of 0.80 metres was used for both faces.

STOPE NAME: **Blue 020**	
Commenced: February 2004 Completed: April 2004 Backfilled:	
Lithology: Contained within GRNB, GRNL & HEM compositions. Alteration: N/A	
Stope adjacency's: Primary stope Stress condition: Low to moderate	
Overbreak: The crown failed, ELOS of 5.43.	
Comments: No primary structures were identified in the area only abundant joint sets, closely spaced in the 51 & 57L. The application of the Matthews stability method for this particular stope was strongly influenced by stopes already developed in the area, due to lack of surrounding development.	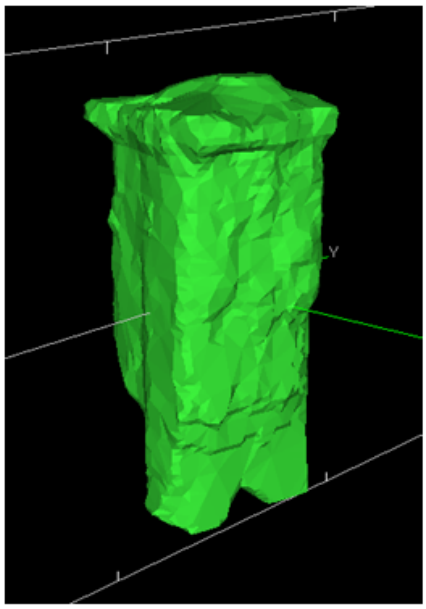 View looking NW

Comments:
Blue 020 crown was plotted in the caving zone though due to greater depth than others previously developed. This proved correct as the crown did indeed fail, with an ELOS of 5.43. Overbreak was consistent across the crown with a maximum of 6.10 metres at the slot raise and a indicative height of 3.30 metres. The 60 metre crown pillar between Blue 020 and overlying Blue 008 and 068 was 60 metres and therefore enough to insulate the stope from a major failure.

The Eastern (NE) wall was predicted to be unstable due to likely exposure of a mafic dyke in the stope wall. The dyke was assumed to have heightened Sericite alteration and a lower RQD. The NE, SE and SW stope walls were all predicted as transition due to this factors but were stable post development and show no signs of significant failure.

STOPE NAME: **Blue 025**	
Commenced: June 2005 Completed: July 2005 Backfilled:	
Lithology: HEMH Alteration: Moderate	
Stope adjacency's: Secondary stope with Blue 020 to the SW. Stress condition:	
Overbreak: Crown surface failure.	
Comments: The overbreak covered the majority of the crown surface, CMS data shows it shadows the drill drive development above.	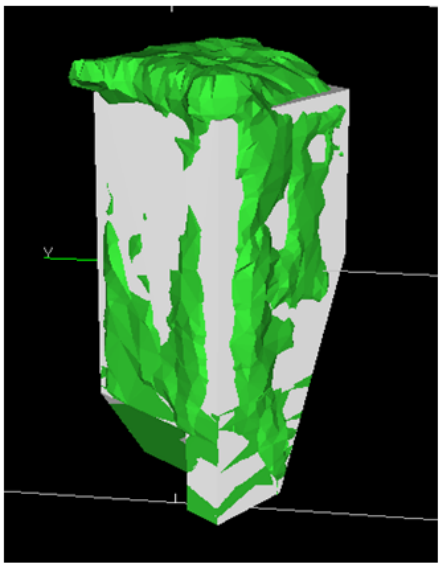 View looking NE

Comments:
The remaining walls of the stope showed only minimal over break with the NW face showing 53% overbreak at a maximum of 4.30 metres and indicative overbreak of 0.90 metres being the most overbreak experienced.
The NW subsequently had an ELOS of 0.81 and was classed as unstable while it was predicted to be unstable. For the NE wall the as with Blue 020 the mafic dyke was anticipated to have a greater impact on wall stability than it did, the NE wall was also expected to suffer from increased stresses due to distribution around Blue 020 and 025. However it had a ELOS of only 0.46 and was therefore stable not unstable. The SE wall performed as expected and the SW wall was adjacent to CAF.

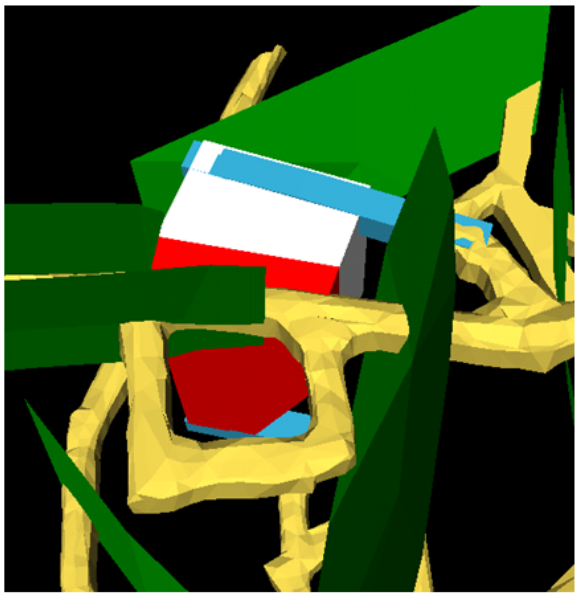

Image displaying the intersecting structures

STOPE NAME: **Blue 117**	
Commenced: September 2007 Completed: October 2007 Backfilled:	
Lithology: Granitic lithologies with small pockets of Hematite throughout it. Alteration: Moderate sericite alteration	
Stope adjacency's: Blue 362 abuts the Southern wall. Stress condition:	
Overbreak: The crown surface failed	
Comments: The crown was plotted as stable however recorded an ELOS of 2.47 with 92% of the surface over breaking with a maximum overbreak of 4.40 metres and the indicative at 2.70 metres. The estimated mining induced stress was only 37 MPa with the assistance of cable bolts the crown was anticipated to plot in the stable segment post production.	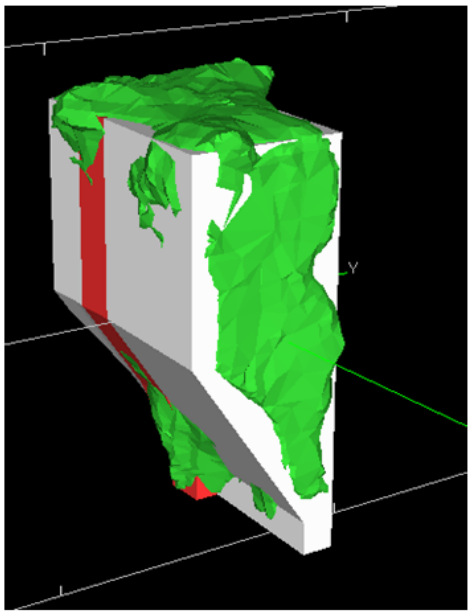 View looking NW

Comments:
The overbreak is a result of the overlying development. In the 45L sub vertical structures intersected the crown and North wall, which answer for the 74% of the North wall over breaking with an ELOS of 1.62 when it was plotted in the stable zone close to the transition boundary.
No issues were found with the East and West walls, they both performed as stable faces as predicted.

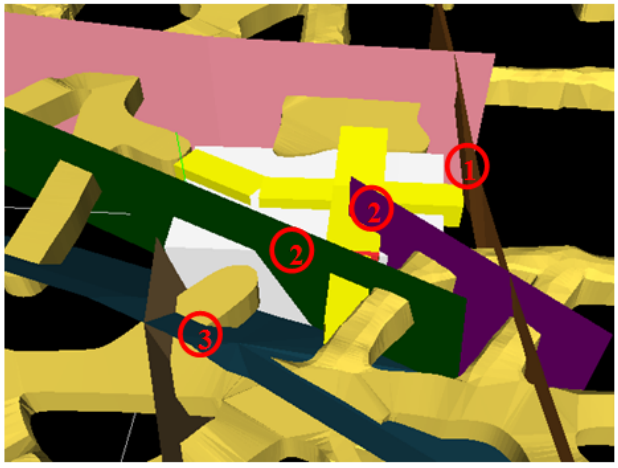

Image displaying Subvertical structure (1) sub-parallel and offset approximately 5 metres from West wall of Blue 117. Subvertical structure (2) intersect Crown and North & East walls. 45° South-West dipping structure (3) intersects North and East Walls below the 45 level.

STOPE NAME: **Cyan 012**	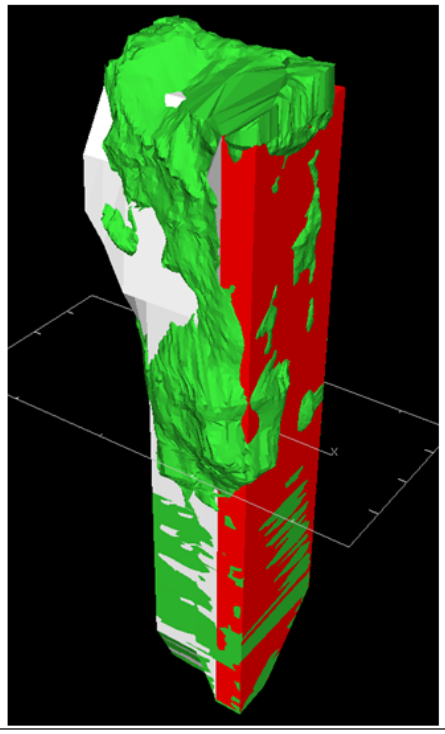
Commenced: March 2005 Completed: May 2005 Backfilled:	
Lithology: Composed of GRNH & GRNL Alteration: Low sericite alteration	
Stope adjacency's: Cyan 12 is a secondary stope, it has a mined adjacent stopes to the north east, Cyan 20. Stress condition: Low	
Overbreak: The crown surface failed	
Comments: The crown of Cyan 12 was expected to be stable with support. Cablebolting of the stope crown was recommended in order to minimise the impact of potential crown overbreak on future stoping in the area. There was always a fault that ran through the crown acknowledged in the pre-production study.	View looking NW

Comments:

The crown failure is likely to stem from a combination of the overlying development, the planar NE dipping structure ~7m above the NE corner & the surrounding previously mined Cyan 020.

The west wall had a higher likelihood of performing unacceptably and the north, south and east walls of Cyan 012 were expected to suffer some dilution. Given the location of Cyan 12, shadowed by Cyan 20 and cyan 23, the walls are expected to be in a low or possibly tensile stress environment during and after excavation. None of the above was realised as all surfaces other than crown were stable.

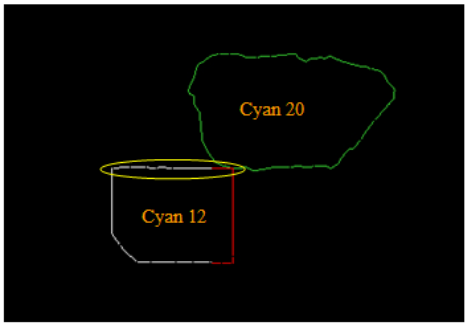

Cyan 112 & Cyan 020 interactions. Plan at ~350 mRL.

STOPE NAME: **Cyan 032**	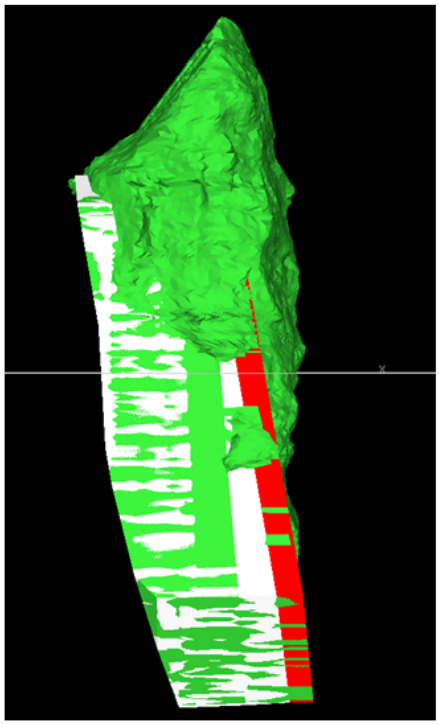
Commenced: August 2004 Completed: February 2005 Backfilled:	
Lithology: Western surface primarily GRNH, eastern & crown surface HEMH,HEM,GRNL & GRNH. Alteration:	
Stope adjacency's: A primary stope. Stress condition: Moderate stress environment	
Overbreak: The crown & eastern surfaces underwent significant overbreak.	
Comments: Cyan 32 was designed to its maximum allowable dimensions with respect to the ore body model in the region, geotechnical constraints, and existing development. In the north-south direction, The Cyan 32 crown has been designed to a dimension of 30 metres, which is the maximum design width of primary stopes in the Cyan area.	View looking north

Comments:
In the east-west direction the stope crown has a dimension of 60 metres. Since the span of the crown is defined as 'the largest circle that fits in the plane of the excavation', the span of the crown of Cyan 32 is 30 metres. The top of the stope was bounded by the position of the unconformity and the RL of existing development, while the base of the stope is limited by Cyan 34. The designed crown of Cyan 32 has been arched in order to increase crown stability and improve the percentage of fill contact with the crown. It appears the 20 m buffer between the crown & the unconformity was not enough & the crown has over broken into this. This overbreak was encouraged by several structures in the area.

The east wall failure is likely to have stemmed from the crown failure & has over broken from it's narrower top width to the wider base width.

STOPE NAME: **Cyan 112**	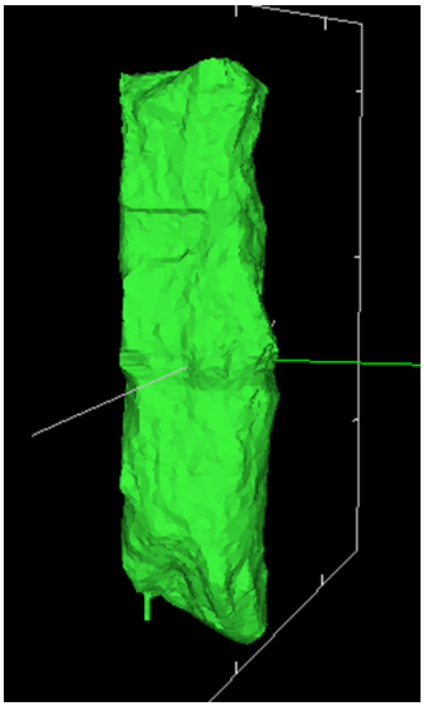
Commenced: March 2005 Completed: May 2005 Backfilled:	
Lithology: Stope walls formed in granitic rocks (GRNL), while the crown is within haematitic (HEM) rich rock. Alteration: Sericite alteration, moderate to high in crown & moderate in walls.	
Stope adjacency's: Cyan 112 has four adjacencies; Cyan 017 to the north, Cyan 001 to the south, Cyan 417 to the east and Cyan 425 to the northeast. Cyan 417 abuts Cyan 112 from the 52L to 58L Stress condition:	
Overbreak: The crown surface failed.	
Comments: The structural influence study highlighted some potential problem structures in the draw point area and in the 52 level. A regional structure was identified to potentially affect the NW corner of the crown and subsequent deterioration of the east wall.	

Comments:
The crown plotted as stable with support. Potential for minor structurally controlled fall-off from the crown was acknowledged. The west wall plotted in the transitional zone.

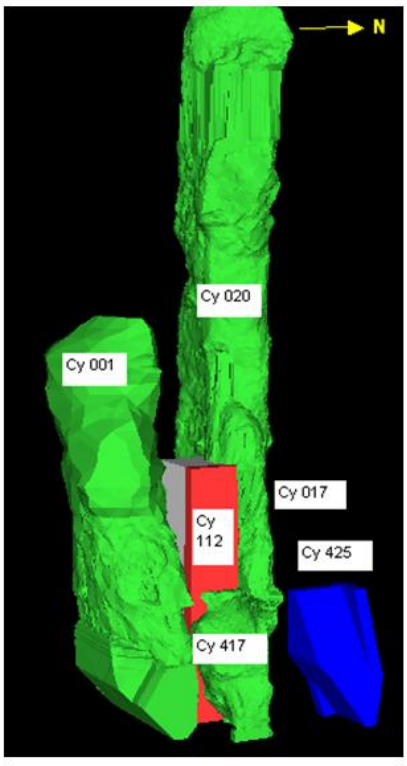

Cyan 112 & surrounding stopes

STOPE NAME: **Cyan 320**	
Commenced: June 2007 Completed: August 2007 Backfilled:	
Lithology: GRNB Alteration: Moderate to high	
Stope adjacency's: Secondary stope with Cyan 332 immediately adjacent to the north. Stress condition:	
Overbreak: The west wall failed	
Comments: There was deterioration of ~60% of the West wall with a maximum overbreak of 9.7 metres and indicative one of 5.6 metres. Although the North wall was adjacent to a 100% CAF filled stope (Cyan 332) there was a small area near the NW corner which remained rock, creating a rock step.	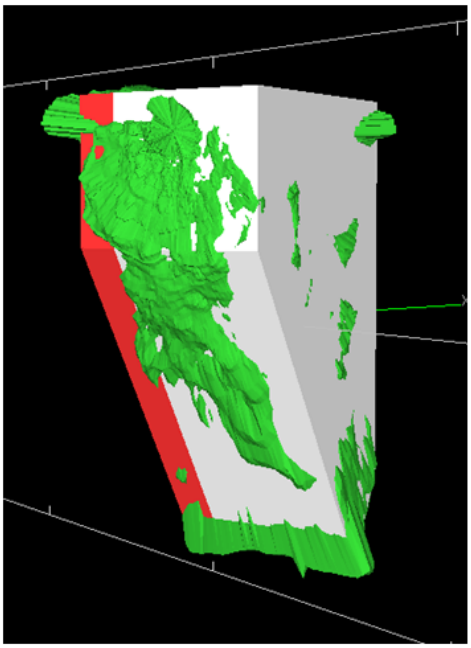 View looking NE

Comments:
This may have been responsible for the unraveling of the West wall coupled with the stress relaxation from the shift in stresses between the South wall of Cyan 320 and Cyan 332. It was expected that the Southern wall would experience the greater of the stress changes and the East and West wall would experience minimal changes, none of which were expected to effect the stopes stability. The west surface ELOS may be bias due to the few areas of high overbreak while the remainder is fairly minimal.

The Crown, South and East walls all shared the same characteristics as the West walls and performed with no ELOS greater than 0.59, with minimal significant overbreak. Minor structurally controlled fall-off was expected in the Crown, South and East walls therefore plotting them in the predicted transition zone. Cable support was used in the crown.

STOPE NAME: **Cyan 393**	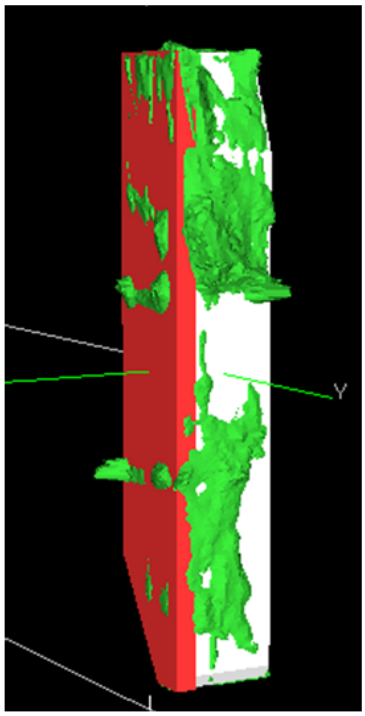
Commenced: April 2006 Completed: September 2006 Backfilled:	
Lithology: GRHNL & GRNH Alteration: Low to moderate Sericite alteration	
Stope adjacency's: Cyan 393 is a secondary stope with 2 direct mined adjacencies. Cyan 393 is located within close proximity of 6 stopes: Above 46L Cyan 393 doesn't have direct adjacencies. Stress condition:	
Overbreak: Failure on the north surface	
Comments: Cyan 393 was mined between 34L and 52L, the surrounding stopes, given size and location in relation to Cyan 393 was expected to create a complex mining induced stress discussed as Upper Cyan 393 and Lower Cyan 393.	View looking SW

Comments:

In the upper segment stress was expected to be elevated in the E-W pillar between Cyan 032 to the South and Cyan 039 to the north. Cyan 393 will be mined East of this pillar experiencing higher stress. It was expected that the mining of Cyan 393 would result in the elevated stress from the pillar being re-distributed around and over Cyan 393. High stress was expected to form in the crown and resulting in some rock noise.

The lower segment was mined in the E-W continuous pillar between Cyan 039, 042 and 048 to the north and Cyan 034 to the south. This area was expected to be elevated in stress from the surrounding stope voids. Mining of Cyan 393 will remove the pillar and cause the stress to re-distribute. Given existing stope voids, the stress is likely to distribute south of Cyan 034 and north around Cyan 042 to respective pillars on each side. The re-distribution expected in the East, South and West walls of the stope could result in de-stressing.

In the 34 level there were several SE and NE dipping regional structures which intersect the stope coupled with a steeply dipping East structure which may have contributed to instability in the North wall. The NE dipping structure continued to interact with the stope on the 41 level potentially contributing to re-distribution and unconfinement of the structure. Throughout the 46 and 52 levels there was little structural effect on the stope recognized apart form the two east dipping structures which had potential to cause some instability in the west wall.

The preliminary study anticipated the crown, east and west walls to be stable and the North and South to be in the transition zone. In reality the crown, south and east walls were stable while the west was unstable and the north failed. The three stable faces showed very little fall off (16 %– 28%). The west wall only experienced 46% of the are with fall off, showing localized fall off occurred with maximum overbreak of 6.94 metres and indicative of 4.2 metres. The likely cause of this overbreak was the steeply dipping east trending structures in the lower levels of the stope.

The northern wall showed significant fall off over 72% of the walls surface area, reaching 10.1 metres at times. The overbreak can be explained by the unraveling of NE dipping structures throughout the 34, 41 and 46 levels coupled with the change in stresses between Cyan 393 and neighboring stopes.

STOPE NAME: **Cyan 425**	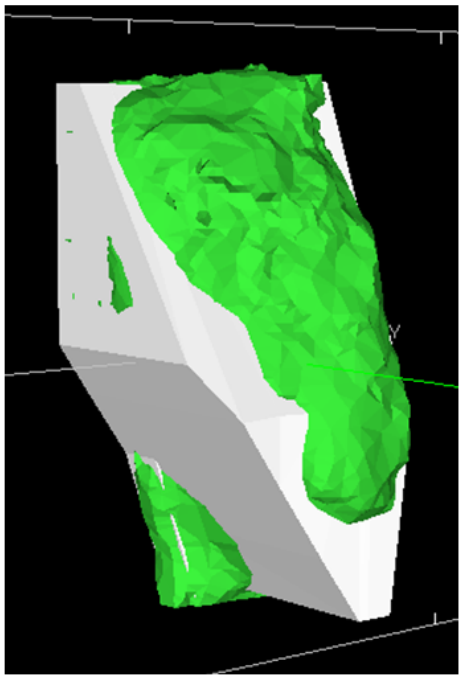
Commenced: March 2006 Completed: May 2006 Backfilled:	
Lithology: GRNH & GRNB Alteration: Low to moderate Sericite alteration	
Stope adjacency's: A pillar between Cyan 425 and Cyan 017 (CAF and rock) is 3m at the narrowest point. Stress condition: High	
Overbreak: The east surface failed	
Comments: A fault dipping 65 degrees to the east was the only structure found to interact with Cyan 425. The East wall of stope was sub parallel to this fault meaning any sympathetic joints had potential to form slabs, which could fall into stope.	View looking SW

Comments:
Postproduction 70% of the crowns surface area had over broken at a maximum depth of 3.1 metres with an ELOS of 1.82 classing it as unstable. This overbreak appears to shadow the overlying development drive, with no evidence of a structural influence.
The north, south and west walls all incurred less than 44% of there surface areas displaying fall off. While the east wall which was expected to be stable failed. The CMS data clearly displays this failure can be attributed to the sub-parallel fault that was identified in the preliminary study.

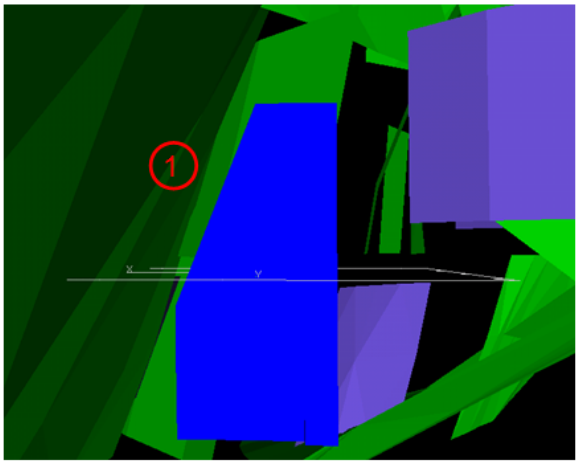

Image showing 1.Fault dipping 65 degrees to the east. East wall of stope is sub parallel to this fault

STOPE NAME: **Cyan 426**	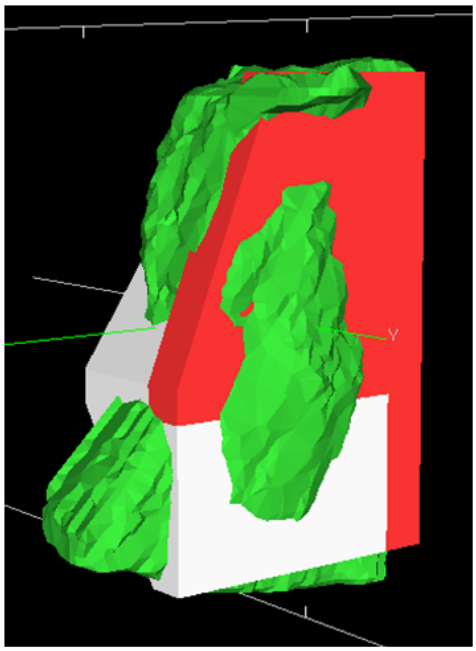
Commenced: January 2009 Completed: March 2009 Backfilled:	
Lithology: The crown and eastern hanging wall consisted of GRNH/GRNB, the majority of the stope is GRNL. Alteration: Moderate Sericite alteration	
Stope adjacency's: Full height adjacency with Cyan 425 to the south & Cyan 031 to the north. Stress condition:	
Overbreak: The eastern surface suffered failure	
Comments: There were several steeply to moderately dipping structures identified to the SE on the crown level. There was one sub-vertical structure on the 58 level in draw point one which intersected the uphole slot.	View looking SW

Comments:
The crown plotted in the stable zone of the supported chart and in the transitional zone on the unsupported chart. The combined crown and hangingwall (Crown-ALL) plots in the caving zone on the unsupported chart. As a result it was recommended that the crown and hangingwall of Cyan 426 be supported with cablebolts. The design eastern wall and hangingwall plot in the transitional zone on the stability chart. As this method dose not fully account for the change in stress state following mining of Cyan 426, failure of an unsupported hanging wall was also expected due to a reduction of the principal stress and confinement following mining of Cyan 426.
The CMS shows that the crown was stable and the eastern wall and hanging wall failed. The failure was not consistent across the face but was up to 9 metres thick. The overbreak on the lower section of the face is more significant and appears the reduction of principal stress and the lack of support has triggered the failure. The upper hanging wall sections failure starts at crown level and looks like a slide structure.

STOPE NAME: **Cyan 442**	
Commenced: March 2005 Completed: April 2005 Backfilled:	
Lithology: GRNH,GRNL & GRNB Alteration: Very low to no alteration	
Stope adjacency's: Cyan 442 was a small primary stope, underlying Cyan 051. There is no CMS data from the lower portions of Cyan 051 because the stope crown failed prior to filling, and the extent of overbreak in the lower portions of this stope is unknown	
Overbreak: The crown surface failed.	
Comments: The regional structural geology model showed a large structure that sub-parallels the east wall of Cyan 442. The structure itself was not of concern but associated sub parallel joints were expected to cause local instability on the east wall.	View looking NW

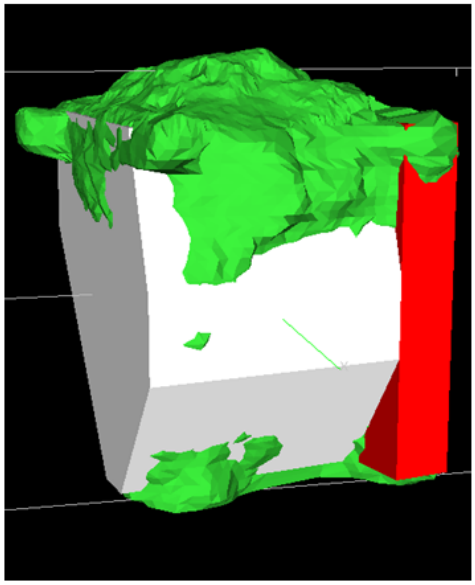

Comments:
The crown of Cyan 442 had a GBI of 3 (two effective block forming joint sets: massive to blocky rock). The drawpoint level of Cyan 442 was not mapped, surrounding mapping indicated GBI 1-2 (massive rock, one or random joint sets only) which was applied.

The crown of Cyan 442 was expected to be stable with support. The study showed that the crown failed, a result of the overlying Cyan 051 coupled with the block GBI. Cyan 051 was known to have failed through the unconformity, and the stope is filled with rock fill. Because the exact location of the base of Cyan 051 is unknown extensive cable bolting was used but did not prevent 99% of the crown surface over breaking to a maximum of 7 metres.

All walls of Cyan 442 were expected to be stable, it was noted in the preliminary study that Poor / variable ground conditions and stope performance were anticipated as a result of the location of the stope in the abutment of the FN Collapse Area. These conditions may not have been adequately represented by the Stability Graph Technique analysis. The east wall was the only one to show any instability, this can be explained by the joint sets noted in the discussion of structures and were not un common for this area of the mine, particularly at this depth.

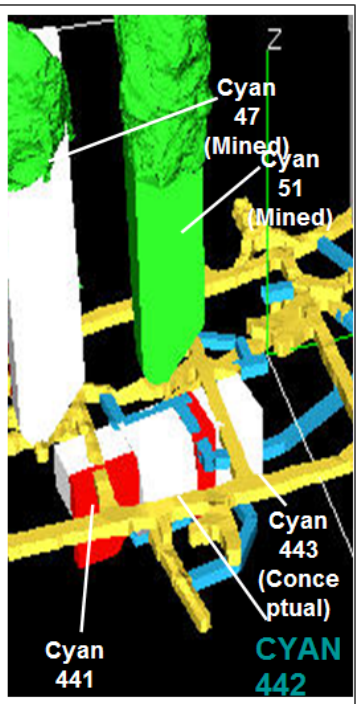

Cyan 442 & surrounding stopes

STOPE NAME: **Jade 025**	
Commenced: November 2006 Completed: February 2007 Backfilled:	
Lithology: GRNL,GRNH & HEMH Alteration: Low on the crown level, increasing to moderate down the stope.	
Stope adjacency's: Direct and full adjacency with CAF filled Jade 026 to the NW Stress condition:	
Overbreak: Both the NE and SW surfaces failed	
Comments: The crown of Jade 025 was highly structured, with two faults and a number of less continuous joints mapped. A number of joints (structures interpreted to have a limited continuity) were mapped in the extraction level.	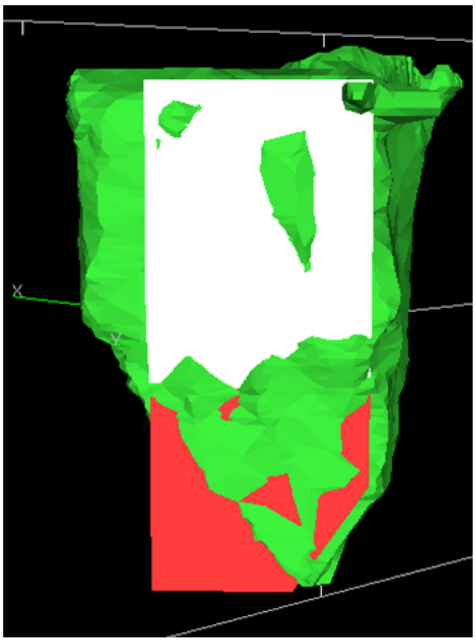 View looking south

Comments:
The crown was plotted on the stable/transitional boundary of the supported chart, but would plot in the caving zone on the unsupported case histories chart. As a result it was recommended that the crown of Jade 025 be supported with cable bolts. The crown was unstable postproduction as predicted. The unravelling that occurred reflects the structures that were identified in the preliminary study.

All the walls were plotted in the stable portion of the stability graph in the preliminary study. This proved true for the SE wall which only had 1% of it's surface area show any overbreak. The NE and SW walls however had 57% and 75% respectively, of there surface areas overbreak. Both being classed as failed surfaces. The only structures which were noted in the stope notes other than those effecting the crown were at the upper levels of the stope, the overbreak extends down the stope face lending to another failure mechanism.

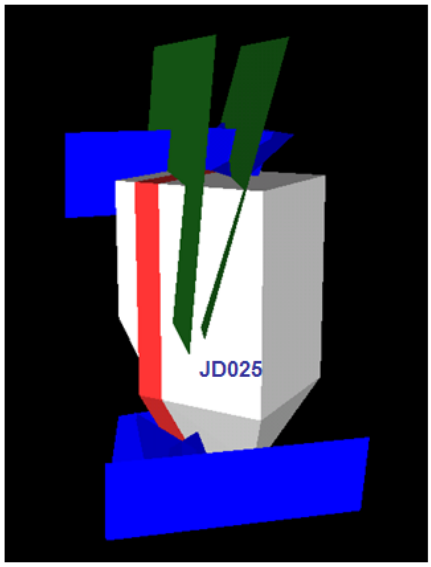

Structures intersecting Jade 025 looking north

STOPE NAME: **Jade 306**	
Commenced: October 2005 Completed: December 2005 Backfilled:	
Lithology: Alteration:	
Stope adjacency's: One partial adjacency, Jade 005 to the south east Stress condition:	
Overbreak: The crown surface failed	
Comments: There were two main instability issues with Jade 306. The first relates to several continuous structures in the crown, the second is a regional structure that intersects the SE wall of the stope. There were several structures in the crown that had the potential to form a wedge.	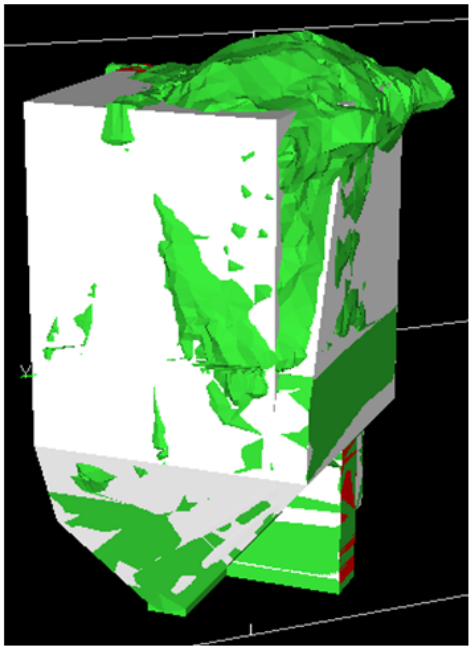 View looking SE

Comments:
Two major continuous structures were mapped on the 26 level around Jade 306. One is a moderate SW dipping structure that daylights along the 26JD3 WDD ACC drive, the other is a steep SE dipping localized structure. These structures combined with several other minor structures may result in crown instability and over break. The Matthews does not acknowledge structural failures.
There was a regional structure identified that intersected the base of the SE wall. This wall is adjacent to Jade 005 stope with only a 15m pillar. As the stope is mined there was the possibility that the SE wall would unravel along this structure resulting in large rocks in the drawpoint.
Post production inspection shows the stope walls performed well however there was significant failure in the crown. The crown failure can be attributed to a moderately (55°) fault, which has resulted in the deterioration of the crown in the SW corner.

STOPE NAME: **Olive 001**	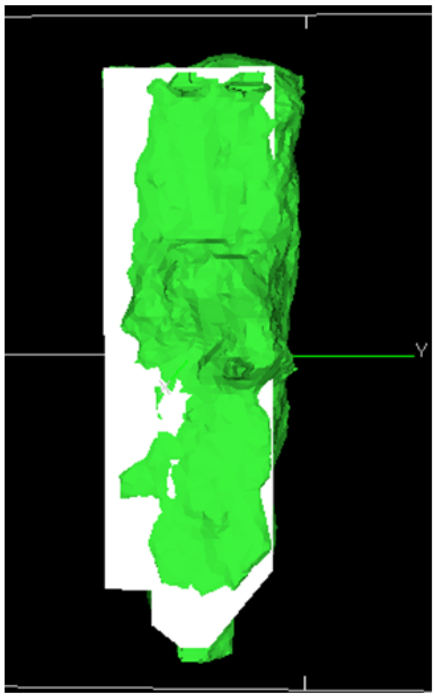
Commenced: September 2008 Completed: December 2008 Backfilled:	
Lithology: Formed within GRNL & HEMH Alteration: Low Sericite alteration	
Stope adjacency's: secondary stope with the following adjacencies, Olive 378 to the west & Olive 008 to the south. Also Olive 020 lies 5 metres to the North-East and Olive 014 lies 5 metres to the North-West Stress condition:	
Overbreak: East surface failed	
Comments: The Crown plotted in the stable zone of the supported case histories chart and in the transition zone of the unsupported case histories chart. The North and East walls plotted in the caving zone close to the transition zone boundary on the unsupported case histories chart.	View looking west

Comments:
This result was primarily dictated by large hydraulic radius, with the rockmass itself assessed as generally good. If rockmass structures were assessed with an adverse orientation then these walls plot well into the caving zone. It was also noted that modelling does not indicate potential for significant stress-driven rockmass damage around Olive 001 after extraction.
The CMS showed the crown and north walls were unstable while the east wall failed with around 50% of the face suffering overbreak up to 9.10 metres thick. The failure appears to have been a result of intersecting sub vertical structures.

STOPE NAME: **Olive 356**	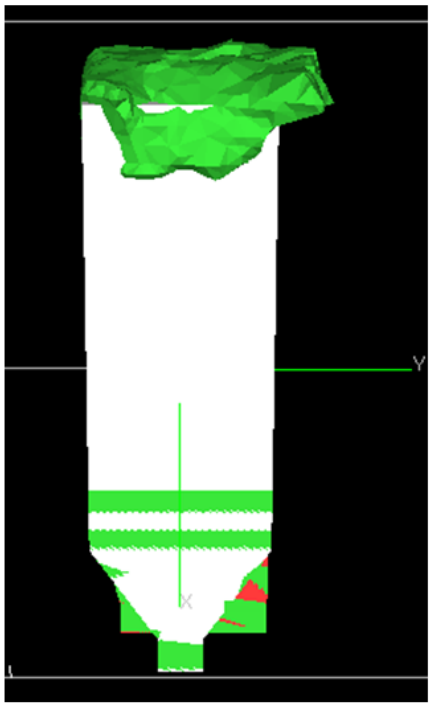
Commenced: January 2006 Completed: February 2006 Backfilled:	
Lithology: HEM & GRNL Alteration: Low alteration	
Stope adjacency's: One adjacency, that was Olive 031 to the North Stress condition: Moderate	
Overbreak: The crown surface failed	
Comments: The following structural influences were noted, the stope is moderately structured. On the 39 level a structure dipping steeply to the NW intersects a moderate-steeply dipping SE structure above the crown of the stope which may result in a steep wedge.	View looking west

Comments:
Crown cable bolt coverage should be adequate to reinforce the wedge. On the 45 level a shallow westerly dipping structure will be present in the backs of the 45 OL31 EXTR DR drawpoint which should be considered when designing the drawpoint cables.
Post production inspection shows all the walls performed well, while the crown which was predicted to be stable failed. The CMS shows the failure of the development drive on the northern edge of the crown, the remaining overbreak is of similar height but doesn't appear to be dictated by any structures. A total of 81% of the crowns surface area has failed to an average overbreak of 2.8 metres.

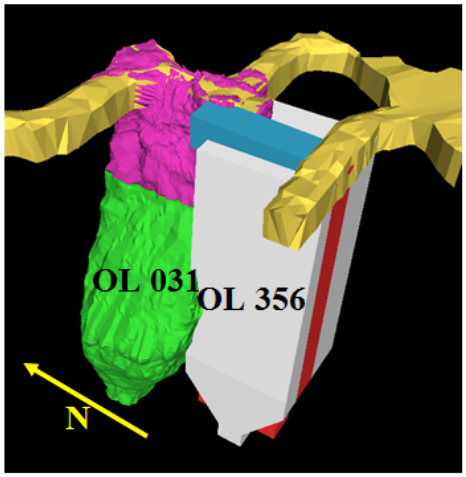

Olive 356 with neighbouring Olive 031

STOPE NAME: **Olive 364**	
Commenced: July 2007 Completed: November 2007 Backfilled:	
Lithology: Formed in HEM & GRNL Alteration: No alteration data	
Stope adjacency's: No direct adjacencies Stress condition: Moderate	
Overbreak: Both the crown & North surfaces failed	
Comments: Due to the orientation of the walls with respect to the virgin stress orientation it was acknowledged all the walls would undergo partial de-stressing. This could explain the full level failure of the northern wall.	View looking west

Comments:
This wall experienced overbreak to 81% of it's surface area at a average depth of 8.80 metres. Another plausible explanation could be the arched geometry of the stope crown.
The crown also underwent significant failure with 67% of it's surface area over breaking to an average height of 3.30 metres. The presence of volcanics may have effected the crown stability, despite crown cabling. The failure evenly hugs the arch shape of the crown down to the northern wall leaving little explanation for the failure other than the arch shape.
The remaining walls of the stope showed minimal overbreak.

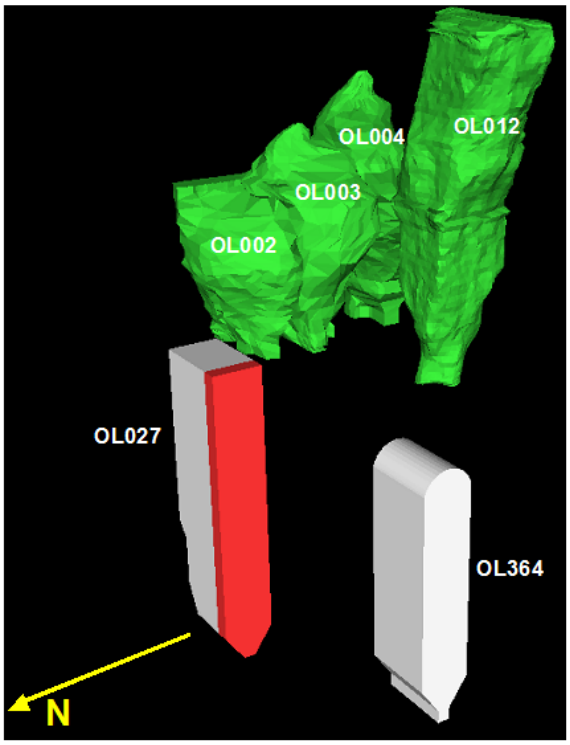

STOPE NAME: **Orange 028**	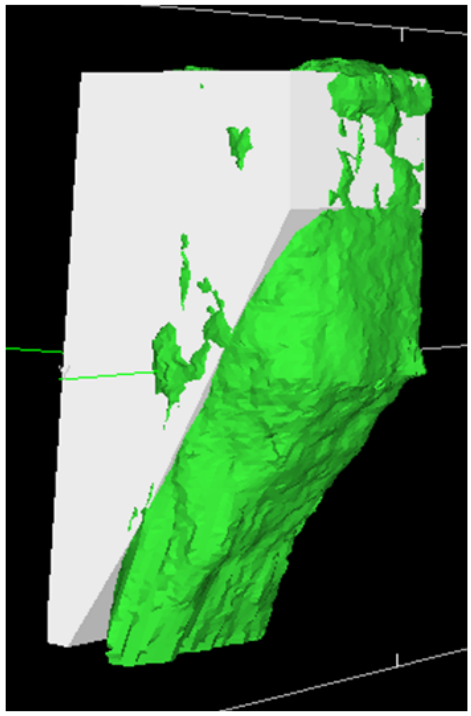
Commenced: March 2005 Completed: August 2005 Backfilled:	
Lithology: The stope crown was of GRNL to HENH composition while the walls had a composition ranging from GRNL to HEM Alteration: Very low Sericite alteration	
Stope adjacency's: Orange 028 three adjacent stopes which are CAF filled, firstly it undercuts Orange 006, Orange 037 lies to the north and Orange 005 to the South Stress condition:	
Overbreak: The west surface failed	View looking SW
Comments: The stope design process does not recognise any major structures only a series of minor ones believed to have minimal impact. Post production inspection shows that the western wall failed, over 50% of the wall failed with a average overbreak of 6.60 metres..	

Comments:
The overbreak is linear to the stope possibly triggered by unidentified sub vertical structures or possibly stress relaxation due to the two adjacencies to the north and south. The remainder of the stope performed without any significant failures.

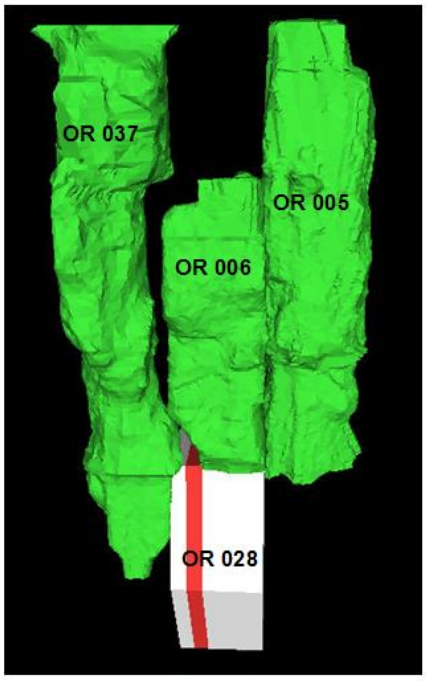

Orange 028 adjacencies looking east

STOPE NAME: **Orange 046**	
Commenced: January 2005 Completed: May 2005 Backfilled:	
Lithology: Primarily composed of GRNL & GRNH Alteration: High Sericite Alteration on the west wall, low to moderate alteration for remainder of stope.	
Stope adjacency's: Orange 046 is a primary stope, Orange 045 sits to the west, with a 15m rock pillar to Orange 046 Stress condition: It was noted the west wall is likely to be highly stressed given the 15m pillar. The crown was in a elevated stress environment as the rock forms a continuous pillar below the "upper oranges".	
Overbreak: Both the crown & west surfaces failed.	
Comments: Mapping of the development near Orange 046 identified two major structures which were continuous in respect of the stope dimensions.	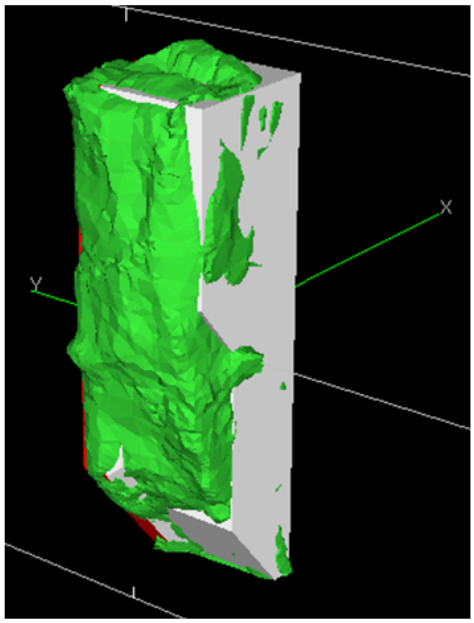 View looking NE

Comments:

Firstly a north-west trending dipping vein was interpreted to truncate the south-western corner of the stope on the 46 level and a north-east trending sub-vertical structure was interpreted to truncate the south-eastern corner of the stope.

The crown was expected to be reasonably stable, although it plotted in the transition portion of the stability graph, cable bolt support was expected to be sufficient. The north and south walls were expected to suffer significant deterioration. The east wall was expected to be unstable but avoid major unraveling. The west wall had a higher likelihood of performing unacceptably, given the wall dimensions and strength. The possibility of local instability/overbreak was identified but the west wall was still plotted in the transition part of the stability graph.

The stope performed in the following ways, the crown failed, as did the east and west walls and the north and south walls were stable. The failure on the west wall is continuous across the entire surface, most probably caused by stress relaxation and the weakened rock strength. The East wall also displays a consistent overbreak across it's surface with an indicative overbreak of around 3.20. The failure on the crown is not as widespread but has an average height of 3.10 metres therefore why it is classed as failed. The north and south walls show very little failures at all, proving the Matthews stability method was very ineffective in predicting the stability of this stope.

The crown failure is locally displaced, with the centre displaying the greatest deterioration, it appears to be structurally controlled or potentially by the relaxation of mining induced stresses due to the minimal pillars between itself and overlying orange stopes.

The west walls fall off is reasonably uniform across the entire face averaging 5.80 metres. It appears the unraveling is a result of the weak Sericite altered rock coupled with the 15m pillar between the face and Orange 045, which was reduced to only a metre or two at the thinnest point. The east face also showed reasonable widespread consistent overbreak across the face averaging 3.10 metres. The sub-vertical north east trending structure appears to have encouraged the unraveling of this face.

STOPE NAME: **Orange 052**	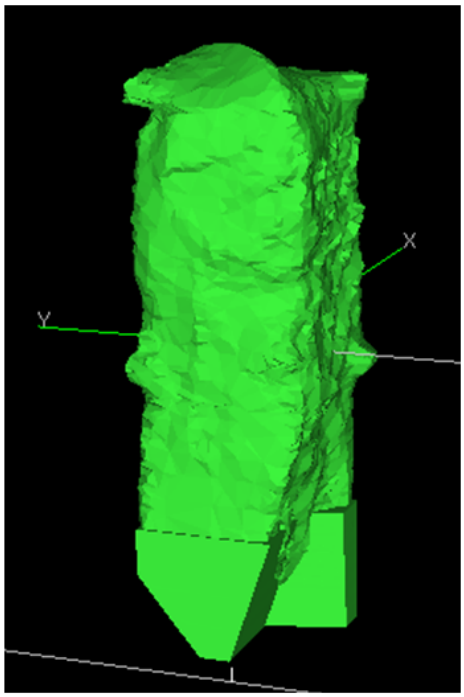
Commenced: October 2004 Completed: March 2005 Backfilled:	
Lithology: The stope was within GRNH lithology with areas of GRNL and GRNB Alteration: Intense Chlorite & Sericite alteration in the NW corner, moderate for the remainder of the stope.	
Stope adjacency's: Primary stope Stress condition:	
Overbreak: Crown surface failed.	
Comments: The structural influence study discussed the presence of the moderate density of continuous structures with low to moderate consistency which are present in the orange stoping block with particular emphasis on a ne/sw dipping set which are particularly continuous within the stope dimensions.	View looking NE

Comments:
The study plotted the crown in the transition zone of the supported case histories chart but noted the lack of background geological information. The walls all plotted in the caving zone of the unsupported case histories chart. It was identified that they may suffer dilution and as a result there may have been large rocks in the draw points.
The CMS shows the north and south walls were stable and the east west walls showed some instability. The crown failed, the failure resembles a north east trend possibly a reflection of the continuous structures noted in the preliminary study.

STOPE NAME: **Pink 325**	
Commenced: June 2005 Completed: July 2005 Backfilled:	
Lithology: Crown & walls predominantly HEM/HEMH Alteration: No alteration data available, but assumed high	
Stope adjacency's: Pink 325 is a secondary stope. Pink 001 (to the south) is its only mined adjacency, it is 100% CAF filled Stress condition: Low to moderate	
Overbreak: The north surface failed	
Comments: The structural influence study identified a fault dipping moderately to the south west was expected to truncate the eastern part of the crown. In the final stability assessment the crown plotted in the stable with support portion of the Supported Case Histories chart.	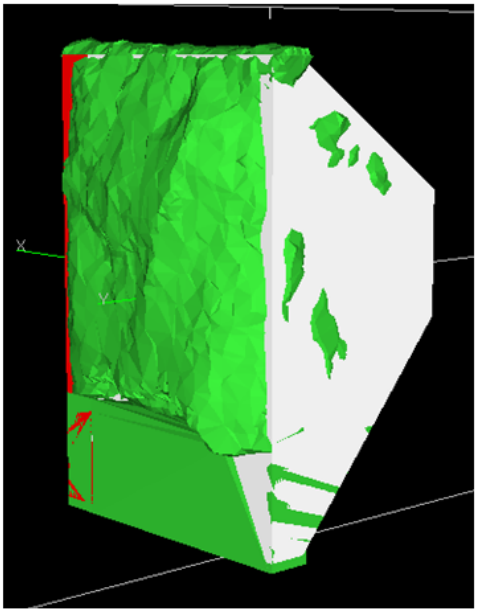 View looking SE

Comments:
It was noted that the crown (with exception of the slot) dipped shallowly and created a pendant wedge against Pink 001 fill. The actual performance of the crown was expected to be worse than indicated by empirical analysis.
It was also be noted that the stability graph method for assessing stope surfaces cannot take into account the influence of the unconformity, which is within 8m of the highest point of the stope crown (existing development backs to unconformity).
The North, West and Eastern walls all plotted within the stable zone on the Unsupported Case Histories chart. This is primarily due to anticipated good ground conditions (high strength, low alteration, high RQD).
The CMS shows the east and west walls were stable, the crown was unstable and the north wall failed. Nothing in the preliminary study highlighted the possibility of this occurring. The failure covers 85% of the stope at an average thickness of 4.5 metres, it could be a result of unidentified sub-vertical structures or stress relaxation.

STOPE NAME: **Purple 128**	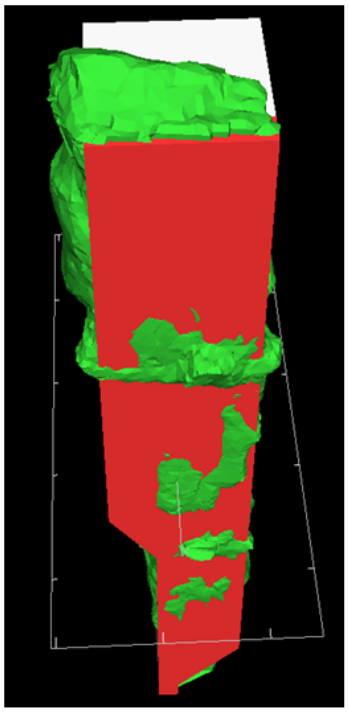
Commenced: April 2005 Completed: August 2005 Backfilled:	
Lithology: The crown was composed of GRNL to HEMH while the walls were GRNL to HEM Alteration: Moderate Sericite alteration	
Stope adjacency's: Purple 128 is positioned within a semicircle of mined stopes it abuts Purple 127 to the north, Purple 129 to the south and Purple 116 to the west Stress condition:The surrounding stopes were expected to form effective stress shadowing for Purple 128, some stress relaxation was expected.	
Overbreak: The crown surface failed	
Comments: The structural influence study showed faults were mapped and interpreted in all levels of development also the fault which had caused instability in the crown and upper levels of other stopes in the area continues through Purple 128. A dolerite dyke was identified in the crown and western wall.	View looking north

Comments: The crown plotted in the caving zone of the unsupported chart but it was believed cables would be sufficient support to prevent instability. The east wall plotted in the transitional zone, local overbreak was expected. The CMS shows the east wall was stable but the crown of Purple 128 failed, with a maximum overbreak of 7.60 metres and an average of 3.60 metres. The failure appears to be influenced by the overlying development.	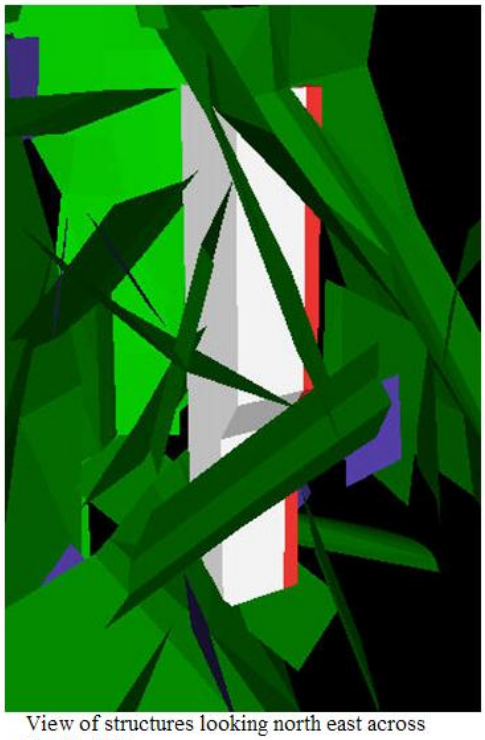 View of structures looking north east across Purple 128.

STOPE NAME: **Purple 232**	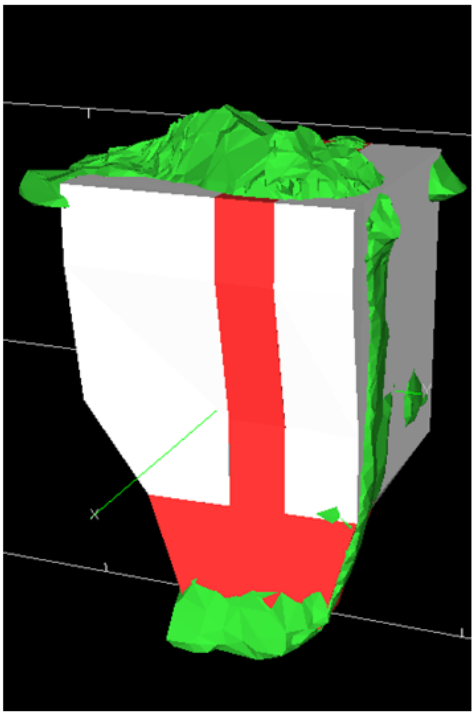
Commenced: November 2008 Completed: December 2008 Backfilled:	
Lithology: Varied from GRNB, GRNH & GRNL Alteration: No model data but expected to be moderate to high.	
Stope adjacency's: Purple 232 had no direct adjacencies but several stopes within close proximity. Stress condition: High	
Overbreak: The crown surface failed	
Comments: The structural influence study showed shallow to moderately dipping regional structures intersecting the undercut west wall dipping to the east. Some instability in the west wall and base of blast packet 4 was expected to occur following blasting of the undercut due to shearing along these structures.	View looking SW

Comments:
Multiple, moderate to steeply dipping structures were identified in the crown of the stope that extend down into blast packets 3 & 4. The orientation of these structures is likely to promote the formation of wedges in the interim crown and northwest corner of the stope. Multiple, flat dipping to steeply dipping structures were present in the crown of the stope. The orientation of these structures is likely to promote the formation of large wedges in the crown. Furthermore, mining of Purple 232 was identified to create a ≈ 10.0m wide pillar to the east, between purple 232 and purple 388. Steep, south-easterly dipping regional structures and faults transect this pillar and may therefore cause some instability in the east wall.
Map 3D modelling indicated high stress and low confinement in the crown of the stope and low confinement to tensile conditions on all the walls. This was thought to potentially lead to unclamping of structures at these locations. The pillar to the east in particular has been highlighted as undergoing significant stress reduction following stope extraction. The crown plotted in the transition zone of the supported chart. All of the walls plotted in the stable zone of the unsupported case histories chart. However, it was noted the Matthew's Stability Chart Method of assessing stope stability does not cope well with instances of low stress.
The CMS shows the crown failed while all other surfaces were stable. The crown has clearly failed along a wedge created by the intersection of two structures coupled with the stress relaxation.

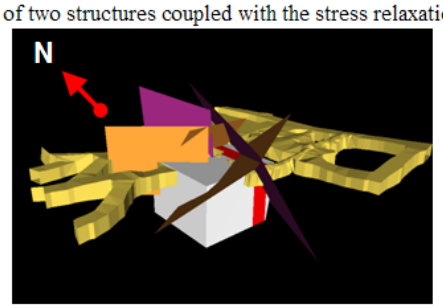

Structures intersecting the crown, view looking north

STOPE NAME: **Purple 269**	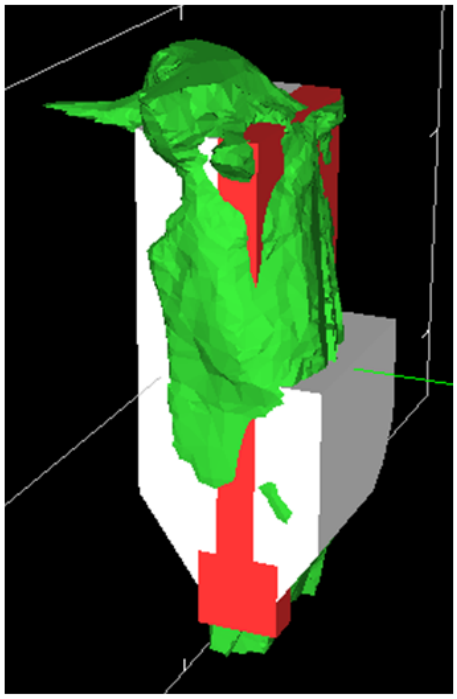
Commenced: January 2008 Completed: March 2008 Backfilled:	
Lithology: GRNH & GRNL Alteration: Moderate to high Sericite alteration	
Stope adjacency's: Purple 269 is a tertiary stope, Purple 034 lies to the west and Purple 080 and 081 lie to the south Stress condition:	
Overbreak: The crown surface failed	
Comments: Two moderately dipping faults were identified to intersect above the Eastern drill drive on the 32 level. Cable bolts were extended past the length identified by the cable bolt graphs to adequately support the undercut.	View looking NW

Comments:
The crown was highly structured. Failure had already occurred at the intersection of the 28 LF63 X-Cut and 27 PL8 NDD. It was recommended that cablebolting lengths and density are higher than that suggested by the analysis due to the presence of these structures, the location of the drives that can be cable bolted and the presence of the existing failure.
The stope footprint plotted in the transition zone of the supported chart and in the caving zone of the unsupported case histories chart. Therefore it was recommended that crown cables were installed on both the 28 and 32 levels.
The Northern wall plotted in the stable zone of the unsupported case histories chart, however the relaxed state of the rockmass wass likely to promote failure of the rockmass due to unclamping of structures which is not accounted for in the stability graph method.
The Eastern wall plotted in the transition zone due to a large HR (13.6) and the presence of a moderately dipping joint set. The "step" in the eastern wall and the low stress environment was expected to further encourage failure in this wall
The north and east walls performed as expected but the crown failed with an average overbreak of 8.60 metres. The CMS shows the failure is as expected of the overlying drill drives due to the intersecting structures.

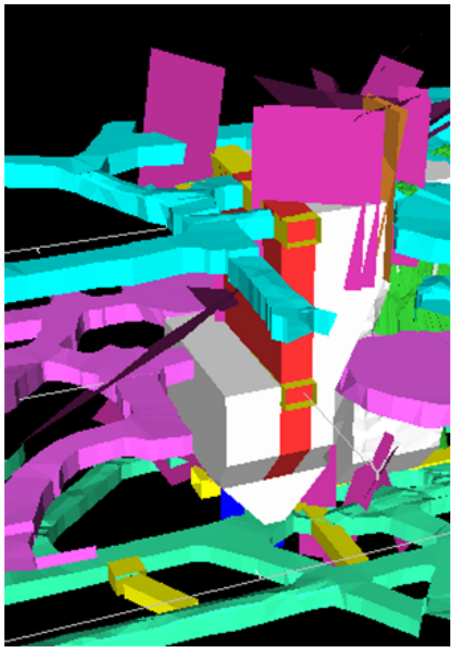

View of the structural influences looking south

STOPE NAME: **Purple 311**	
Commenced: September 2006 Completed: October 2006 Backfilled:	
Lithology: Alteration:	
Stope adjacency's: Purple 311 have two immediate adjacencies. Purple 001 sits to the south and abuts most of the south wall of the stope Stress condition:	
Overbreak: The crown surface failed	
Comments: Purple 008 is below Pu311, the crown of which is adjacent to extraction development of the Pu311 on the 32 Level. Records show that Purple 008 was rock filled with no placement of CAF to tight fill.	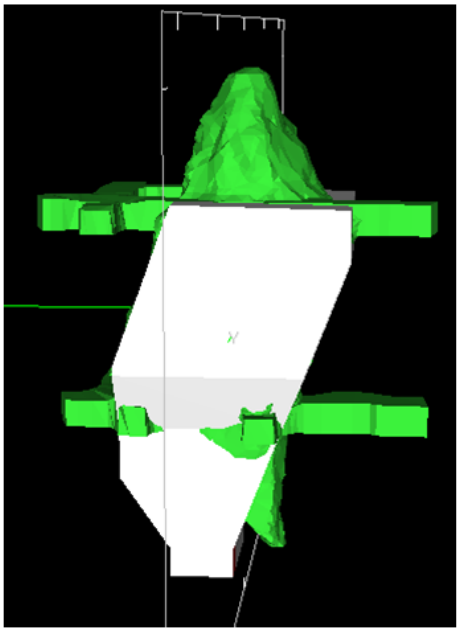 View looking South

Comments:
However, probe drilling revealed that there is CAF in Purple 008.
The CMS shows the north and west walls of Purple 311 were stable while the east wall was unstable as predicted and the crown failed. The overbreak experienced reached 21.70 metres, the shape and extent of the overbreak implies the failure was controlled by the unconformity coupled with the notoriously fractured ground in the northern end of the mine.

STOPE NAME: **Scarlet008**	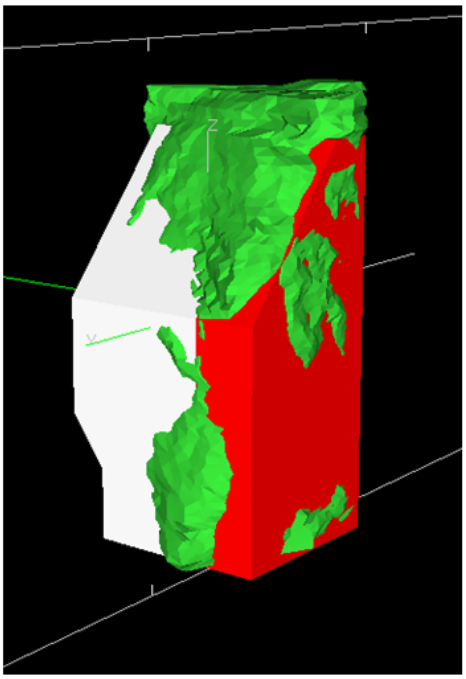
Commenced: October 2005 Completed: November 2005 Backfilled:	
Lithology: Formed in a combination of GRNB & GRNH. Alteration: No alteration model data available but inferred to be moderate Sericite alteration.	
Stope adjacency's: Secondary stope with only Scarlet 009 (CAF filled) abutting the south west corner over 10m of the 30m stope wall Stress condition:	
Overbreak: The crown & west surfaces failed	
Comments: Steeply dipping NS and NE-SW trending structures are predominant in the region and were identified to affect the stability of the northern and southern walls. The crown is stable without support.	View looking SE

Comments:

The crown plotted within the stable zone of the supported and unsupported charts. The western wall, which had slightly better ground conditions based on window mapping in the area, plotted in the stable zone of the unsupported chart. Some minor overbreak was expected as the western wall abuts the slot for SC008 and will be the first wall to reach design dimensions. The northern and southern walls plot in the transitional zone, the eastern wall plotted in the stable zone of the unsupported chart.

The CMS shows the north and east walls were stable, the south unstable and the crown and west failed. This was quite unexpected for both these surfaces. The crown simply broke into the overlying drill drive while the west wall suffered planar failure over 95% of it's surface area, with no identified sub-vertical structures to justify this failure. It is likely the location of the slot was the primary cause.

STOPE NAME: **Scarlet 346**	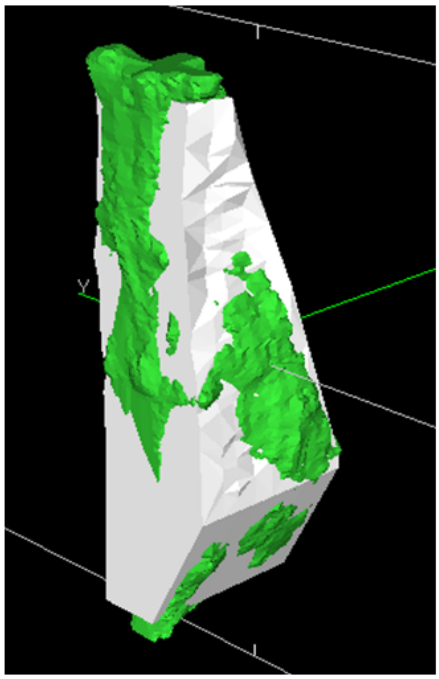
Commenced: December 2006 Completed: March 2007 Backfilled:	
Lithology: The crown of the stope is within GRNH & GRN, the E wall is GRNL, the W wall was GRNL/HEMH. Alteration: The model only extends for lower half of the stope, on the E wall it is low & moderate on the W wall	
Stope adjacency's: Full adjacencies to the north with Scarlet 055 and to the south with Scarlet 061 Stress condition: Low to moderate	
Overbreak: The crown surface failed	
Comments: The crown was on the 45 level the structural influence study identified two vertical discontinuous structures intersecting the crown. Two regional scale structures mapped on the eastern side of the stope.	View looking NE

Comments:
They both dipped to the west, and thus probably intersect the eastern wall of the stope. There were no structures projected to intersect the western wall.
The crown plotted well within the stable zone because of it's small size. The west wall plotted in the transitional zone. The east wall also plotted in the transitional zone, due mainly to unfavourably oriented structures present which dip into this wall. The lower stability was also due to the less stable shape (inclined east wall versus the vertical west wall). The area is within a high stress area. Instability due to high stress is not accounted for by the Stability Graph method.
The CMS data shows the east and west walls both remained stable but the crown failed with an average overbreak of 4.80 metres. The crown has failed along the drill drive.

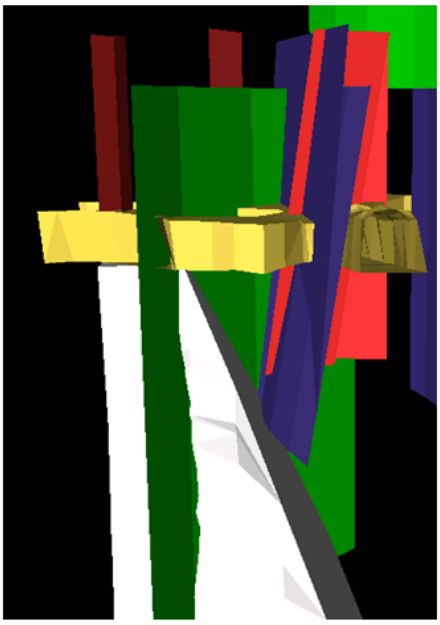

Overlying development & structural influences

STOPE NAME: **Scarlet 353**	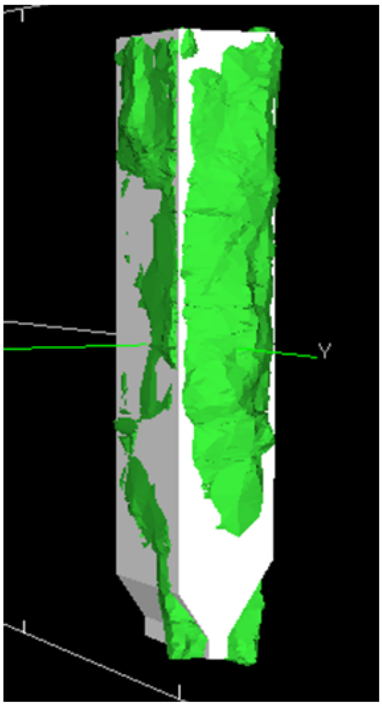
Commenced: September 2006 Completed: January 2007 Backfilled:	
Lithology: The crown of the stope was within GRNL and GRNH, the walls were predominantly HEM with GRNL and HEMH Alteration: No alteration model available, but u/g observations indicate low to moderate alteration	
Stope adjacency's: No existing direct adjacencies, a 5m wide partial pillar is formed between Scarlet 353 and Scarlet 043 Stress condition:	
Overbreak: The north surface failed	View looking SW
Comments: No major structures were identified in the structural influence study, some minor joint sets were identified but not expected to have an effect on the stability of the stope. The crown plotted in the transition zone on the supported case histories chart.	

Comments:
The north and south walls plotted within the transitional zone and the east and west walls plotted within the caving zone. This is due to the large dimensions of these walls (26m x 160m and 35m x 160m respectively) and to the blocky nature of the rock mass. The rock mass in the top half of the stope was identified as blocky, while below the 45L the rock mass became massive.
The CMS shows the south wall was unstable, the north wall failed and the remainder were stable. These results are indifferent to the results of the Mathews stability graph prediction. From the preliminary study and looking at the CMS no direct cause of the north wall failure could be identified.

STOPE NAME: **Scarlet 388**	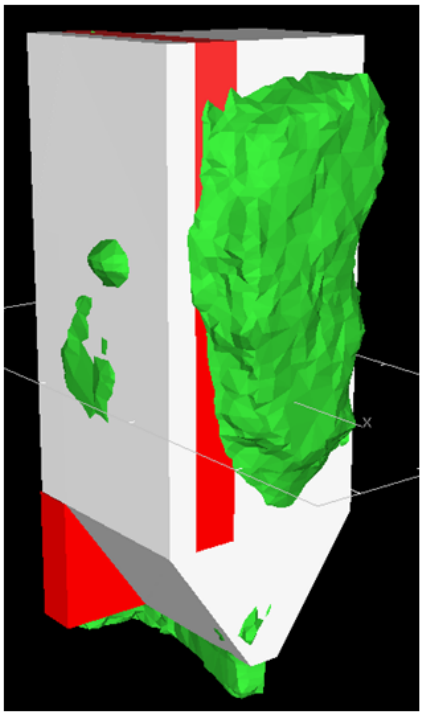
Commenced: February 2007 Completed: June 2008 Backfilled:	
Lithology: Backs & walls were formed in majority of HEMH and some GRNL Alteration: Low to moderate alteration.	
Stope adjacency's: Secondary stope with Scarlet 060 directly to the South. Stress condition: Moderate	
Overbreak: The east surface failed	
Comments: There were very few major structures identified in the structural influence study, the majority of faults which were mapped near Scarlet 388 were NE-SW striking, steeply dipping and not very continuous.	View looking NW

Comments:
The crown plotted in the transition zone of the supported case histories chart, the east and walls also plotted in the transition zone while the north was expected to be stable.
The CMS shows all surfaces of the stope performed well other than the east wall which failed. The failure was planar across the face, nothing in the preliminary study identified potential for east wall failures.

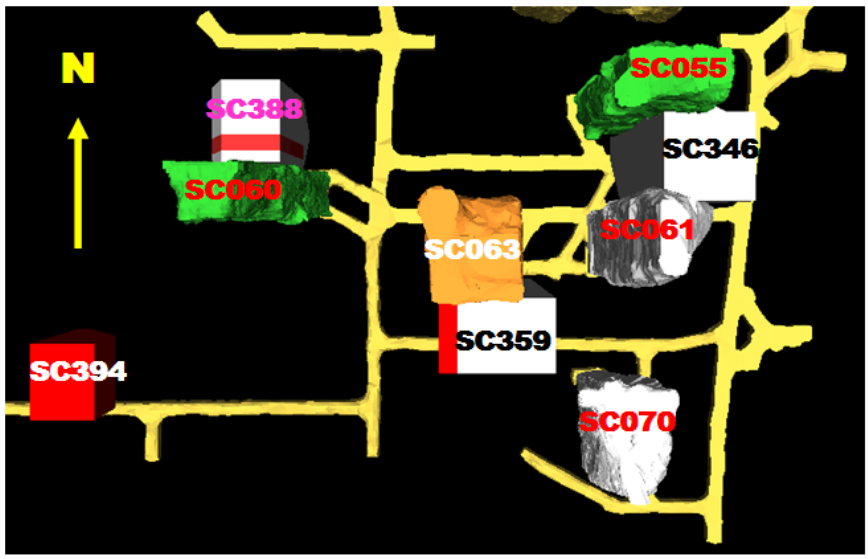

Image showing Scarlet 388 with surrounding stopes & development.

STOPE NAME: **Yellow 004**	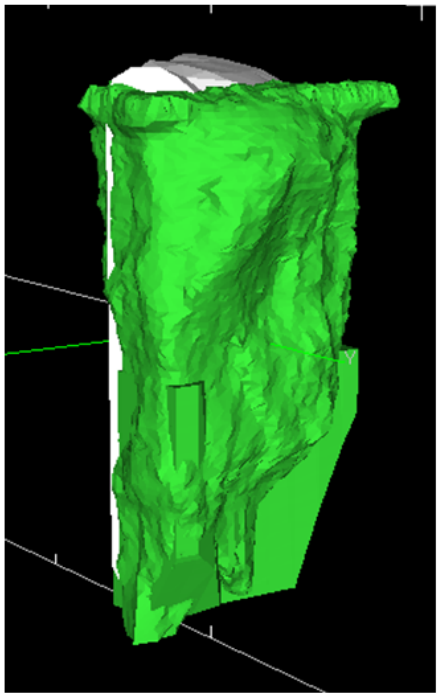
Commenced: January 2005 Completed: April 2005 Backfilled:	
Lithology: GRNB, GRNH & GRNL Alteration: Pervasive Sericite alteration	
Stope adjacency's: Secondary stope with both Yellow 024 & 025 directly to the South. Stress condition:	
Overbreak: North surface failed	
Comments: The structural influence study identified three major fault orientations which were continuous in respect of the stope dimensions: steep SE dipping and steep SSW dipping. The more significant joint orientations were similar to the fault orientations mentioned above and a moderately continuous shallow to flat dipping set was also been	View looking SW

Comments:
identified. The crown of Yellow 004 was expected to be stable with support and cable bolting was recommended. The east and west walls of Yellow 004 were expected to be stable with some dilution . The north and south walls were expected to suffer dilution, they plotted well into the "caving zone" on the "Unsupported Case Histories" chart. Whilst the performance of this stope was regarded as potentially unsatisfactory, it was not of serious concern as was the last planned stope in the area. It was identified the location of development to facilitate parallel hole drilling may act as a site for initiation of overbreak on the northern wall.
The CMS data shows the only failure which occurred was on the north wall, the crown and south walls were unstable and the east west walls were stable. The northern wall suffered overbreak of up to 12.40 metres with an average of 5 metres across 90% of the surface area. As identified in the stability analysis the failure appears to be exaggerated around the development, indicating this as the most likely instigator of instability.

Appendix F: Rock property data provided to BE for use in LR2

Rock Mass Zones			Mean	Lower Quartile							Hoek & Diedrichs (2006)
No	Geological	Geotechnical	Area	GSI	GSI	mi	UCS [MPa]	Density [t/m³]	E Lab [MPa]	Poissons ratio	Erockmass [MPa]
1	ZAL	ZG1 Undeformed		71	65	12	76	2.61	60000	0.26	13502
2	ZAL	ZG1 Deformed	Mashers	61	52	12	50	2.61	39470	0.26	5107
3	ZWAR	ZG2A Undeformed		73	68	17	100	2.6	39000	0.2	9646
4	ZWAR	ZG2A Deformed	Mashers	66	57	17	65	2.6	25350	0.2	4387
5	ZWAR	ZG2B Undeformed		73	68	17	100	2.6	39000	0.2	9646
6	ZWAR	ZG2B Deformed	Mashers	66	57	17	65	2.6	25350	0.2	4387
7	ZWAR	ZG3 Undeformed		78	74	22	132	2.52	55000	0.22	16713
8	ZWAR	ZG3 Deformed	Mashers	69	62	22	89	2.52	37080	0.22	7544
9	ZWAW	ZG4 Undeformed		76	71	20	148	2.5	65000	0.19	18288
10	ZWAW	ZG4 Deformed	Mashers	68	62	20	95	2.5	41720	0.19	8053
11	ZWC	ZG5 Undeformed		77	74	22	117	2.39	44000	0.22	12877
12	ZWC	ZG5 Deformed	Mashers	70	64	22	93	2.39	34970	0.22	7488
13	ZWT	ZG6A Undeformed		73	69	11	118	2.5	40000	0.2	9893
14	ZWT	ZG6A Deformed	Mashers	65	59	11	95	2.5	32200	0.2	5258
15	ZWT	ZG7 Undeformed		71	70	9	75	2.73	28000	0.23	6301
16	ZWT	ZG7 Deformed	Mashers	68	66	9	60	2.73	22400	0.23	4324
17	Granite	Granite 1		81	78	22	135	2.85	60480	0.25	20354
18	Granite	Granite 2		79	76	19	109	2.85	48832	0.25	16380
19	Granite	Granite 3_4		74	70	12	95	2.89	42560	0.25	11008
20	Granite	Granite 5_6		77	75	22	135	2.88	60480	0.25	17700
21	HEM_BX 1	HEM_BX1		80	77	28	190	3.86	74860	0.33	24394
22	HEM_BX 2&3	HEM_BX2_3		77	73	28	190	3.86	74860	0.33	21909
23	HEM_BX 4&5	HEM_BX4_5		68	61	28	190	3.86	74860	0.33	14451
24	HEM_BXN	HEM_BXN		77	73	24	190	3.86	74860	0.33	21909
25	HEM1	HEMQ		76	73	20	150	3.62	75300	0.3	21186
26	KASH	KASH		60	56	12	30	2.85	14000	0.19	1706
27	KHEMQ	KHEMQ		76	69	22	104	3.45	69000	0.3	19414
28	VOLC_BX	VOLC_BX		77	74	20	90	3.6	43000	0.31	12585
29	Sand	Sand						2	10	0.35	

Shear properties of unit boundaries			Disturbance	1
	ϕ [°]	coh [Pa]		
ZAL/ZWAR	27	0		
ZWAR/ZWAW	34	0		
ZWTU	34	0		
ZWTL	22	0		
ZWT/Granite	22	0		

Mohr-Coulomb failure criterion